Connectivity gradients reveal functional reorganisation and cognitive outcomes after stroke

Ramya Balakrishnan

Doctor of Philosophy

University of York

Psychology

June 2026

Abstract

Stroke produces widespread disturbances in whole-brain organisation, yet the mechanisms through which focal lesions alter functional connectivity and how structurally intact regions reorganise remain incompletely understood. Connectivity gradients provide a framework for characterising macroscale functional architecture, capturing continuous axes of organisation that extend beyond discrete network boundaries. This thesis examines how stroke affects these gradients and evaluates whether gradient changes explain variation in post-stroke cognition. The thesis also explores the use of structural imaging for modelling post-stroke functional reorganisation, assessing its value in contexts where resting-state fMRI is not routinely obtained in clinical settings. This work draws on two chronic stroke cohorts: a group of individuals with semantic aphasia and a subset of the PLORAS dataset. Resting-state fMRI from both cohorts (mean post-stroke interval > 4 years) was used to characterise long-term functional changes. First, in semantic aphasia, lesion information from structural MRI was used to model the direct effects of stroke in connectivity space and to test whether simulated post-stroke gradients predicted semantic control impairments. Second, connectivity gradient reorganisation was characterised in the PLORAS cohort to determine whether large-scale organisational changes in the unlesioned cortex were linked to language outcomes. Third, an iterative propagation simulation model was evaluated, capturing direct and indirect effects of stroke across the cortex, and tested to determine whether gradient–behaviour associations observed in the simulations were reflected in empirical stroke gradients. Across the three empirical studies, the thesis demonstrates that stroke consistently attenuates the brain's principal connectivity gradient axes, reducing differentiation between transmodal and unimodal systems, visual and motor networks, and control-default mode regions. In semantic aphasia, lesion-based simulations reproduced the empirically observed reorganisation moderately well, particularly along the transmodal–unimodal axis. These simulations revealed that shifts of the left inferior frontal gyrus toward a more unimodal connectivity profile were associated with poorer semantic control, highlighting how altered embedding within large-scale hierarchies contributes to semantic deficits. In the larger and more diverse PLORAS cohort, distributed reorganisation of connectivity gradients in the unlesioned cortex explained language outcomes beyond the effects of focal lesions. Shifts along the control-default mode axis, particularly within the left inferior frontal gyrus, were associated with better speech but poorer writing performance. The final study showed that iterative propagation simulations improved correspondence with empirical gradients, especially for the visual-motor axis. One replicated finding was that a shift of the right inferior frontal gyrus toward the motor end of the visual–motor axis was associated with better phonology and working memory. Together, these findings show that connectivity gradients provide a low-dimensional, clinically informative framework for understanding how focal lesions and distributed reorganisation shape post-stroke cognition. They also highlight the current potential and limitations of structural imaging-based simulations for modelling post-stroke functional reorganisation.

List of Contents

Abstract 2
List of Contents 3
List of figures 9
List of tables 11
List of Abbreviations 12
Acknowledgements 13
Author's Declaration 15
Supervisor's Declaration 16
Chapter 1 17
Literature review 17
1.1. Introduction: Stroke as a Network Disorder 17
1.2. Whole-brain network disruption and post-stroke behavioural impairments 18
1.2.1 Distributed organisation of cognitive function 18
1.2.2. Aphasia as a disorder of language and domain-general control 18
1.2.3. Executive dysfunction and frontoparietal control systems 20
1.2.4. Semantic aphasia and the semantic control network 21
1.2.5. Neglect as a large-scale attention network disorder 22
1.2.6. Sensorimotor disconnection and motor–cognitive coupling 23
1.3. Reorganisation after stroke and its role in behaviour 24
1.4. Overview of lesion mapping methods 27
1.4.1 Lesion symptom mapping 28
1.4.2. Direct structural disconnectome-based symptom mapping 28
1.4.3. Indirect structural disconnectome-based symptom mapping 30
1.4.4. Direct functional disconnection-based symptom mapping 31
1.4.5. Indirect functional disconnectome-based symptom mapping 33
1.4.6. Functional connectivity analyses 34
1.5. Functional organisation from a gradient perspective 35
1.5.1. Functional connectivity gradients 35

1.5.2. Functional connectivity gradients and correlates of cognition 38
1.5.3. Atypical connectivity gradients 39
1.6. Overview of the thesis 41
Chapter 2 44
Lesion-gradient mapping: effects of stroke on connectivity gradients 44
in semantic aphasia 44
2.1. Abstract 44
2.2. Introduction 45
2.3. Methods 48
2.3.1. Overview 48
2.3.2. Participants 48
2.3.3. Semantic cognition testing 49
2.3.4. MRI acquisition: Stroke patients and aged controls 50
2.3.5. Lesion segmentation 51
2.3.6. Resting-state fMRI data preprocessing 52
2.3.7. Whole-brain functional connectivity 52
2.3.8. Functional connectivity gradient extraction 53
2.3.9. Simulated post-stroke gradients 53
2.3.10. Post-stroke gradient differences 55
2.3.11. Phase 1: Statistical analyses 56
2.3.12. Phase 2: Statistical analyses 56
2.4. Results 57
2.4.1. Lesion Analysis 57
2.4.2. Phase 1: Effects of stroke on connectivity gradients extracted from resting-state fMRI 58
2.4.3. Phase 1: Comparisons of gradient changes in resting-state fMRI and simulated from structural MRI 59
2.4.4. Phase 1: Association between lesion size and the level of similarity captured by the simulation 62
2.4.5. Phase 2: Post-stroke simulated gradient changes compared with healthy controls ... 63

2.4.6. Phase 2: Association between simulated gradient changes and semantic impairment in the semantic control network 64
2.4.7. Phase 2: Whole-brain associations between simulated gradient changes and semantic impairment 65
2.5. Discussion 66
2.5.1. Functional connectivity gradients capture whole-brain changes post-stroke 66
2.5.2. Role of the left IFG in semantic control 68
2.6. Future directions 70
2.7. Conclusion 71
Chapter 3 72
Reorganisation of functional connectivity gradients in post-stroke aphasia 72
3.1. Abstract 72
3.2. Introduction 73
3.3. Methods 74
3.3.1. Participants 74
3.3.2. Comprehensive aphasia test 76
3.3.3. Lesion segmentation 76
3.3.4. Resting-state fMRI data preprocessing 76
3.3.5. Whole-brain functional connectivity 78
3.3.6. Functional connectivity gradient extraction 78
3.3.7. Post-stroke gradient differences 79
3.3.8. Statistical analyses 79
3.4. Results 80
3.4.1. Principal Component Analysis: Comprehensive Aphasia Test 80
3.4.2. Lesion symptom mapping 81
3.4.3. Post-stroke gradient differences 82
3.4.4. Association between post-stroke functional connectivity gradient changes and language outcomes within the language network 85
3.5. Summary of results 87
3.6. Discussion 87

3.6.1. Interpretation of lesion-symptom mapping 87
3.6.2. Reorganisation of gradient-based functional connectivity 89
3.6.3. Integrating lesion location and gradient organisation 90
3.8. Conclusion 92
Chapter 4 93
A Connectivity-gradient simulation model captures stroke reorganisation 93
and language outcomes 93
4.1. Abstract 93
4.2. Introduction 93
4.3. Methods 96
4.3.1. Participants 96
4.3.2. Comprehensive Aphasia Test 97
4.3.3. Lesion segmentation 97
4.3.4. Resting-state fMRI data preprocessing 98
4.3.5. Whole-brain functional connectivity 98
4.3.6. Functional connectivity gradient extraction 98
4.3.7. Simulated lesion functional connectivity 99
4.3.8. Post-stroke gradient differences 104
4.3.9. Highest-correlation α–γ parameter 104
4.4. Statistical analyses 105
4.4.1. Spatial correlation analyses 105
4.4.2. Lesion–gradient symptom mapping 106
4.4.3. Validation of lesion–gradient symptom mapping of simulation 107
4.5. Results 107
4.5.1. Lesion analysis 107
4.5.2. Principal Component Analysis: Comprehensive Aphasia Test 109
4.5.3. Single-case illustration of the lesion simulation model 109
4.5.4. Spatial correlation: Focal effects simulation vs. iterative propagation simulation 110
4.5.5. Post-stroke connectivity gradients 111

4.5.6. Post-stroke connectivity gradient changes: observed versus simulated gradients from the iterative propagation model 113
4.5.7. Comparisons of network organisation in gradients between observed and stimulated stroke 115
4.5.8. Validation of simulated post-stroke gradient–language outcome associations in observed stroke gradients 118
4.6. Discussion 121
4.6.1. Iterative propagation approach to model lesion effects on cortical gradients 121
4.6.2. Post-stroke connectivity gradients 123
4.6.3. Simulation captured functional reorganisation changes associated with language outcomes 123
4.7. Future directions 125
4.8. Conclusions 126
Chapter 5 127
General Discussion 127
5.1. Scope and aims of the thesis 127
5.2. Summary of empirical chapters 127
5.2.1. Chapter 2: Lesion-gradient mapping in semantic aphasia: comparisons of observed and simulated effects of stroke on connectivity gradients 127
5.2.2. Chapter 3: Reorganisation of functional connectivity gradients in post-stroke aphasia 129
5.2.3. Chapter 4: A connectivity-gradient simulation model captures stroke reorganisation and language outcomes 130
5.3. Key Themes from the Empirical Chapters 131
5.3.1. Methodological rationale for connectivity gradients 131
5.3.2. Global attenuation of connectivity gradients after stroke 137
5.3.3. Gradient-specific shifts of the inferior frontal gyrus after stroke 138
Interpreting the IFG's position in connectivity gradients 138
5.3.4. Functional reorganisation of the inferior frontal gyrus across connectivity gradients 141
Left IFG shift toward unimodal connectivity in semantic aphasia 141
Right IFG's visuomotor shift and phonology 144

5.4. Future directions 147
5.5. Conclusions 149
Supplementary materials 151
Chapter 2 supplementary materials 151
Chapter 3 supplementary materials 155
Chapter 4 supplementary materials 160
References 172

List of figures

Figure 1.1. Workflow for indirect structural disconnectome mapping. 31
Figure 1.2. Functional connectivity gradients. 37
Figure 2.1. Processing pipeline for simulated post-stroke gradients for each lesion.... 55
Figure 2.3. Post-stroke changes in connectivity gradients 60
Figure 2.4. Relationship between lesion size and simulation accuracy. 62
Figure 2.5. Permutation test results for Gradient 1 and lesion distribution 63
Figure 2.6. Semantic control network ROI analysis. 65
Figure 3.1. Overlap map of stroke lesions (N = 60). 75
Figure 3.2. Processing pipeline for functional connectivity gradients in stroke participants and aged matched controls. 77
Figure 3.3. Lesion–symptom associations with PCA-derived language outcomes. 81
Figure 3.4. Functional connectivity gradients for age-matched controls and stroke participants 83
Figure 3.5. Significant post-stroke gradient changes for Gradients 1–3 84
Figure 3.6. Permutation test results within the language ROI. 86
Figure 4.1. Processing pipeline for simulated post-stroke gradients for each lesion using the iterative propagation model. 103
Figure 4.2. Lesion distribution across the stroke cohort. 108
Figure 4.3. Visual correspondence between observed and simulated stroke connectivity. 110
Figure 4.4. Functional connectivity gradients for age-matched controls, observed stroke, and simulated stroke. 112
Figure 4.5. Distribution of correlation values for iterative propagation and direct lesion effects simulation. 113
Figure 4.6. Comparisons of significant post-stroke functional changes between observed and simulated gradients from permutation tests. 115
Figure 4.7. Network-level shifts of observed and simulated stroke in gradient space. 117
Figure 4.8. Permutation test results within the language ROI. 120
Figure 5.1. Behaviourally significant IFG clusters identified across the three empirical chapters, their positions in gradient space, and their relation to large-scale control networks. 139
Supplementary Figure 2.S1. Steps followed for generating the lesion matrix: 151
Supplementary Figure 2.S2. Topographic organisation of connectivity gradients. 152
Supplementary Figure 2.S3. Permutation test results for Gradient 2 and lesion distribution. 154
Supplementary Figure 3. S1. Principal component analysis results of the CAT. 155

Supplementary Figure 3.S2. Post-stroke functional connectivity differences after removing aging effects. 156
Supplementary Figure 3.S3. Permutation test results within the language ROI. 157
Supplementary Figure 3.S4. Permutation test results at the whole-brain level. 159
Supplementary Figure 4.S1. Principal component analysis results of the CAT. 160
Supplementary Figure 4.S2. Heatmap showing spatial correlations between the observed and simulated Gradient 1 maps across α–γ parameter combinations. 161
Supplementary Figure 4.S3. Heatmap showing spatial correlations between the observed and simulated Gradient 2 maps across α–γ parameter combinations. 162
Supplementary Figure 4.S4. Bar plots showing the α–γ parameter combinations that produced the highest correlation between simulated and observed stroke gradients. . 163
Supplementary Figure 4.S5. Relationship between lesion hemisphere and simulation accuracy. 164
Supplementary Figure 4.S6. Relationship between lesion size and simulation accuracy for Gradient 1 and Gradient 2. 166
Supplementary Figure 4.S7. Comparison of post-stroke gradient changes between observed resting-state gradients and simulated gradients from the iterative propagation model. 167
Supplementary Figure 4.S8. Network-level comparisons between observed and simulated stroke across connectivity gradients. 169
Supplementary Figure 4.S9. Comparison of observed and simulated stroke-related gradient differences across functional networks. 170
Supplementary Figure 4.S10. Significant clusters from lesion–symptom mapping conducted on the simulation 171

List of tables

Table 2.1. Semantic performance scores for Camel and Cactus test and Ambiguity task 51

Table 2.2. Lesion location, size and spin permutation results for Gradient 1 and Gradient 2 61

Supplementary Table 2.S1. 153

Supplementary Table 4.S1. Spatial correlations between observed and simulated post-stroke gradient changes for each lesion. 165

List of Abbreviations

Abbreviation	Definition
AD	Alzheimer's disease
BOLD	Blood oxygen level-dependent
CAT	Comprehensive Aphasia Test
CCT	Camel and Cactus Test
CONN	CONN functional connectivity toolbox
DMN	Default Mode Network
DTI	Diffusion Tensor Imaging
FC	Functional Connectivity
fMRI	Functional Magnetic Resonance Imaging
FPN	Frontoparietal Network
FSL	FMRIB Software Library
FWE	Family-Wise Error
GLM	General Linear Model
HCP	Human Connectome Project
ICA	Independent Component Analysis
IFG	Inferior Frontal Gyrus
IFOF	Inferior Fronto-Occipital Fasciculus
IQR	Interquartile Range
LIFG	Left Inferior Frontal Gyrus
MDN	Multiple-Demand Network
MNI	Montreal Neurological Institute
MRI	Magnetic Resonance Imaging
OASIS	Open Access Series of Imaging Studies
PCA	Principal Component Analysis
PLORAS	Predicting Language Outcome and Recovery After Stroke
ROI	Region of Interest
rs-fMRI	Resting-State Functional Magnetic Resonance Imaging
SA	Semantic Aphasia
SCN	Semantic Control Network
SD	Standard Deviation
SN	Salience Network
SPM	Statistical Parametric Mapping
TE	Echo Time
TFCE	Threshold-Free Cluster Enhancement
TMS	Transcranial Magnetic Stimulation
TR	Repetition Time

Acknowledgements

I would like to express my deepest gratitude to Professor Beth Jefferies, whose support, insight, and encouragement have shaped every stage of this thesis. Working with her has been an enriching experience. She consistently encouraged me to think beyond the obvious, to question assumptions, and to approach problems creatively. Her enthusiasm for developing new methods by integrating ideas across different domains, together with her openness to exploring unconventional approaches, made this research journey both stimulating and rewarding. She placed great trust in my ability to pursue ambitious projects and was exceptionally supportive of new directions and ideas. I am profoundly grateful for the time, energy, and care she invested in my development as a researcher, and for fostering an environment that made learning both rigorous and enjoyable.

I am deeply grateful to Professor Cathy J. Price for generously sharing the PLORAS dataset, which formed the basis for much of this thesis, and for the opportunity to work with her. I greatly appreciated her support and insightful discussions, particularly in helping me interpret the findings and identify the most important aspects of the results. Her contributions to the field of stroke and language neuroscience have been a great source of inspiration. I am sincerely thankful for her time, insight, and encouragement, and for the opportunity to work with and learn from her.

I would like to thank Tirso R. J. Gonzalez Alam and Theodoros Karapanagiotidis for introducing me to the foundations of gradient extraction and for generously sharing their scripts, expertise, and time.

I would like to thank my FLEXSEM lab members for creating such a friendly and intellectually stimulating environment. The many discussions we shared helped shape aspects of this thesis, and I greatly appreciated the supportive atmosphere within the lab. Special thanks to Katya Krieger-Redwood, Ximing Shao, Nicholas E Souter, Meichao Zhang, Susanne Eisenhauer, Lidon Marin Marin, Hannah Thompson, Rebecca Jackson, Darren Millward, and Jiayu Liu for their support and encouragement throughout this journey.

I would like to thank Joe Lyons, Richard Aveyard, Jennifer Ashton, Andre Gouws, Jackie Mayhew, and all the other YNiC staff for their support throughout this project. Their expertise and assistance with the technical aspects of the work were invaluable, and I am very grateful for their patience and willingness to help whenever needed.

I am grateful to the stroke patients and their caregivers who contributed to the York study and the PLORAS dataset. Their willingness to participate in research and share their time and experiences made this work possible. I would like to dedicate this thesis to them, in recognition of their invaluable contribution to stroke research and to our understanding of post-stroke functional reorganisation.

I am also grateful to my friends outside the university, whose support, encouragement, and steady presence have meant a great deal throughout this journey. I am thankful for their friendship and understanding, and for helping me maintain perspective beyond the PhD. Their kindness and support made the more challenging moments easier to navigate.

I am deeply grateful to my mother, Nirmaladevi Balakrishnan, my sister, Anusha Balakrishnan, and my brother, Janagan Balakrishnan, for their constant support from Sri Lanka. Despite the distance between us, their encouragement, care, and unwavering belief in me have been a continuous source of strength throughout this journey. I am deeply appreciative of their love and support over the years.

Above all, I would like to thank my husband, Prashanth Chanmugam, for his unwavering support throughout this journey. His understanding, encouragement, and constant belief in me meant a great deal during the many challenges of the PhD. I am especially grateful for the way he took on additional responsibilities at home during the final stages, allowing me to focus fully on completing this thesis. I am profoundly grateful for his patience, support, and love throughout these years.

Author's Declaration

I, Ramya Balakrishnan, declare that this thesis is a presentation of original work and that I am the sole author, under the supervision of Professor Beth Jefferies. This work has not previously been presented for an award at this, or any other, University. All sources are acknowledged in the References.

Generative artificial intelligence tools were used solely to assist with proofreading and improving the clarity and grammar of the text. All scientific content, analyses, interpretations, and conclusions are the original work of the author, who takes full responsibility for the content of this thesis.

Parts of the work presented in Chapters 2 and 3 have been submitted for publication and have undergone peer review. Pre-print versions of these manuscripts are available:

Chapter 2

Balakrishnan, R., Alam, T. R. del J. G., Mckeown, B. L. A., Souter, N., Karapanagiotidis, T., Smallwood, J. E., Krieger-Redwood, K., & Jefferies, E. (2026). Lesion-Gradient Mapping in Semantic Aphasia: Comparisons of Observed and Simulated Effects of Stroke on Connectivity Gradients. *BioRxiv*, 2026.06.12.731654. https://doi.org/10.64898/2026.06.12.731654

Chapter 3

Balakrishnan, R., Del, R., Gonzalez Alam, J., Leech, R., Price, C. J., & Jefferies, E. (2026). Reorganisation of Functional Connectivity Gradients in Post-Stroke Aphasia. *BioRxiv*, 2026.06.07.730675. https://doi.org/10.64898/2026.06.07.730675

Supervisor's Declaration

As the primary supervisor of Ramya Balakrishnan, I confirm that this thesis is the work of the candidate. Where I am named as a co-author on publications arising from this thesis, this reflects my role in providing intellectual and methodological contributions, together with guidance in the preparation of manuscripts. The contributions of other collaborators are acknowledged where appropriate.

Chapter 1
Literature review

1.1. Introduction: Stroke as a Network Disorder

Stroke was initially viewed as a focal disease: damage to a specific brain region was thought to produce a corresponding deficit associated with that location. This view originated from Paul Broca's influential work showing that lesions in the left inferior prefrontal cortex (LIPC) and neighbouring regions cause non-fluent speech in stroke patients (Broca, 1861a; Gajardo-Vidal et al., 2021). Over time, this view has changed. Stroke causes damage to focal brain regions, but also global functional and structural network perturbations that emerge along anatomical pathways, from the cortex to subcortical regions, the brainstem, and the spinal cord (Latifi & Carmichael, 2024). This disruption reflects both the primary injury to local neural tissue and alterations in brain networks that are spatially and temporally remote from the lesion (Shi et al., 2019). Brain regions that are directly and indirectly affected by stroke are embedded within functional networks that maintain dynamic balance through synchronised interactions with other networks (Siegel et al., 2016). This interconnected framework explains how a lesion in a specific brain location can affect neurological functions far beyond the focal lesion site (Corbetta, 2012). The widespread effects of stroke at the whole-brain level are now conceptualised as a 'disconnectome' (Latifi & Carmichael, 2024) or network disorder (Esser et al., 2025). A recent study provided evidence consistent with this interpretation by showing the mechanisms underpinning whole-brain network disruption: Wu et al. (2025) showed that stroke-induced white-matter disconnections provide the neuroanatomical basis linking widespread functional connectivity disruptions to behavioural impairment.

Over 130 years ago, von Monakow proposed the concept of diaschisis, which served as a prelude to the network dysfunction framework. Diaschisis originally referred to a distant loss of excitability and changes in energy metabolism, or 'functional stillstand', in regions remote from the lesion (von Monakow, 1914). Modern neuroimaging has expanded this concept to show that post-stroke injury and repair extend well beyond the lesion site, triggering imbalances in networks connected to the stroke core. Damage-related signals spread across these networks and establish new connections in distant regions (Carmichael, 2015). The hemispheric engagement and disengagement pattern provides supporting evidence for whole-brain functional organisational change. Stroke results in an abnormal increase in asymmetrical hemispheric connections, characterised by decreased interhemispheric connectivity and increased intra-hemispheric connectivity between networks that are

normally more modular (Carter et al., 2010; Ramsey et al., 2016; Frías et al., 2018). These hemispheric functional changes are associated with dysfunction across multiple domains (Siegel et al., 2016). These broad effects explain why behavioural impairments are not strictly tied to lesion location, a pattern consistent with diaschisis (Carrera & Tononi, 2014).

1.2. Whole-brain network disruption and post-stroke behavioural impairments

Stroke produces behavioural impairments that extend beyond the anatomical boundaries of the lesion. This section focuses on how disruption of distributed brain networks contributes to post-stroke dysfunction across multiple domains. Rather than considering recovery or compensatory mechanisms, the emphasis here is on the immediate consequences of network disruption and on how alterations within and between large-scale systems give rise to the diverse cognitive, language, and motor impairments observed after stroke.

1.2.1 Distributed organisation of cognitive function

Stroke affects multiple domains, including executive function, motor control, language, memory, visuospatial skills, visuoconstruction, attention, and global cognitive function (Melkas et al., 2014). The co-occurrence of multiple impairments and their varying levels of severity suggest that this complexity cannot be attributed solely to the lesion site; rather, it reflects widespread functional disruptions both within and between networks (Wu et al., 2025). These deficits can be explained by the view that cognitive functions emerge from the topology of the whole-brain rather than from isolated regions behaving as autonomous modules (Bullmore & Sporns, 2009; Sporns et al., 2005). Several "rich-club" regions (e.g., the precuneus, superior frontal cortex, and superior parietal cortex) are characterised as high-degree nodes that are densely interconnected and facilitate high-level information transfer across the global network (van den Heuvel & Sporns, 2011). These regions are not limited to a single specific task; instead, they function as integrators that allow information to flow between otherwise segregated subdomains, thereby conferring robustness to the system (van den Heuvel & Sporns, 2011). One such example is Broca's area, which does not function as a simple speech-production unit but is involved in drawing representational inputs from the temporal cortex (semantic store) to their corresponding articulatory outputs in the motor cortex, thereby coordinating information transfer across large-scale networks (Flinker et al., 2015). This intrinsic architecture explains why a lesion at a specific site can cause multifaceted deficits that are not tied to the physical location of the damage.

1.2.2. Aphasia as a disorder of language and domain-general control

Post-stroke aphasia illustrates the interconnected network paradigm, affecting subdomains of language including phonological, morphological, semantic, syntactic, and speech processes (Sheppard

& Sebastian, 2020) and non-language cognitive domains such as attention, thinking, memory, and executive functions (Sheppard & Sebastian, 2020; Ivanova et al., 2015; Kuptsova et al., 2021; Murray, 2012). Most aphasia patients present with some level of impairment in comprehension, speech production, reading, and writing (Sheppard & Sebastian, 2020). Language is a complex function that requires interaction between multiple brain regions (Fedorenko & Thompson-Schill, 2014; Hagoort, 2019).

Hickok and Poeppel (2004) proposed a framework explaining how ventral and dorsal streams support different language functions. The cortical language system divides into two processing streams: a ventral stream linked to mapping sound onto meaning, and a dorsal stream supporting the mapping of sound onto articulatory-motor representations. The ventral pathway runs ventrolaterally toward the posterior inferior temporal region, serving as an interface between the superior temporal gyrus involved in sound-based representations and distributed conceptual representations. The dorsal pathway runs dorsoposteriorly toward a region in the posterior Sylvian fissure at the parietal–temporal border and connects to frontal regions, forming a network involved in auditory and motor representations of speech. These two streams interact with each other (Saur, 2024). A study examining the neuroanatomical basis of the dual streams using diffusion tensor imaging and fMRI found that the dorsal stream connecting the superior temporal lobe and premotor cortex through the arcuate and superior longitudinal fasciculi subserves speech repetition, whereas a ventral stream connecting the middle temporal lobe and ventrolateral prefrontal cortex through the extreme capsule supports higher-level language comprehension (Saur et al., 2008). To further expand on the dorsal pathway, posterior temporo-parietal cortex contributes to lexical, semantic, and phonological processing, and this information is passed to the inferior frontal gyrus via the arcuate fasciculus, where phonological information is converted into articulatory codes for motor output (Hickok et al., 2011).

However, language function is also supported by regions beyond the dorsal and ventral pathways. Core regions of the language network include lateral frontal and temporal areas, while the extended language network includes homotopic regions in the non-dominant hemisphere, midline cortical regions, the ventral temporal surface, and subcortical and cerebellar structures (Fedorenko et al., 2020). These observations indicate that language function relies on a widely distributed network architecture. The presentation of aphasia symptoms varies from patient to patient (Marinelli et al., 2017). Lesions affecting Broca's and Wernicke's areas do not always cause language dysfunction, and comprehension and speech impairments can arise from lesions affecting other brain regions (Blank et al., 2002; Price et al., 2010; Schäffler et al., 1993). For clinical purposes, aphasia is classified into non-fluent and fluent variants. In fluent aphasia, speech remains fluent but difficulties in comprehension, naming, and repetition are observed, whereas in non-fluent aphasia, speech production is effortful and reduced in phrase length and words per minute (Clough & Gordon, 2020).

However, both variants show anomia, a deficit in retrieving words for people, objects, and actions (Kristinsson et al., 2021). A recent study reported that naming difficulties in aphasia were associated with white-matter disconnection within the ventral and dorsal language pathways, while executive dysfunction was associated with white-matter disconnection within executive networks. Difficulties in reading, naming, and repetition were associated with lesions affecting the left inferior frontal gyrus, superior temporal gyrus, and Heschl's gyrus (Døli et al., 2021). A plausible interpretation is that speech impairments can arise from lesions affecting both white- and grey-matter regions.

Aphasia often involves varying degrees of damage in the language network and domain-general networks, subsequently affecting language domains such as phonology, semantics, and syntax, with impairments at different lexical levels (Wilson & Hula, 2019). A recent study examined structural and functional coupling in post-stroke aphasia and found decreases in whole-brain structural and functional coupling, and decoupling in the limbic network, default mode network, somatomotor network, and frontoparietal network, suggesting the involvement of multiple systems in language (Xu et al., 2026). Overall, this evidence indicates that post-stroke aphasia is associated with widespread, whole-brain disruption.

Executive dysfunctions often generate cascading effects on other functional domains (e.g., language, semantic cognition, and motor) (Tarantino et al., 2021). In aphasia patients, executive impairments are frequently observed, and a possible explanation for the co-occurrence of these deficits is that language and executive functions depend, to a certain extent, on overlapping neural substrates (Murray, 2012; Olsson et al., 2019). Language abilities in aphasia can be strongly linked with linguistic and non-linguistic executive control (Obermeyer et al., 2019; Olsson et al., 2019; Jefferies & Lambon Ralph, 2006). Several studies have identified executive control problems in aphasia, manifested as difficulties in inhibition, working memory, or cognitive flexibility (Jefferies et al., 2008; Schumacher et al., 2019; Vallila-Rohter & Kiran, 2012). All the evidence above implies a tight coupling between the language and executive control systems (Meier et al., 2022).

1.2.3. Executive dysfunction and frontoparietal control systems

Executive impairments are classically associated with lesions to the frontal lobes (Funahashi & Andreau, 2013). The prefrontal cortex supports a broad set of executive functions, including planning, organising, problem solving, multitasking, cognitive control, inhibition, switching, and monitoring (Veldsman et al., 2020). These functions are driven by working-memory mechanisms, in which attention and memory are controlled and coordinated by a central executive system (Baddeley & Hitch, 1974). Several studies show that damage to the dorsolateral prefrontal cortex leads to deficits in working memory, attention, and executive control (Badre et al., 2009; Godbout et al., 2005; Thompson-Schill et al., 2002; Voytek et al., 2010). These impairments frequently co-occur because they rely on a common frontoparietal network (Marek & Dosenbach, 2018). The frontoparietal

network, formed by the dorsolateral prefrontal cortex and posterior parietal cortex (Seeley et al., 2007), acts as a flexible hub for goal-directed behaviour (Cole et al., 2013). The frontoparietal network (FPN) and salience network (SN) typically operate together during cognitively demanding tasks (Chen et al., 2013; Vanhaudenhuyse et al., 2011). Both networks show task-dependent anticorrelation with the default-mode network (DMN), which supports internally oriented processes. The SN plays a critical role in initiating the transition from DMN-dominated states to FPN engagement for external events (Menon, 2011; Braunlich et al., 2014). Because these networks work in tandem, lesions affecting the prefrontal cortex can disrupt the coordinated functioning of the SN and FPN.

In addition, working memory and spatial attention are supported by partially overlapping brain networks (intraparietal sulcus, ventral precentral sulcus, supplementary motor area, and right insula), indicating that these domains share common cognitive mechanisms involved in the dynamic allocation of attentional resources (Labar et al., 1999). This complex network architecture provides a mechanistic explanation for the co-occurrence of attention, working memory, and executive impairments commonly observed after stroke. Notably, executive dysfunction is not restricted to prefrontal lesions. Damage to the mediodorsal thalamus or basal ganglia can also elicit attention and executive deficits (Van Der Werf et al., 2003; Obayashi, 2021; Ye et al., 2022; Zuo et al., 2023; Wolff & Halassa, 2024). The prefrontal cortex has strong reciprocal connections with the mediodorsal thalamus (Wolff & Halassa, 2024), and it also participates in prefrontal–basal ganglia–thalamus circuits that support sensory gating and the selection of relevant inputs over distractors. This circuitry enhances sensory discrimination and supports goal-directed behaviour through noise suppression (Nakajima et al., 2019; Wimmer et al., 2015). Together, these findings show that executive dysfunction arises from disruption of distributed brain networks rather than damage to a single cortical structure.

1.2.4. Semantic aphasia and the semantic control network

Semantic aphasia provides another clear example of how control impairments lead to difficulties with language and semantic tasks after stroke. Patients with semantic aphasia have difficulty retrieving conceptual information in a flexible, adaptable, and context-specific manner, a deficit referred to as impaired semantic control (Jefferies and Lambon Ralph, 2006). Head (1926) used the term semantic aphasia to describe two way difficulties in comprehension and naming in patients injured in war. Later, Jefferies and Lambon Ralph (2006) expanded the definition to describe patients who show deregulated semantic cognition while preserving semantic knowledge, resulting in difficulty accessing semantic control following left hemisphere stroke. These problems arise as difficulty in flexibly retrieving concepts appropriate for a given task or context. These patients show varying levels of performance across tasks, which does not depend on the items themselves but instead on the level of control required (Jefferies and Lambon Ralph, 2006). Diverse characteristics have been noted in these

patients. They may find it difficult to inhibit highly relevant but inappropriate information for the task (Hallam et al., 2016), to choose among competing items when a target and highly related distractors are presented (Saygin et al., 2003), and to sustain focus on the goal of a task, particularly when this goal changes during the task (Thompson et al., 2015). Semantic control difficulties are observed across modalities, including verbal and non-verbal tasks such as picture, sound, and action understanding. These semantic retrieval difficulties are multimodal in nature, affecting both language and non-verbal behaviour (Thompson and Jefferies, 2013). However, the semantic knowledge store in the anterior temporal lobes is largely spared in these patients (Jefferies, 2013).

Semantic aphasia typically results from stroke affecting the left inferior frontal or temporoparietal regions (Jefferies and Lambon Ralph, 2006). Semantic cognition relies on interactions between the anterior temporal cortex, which supports conceptual representation, and two networks occupying adjacent cortical regions that guide controlled semantic retrieval (Wang et al., 2024): the semantic control network and the multiple demand network. The multiple demand network, including bilateral inferior frontal sulcus and intraparietal cortex, responds to domain general executive demands (Duncan, 2010; Fedorenko et al., 2013). The semantic control network, which partially overlaps with both the multiple demand network and the default mode network, includes the left inferior frontal gyrus, posterior temporal cortex and dorsomedial prefrontal cortex, and supports flexible, context-dependent semantic retrieval (Jackson, 2021; Noonan et al., 2013). Since people with semantic aphasia typically have damage affecting regions at the intersection of the multiple demand network and the semantic control network, they often present with both semantic and non-semantic control deficits. However, these patterns of impairment are associated with different patterns of disconnection: between left inferior frontal gyrus and posterior temporal areas for semantic control, and between left and right prefrontal regions for domain general aspects of executive control (Souter et al., 2022). In summary, semantic aphasia disrupts the coordinated engagement of the semantic control network with multiple demand and default mode network regions, leading to impaired semantic control and multimodal semantic deficits (Hallam et al., 2018; Hallam et al., 2016).

1.2.5. Neglect as a large-scale attention network disorder

Neglect is another example of stroke-induced brain network disruption (Bartolomeo et al., 2007) that results in various forms of spatial impairment and affects multiple cognitive domains (Zebhauser et al., 2019). Neglect refers to the inability to perceive, respond to, or direct attention toward meaningful stimuli presented in the space opposite to the lesion site (Li & Malhotra, 2015). It is a highly heterogeneous syndrome that can manifest as sensory, motor, or representational neglect, occurring within egocentric (body-centred) or allocentric (object-centred) reference frames (Zebhauser et al., 2019). Although neglect most commonly follows right hemisphere lesions, particularly in the right posterior parietal cortex, damage to the left hemisphere, thalamus, basal ganglia (Sperber et al., 2025), and cerebellum can also produce neglect (Moore et al., 2021). Visuospatial neglect is the most

frequently observed subtype, reflecting impaired allocation of attention toward visual stimuli in contralesional space (Chechlacz et al., 2012; Moore et al., 2021). This form of neglect strongly influences motor recovery, mobility, balance, and postural control (Embrechts et al., 2021), as well as language-related behaviours such as reading and writing (Gajardo-Vidal et al., 2018).

Just as the anterior temporal lobe functions as a semantic hub that integrates information from various sensory modalities to form coherent conceptual representations, the posterior parietal cortex integrates multimodal input to support spatial representations and spatial cognition (Cohen & Andersen, 2004; Husain & Nachev, 2007). It is functionally connected with the frontal eye fields—regions in the prefrontal cortex involved in attention and eye movements toward external targets (Zhang et al., 2022). Spatial cognition and attention are driven by the frontoparietal network, including the frontal eye fields and the posterior parietal cortex for spatial attention, and by the right-lateralised ventral frontoparietal network, which mediates reactions to unexpected events or stimuli through spatial control mechanisms (Corbetta & Shulman, 2011). Disruption of these frontoparietal–cingulate networks explains why neglect is multimodal (Mesulam, 2002) and why it can arise from lesions both within and beyond the parietal cortex.

1.2.6. Sensorimotor disconnection and motor–cognitive coupling

Sensorimotor impairments experienced after stroke are a classic example of neural disconnection. Stroke can affect movement control of the face, arm, and leg on the contralateral side of the body (Einstad et al., 2021) and frequently causes somatosensory disturbances in light touch, pain, and proprioception, which are closely linked with motor deficits (Kessner et al., 2019; Semrau et al., 2015). These impairments reflect the fact that controlled movement depends on coordinated interactions between sensory and motor systems, and this sensorimotor integration occurs across multiple levels of the nervous system, including the thalamus, basal ganglia, cerebellum, and several cortical regions (Asan et al., 2022). This also means that the primary motor cortex is not the sole structure governing motor control. Motor behaviour relies on somatosensory cortices and the sensory thalamus for processing somatosensory input, as well as secondary motor regions such as the supplementary motor area and premotor cortex, which integrate sensory information to guide movement (Nudo et al., 1996). Lesions affecting pathways between these structures, or disconnections involving non-sensorimotor regions, have been consistently linked to motor impairments (Esser et al., 2025).

Motor impairments after stroke are also associated with deficits in executive, attentional, and language functions, highlighting the interdependence between motor and cognitive systems (Schwarz et al., 2026). Motor and language functions share overlapping neural networks, with pathways centred around Broca's area playing a key role in both movement and language fluency (Saber-Moghadam et al., 2024). Neuroimaging studies indicate that motor-related regions are implicated in action-related

language comprehension, such that sensorimotor systems engaged during real-world actions may also become active when processing language that describes those actions (e.g., “throw a ball”; Desai et al., 2009; Ahrens et al., 2022). Motor learning requires controlled cognition to adapt movements to changing task demands and environmental conditions, involving sensory integration, interpretation, response selection (executive function), sustained attention (Wulf et al., 2001), and memory (Rajda et al., 2025). Evidence also links the default mode network (DMN) with motor learning in both stroke and neurotypical populations (Dahms et al., 2024; Rezaei et al., 2025), further demonstrating that motor behaviour engages distributed neural systems beyond classical motor pathways. Taken together, this evidence points to the broader conclusion that stroke induces whole-brain disruption, with effects extending far beyond the focal lesion to influence motor, sensory, cognitive, and language domains. This pattern is thought to reflect the distributed and interconnected nature of the neural systems that support behaviour. Stroke interrupts this network architecture, producing multiple co-occurring impairments that cannot be explained by the lesion site alone. Building on this, the next section will examine post-stroke functional reorganisation and consider how these network-level changes shape behavioural outcomes.

1.3. Reorganisation after stroke and its role in behaviour

Although stroke initially disrupts large-scale brain networks, these disturbances are not confined to the anatomical boundaries of the lesion. Surviving regions and networks undergo structural and functional reorganisation that can either support recovery or contribute to persistent impairments. This section examines evidence for post-stroke reorganisation and considers how dynamic changes in network interactions influence behavioural outcomes over time.

Spontaneous reorganisation refers to the brain’s innate ability to adapt and improve cognitive and emotional functions affected by stroke (Fang et al., 2025). These changes emerge over weeks to months, particularly in regions neighbouring the infarct and in networks connected to it (Regenhardt et al., 2020). These changes are interrelated and occur at both the structural levels, which include molecular, cellular and tissue processes, and the functional levels, which include excitability, cortical maps and networks (Pascual-Leone et al., 2005; Cui et al., 2023). Functionally, spontaneous reorganisation involves processes such as synaptogenesis and is driven by surviving neural networks attempting to compensate for functions lost due to tissue damage, as described by Campos and colleagues in 2023. Recent studies show that stroke-induced network disruptions can be partially offset through the formation of new connectivity patterns (Fang et al., 2025; Latifi and Carmichael, 2024; Olafson et al., 2021). This rewiring process is conceptually aligned with the remapping hypothesis, which originated from the theory of vicariation, proposed in the late nineteenth century, stating that after focal injury a surviving part of the brain reorganises and subsumes the lost functions

of the damaged tissue (Finger, 2009). With the application of modern neuroimaging techniques, this theory has been expanded to the idea that spared neural tissue in adjacent areas, or in regions functionally related to the lesion, may change its activity to take on the role of the damaged tissue (Murphy & Corbett, 2009), and several patterns of reorganisation have been observed (Saur et al., 2006). Patterns of reorganisation following stroke have been associated with both recovery and persistent impairments (Campos et al., 2023). Surviving neurons reorganise their connectivity patterns by either supporting partial restoration or providing compensatory substitution for lost functions, although these mechanisms are interrelated (Jones & Adkins, 2015). Peri-infarct regions are strongly engaged in remapping because the neurons and circuits within them share similar functional properties or long-range connectivity with the lesioned core (Campos et al., 2023). Examples of peri-infarct regions involved in rewiring have been observed in language and motor recovery. In middle cerebral artery infarcts, primary motor cortex activation decreases, while activity in premotor or parietal regions increases depending on infarct location and size (Fridman et al., 2004). Increased activation has been noted in premotor regions such as the dorsal premotor cortex, ventral premotor cortex, and the supplementary motor area (Dimyan & Cohen, 2011). These are neighbouring regions of the primary motor cortex and assume previously subserved functions, resulting in adaptive motor change through parallel descending tracts (Falaschi et al., 2025; Pineiro et al., 2001).

In relation to language recovery, although perilesional tissue and homologue language regions have been shown to upregulate the undamaged language network, left-hemispheric infarcts, particularly those affecting language show another pattern of functional reorganisation (Crinion & Price, 2005; Leff et al., 2002; Saur et al., 2006; Stockert et al., 2020). A recent longitudinal study on post-stroke language recovery noted distinct patterns of functional reorganisation, particularly in regions within and across the language and multiple-demand networks (Jiang et al., 2025). These patterns were observed in left-hemispheric infarcts with lesions either in frontal or temporoparietal regions (Jiang et al., 2025). For large lesions, right-hemisphere homologues and bilateral domain-general areas supported language functions. These findings imply that remapping of perilesional areas is one pattern of reorganisation but not a generalisable phenomenon across all stroke types or levels of impairment. There is evidence against the view that peri-infarct remapping alone drives recovery. Long-range functional connectivity involved in remodelling and driving shifts in large-scale topology at the network level jointly contributes to cognitive recovery (Bonkhoff et al., 2021; Corbetta et al., 2015).

Right-hemispheric infarct patients within three months of stroke showed reduced intrahemispheric functional connectivity between anterior and posterior regions in the right hemisphere, and this reduction was associated with working-memory deficits (Marti et al., 2025). In contrast, increased interhemispheric functional connectivity between the right middle and inferior frontal gyri and contralateral parietal regions was associated with better performance on

working-memory tasks (Marti et al., 2025). This study is an example of compensatory engagement of the intact hemisphere. The engagement of contralesional activation is mediated through callosal projections, which drive functional rebuilding (Carter et al., 2010). Functional reorganisation linked with visuospatial neglect and upper-limb motor recovery in right-hemispheric stroke shows a contrasting pattern within four weeks of stroke. Carter et al. (2010) noted an opposite trend, where interhemispheric functional connectivity disruption between homologues of the dorsal attention network was associated with visuospatial neglect. A similar pattern was noted in the motor system, where loss of interhemispheric functional connectivity in the somatomotor network correlated with upper-extremity impairment. The default mode network (DMN) shows another pattern of functional reorganisation in different phases of stroke. In right-hemispheric infarcts, reduced connectivity in DMN regions such as the posterior cingulate cortex, precuneus, medial frontal gyrus, and inferior parietal lobes has been observed one month after stroke (Park et al., 2014). DMN connectivity in these brain areas was almost restored to normal levels three months after stroke. Another striking observation was that dorsolateral prefrontal cortex connectivity with the DMN in the contralesional hemisphere was strongly associated with cognitive function recovery (Park et al., 2014). This suggests long-range compensatory functional reorganisation.

All these findings indicate that functional reorganisation after stroke is a dynamic process. The changes are associated with cognitive processes that can either support or impair recovery. Post-stroke recovery follows a non-linear trajectory, with patients regaining some level of function over time and often continuing to improve during the chronic phase. This highlights that brain reorganisation can occur over long periods, have long-lasting effects, and can contribute to both recovery and persistent impairments. The studies cited above used heterogeneous designs, patient samples, lesion loads, deficits, and hypotheses, and they focused on reorganisation within specific networks rather than at the whole-brain level. These findings stress the importance of examining whole-brain level functional reorganisation, as this approach may reveal how surviving transmodal and unimodal regions, particularly those involved in long range connectivity, contribute to recovery and impairments in addition to homologue and perilesional perspectives.

The examples listed above focused on functional reorganisation, but there is also evidence supporting structural changes as a form of post-stroke brain reorganisation linked with behavioural outcomes. Longitudinal grey-matter changes have been observed in left-hemispheric infarcts one year after stroke. Hope et al. (2017) reported an interesting pattern in which hypertrophy of the right anterior temporal lobe was associated with better language skills, whereas hypertrophy of the right precentral gyrus correlated with poorer language outcomes. Several studies have also reported white-matter plasticity following therapy in chronic post-stroke aphasia, particularly showing that bilateral tracts are associated with language recovery (Blom-Smink et al., 2020; Braun et al., 2022; Keser et al., 2020). Another study on post-stroke motor recovery showed that severe corticospinal

tract injury was positively associated with fractional anisotropy in callosal fibres interconnecting the primary motor cortices and the superior longitudinal fasciculus, and with improvements in upper-limb function (Domin et al., 2023).

Several lesion-mapping approaches have been developed to characterise how stroke lesions influence behaviour by relating post-stroke outcomes to the structural and functional consequences of brain damage. No single technique serves as a gold standard, and each has distinct strengths and limitations. Understanding these differences is essential for improving existing methods or combining complementary approaches to produce more clinically useful and cost-effective prediction tools. The evidence reviewed above shows that the post-stroke brain undergoes continuous structural and functional change, and these dynamic processes strongly shape behavioural outcomes. As stroke incidence rises with population ageing (Grefkes et al., 2020) and cognitive dysfunction often persists for years (Tarantino et al., 2021), it becomes increasingly important to understand how lesions alter brain structure and function, and how spared regions reorganise to support recovery. Such knowledge can support patient stratification for rehabilitation, guide therapy intensity, enable early identification of individuals at risk of secondary complications such as dementia, and facilitate the formation of well-defined clinical-trial cohorts.

Taken together, these studies show that functional reorganisation after stroke is highly heterogeneous, varying with lesion location, stroke severity, time post-stroke, behavioural domain, and the imaging approach used. Some studies emphasise perilesional remapping, others highlight distributed network-level changes or contralesional recruitment. These inconsistencies suggest that recovery cannot be explained by a single mechanism. Instead, whole-brain approaches that capture large-scale organisational change may be necessary to characterise post-stroke functional reorganisation.

1.4. Overview of lesion mapping methods

Stroke-induced behavioural problems are mapped using different features of the lesion—generally referred to as symptom-mapping techniques. These mapping techniques can be broadly divided into direct and indirect methods. Direct methods use features derived from the patient's imaging data to map their behavioural profiles. Within direct approaches, traditional lesion–symptom mapping has played a pivotal role in generating evidence for the dynamic organisation of the brain supporting various neurological functions (Bates et al., 2003, Thielen et al., 2025). This method focuses on the statistical association between the anatomy of the lesion location and behavioural impairments, and the role of lesion location in post-stroke dysfunction is well established (Bates et al., 2003). Connectome-based lesion–symptom mapping is another direct approach that examines the statistical

association between stroke-related connectome injury and behavioural problems (Ding et al., 2024). This approach is used to examine the impact of lesions on structural and functional connectivity. Indirect methods estimate lesion impact on the connectome by overlaying lesion masks from structural brain images onto a normative white matter atlas or functional connectivity template (Ding et al., 2024; Salvalaggio et al., 2020). These approaches infer the likely disconnection pattern without requiring patient specific connectivity data (Salvalaggio et al., 2020). The following sections discuss each method in detail.

1.4.1 Lesion symptom mapping

Traditional univariate voxel based lesion symptom mapping is a voxel wise statistical method for identifying brain regions that are statistically associated with behavioural impairments (Bates et al., 2003). The univariate approach has two fundamental problems. First, it does not account for the spatial continuity of lesioned voxels that arise from the same underlying pathology. For example, a lesion in the middle temporal gyrus often extends into the neighbouring superior temporal gyrus (Herbet et al., 2015; Mah et al., 2014). Second, it does not consider stroke-induced disconnection of white matter tracts (Corbetta et al., 2015). Studies examining lesions affecting both white matter tracts and grey matter show that these structures are interconnected and jointly contribute to behavioural deficits. In contrast, multivariate voxel based lesion symptom mapping examines all lesioned voxels simultaneously and identifies inter voxel correlations—voxels that tend to be affected together because of lesion distribution across the brain—associated with behavioural deficits. Various machine learning approaches have been explored (Khalilian et al., 2024), including support vector machines, support vector regression, random forests, Gaussian process regression, and Bayesian networks (Wilson & Hula, 2019). Support vector regression (Schumacher et al., 2019) and sparse canonical correlation analysis (Pustina et al., 2018) have shown greater efficiency in linking lesioned brain structures with post-stroke functional impairments. These approaches provide a unidimensional topological view by identifying particular grey matter regions linked with behavioural impairments, but they do not show how a lesion affects structural connections between several brain regions and white matter tracts, which in turn impacts behaviour (Thielen et al., 2025). Similarly, they do not capture the impact of the lesion on functional network connections. In addition to these direct effects on structural and functional connections, they also fail to account for lesion related effects on undamaged parts of brain networks (Moore et al., 2024). Another limitation is that structural and functional reorganisation associated with behavioural outcomes is not captured.

1.4.2. Direct structural disconnectome-based symptom mapping

Stroke infarcts in white-matter tracts disrupt the structural connectome, affecting the networks that assist and regulate normal brain function (Schlemm et al., 2021). Post-stroke cortical deafferentation is usually extensive and not captured on conventional structural MRI, such as T1- or T2-weighted

images (Bonilha et al., 2014). White-matter tract integrity is studied using diffusion-weighted imaging, and these imaging data are used to map white-matter injury in relation to behaviour using a method called structural disconnectome-based mapping. This method was developed as a complement to voxel-based lesion–symptom mapping, showing that disruptions of structural connections are also involved in post-stroke symptoms (den Ouden et al., 2019; Ding et al., 2024). A recent study examined the association between changes in white-matter tracts and language performance in chronic aphasia patients (Zhang et al., 2025). The authors focused on how regions less affected by stroke, particularly white-matter pathways below the tentorium, can still contribute to language network disorder (Zhang et al., 2025). Fractional anisotropy measures the directionality of white-matter microstructure (e.g., myelin, microtubules, axons), reflecting tract integrity (Freire et al., 2024). Fractional anisotropy values of the middle cerebellar peduncle, left inferior cerebellar peduncle, and left corticospinal tract were positively associated with language skills measured using the Western Aphasia Battery–Revised (Zhang et al., 2025). This study provided new insights, showing that network dysfunction is not restricted to the cortex but also extends to cerebellar pathways. A longitudinal study showed associations between DMN white-matter tracts such as the anterior thalamic radiation, splenium, genu of the corpus callosum, cingulum, and the thalamus–precuneus tract with post-stroke cognitive outcomes after three months (Fruhwirth et al., 2024).

Although disconnectome-based mapping clarifies how white-matter pathway disruptions extend beyond focal grey-matter injury, the method is constrained by the technical limitations of diffusion imaging and by practical acquisition constraints. Diffusion tensor imaging provides only a simplified representation of intravoxel fibre architecture and is known to be less reliable in regions containing crossing fibres, which may influence structural disconnection maps (Koch et al., 2016). For example, the arcuate fasciculus and inferior fronto-occipital fasciculus (IFOF) are crossing fibres, and these long association fibres cross numerous pathways along their entire length (Schevenels et al., 2022). The IFOF connects several regions of the occipital lobe, inferior temporal area, and superior parietal lobule to the frontal lobe (Herbet et al., 2018). This tract is implicated in orthographic and semantic processing (Schevenels et al., 2022). Although studying the arcuate fasciculus and IFOF in stroke is beneficial for diagnosis, prediction of long-term prognosis, and understanding the recovery mechanism of aphasia, DTI can only estimate one fibre direction per voxel in regions containing the arcuate fasciculus and IFOF (Jones, 2009; Jang, 2013).

Further, the validity of axonal pathways reconstructed through lesioned tissue remains uncertain, because stroke pathology can alter the diffusion-weighted imaging signal (Sperber et al., 2022). Moreover, precise localisation of a lesion along a damaged white-matter pathway is often not necessary to explain the clinical presentation after stroke. For instance, lesions occurring anywhere along the corticospinal tract (periventricular white matter, internal capsule, midbrain, pons, medulla oblongata, or spinal cord) can produce hemiparesis (Feng et al., 2015). These considerations suggest

that the usefulness of structural disconnectome mapping depends on the specific clinical or research context. In practice, the main limitations of this method are its cost and the fact that the required data are not routinely acquired in clinical settings. To overcome these constraints, researchers have developed an indirect structural-disconnectome-based symptom-mapping approach.

1.4.3. Indirect structural disconnectome-based symptom mapping

Indirect structural disconnectome-based symptom mapping estimates white-matter–related behavioural dysfunction without relying on diffusion imaging from stroke patients (Salvalaggio et al., 2020). This mapping technique derives structural disconnection for a stroke patient by integrating the spatial lesion map with anatomical information from white-matter data of healthy participants (Salvalaggio et al., 2020; Sperber et al., 2022). The patient's lesion map is embedded into normative structural connectome data acquired from healthy, age-matched participants to model the lesion effects on white-matter tracts (Sperber et al., 2022) (Figure 1.1). The mapping approach examines the association between the estimated structural disconnection and behavioural measures (Salvalaggio et al., 2020; Sperber et al., 2022). This method commonly uses probabilistic fibre tract atlases, referred to as the tract-wise or hodological approach, where disconnection estimation is derived from canonical white-matter fibre tracts (e.g., the superior longitudinal fasciculus and corticospinal tract) (Rudrauf et al., 2008; Thiebaut De Schotten et al., 2014). A recent study found that a strategic structural disconnection pattern focused on the left prefrontal cortex, thalamus, and basal ganglia was implicated in global post-stroke cognitive impairment using indirect structural disconnection analysis (Pan et al., 2023). Another study found that structural disconnections involving the right insula, right frontotemporal regions, and right putamen were associated with general cognitive deficits (Kolskår et al., 2022). Although these findings align with the brain-behaviour literature, they provide a unidimensional perspective and fail to capture how spared white-matter tracts are involved in brain reorganisation, given that a stroke brain's rewiring continues in the chronic phase. Another issue is that this method heavily depends on lesion–tract overlap and is incapable of quantifying participants with zero overlap between lesion maps and tract masks (Domin et al., 2025).

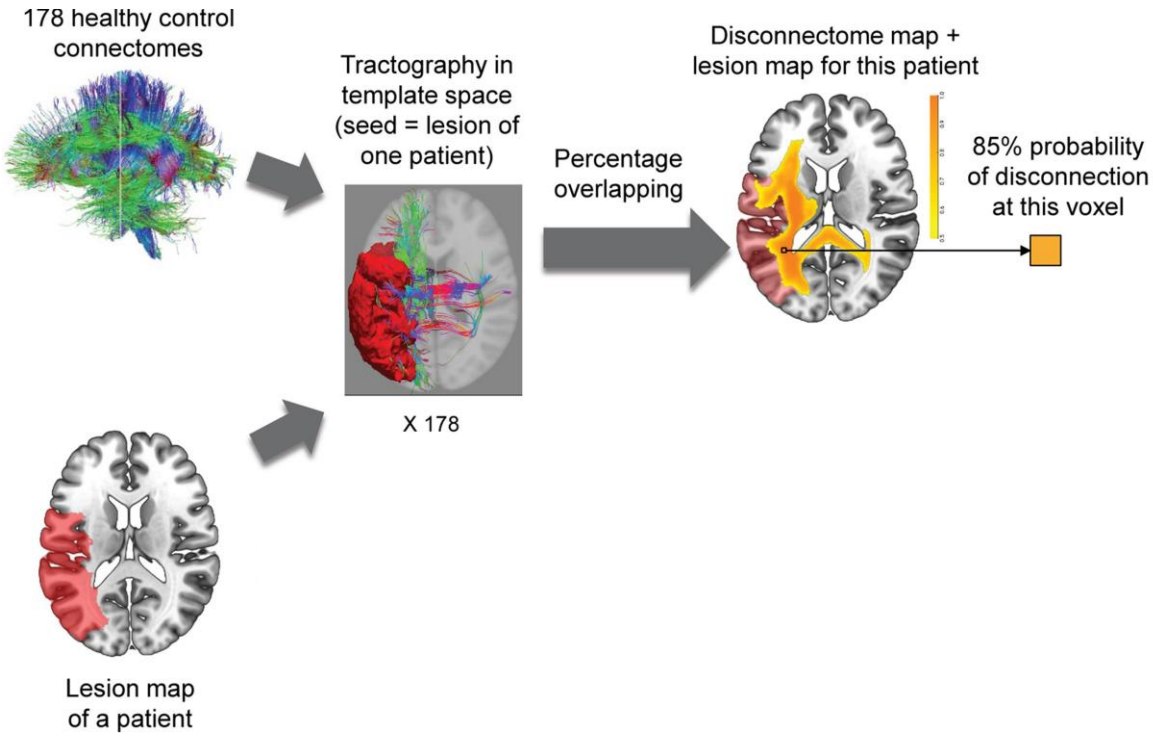

Figure 1.1. Workflow for indirect structural disconnectome mapping. Image source: Akinina et al. (2022), structural disconnection associated with language outcomes in chronic stroke. The figure illustrates the procedure for generating an indirect structural disconnectome map. A patient's lesion mask is used as a seed region for tractography within a normative dataset of 178 healthy control connectomes. The degree of overlap across tractography results is then combined with the lesion mask to produce a voxelwise probabilistic map, where values represent the percentage likelihood of white-matter disconnection at each location.

1.4.4. Direct functional disconnection-based symptom mapping

Functional disconnection-based symptom mapping examines how the strength of functional connectivity between brain regions relates to behavioural outcomes (Tsiakiri et al., 2024). Functional connectivity refers to the temporal coordination of activity between spatially distinct regions during tasks or at rest, as measured by functional imaging (Friston, 2011). Resting-state functional magnetic resonance imaging (rs-fMRI)—a rapidly evolving technique—uses functional connectivity to estimate intrinsic spatial patterns of synchronised neural activity in spontaneous, low-frequency blood-oxygen-level-dependent (BOLD) signals below 0.1 Hz (Wang et al., 2015). In situations where no direct white-matter tract links two regions, strong BOLD-signal correlations suggest that functional

coordination can rely on indirect anatomical pathways rather than only on direct structural connections (Koch et al., 2002).

Rs-fMRI studies have identified distributed sets of brain regions that show correlated activity in the absence of explicit tasks or stimuli, termed resting-state networks (RSNs). These networks comprise functionally connected brain regions that maintain relatively high, ongoing connectivity at rest despite being anatomically separated (van den Heuvel & Hulshoff Pol, 2010). Resting-state networks show substantial overlap with networks identified in task-based fMRI, and their instantaneous activity has been linked to behaviour (Carter et al., 2010). Mapping resting-state networks to functional deficits offers several advantages over task-based fMRI, particularly for stroke patients. Resting-state scans are less cognitively and physically demanding, reduce the risk of movement artefacts, require shorter acquisition times, and remain feasible even for patients with severe motor impairments (e.g., hemiplegia) who may be unable to perform the movements required in task-based paradigms. A recent systematic review identified reduced functional connectivity in key regions—including the medial prefrontal cortex, precuneus, inferior frontal gyrus, anterior and posterior cingulate cortices, and hippocampus—in association with post-stroke cognitive impairment (Sagues et al., 2025). This indicates that altered connectivity in transmodal regions contributes to cognitive deficits after stroke (Hallam et al., 2018). A longitudinal functional connectivity study observed an interesting pattern between the limbic and dorsal attention networks: connectivity between these two networks at the first scan reliably predicted motor outcomes at the second time point in patients with chronic subcortical infarcts (Li et al., 2022). This study highlighted the importance of functional coupling between the dorsal attention and limbic networks. Sections 1.2 and 1.3 considered how alterations in large-scale networks contribute to behavioural impairments and recovery after stroke. The following section shifts from these neurobiological findings to the methods used to characterise functional connectivity from resting-state fMRI data.

Resting state fMRI captures functional coordination between spatially distant regions through the temporal synchrony of BOLD signals (Biswal et al., 1995). It measures intrinsic interactions between grey matter regions without requiring an explicit task (Fox & Raichle, 2007). Resting state approaches have been widely used to characterise functional connectivity after stroke, providing insight into how focal lesions alter large-scale network organisation (Aziz et al., 2025; Christidi et al., 2024). A major advantage over task based paradigms is that resting state scanning does not impose task demands or require overt responses, making it suitable for stroke populations with heterogeneous cognitive, linguistic, or motor impairments (Fan et al., 2015). In contrast, task based fMRI requires all patients to complete the same language paradigm, which is often not feasible for individuals with severe language or motor deficits. Resting state paradigms are therefore particularly valuable in clinical aphasia research, including the acute stage when tools for mapping deficits and estimating prognosis are needed. They allow the integrity of functional networks supporting different cognitive

domains to be assessed, providing insight into how stroke disrupts network balance and how these disruptions relate to cognitive, language, and motor impairments. Tracking functional connectivity across different stages of stroke also helps characterise how the brain reorganises using tissue spared from the lesion, and to what extent spontaneous neuroplastic changes contribute to recovery (Aziz et al., 2025; Fan et al., 2015).

However, resting-state fMRI also has important limitations in the context of stroke. Stroke can alter neurovascular coupling and haemodynamic response properties, although these effects are most pronounced in the acute and subacute stages and tend to stabilise in chronic stroke (Bonakdarpour et al., 2007; Braban et al., 2023; Promjunyakul et al., 2013). Lesions can introduce signal dropout, distort spatial normalisation, and increase head-motion artefacts, all of which can bias functional connectivity estimates (Siegel et al., 2017). There are established preprocessing and modelling strategies to mitigate many of these limitations, including approaches that estimate or correct for vascular confounds, but developing or evaluating such methods is beyond the scope of this thesis.

1.4.5. Indirect functional disconnectome-based symptom mapping

The indirect method used to understand functional disconnection–behaviour relationships is commonly referred to as lesion network mapping (Bowren et al., 2022). Functional disruption is estimated without requiring resting-state data from stroke patients, but using clinically available lesion data (Salvalaggio et al., 2020). In this method, lesion effects on networks are estimated by mapping each lesion onto high-quality functional connectome data from age-matched controls (Salvalaggio et al., 2020). A proxy association between inferred network disruption and behavioural dysfunction is then examined. This method has lower predictive value compared with indirect structural disconnectome-based symptom mapping and traditional lesion–symptom mapping (Salvalaggio et al., 2020). It may not be suitable for large lesions when performing seed-based connectivity analyses, as the seed region may consist of several distributed areas (Boes, 2021). Averaging the time series of those regions within the lesion area can provide misleading estimates of network disruption. This method estimates direct disconnection between the seed region and networks but does not account for indirect functional interactions linked with the lesion (i.e., indirect functional connections through polysynaptic pathways) (Corbetta et al., 2018).

A recent study reported opposite results to those of Salvalaggio et al. (2020). Bowren et al. (2022) found that structural and functional network mapping predicted behavioural variance better than lesion–symptom mapping, and that indirect functional lesion network mapping had the strongest predictive ability for language deficits compared with other methods. However, the patients in this study were assessed 3–12 months after stroke, a period characterised by substantial functional reorganisation (Cui et al., 2023). Because lesion network mapping relies on normative connectivity

rather than patient-specific post-stroke connectivity, it does not capture these dynamic changes. This mismatch may contribute to the method's predictive performance in the subacute–chronic phase. Therefore, lesion network mapping should be interpreted in a complementary and context-dependent manner.

1.4.6. Functional connectivity analyses

The conventional functional connectivity analyses used for resting-state fMRI data are broadly divided into hypothesis-dependent and data-driven methods. Seed-based correlation approaches are hypothesis-dependent, whereas independent component analysis (ICA), principal component analysis (PCA), and clustering methods are data-driven (van den Heuvel & Hulshoff Pol, 2010). Seed-based methods, also known as region-of-interest (ROI)-based functional connectivity, identify regions whose BOLD-signal time series correlate with a predefined seed region. A small cluster of voxels is selected as the seed, and their averaged time series is extracted. This seed time series is then correlated with the time series of every other voxel in the brain, producing a spatial map of correlation strengths (Biswal et al., 1995). Seed regions can be defined using anatomical landmarks or functional results, such as peak clusters from statistical maps. This approach requires an a priori specification of the seed region based on a hypothesis. Functional connectivity estimates change when the seed changes, and this dependence on seed selection is a major limitation, as it introduces susceptibility to bias (Lv et al., 2018). In addition, seed-based analysis does not characterise intrinsically connected networks or their interactions; it only describes connectivity patterns of the chosen seed (Joel et al., 2011). As a result, it focuses on a narrow aspect of brain organisation rather than the whole-brain network structure.

In contrast to seed-based analysis, independent component analysis (ICA) examines the full four-dimensional fMRI dataset and identifies coherent patterns of activity without requiring predefined seed regions. ICA examines the full four-dimensional fMRI dataset to identify coherent patterns of activity without specifying seed regions. It models the observed BOLD signal as a linear mixture of spatially independent sources, including intrinsic neural fluctuations, head motion, physiological noise, and other artefactual processes. Each source contributes its own time course to the data, and ICA separates these components by maximising statistical independence (McKeown et al., 1998). The decomposition yields spatially independent components, each associated with a characteristic time course. Several algorithms have been developed for this purpose, most of which optimise spatial independence (Hyvärinen, 1999). Dacosta-Aguayo et al. (2014) used ICA to characterise intrinsic functional connectivity patterns following sub-acute ischaemic stroke and their relationship to cognitive recovery. They identified 18 components corresponding to the major resting-state networks. This model order provides a mid-level decomposition that captures canonical networks but not the finer subdivisions that emerge at higher model orders. The small sample size further reduces component stability and limits generalisability. ICA components can also be

challenging to interpret because they may contain mixtures of neural and non-neural signals, and their identification depends on algorithm choice, model order, and sample characteristics (Lu et al., 2017). These factors make network-level inference less straightforward, particularly in clinical populations, and limit the suitability of ICA for routine clinical applications, although it remains a valuable tool in research settings. Moreover, ICA identifies spatially independent networks but does not, on its own, characterise interactions between these networks. Examining between-network connectivity is important for understanding post-stroke reorganisation, so additional analyses are required to address these questions.

Another data-driven approach, principal component analysis (PCA), extends this decomposition framework by focusing on variance rather than statistical independence. PCA is a dimensionality reduction technique that reduces the dimensionality of resting-state fMRI data while preserving the dominant patterns of variance (Jolliffe & Cadima, 2016). When applied to voxel time series, PCA treats the fMRI dataset as a time-by-voxel matrix and decomposes it into a set of orthogonal temporal components and their associated spatial loadings. These components reflect the dominant temporal patterns shared across voxels, providing a compact, low-dimensional representation of the underlying structure in the data. The ordering and number of components are determined by the covariance structure of the time series, with the first components explaining the greatest proportion of variance (van De Ven et al., 2004). Because PCA transforms correlated voxel signals into uncorrelated directions of variation, it can reduce problems caused by collinearity in multivariate analyses. However, the orthogonality constraint is mathematical rather than biological, which limits the interpretability of PCA components and makes them less suitable for identifying meaningful network structure compared with ICA (Viviani et al., 2005). Taken together, these limitations highlight the need for approaches that characterise whole-brain organisation as continuous rather than as a set of discrete regions or networks. In addition, whole-brain voxelwise connectivity matrices contain an enormous number of pairwise relationships, making their organisation difficult to interpret. Functional connectivity gradients address these limitations by providing a low-dimensional representation of whole-brain connectivity that captures systematic patterns of cortical organisation, as discussed in Section 1.5.

1.5. Functional organisation from a gradient perspective

1.5.1. Functional connectivity gradients

Connectivity gradients decompose whole-cortex patterns of connectivity into a small number of dimensions that represent similarities in connectivity profiles between brain regions. Traditional lesion-mapping and network-based approaches typically characterise brain organisation in terms of discrete regions or networks. However, increasing evidence suggests that large-scale brain organisation is better described as a continuous hierarchy rather than a set of sharply bounded

modules. Connectivity gradient approaches capture this systematic organisation by representing brain regions along low-dimensional axes that reflect similarities in connectivity patterns. This framework therefore provides a complementary perspective on brain organisation and may be particularly useful for studying distributed network disruption following stroke.

The human brain has a unique and highly complex structural and functional organisation. Morphological transitions span from molecules to cells, through white-matter pathways, to large-scale structural networks (von Economo & Koskinas, 2007). Graded changes occur from the cellular to the macroscale level of network organisation (Bernhardt et al., 2022). This continuously changing feature, referred to as "gradients", is observed across multiple levels of brain organisation (Royer et al., 2024). Because of the spatial continuity of the cerebral cortex, adjacent regions that are structurally and anatomically coupled allow signals to propagate in a spatially organised manner (Betzel et al., 2026). The gradient concept is also evident in task-based activation and deactivation patterns, as well as in structural and functional connectivity (Margulies et al., 2016; Bernhardt et al., 2022). Functional connectivity gradients provide a low-dimensional representation of whole-brain connectivity patterns, reducing the complexity of voxelwise connectivity while preserving biologically meaningful relationships between regions (Margulies et al., 2016; Hong et al., 2020). They project functional connectivity patterns into a low-dimensional space, where different dimensions capture different functional relationships (Margulies et al., 2016). In other words, each axis explains a unique functional relationship, and regions with similar functional profiles are positioned next to each other (Huntenburg et al., 2018; Mckeown et al., 2020).

The principal gradient captures the systematic transition from unimodal to transmodal regions, whereas the second and third gradients capture the next most important differences in connectivity profiles across the cortex. Specifically, Gradient 2 reflects sensory-motor organisation, with visual regions occupying one end and motor regions the other, while Gradient 3 characterises variation within transmodal systems and has been interpreted as a control-to-DMN axis (Margulies et al., 2016) (Figure 1.2). Some gradients exhibit fractal repetition across cortical lobes, forming large-scale axes, while each region participates in multiple functional organisations (Margulies et al., 2016; Royer et al., 2024). For example, transmodal regions such as the posterior cingulate cortex and angular gyrus occupy high positions on both Gradient 1 (unimodal → transmodal hierarchy) and Gradient 3 (control → DMN axis), integrating sensory information while facilitating executive control and internally directed thought.

Connectivity gradients are derived from resting-state fMRI by constructing a functional connectivity matrix that reflects each region's connectivity profile with the rest of the brain (Margulies et al., 2016). Diffusion embedding is then applied to identify components that best describe similarity patterns across these profiles. Although conceptually similar to PCA, diffusion embedding does not

impose linearity and instead extracts nonlinear axes that explain the greatest variance in intrinsic connectivity (Katsumi et al., 2023). These axes are neurobiologically meaningful: recent work integrating transcriptional and connectivity gradients has shown that imputed cell type distributions recapitulate the hierarchical functional organisation of the cortex (Zhang et al., 2024). It is important to note, however, that gradients are not fixed entities. Their precise ordering and interpretation can vary depending on the sample, preprocessing pipeline, parcellation scheme, and embedding method. Studies may therefore extract sample specific gradients or, alternatively, rotate their gradient solution to maximise correspondence with canonical gradients derived from the large HCP dataset (Margulies et al., 2016), which improves interpretability and facilitates comparison across studies.

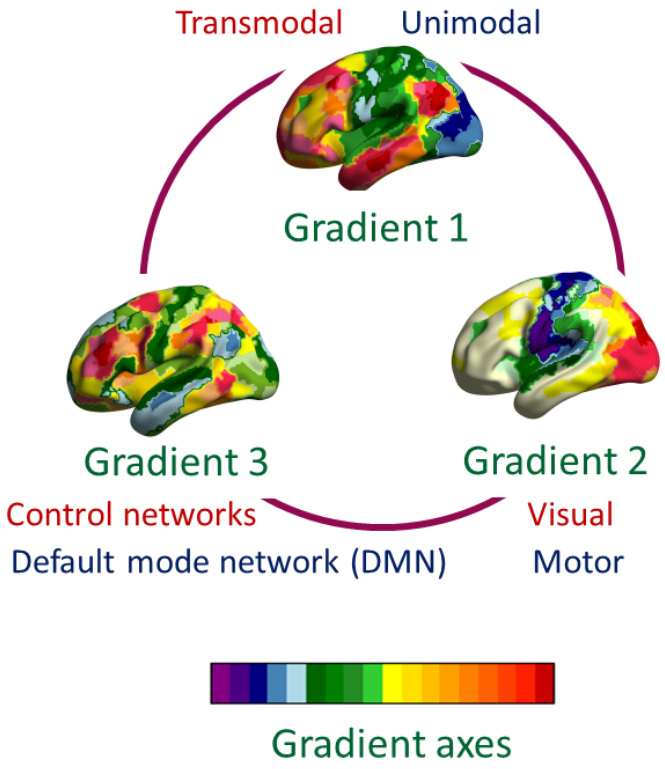

Figure 1.2. Functional connectivity gradients. Gradient 1 represents the transmodal–unimodal axis, Gradient 2 captures the visual–motor axis, and Gradient 3 reflects variation between control networks and the default mode network. Along all gradients, cool colours indicate the lower end of the axis and warm colours indicate the higher end.

1.5.2. Functional connectivity gradients and correlates of cognition

Connectivity gradients not only map the spatial functional transitions across the cortex but also provide insight into how cognitive functions emerge from coordinated interactions of distributed networks. Gradient 1 captures a key organisational principle of the cortex, spanning from unimodal regions associated with sensory-motor processing at one end to transmodal regions implicated in higher cognitive functions at the other (Margulies et al., 2016; Wang et al., 2025). This continuum—from local functional specialisation to global integration—provides a useful framework for understanding language processing, which spans sensory inputs and higher-level semantic representation. For example, auditory comprehension aligns with this axis: the auditory cortex handles basic sound processing near the unimodal end, while transmodal regions like the anterior temporal lobe contribute to word comprehension near the opposite end. This organisation is conceptually consistent with the ventral stream of the dual-stream model of speech and language processing (Hickok & Poeppel, 2007). Gradient 3 delineates a higher-order dimension relating the default mode network (DMN) to control networks (Wang et al., 2020; Shao et al., 2022). Speech production can be interpreted within this framework, where conceptual retrieval engages DMN regions and contextually appropriate articulation involves control networks. This gradient-based perspective offers a complementary large-scale description that aligns conceptually with interactions between the ventral (semantic) and dorsal (articulatory) streams in the dual-stream model (Hickok & Poeppel, 2007).

Connectivity gradients are not restricted to language processing but extend to a wide array of cognitive processes. Gao et al. (2022) identified that gradients' axes have a flexible property that supports semantic cognition based on task demands. They explored the gradient correlates of associative strength between two words. Strong associations between word pairs showed greater separation between unimodal and transmodal poles. This indicated that long-term-memory-driven cognition relies on wider informational separation from sensory-motor features. Weak associations showed reduced separation between unimodal and transmodal poles. This reflects that retrieving weakly related concepts requires greater reliance on intermediate, multimodal regions and closer interaction between sensory-motor features and control-based semantic processes. McKeown et al. (2020) explored how individual differences in macroscale cortical gradients are associated with ongoing internal thought patterns during rest. They observed that variation in the principal gradients predicted unique aspects of spontaneous cognition. Greater differentiation along Gradient 1 was associated with more detailed and internally oriented thought, anchored by the DMN at the transmodal end. Gradient 2 reflected sensory- and imagery-based visual content, and Gradient 3 captured the separation between spontaneous and goal-directed thinking. These findings indicate that connectivity gradients shape stable individual differences in ongoing thought. Another study investigated how individual differences in the principal connectivity gradient (the unimodal–transmodal axis) link to creative ability (Huo et al., 2022). In this study, the alternative uses task

probed divergent thinking as a measure of creativity. Individuals with greater unimodal–transmodal axis expansion showed higher creativity. They also found that higher creativity was associated with greater gradient values within the ventral attention network, reflecting a shift of VAN toward transmodal regions such as the DMN and FPN (Huo et al., 2022). The evidence above clearly shows how changes in gradient axes, which reflect segregation and global integration, are required for different aspects of cognition.

1.5.3. Atypical connectivity gradients

The multidimensional network perspectives offered by gradients make them a valuable tool for understanding how the brain's highly interconnected organisation is disrupted in stroke and other neurological disorders. A recent study reported functional disturbances in the visuomotor axis (G2) in stroke patients, relating these findings to difficulties in activities driven by unimodal regions (Koba et al., 2025). Another study noted greater suppression of the transmodal–unimodal axis in Alzheimer's disease than in amnestic mild cognitive impairment (He et al., 2023). In frontotemporal dementia, similar alterations in the transmodal–unimodal axis were observed, while Gradient 2 (visuomotor axis) exhibited widespread alterations affecting interactions among all networks (Bouzigues et al., 2024). Semantic and non-fluent variants of frontotemporal dementia showed specific disruptions in limbic and sensorimotor networks. Functional neurological disorder (FND) is a disabling condition that has recently gained increasing attention in both psychiatry and neurology (Westlin et al., 2025). Patients with FND experience a wide range of symptoms affecting motor, sensory, and cognitive functions, as well as seizure-like episodes. Emerging evidence suggests that FND is associated with disturbances across multiple brain networks (Weber et al., 2025). Using connectivity gradients, Bègue et al. (2025) examined network profiles in patients with FND and reported alterations across all three gradient dimensions. Specifically, sensorimotor regions exhibited connectivity patterns resembling association cortex in Gradient 1, while Gradient 2 showed reduced separation between motor and visual regions. Functional differentiation was also altered along Gradient 3, particularly between representational and modulatory regions.

Multiple sclerosis has received increased consensus as a brain network disorder, with network disturbances caused by neuroinflammatory and neurodegenerative processes involving the central nervous system. Similar to other brain network disorders like stroke, multiple sclerosis encompasses a broad range of clinical presentations, including visual, sensory, motor, and cognitive impairments (Filippi et al., 2018). Cognitive impairments experienced in multiple sclerosis include delays in information processing, deficits in attention, executive control, and episodic memory (Schoonheim et al., 2022). De Rosa et al. (2024) explored the changes in cortical hierarchy and their association with the symbol digit modality test, used to measure information processing speed. The gradients extracted in this study were different from the gradient dimensions observed by Margulies et al. (2016) and described above. They are visuo-motor and transmodal-unimodal axes. De Rosa et al. (2024)

observed attenuation of the transmodal-unimodal axis, and higher gradient values within limbic and default mode networks were associated with higher symbol digit modality test scores. They also reported that a lower position of the ventral attention network on the transmodal-unimodal axis was associated with higher predicted symbol digit modality test scores. This study showed how the position of the default mode network within gradient space affects information processing speed, as this network functions as a central hub involved in processing and integrating transmodal information.

All the above studies were conducted in neurological conditions in aging populations. Connectivity gradients are also employed to understand brain organisation in neurodevelopmental disorders such as autism. Hong et al. (2019) found atypical functional connectivity transitions between sensory systems and transmodal regions in autism. Disease-specific changes in functional gradients showed reduced separation between unimodal and transmodal regions in autism. They also found a reduced hierarchical division across the cortex, reflecting altered transitions from sensory systems to transmodal cortices, and gradient changes predicted social and behavioural difficulties in individuals with autism (Hong et al., 2019). All of these studies clearly demonstrate that understanding how connectivity gradients become less differentiated helps to untangle various patterns of cognitive impairments caused by different brain pathologies. The studies listed above are network disorders, but connectivity gradients captured the unique patterns of network disruptions linked with specific pathology. In contrast to this overall narrowing of gradient axes, some brain regions show expanded gradient positions. Liu et al. (2026) observed that the right medial superior frontal gyrus and bilateral angular gyri occupied higher gradient positions along the DMN to somatomotor axis in Alzheimer's disease compared with healthy controls. The authors proposed that these regional gradient expansions may reflect compensatory functional reorganisation, whereby increased functional differentiation helps preserve network integration despite widespread disease-related disruption.

Although a few studies have used connectivity gradients to characterise stroke-related whole-brain functional disruptions (Bayrak et al., 2019; Chen et al., 2026; Koba et al., 2025), no work has examined gradient changes in relation to semantic control deficits or aphasia after stroke. Existing studies have not linked gradient alterations to detailed behavioural measures, particularly those assessing performance across a range of language and semantic cognition tasks. This thesis investigates functional reorganisation captured by connectivity gradients in relation to language and semantic cognition.

1.6. Overview of the thesis

The overarching aim of this thesis is to examine how stroke disrupts network-wide functional connectivity and how functional reorganisation in preserved brain regions relates to language and semantic cognition. Building on the view of stroke as a distributed network disorder, this work investigates whether connectivity gradients provide a mechanistic account of post-stroke behavioural outcomes that is not captured by traditional region-based or network-based approaches. The central focus is on how functional reorganisation within the surviving brain influences cognition and language functions in chronic stroke.

A first aim is to determine whether stroke lesions produce systematic alterations along the principal axes of cortical organisation, and whether these alterations reflect the distributed nature of post-stroke functional disruption. A second aim is to evaluate whether changes in gradient position are linked to language and semantic control outcomes, focusing on whether variation along specific gradient dimensions corresponds to deficits in controlled semantic retrieval and broader language performance. A third aim is to use connectivity gradients in a novel way to simulate lesion effects within gradient space, modelling stroke-specific disruptions separately from individual variability in intrinsic cortical organisation. This involves using lesion information derived from structural MRI to characterise functional reorganisation in chronic stroke and to provide a mechanistic account of how focal damage alters large-scale connectivity. A fourth aim is to evaluate the utility of these simulated gradients, examining whether gradient solutions derived from lesion maps can approximate aspects of resting-state functional organisation, particularly in situations where resting-state data are not available. This aim also tests whether simulated stroke gradients can predict semantic cognition and language outcomes. A final aim is to assess whether relationships between gradients and behaviour offer insights that could support future clinical understanding of language and semantic outcomes, including whether gradient-linked measures capture aspects of impairment not explained by lesion location. The following section outlines how these aims are addressed in Chapters 2, 3, and 4.

Chapter 2 examined functional connectivity changes in stroke survivors with semantic aphasia using a connectivity-gradient decomposition approach. Because semantic control deficits arise at the interface between domain-general control systems and semantic representational networks, semantic aphasia provides a particularly useful test case for approaches that characterise the continuous organisation of brain networks, such as connectivity gradients. This chapter assessed whether cortical lesion information from structural MRI could model aspects of the functional changes observed in empirical resting-state data. This proof-of-concept analysis was conducted in a small subset of eight patients with both resting-state fMRI and structural lesion maps, allowing comparison between simulated and observed post-stroke gradients. The simulation modelled each

lesioned parcel's influence on the remaining cortex, reflecting a direct lesion-effects approach. The chapter also investigated whether simulated gradient changes within unlesioned regions of the semantic control network were associated with retrieval difficulties in a larger sample of 21 individuals with semantic aphasia.

Chapter 3 investigated post-stroke reorganisation of connectivity gradients in a large and heterogeneous cohort of individuals with aphasia drawn from the PLORAS database. PLORAS, established in 2008, provides an extensive resource for predicting language recovery after stroke, combining structural and functional imaging with detailed behavioural assessments. The project has been used to characterise long-term language outcomes from structural scans and to understand inter-subject variability in post-stroke reorganisation (Seghier et al., 2016). For example, Gajardo-Vidal et al. (2021) used PLORAS to dissociate the effects of injury to Broca's area from damage to adjacent white-matter pathways, showing that persistent language production deficits following left frontal infarcts were linked to the anterior arcuate fasciculus rather than Broca's area itself. Building on this foundation, Chapter 3 applied connectivity-gradient analysis to PLORAS for the first time, using data from 60 stroke survivors with structural MRI, resting-state fMRI, and detailed language and cognitive assessments from the Comprehensive Aphasia Test. This chapter first identified the lesion locations most strongly associated with specific language subdomains, replicating and extending conventional lesion–symptom mapping within this large cohort. It then introduced a novel analysis by examining how connectivity-gradient changes in the preserved cortex explained additional variance in language outcomes beyond the effects of focal damage. This approach allowed the chapter to test whether distributed reorganisation along key gradient dimensions provides behaviourally meaningful information that is not captured by lesion location alone. Together, these analyses clarified how both focal injury and large-scale functional reorganisation jointly support or constrain language function in chronic stroke.

Chapter 4 also used the PLORAS dataset, analysing 52 stroke survivors with both structural and resting-state fMRI. This chapter extended the simulation framework introduced in Chapter 2 by developing a more comprehensive model of lesion impact on connectivity gradients. Because the simulation approach required cortical lesion information, eight cases with purely subcortical lesions were excluded. Building on the direct lesion-effects simulation from Chapter 2, Chapter 4 introduced an iterative-propagation model that incorporated all edge-wise connections, thereby modelling both direct and indirect (diaschisis-like) effects across the cortex. The chapter evaluated whether this additional propagation step improved the accuracy with which simulated gradients reproduced empirically observed stroke gradients derived from resting-state fMRI. This work provided an initial evaluation of whether lesion-derived simulations can approximate aspects of resting-state functional

organisation, offering a potential complementary approach in situations where functional imaging is unavailable.

Chapter 2
Lesion-gradient mapping: effects of stroke on connectivity gradients in semantic aphasia

2.1. Abstract

Post-stroke semantic aphasia is characterised by multimodal semantic deficits arising from disruption to a distributed network spanning frontal and temporal regions. Although long-term conceptual knowledge is largely preserved, controlled retrieval is impaired because the interaction between control processes and underlying semantic representations is disrupted. Connectivity gradients, which capture major axes of whole-brain functional connectivity variation, offer a useful framework for assessing the global impact of stroke. They provide a dimensional perspective on how stroke disrupts the interaction between the semantic control system and the semantic store across different input modalities. This study examined whether post-stroke changes in connectivity gradients help explain semantic-aphasia deficits. First, we tested whether lesion location and lesion-load information from structural MRI could predict gradient changes observed in resting-state fMRI, in a proof-of-principle analysis of eight cases. Simulated post-stroke gradient changes derived from structural MRI correlated with actual resting-state gradient alterations caused by stroke, particularly for the principal gradient separating unimodal and heteromodal cortex. Second, we assessed whether simulated gradient changes predicted the severity of semantic impairment (N = 21). Semantic deficits were associated with simulated connectivity shifts along this principal gradient: left prefrontal regions supporting controlled semantic retrieval showed stronger connectivity to unimodal cortex in patients with more severe semantic impairment. Overall, these findings demonstrate that connectivity gradients capture a macroscale reorganization of brain networks that is linked to semantic impairment. Furthermore, the ability to approximate these shifts from structural MRI indicates a promising direction for future clinical applications.

2.2. Introduction

Semantic aphasia (SA) is associated with infarcts affecting the left inferior frontal and/or temporoparietal cortex and is often defined as a comprehension impairment affecting both verbal and non-verbal tasks (Jefferies & Lambon Ralph, 2006; Robson et al., 2012). These problems are thought to reflect difficulties controlling semantic retrieval so that it is appropriate to the current task or context, rather than a loss of long-term conceptual knowledge (Jefferies & Lambon Ralph, 2006; Jefferies et al., 2008; Lambon Ralph et al., 2017; Jefferies, 2013; Souter et al., 2022). Irrespective of modality, SA patients show difficulties in flexibly retrieving information (Corbett et al., 2011) and perform poorly when retrieving weak or subordinate meanings (Noonan et al., 2010). They also show impairments on semantic tasks involving pictures, environmental sounds (Jefferies & Lambon Ralph, 2006; Thompson & Jefferies, 2013), and unusual object use (Corbett et al., 2009, 2011). These deficits are thought to reflect problems tailoring semantic retrieval to suit the circumstances, particularly when meanings are ambiguous or competing alternatives must be resolved (Jefferies & Lambon Ralph, 2006; Jefferies, 2013). Semantic control deficits occur in transcortical sensory aphasia, in patients with fluent speech and good repetition, but they can also be accompanied by degrees of dysfluency and repetition difficulty (Jefferies & Lambon Ralph, 2006). According to the controlled semantic cognition framework, semantic cognition draws on unimodal features that are integrated within the anterior temporal lobes to form heteromodal concepts (Patterson et al., 2007; Lambon Ralph et al., 2017). Semantic control processes then shape retrieval so that less strongly instantiated knowledge can be prioritised when relevant (Jefferies, 2013). Computational modelling work has suggested that this might involve control over the activation of unimodal features, which are then integrated into the heteromodal conceptual store in a way that prioritises task-relevant information (Jackson et al., 2021). In this way, semantic control deficits in semantic aphasia can be understood as a failure to flexibly weight features of multi-dimensional concepts flexibly according to the current context.

Neuropsychological studies of semantic control converge with neuroimaging and neurostimulation approaches in revealing a left-lateralised distributed network of brain regions associated with semantic control, including left inferior frontal gyrus (IFG), posterior temporal cortex, and dorsomedial prefrontal cortex (Hallam et al., 2016; Whitney et al., 2011; Jackson, 2021). These regions partially overlap with the multiple-demand network and also interface with regions of the default mode network during semantic judgements, reflecting the need to integrate conceptual information with executive goal representations (Davey et al., 2016; Chiou et al., 2022; Wang et al., 2024). The semantic control network responds across modalities of input (Krieger-Redwood et al., 2015; Davey et al., 2015) and interacts with anterior temporal regions implicated in long-term heteromodal semantic memory (Bonner & Price, 2013; Jefferies et al., 2020; Chiou et al., 2018; Pobric et al., 2007); moreover, this network changes its pattern of connectivity along the unimodal-

transmodal hierarchy depending on semantic control demands, shifting its connectivity towards the transmodal default mode network when strong associations are retrieved, and towards sensory-motor regions during the controlled retrieval of weaker associations (Gao et al., 2022). The semantic control network may therefore play a key role in flexibly modulating the way that heteromodal and unimodal aspects of knowledge are integrated.

Given the semantic control network is highly distributed and draws together both the multiple-demand network and the default mode network (Davey et al., 2016; Chiou et al., 2022; Wang et al., 2020), semantic aphasia likely reflects more than focal tissue loss and may involve broad disruption of whole-brain organisation (Souter et al., 2022; Hallam et al., 2018). This macroscale perspective is able to explain a key clinical observation in SA: patients often present with similar behavioural deficits despite having anatomically distinct lesions in either frontal or posterior temporal regions (Jefferies & Lambon Ralph, 2006; Noonan et al., 2010; Thompson et al., 2022). While lesion size and location are useful clinical predictors of post-stroke deficits (Plowman et al., 2012), a fuller picture is provided by mapping post-stroke changes to large-scale functional brain organisation (Hannan et al., 2023). Lesion-network mapping has emerged as a tool for this purpose, using normative connectomes to estimate how a specific infarct might 'disconnect' functional networks (Boes et al., 2015; Fox, 2018). Lesion-network mapping has been used to link network disruption to cognitive symptoms (Fox, 2018; Pini et al., 2021), including mind-wandering, impaired face recognition, and sensory processing (Philippi et al., 2020; Cohen et al., 2019; Schlemm et al., 2023). However, the success of this approach has been inconsistent across studies (Souter et al., 2022; Zhao et al., 2023; Salvalaggio et al., 2020; Pini et al., 2021) and important limitations of lesion-network mapping have been identified: i) it measures direct disconnections, potentially ignoring shifts in functional interactions among brain areas not directly connected to the lesion (Pini et al., 2021); ii) it often identifies extensive networks but fails to pinpoint which aspects of altered connectivity are causally related to symptoms (Boes, 2021); and iii) it treats connectivity as a unidirectional magnitude, overlooking the dynamic ways that regions reorganise their network activity over time. For example, stroke may induce changes in specific functional relationships, leaving other aspects of connectivity for the same regions intact.

To move beyond traditional disconnection models of semantic impairment, we use lesion–gradient mapping, a relatively novel method for characterising the complex macroscale organisation of the cortex (Bayrak et al., 2019). This approach leverages connectivity gradients (Margulies et al., 2016), which describe the cortex not as a set of discrete regions but as a continuous landscape of functional transitions. By projecting the brain into a low-dimensional functional “gradient space,” each cortical region can be assigned coordinates along multiple axes of functional variation. This allows us to track a region’s functional identity—how it maintains its distance from primary sensory systems or interfaces with high-level transmodal hubs—and to examine how these properties are

altered following stroke. Unlike traditional seed-based or network-based approaches, the gradient framework avoids the need to predefine regions of interest. It also allows individual regions to contribute to multiple functional relationships across different cognitive states. By emphasising the dominant, large-scale axes of brain organisation, this method potentially provides a more sensitive measure of how a focal lesion can shift the global "position" of structurally spared tissue in the connectivity landscape.

In this study, we compare connectivity gradients for people with SA to age-matched healthy controls, with the aim of identifying post-stroke changes in intrinsic connectivity associated with semantic impairment in this group. We focus on the top two gradients that explain the most variance, since individual differences in semantic cognition have been linked to individual differences in both of these dimensions (Shao et al., 2022). The principal gradient captures a continuum from unimodal to heteromodal cortex, with primary sensory–motor regions at one end and default-mode regions at the other. It also reflects the orderly arrangement of major functional networks (Margulies et al., 2016), and individual differences along this axis relate to the efficiency of controlled semantic retrieval (Shao et al., 2022). During semantic retrieval, the semantic control network shifts its position along this gradient—showing greater similarity to the transmodal end for strong associations and to the unimodal end for weak associations (Gao et al., 2022), consistent with its role in shaping access to task-relevant conceptual features. The second gradient describes an orthogonal axis separating visual from auditory–motor connectivity patterns (Margulies et al., 2016), and variation along this dimension relates to picture- versus word-based semantic performance (Shao et al., 2022). Alterations to either gradient following stroke may therefore influence semantic cognition. Although Bayrak et al. (2019) examined stroke-related changes in connectivity gradients at a global level, they did not assess how these alterations relate to cognitive outcomes.

We use two previously published datasets of patients with semantic aphasia (Souter et al., 2022; Hallam et al., 2018) to ask whether structural MRI, which is commonly available in clinical settings, can be used to simulate stroke-induced changes in connectivity gradients, in place of resting-state fMRI, which is not routinely collected as part of clinical practice. We attempt to validate the simulated gradients in two ways: Phase 1 (N = 8), a proof-of-principle analysis, compares simulated connectivity gradients (derived from lesion data) with actual gradients extracted from resting-state fMRI in the same individuals. Phase 2 (N = 21) tests whether simulated gradient changes predict the severity of the semantic impairment in a group of SA patients. We simulate lesion effects on functional gradients by identifying each cortical lesion's shape, size, and location from structural MRI, and then model the expected disruption to functional connectivity gradients using a healthy control connectome (N = 39), in a fashion conceptually similar to lesion-network mapping. While lesion-gradient mapping could be applied to other stroke-related impairments (e.g., motor, phonological, fluency, or attentional deficits), here we focus on semantic aphasia as a test case given

previous research has linked gradient organisation to semantic cognition (Shao et al., 2022; Gao et al., 2022).

2.3. Methods

2.3.1. Overview

In Phase 1, as a proof-of-principle in a small sample, we asked whether changes in brain connectivity gradients seen in patients' resting-state fMRI scans after stroke correlate with changes that can be predicted from their lesions using structural MRI data. This comparison assesses how accurately simulated cortical gradients can capture key changes to dimensions of connectivity following stroke. To estimate gradient changes in stroke survivors, we used a functional cortical parcellation, calculated the proportion of each parcel that was damaged by the lesion, considered the extent to which each *pair* of parcels was intact, and then reduced the strength of the functional connectivity matrix for each pair of parcels by this value and computed the impact of this reduction on connectivity gradients. This approach is conceptually similar to other methods in which lesion data is used to simulate changes in connectivity – for example, structural disconnection analyses take lesioned regions and estimate which white matter pathways are likely to be disrupted by a pattern of brain injury (Jiang et al., 2023; Thiebaut de Schotten et al., 2020), while lesion-network mapping uses lesions from structural MRI as seeds in functional connectivity analysis to model possible network disruption (Fox, 2018; Pini et al., 2021). In such studies, the distant and distributed effects of focal lesions are simulated using normative connectome data to predict the impact of stroke. Here, we estimate how lesions affect two principal dimensions of functional connectivity, Gradients 1 and 2. In Phase 2, we use simulated changes in these gradients, derived from structural MRI lesion data, to predict semantic control deficits. This allows us to test whether structural MRI, which is far more widely available than functional MRI in stroke survivors, can be used to predict cognitive outcomes in patients with left-hemisphere stroke.

2.3.2. Participants

A total of twenty-one stroke patients (9 females; mean age: 62.2 ± 11.9 years) participated in this research. All participants were right-handed native English speakers who were at least 6 months post-stroke (mean duration: 6.7 ± 5.5 years). Inclusion criteria were an infarction in the left hemisphere and a confirmed impairment in semantic control. Patients who were undergoing rehabilitation at the time of testing, had a history of traumatic brain injury, or had suspected or confirmed neurodegenerative disorders were excluded. On average, the patients left formal education at 16.3 ± 1.5 years of age. The analysis was conducted in two parts: Phase 1 (validation subset) included a subset of eight patients (5 females; mean age: 58.6 ± 11.6 years) who had both resting-state fMRI and structural MRI. This

sample was used to compare empirical connectivity gradients with those simulated from structural lesion data. In Phase 2, the full cohort of 21 patients was used to test whether simulated gradient changes predicted the severity of semantic impairment. A sample of 39 healthy controls (22 females; mean age: 66.8 ± 6.9 years) was used for comparison with the patients in both phases. The study was approved by the York Neuroimaging Centre Research Ethics Committee.

2.3.3. Semantic cognition testing

Patients were identified on the basis of impaired performance on at least one verbal and one non-verbal measure of semantic cognition. Four tasks were used for screening: word and picture versions of the Camel and Cactus Test (CCT), the non-verbal Alternative Object Uses task (Corbett et al., 2011) and comprehension of subordinate meanings of ambiguous words (Noonan et al., 2010). Individual scores are presented in Table 2.1; impairment was defined as performance more than two standard deviations below the healthy control mean (Thompson et al., 2017; Corbett et al., 2009). Camel and Cactus Test (CCT) (Adlam et al., 2010): Participants selected which of four items was semantically associated with a probe. Control demands were high because participants had to ignore strong but irrelevant relationships among response options. Sixteen patients were impaired on the word version and ten on the picture version. Alternative Object Use (Corbett et al., 2011): Participants selected an object to perform a specific action (e.g., “crack a nut”). Canonical trials used typical objects (e.g., a nutcracker), while alternative trials required access to non-dominant object knowledge (e.g., a hammer), placing higher demands on semantic control. Twenty patients completed this task; 19 were impaired on the alternative use trials (scoring below the control-derived cut-off), while performance was significantly higher on canonical trials [Mean (SD) = 92.7% (7.5) vs. 59.5% (19.7)].

Ambiguity Task: Participants matched words with ambiguous meanings to a probe (e.g., "bank"), in the uncued version of this task from Noonan et al. (2010). The dominant condition involved the more common meaning, while the subordinate condition required retrieval of the less frequent meaning and both versions of the task involved suppressing irrelevant interpretations. Twenty of 21 patients were impaired on dominant trials, and all 21 were impaired on subordinate trials. Given the near-universal impairment across both conditions, the average score across dominant and subordinate trials was used for subsequent analyses.

To derive a single factor representing semantic cognition, a Principal Component Analysis (PCA) was performed. The Alternative Object Use task was excluded from the PCA because one patient did not complete it. The remaining scores (CCT words, CCT pictures, and the ambiguity average) were highly correlated (CCT word–picture $r = 0.83$; CCT word–ambiguity $r = 0.95$; CCT picture–ambiguity $r = 0.96$; all $p < 0.001$). PCA with oblique rotation yielded a single component (eigenvalue = 2.6) explaining 87% of the variance (loadings: CCT words = 0.95; CCT pictures = 0.92; ambiguity = 0.92). To ensure the robustness of this composite score, we checked for outliers using the

interquartile range (IQR) criterion; there were no scores falling more than 1.5 times the IQR above the third quartile or below the first quartile. This semantic composite score was used as the behavioural dependent variable in the Phase 2 lesion-gradient mapping analysis.

2.3.4. MRI acquisition: Stroke patients and aged controls

Whole-brain resting-state functional MRI images were acquired for both stroke patients and aged controls using a 3T GE HDx scanner equipped with an eight-channel phased array head coil. For the stroke patients, a GE-EPI (Gradient-Echo Planar Imaging) sequence was used with the following acquisition parameters: repetition time (TR) = 3s, echo time (TE) = minimum full, flip angle = 90°, field of view = 19.2 cm (matrix size = 64 x 64), 60 interleaved slices per volume with a slice thickness of 3 mm, voxel size = 3x3x3 mm^3, total volumes = 180, and a scan duration of 9 minutes. For the aged controls, a single shot 2D gradient echo planar imaging sequence was used with similar parameters, including TR = 3s, TE = minimum full, matrix size = 64 x 64, 60 slices, and voxel size = 3x3x3 mm^3, with 180 volumes. Participants were instructed to fixate on a black fixation cross on a grey background during the scan. For both groups, T1-weighted structural images were acquired using a 3D fast spoiled gradient echo sequence: the acquisition parameters for the stroke patients included TR = 7.8 ms, TE = minimum full, flip angle = 20°, matrix size = 256 x 256, 176 slices, and voxel size = 1.13 x 1.13 x 1 mm, while the structural scan for the aged controls included 178 slices.

Table 2.1. Semantic performance scores for Camel and Cactus test and Ambiguity task

Patient ID	Object Use		Camel and Cactus Test		Ambiguity	
	Alternative	Canonical	Word	Picture	No Cue Dominant	No Cue Subordinate
P01	24	35	54	54	26	23
P02	NT	NT	41	46	19	10
P03	12	30	42	44	21	13
P04	9	31	16	15	11	10
P05	13	31	33	13	23	10
P06	24	37	39	36	23	13
P07	31	37	60	61	29	24
P08	22	35	56	61	25	16
P09	21	35	53	56	22	14
P10	14	29	29	45	24	14
P11	22	33	57	54	27	19
P12	13	31	43	44	18	9
P13	32	37	56	61	27	21
P14	26	37	61	53	28	21
P15	14	32	39	31	22	11
P16	27	37	48	51	25	18
P17	22	35	52	57	26	17
P18	29	37	60	61	28	19
P19	24	33	50	59	27	17
P20	34	37	59	45	24	19
P21	27	37	48	54	23	19
Mean	22	34.4	47.4	47.7	23.7	16.1
Cut off	33.7	35.9	56.6	52.7	28.4	27.6

NT = Not available for testing. Poor semantic performance scores were observed in the object use task, the word and picture versions of the CCT, and in both the dominant and subordinate trials of the ambiguity task, shown in bold numbers.

2.3.5. Lesion segmentation

Brain extraction and lesion segmentation were performed in native space. The brains were extracted using ANTs (Advanced Neuroimaging Toolkit), utilising a template from the OASIS brain project (https://www.oasis-brains.org/; Marcus et al., 2010) based on the patients' T1-weighted volumes.

Lesions were manually segmented using MRIcron. We used a combination of the 3D fill feature and subsequent slice-by-slice validation. While delineating the lesions, care was taken to avoid including enlarged sulci or ventricles; instances where these were incorrectly included by the 3D tool were identified through visual inspection, cross-referencing axial, coronal, and sagittal views. After segmentation, the native-space T1 images were registered to MNI152 space using ANTs linear registration (version 2.1.0; Avants et al., 2011, 2014), which employs a symmetric normalization model. The following default parameters were used: aligning centres and orientations, followed by an affine transformation accounting for scaling factors, with optimisation of the cost function (Avants et al., 2011). Lesions were not included in the cost function during registration, consistent with standard PLORAS procedures (Seghier et al., 2016). The resulting transformation matrix was then applied to the lesion masks to bring them into template space.

2.3.6. Resting-state fMRI data preprocessing

The resting-state fMRI data from both stroke participants and age-matched controls were preprocessed using the CONN toolbox (v.18b; Whitfield-Gabrieli and Nieto-Castanon, 2012) implemented in Matlab R2018a. CONN's default preprocessing pipeline was employed, including motion estimation and correction by volume realignment with a six-parameter rigid-body transformation, slice-time correction, and simultaneous segmentation and normalisation of white matter, grey matter, and cerebrospinal fluid to MNI152 stereotactic space (2 mm isotropic voxel size) for both functional and structural scans. Functional and structural images were normalised using CONN's unified segmentation and normalisation procedure, which estimates tissue classes and spatial transformations jointly. After preprocessing, potential confounds were statistically controlled for, including the six motion parameters and their first and second derivatives, volumes with excessive motion (greater than 0.5 mm) or global signal changes ($z > 3$), linear drifts, and five principal components from white matter and CSF signals (CompCor method; Behzadi et al., 2007). Time series were then band-pass filtered between 0.01 and 0.1 Hz. Global signal regression was not performed. All participants exhibited mean head motion below 0.35 mm; therefore, no participants were excluded from further analyses.

2.3.7. Whole-brain functional connectivity

The functional connectivity matrix for each participant was extracted after preprocessing and denoising the resting-state data. First, we extracted the mean functional time series for each of the 400 parcels from the Schaefer parcellation (Schaefer et al., 2018) (https://github.com/ThomasYeoLab/CBIG/tree/master/stable_projects/brain_parcellation/Schaefer2018_LocalGlobal). These 400 ROIs were assigned to the seven networks from an influential whole-brain parcellation (Yeo et al., 2011) based on their overlap. The Schaefer parcellation provides a standardized framework for functional connectivity analysis, capturing the organization of resting-

state networks while preserving homogeneity and aligning with histological boundaries (Yan et al., 2023). Subsequently, for each participant, a 400 × 400 functional connectivity matrix was generated by computing the Pearson correlation between the mean time series of each ROI and all other ROIs. At this stage, lesioned ROIs were not removed; instead, a complete functional connectivity matrix is necessary to extract connectivity gradients. We assume that lesioned parcels do not contribute significantly to explaining the variance in functional connectivity patterns and therefore do not influence the gradient structure. However, lesioned parcels were masked out in subsequent analyses to examine connectivity-gradient changes in the unlesioned brain. Individual functional connectivity matrices were subjected to Fisher Z-transformation and averaged to obtain a group-level connectivity matrix.

2.3.8. Functional connectivity gradient extraction

Using the BrainSpace toolbox (Vos de Wael et al., 2020), we extracted connectivity gradients from functional connectivity matrices parcellated with the Schaefer-400 atlas (Schaefer et al., 2018). Ten individual-level gradients were computed for each stroke patient, while ten group-level gradients were derived from the group-averaged connectivity matrix of the aged controls. Connectivity matrices were thresholded at 90% sparsity (retaining the top 10% of weighted connections per row), transformed with a normalized angle kernel, and projected into a low-dimensional space using diffusion map embedding. To ensure comparability across the sample, the group-level control gradients and individual patient gradients were aligned via Procrustes rotation to canonical reference gradients derived from Human Connectome Project (HCP) data (n = 217; 122 women; mean ± SD age = 28.5 ± 3.7 years; see Vos de Wael et al., 2018). This orthogonal transformation (rotation and reflection, with scaling) achieves maximum correspondence between matrices while preserving the underlying subject-specific connectivity geometry (Goodall, 1991; Siegel et al., 2017). Aligning gradients in this way provides a standardized coordinate system that increases the interpretability of stroke-related shifts relative to a normative reference space (Gonzalez Alam et al., 2021; McKeown et al., 2020). Although we extracted ten gradients to improve the mathematical correspondence with canonical solutions (Margulies et al., 2016), our analyses focused on the first two gradients, as they explain the greatest variance and characterise primary patterns of functional variation linked to semantic cognition.

2.3.9. Simulated post-stroke gradients

We simulated the effects of stroke on connectivity gradients using structural lesion data. For each participant with semantic aphasia, we created a simulated functional connectivity lesion matrix to model the impact of stroke on parcel-to-parcel connectivity, using segmented lesion maps derived from T1-weighted images (see Figure 2.1). The steps were as follows: 1) The segmented, binarised lesion map for each patient was multiplied by the Schaefer parcellation (400 parcels assigned to 7 Yeo

networks; Yeo et al., 2011) using FSL's fslmaths tool, aligning the lesion map to the Schaefer parcellation template. This step identifies which parcels are affected by the lesion and computes the proportion of each parcel that is damaged (lesion load). These lesion load values were then used to estimate the amount of spared tissue in each parcel for subsequent modelling of connectivity changes. 2) The proportion of tissue in each parcel spared by the lesion (i.e., the complement of the parcel) was extracted, producing 400 values that indicate the amount of intact brain tissue in each parcel after stroke. 3) A 400 x 400 lesion matrix was then constructed by multiplying each spared tissue value by every other value in the set (calculate the pairwise products of all elements), so that each entry in the matrix represents the estimated connectivity between two parcels based on the amount of intact tissue in both (See Supplementary Figure 2.S1 in the supplementary material for the steps involved in the generation of the lesion matrix). This estimates the connectivity between intact tissue in each parcel and all other parcels, resulting in a 400 x 400 matrix. 4) Each lesion matrix was then multiplied element-wise with the 39 functional connectivity matrices from the aged control group to simulate the functional disruption caused by each lesion. The underlying assumption is that a fully intact parcel maintains its normal level of functional connectivity across the cortex, and that partial damage reduces this capacity proportionally to the amount of spared tissue. For example, if a parcel retains 50% intact tissue, its effective contribution to functional connectivity is modelled as 0.5; if two parcels each retain 50% intact tissue, their joint capacity to maintain a connection is modelled as $0.5 \times 0.5 = 0.25$. The aim of this step was to model how introducing a lesion affects functional connectivity in a healthy brain, thereby isolating the direct effects of the lesion independently of other neurological conditions present in patients' brains. This operation generated 39 simulated versions of how each lesion could impact the brain's functional connectivity pattern. This approach is conceptually similar to established lesion-network-mapping methods, which estimate a lesion's network connectivity in a normative connectome to generate a disconnection map capturing how each lesion affects network organisation (e.g., Fox, 2018; Boes et al., 2015). 5) We computed the element-wise average of these 39 simulated matrices for each lesion, providing an overall estimate of the lesion's impact on functional connectivity. 6) Finally, simulated post-stroke gradients were extracted using the average simulated functional connectivity lesion matrix for each lesion, following the same methods used for the extraction of the stroke gradient from the resting state data described above. These individual-level simulated gradient maps for each lesion were aligned to the group-level gradients using Procrustes rotation, resulting in ten individual-level simulated lesion gradients for each lesion. These gradients demonstrated significant variance in whole-brain connectivity in descending order.

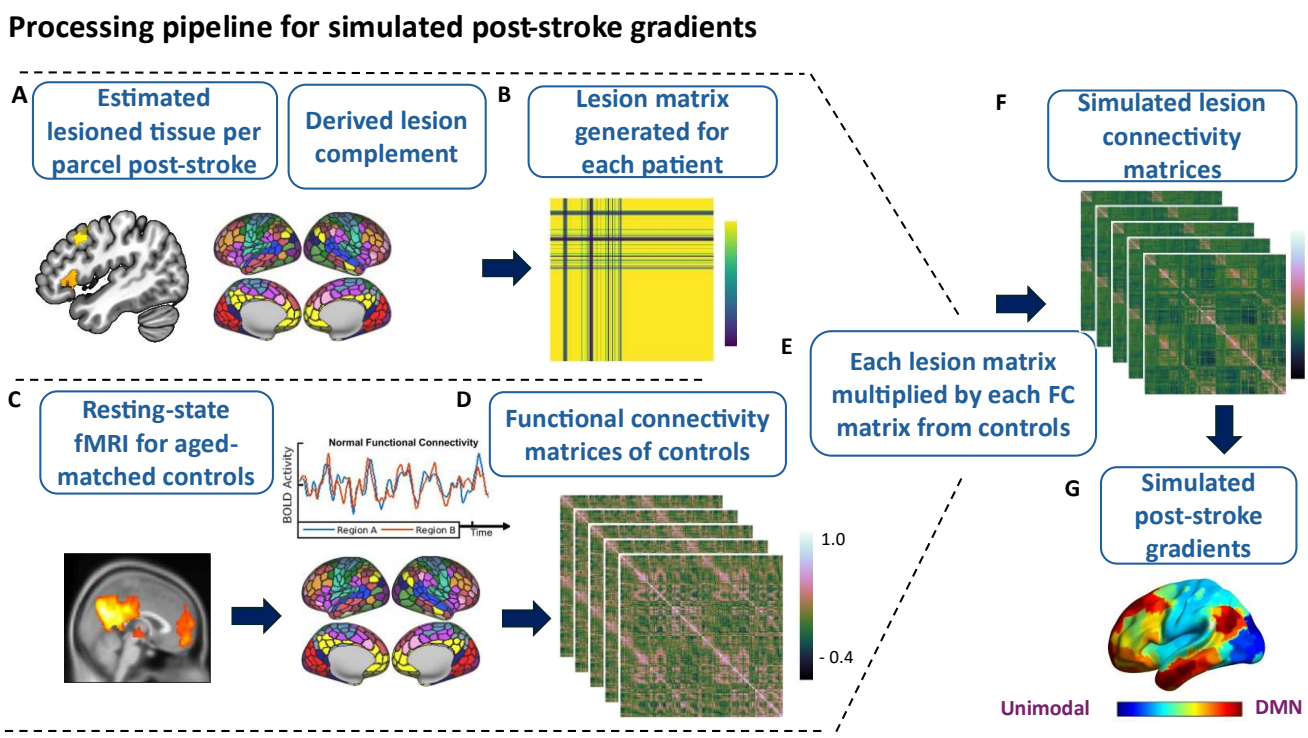

Figure 2.1. Processing pipeline for simulated post-stroke gradients for each lesion. A) The T1-weighted brain map for each lesion was multiplied by the Schaefer parcellation (400 parcels) to identify lesioned parcels. Lesion complements were then estimated from the lesioned parcels for each lesion. B) Lesion complement values were used to generate lesion matrices. C) Resting-state data from each aged control subject were pre-processed individually. D) A connectivity matrix for each control was generated by computing the Pearson correlation between the mean time series of each of the 400 ROIs, resulting in a 400 × 400 connectivity matrix per participant. E) Each lesion matrix was element-wise multiplied with the 39 individual functional connectivity matrices from the aged control group. F) For each lesion, the 39 simulated functional connectivity lesion matrices were averaged to create a single lesion-specific average matrix. G) Simulated post-stroke gradients were then extracted for each lesion using this average simulated functional connectivity lesion matrix.

2.3.10. Post-stroke gradient differences

To isolate stroke-specific effects, we generated gradient difference maps by subtracting the individual post-stroke gradients from the group-averaged aged-control template. By removing the shared normative gradient structure, these difference maps highlight the functional displacement that is specifically attributable to the stroke rather than baseline organisational features common to the healthy connectome. This subtraction procedure was applied to both observed and simulated

gradients, providing a standardised basis for evaluating the accuracy of our simulation approach and its relationship to behavioural impairment.

2.3.11. Phase 1: Statistical analyses

We used spin permutation testing to evaluate how accurately the simulated post-stroke gradient changes captured the effects of stroke in each participant with aphasia. This method addresses spatial autocorrelation—an innate property of brain imaging where nearby regions exhibit more similar activity than distant regions (Alexander-Bloch et al., 2018; White et al., 2022). Spin permutation tests were conducted on post-stroke gradient difference maps, comparing each lesion's observed and simulated stroke effects, using the Neuromaps Python library (Markello et al., 2022). First, Neuromaps converted the post-stroke difference maps from MNI152 volumetric space to cortical surface space. Next, a set of N=5000 randomised rotated versions of the simulated gradient maps were generated by applying spherical rotations ("spins") to the data, creating a null distribution of simulated gradient maps that preserve spatial autocorrelation. For each permuted simulated map, the Pearson correlation with the observed gradient difference map was calculated, producing a null distribution of correlation coefficients. The observed correlation between the actual simulated and observed maps was then compared against this null distribution to obtain a p-value, assessing the significance of their correspondence while accounting for spatial dependencies. To ensure that findings were not driven by missing tissue, lesioned parcels were excluded from both observed and simulated gradient difference maps prior to spin-permutation testing.

2.3.12. Phase 2: Statistical analyses

Phase 2 focused on two research questions: what are the post-stroke changes in functional connectivity captured by simulated gradients and are there any associations between the simulated post-stroke gradient changes and semantic impairment? We used a general linear model (GLM) to examine the association between stroke-induced simulated gradient changes and semantic cognition. We refer to this approach as lesion–gradient mapping. For each patient, the simulated difference gradient maps were entered into the model with the semantic composite score as the primary covariate. We also entered lesion size, age, and post-stroke duration as covariates of no interest. Nonparametric t-tests were performed in Randomise (Winkler et al., 2014; https://fsl.fmrib.ox.ac.uk/fsl/fslwiki/Randomise/UserGuide), using 5000 permutations. Analyses were conducted both across the whole-brain, to capture distributed disruptions in SA, and within a targeted semantic control mask (Jackson, 2021).To ensure results were driven by functionally reorganised rather than missing tissue, we excluded voxels damaged in more than 25% of the sample from the whole-brain mask and masked out all lesioned voxels from the ROI analysis (see Figure 2.5A). Output images from the nonparametric t-tests were thresholded at 0.95 to visualise regions significantly associated with behaviour at $p < 0.05$. Randomise produces TFCE-corrected 1–p maps,

with values closer to 1 indicating stronger statistical evidence. We therefore thresholded the 1–p images at 0.95 to visualise the significant clusters ($p < 0.05$). We also performed lesion–symptom mapping to investigate the association between lesion location and semantic control deficits. A general linear model was constructed, similar to the lesion–gradient mapping analysis, in which binarised lesion maps and the semantic composite score were entered as variables of interest, and the same covariates of no interest (lesion size, age, and post-stroke period) were included. This analysis was also implemented using nonparametric t-tests in Randomise (Winkler et al., 2014) with 5000 permutations. Threshold-Free Cluster Enhancement (TFCE) was used to identify significant lesion clusters. The same thresholding approach used in lesion–gradient mapping was applied here: significance was defined as $p < 0.05$ (FWE-corrected), visualised using thresholded 1–p maps with a 0.95 cut-off.

2.4. Results

2.4.1. Lesion Analysis

For the 8 patients with left frontal and temporal infarcts included in Phase 1, the maximum lesion overlap within grey matter was in the left insular and central opercular cortex (damaged in 6 out of 8 patients; Figure 2.2A). Figure 2.2B shows the grey-matter lesion overlap map for the 21 cases included in Phase 2; more than half had infarcts in the left insular cortex, lateral occipital cortex, and inferior frontal gyrus (IFG), with the maximum lesion overlap in the left middle frontal gyrus. Details of lesion location and lesioned voxels for participants included in both phases of the study are provided in the supplementary materials (Supplementary Table 2.S1).

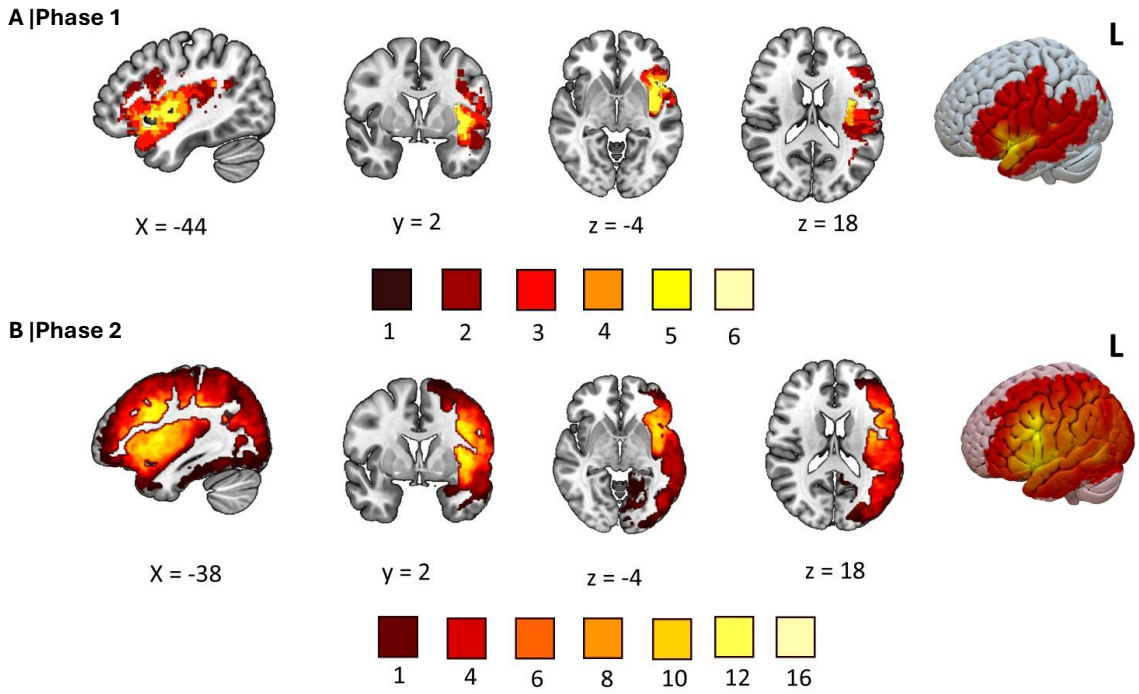

Figure 2.2. Lesion overlap maps. (A) Overlap map of stroke lesions in Phase 1 (N = 8). (B) Overlap map of lesions in Phase 2 (N = 21). Binary lesion maps were generated using FSLmaths (Jenkinson et al., 2012) and displayed in MNI space with MRIcroGL. Brighter colours indicate a greater degree of lesion overlap across stroke patients.

2.4.2. Phase 1: Effects of stroke on connectivity gradients extracted from resting-state fMRI

Phase 1 compared observed changes in intrinsic connectivity gradients derived from resting-state fMRI in semantic aphasia with changes predicted from structural MRI only using information about the lesion. Empirical and simulated gradient changes in SA were both estimated by comparing the gradients for each stroke participant with the average gradient in age-matched controls. We first extracted Gradients 1 and 2 from resting-state fMRI data for the patients and age-matched controls, as shown in Supplementary Figure 2.S2. Both groups showed a principal gradient (i.e., Gradient 1) which captured the separation of heteromodal from unimodal cortex, and a second gradient that distinguished between visual and auditory-motor cortex, as described by Margulies et al. (2016).

The left-hand panel in Figure 2.3 illustrates these empirical gradient changes for the eight participants in Phase 1. Although this limited subset is not intended to provide a generalisable map of stroke effects, a distinct pattern of reorganisation emerged (Koba et al., 2025) that served as our target for simulation. Regions in warm colours depict areas where patients had lower values than controls (i.e. positive values following the subtraction of patients from controls); conversely, regions shown in cool colours depict areas where patients had higher values than controls. For Gradient 1 (transmodal-

unimodal), transmodal regions of the default mode and frontoparietal networks which normally anchor the upper end of Gradient 1 (including lateral temporal, and lateral and medial prefrontal and parietal cortices, highlighted in warm colours), shifted toward more unimodal-weighted positions (Figure 2.3, top left). This movement indicates that these higher-order regions no longer maintain their characteristic functional distance from sensory-motor systems. Simultaneously, unimodal regions such as the motor cortex and insula shifted toward the transmodal end. This convergence suggests a 'compression' of the principal gradient axis and a loss of functional differentiation along this axis post-stroke. However, this compression of Gradient 1 was not found in all cortical regions: medial visual regions typically located at the extreme unimodal end shifted even further toward this pole post-stroke, exaggerating their usual position. Gradient 2 showed a similar reduction in differentiation, with decreased separation between visual and motor regions relative to age-matched controls (Figure 2.3, bottom left), indicating that the functional distinction between unimodal systems was also compromised.

2.4.3. Phase 1: Comparisons of gradient changes in resting-state fMRI and simulated from structural MRI

To validate our simulation approach, we used spin permutation tests to compare the average simulated gradient changes with those observed in resting-state fMRI data. At the group level, Gradient 1 showed a significant correlation between empirical and simulated gradient changes ($r = 0.63$, $p = 0.0004$), indicating that the simulation successfully captured functional reorganisation along the primary axis. However, Figure 2.3A shows that lateral visual cortex shifted toward the heteromodal end of Gradient 1 in the observed data, whereas the simulated gradients (Figure 2.3B) did not reproduce this specific shift. Gradient 2 showed a weaker, though still significant, correlation ($r = 0.20$, $p = 0.03$). Both the observed data and the simulations showed a shift toward the motor end of Gradient 2 in medial and lateral visual cortex after stroke. However, the shift of motor cortex toward the visual end of Gradient 2, evident in the resting-state fMRI data, was not captured by the simulated gradients.

Next, for each individual lesion, the correspondence between observed post-stroke gradient changes and simulated post-stroke gradient changes was estimated using spin permutations, and the results for each gradient are reported in Table 2.2. Spatial correlations between observed and simulated post-stroke changes were significant in 7 out of 8 cases for Gradient 1 (individual r values = 0.20–0.62; group mean = 0.423; SD = 0.145). For Gradient 2, significant correlations were found in 5 out of 8 SA patients (individual r values = –0.33–0.42; group mean = 0.153; SD = 0.218). These analyses suggest that the simulation captured Gradient 1 effects moderately well, whereas correspondence was lower for Gradient 2.

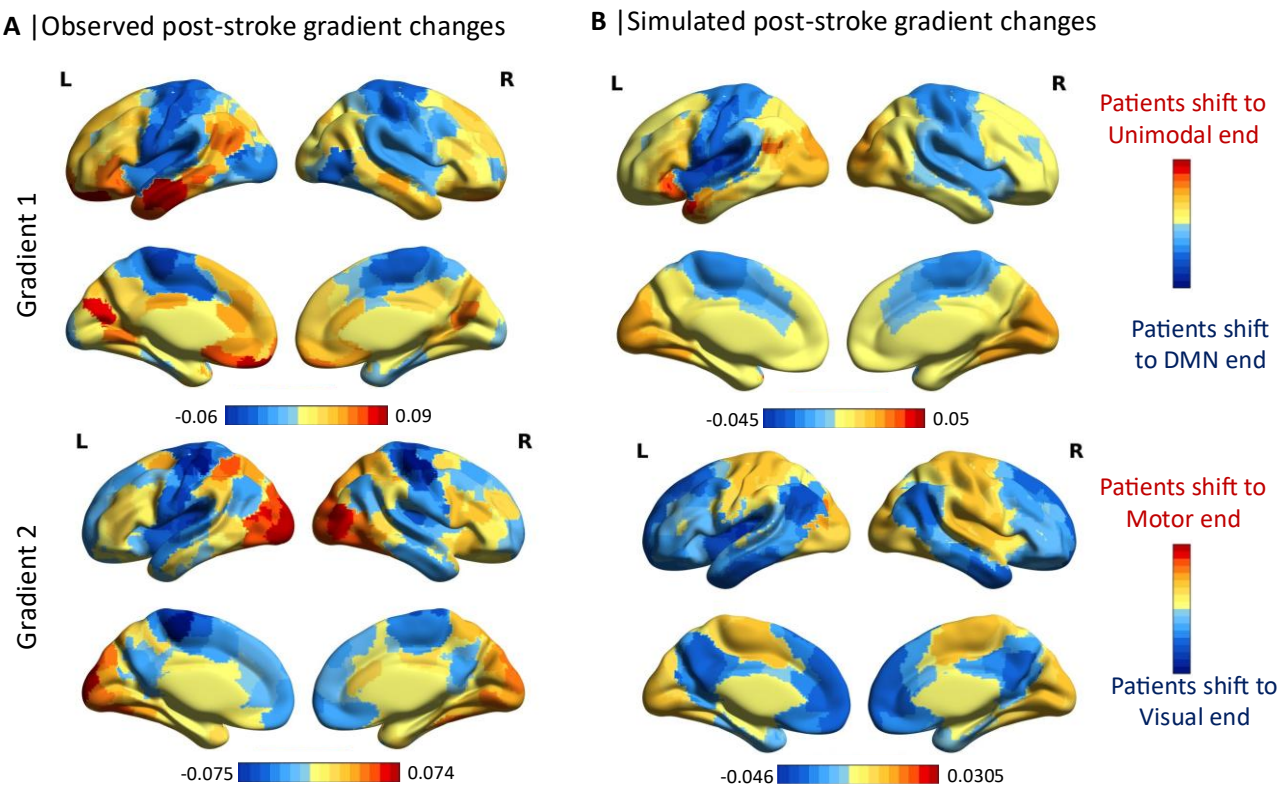

Figure 2.3. Post-stroke changes in connectivity gradients. (A) Post-stroke changes in Gradients 1 and 2 derived from resting-state fMRI data, comparing semantic aphasia (SA) patients with age-matched controls. (B) Simulated post-stroke changes in Gradients 1 and 2 derived from lesion data. The maps depict stroke-related effects by computing the difference between either observed or simulated gradients in each SA patient and the corresponding gradients of age-matched controls. Warm colours indicate regions where patients had lower gradient values than controls, whereas cool colours indicate regions where patients had higher gradient values than controls.

Table 2.2. Lesion location, size and spin permutation results for Gradient 1 and Gradient 2				
ID	Lesion Location	Lesion Volume(voxel)	Spin permutation results for Gradient 1	Spin permutation results for Gradient 2
09	Inferior frontal gyrus Parietal operculum cortex Angular gyrus	762	r = 0.62 (p = 0.001)	r = -0.3266 (p =0.009)
10	Middle frontal gyrus Inferior frontal gyrus Frontal operculum cortex Temporal lobe Angular gyrus Lateral occipital cortex	14491	r = 0.46 (p = 0.001)	r = 0.1036 (p = 0.55)
11	Frontal orbital cortex Insular cortex Central opercular cortex Inferior frontal gyrus	7318	r = 0.34 (p = 0.001)	r = 0.25 (p =0.048)
13	Frontal orbital cortex Insular cortex Central opercular cortex Postcentral gyrus	4307	r = 0.432 (p = 0.001)	r = 0.2543 (p =0.0039)
14	Insular cortex	16	r = 0.2 (p = 0.263)	r = 0.42 (p = 0. 0011)
15	Temporal pole Insular cortex Central opercular cortex Postcentral gyrus	2286	r = 0.55 (p = 0.001)	r = 0.11 (p =0.39)
17	Postcentral gyrus Lateral occipital cortex	592	r = 0.266 (p = 0.019)	r = 0.222 (p = 0.072)
18	Frontal pole Temporal pole Frontal orbital cortex Insular cortex	3700	r = 0.522 (p = 0.0019)	r = 0.189 (p = 0.0383)

2.4.4. Phase 1: Association between lesion size and the level of similarity captured by the simulation

We examined whether the similarity between simulated and observed post-stroke gradient changes was influenced by lesion size. To test this, we assessed the relationship between lesion size and the simulation accuracy (estimated by the spatial correlations from spin permutation tests between empirical and simulated post-stroke gradient changes) for each gradient separately using Spearman's rank correlation coefficient. Because of the small sample size and data that were not normally distributed, this correlation was evaluated using a subject-level permutation test. The relationship between lesion size and simulation accuracy was randomly permuted across all possible pairings (8! = 40,320 permutations), and the Spearman correlation was recomputed for each permutation to generate a null distribution. This analysis indicated that simulation accuracy was not dependent on lesion size for either gradient (Gradient 1: r = 0.24, permuted p = 0.582; Gradient 2: r = –0.21, permuted p = 0.619) (Figure 2.4).

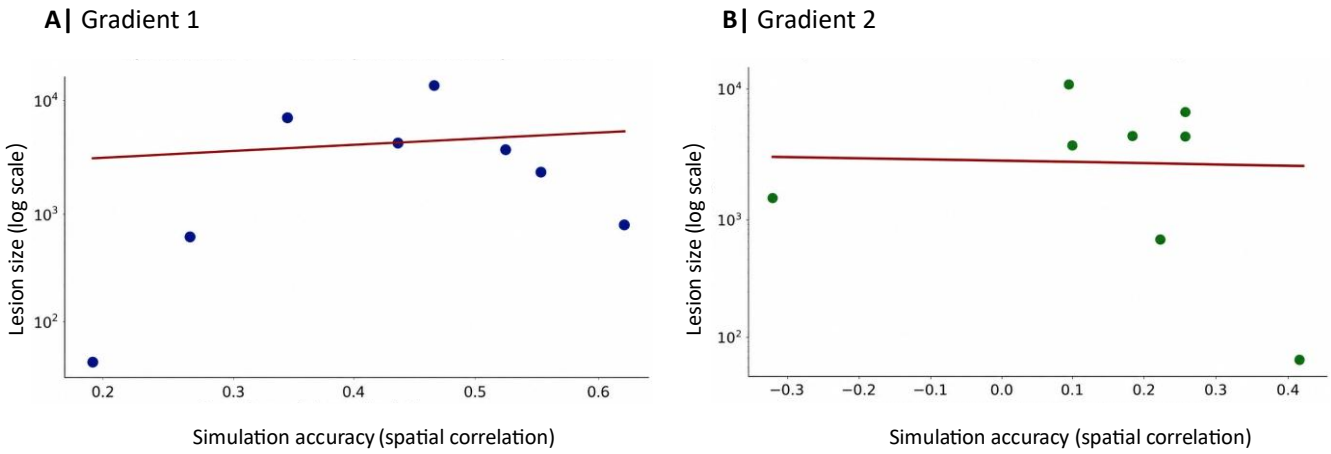

Figure 2.4. Relationship between lesion size and simulation accuracy. Scatter plots showing the association between lesion size and simulation accuracy, quantified as the spatial correlation between observed and simulated post-stroke gradient changes. The x-axis represents simulation accuracy (spatial correlation), and the y-axis represents lesion size on a logarithmic scale. Each point corresponds to a single lesion. (A) Gradient 1. (B) Gradient 2.

2.4.5. Phase 2: Post-stroke simulated gradient changes compared with healthy controls

Phase 1 suggests that post-stroke gradient changes in SA patients can be simulated, at least to some extent, using structural MRI, with significantly higher accuracy for the principal gradient (Gradient 1) than for the second axis (Gradient 2). Next, we asked if this method could identify consistent patterns of reorganization across a larger sample of 21 SA patients who only had structural MRI available. Permutation tests were performed on difference maps representing the predicted impact of each patient's lesion (calculated as the shift from the healthy control mean). These analyses revealed areas of significant gradient change in SA patients versus controls that were reliable across the group (Figure 2.5). For Gradient 1, transmodal regions including the inferior frontal gyrus, anterior temporal pole, middle temporal gyrus, angular gyrus, precuneus and posterior cingulate cortex showed a significant shift towards the unimodal end following stroke. Visual cortex also showed a shift toward the unimodal end of Gradient 1, although Phase 1 suggests these simulated gradient changes may not be accurate. Conversely, motor cortex and some auditory regions showed a shift toward the transmodal end. These patterns indicate that in a larger group of 21 SA cases, simulated changes in connectivity gradients consistently show reduced separation between the unimodal and transmodal ends of the principal gradient, similar to Phase 1, although some brain regions show conflicting effects. Parallel analyses were conducted for Gradient 2 (auditory-motor-to-visual), which suggested a shift in visual and motor regions toward a more motor-like connectivity profile. However, given the lower simulation accuracy for this axis identified in Phase 1, these results are provided in the Supplementary Materials (Supplementary Figure 2.S3).

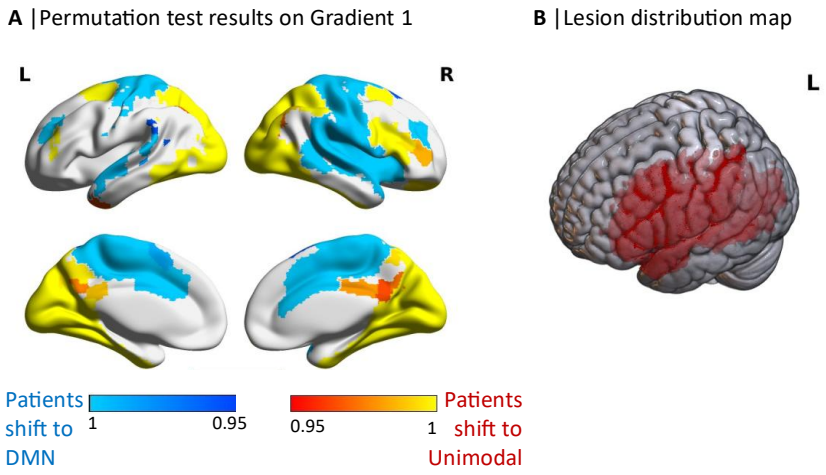

Figure 2.5. Permutation test results for Gradient 1 and lesion distribution. (A) Regions showing significant post-stroke changes in Gradient 1. Warm colours indicate areas where patients had significantly lower gradient values than controls, whereas cool colours indicate areas where patients had significantly higher values. Clusters correspond to thresholded 1 − p images (cut-off = 0.95). (B) Lesion distribution map showing all lesioned voxels across the 21 semantic aphasia (SA) patients.

2.4.6. Phase 2: Association between simulated gradient changes and semantic impairment in the semantic control network

To examine whether post-stroke simulated changes in Gradient 1 are associated with deficits in semantic cognition, we performed nonparametric t-tests using FSL's Randomise (Winkler et al., 2014), with 5000 permutations. The model included the semantic cognition composite score, as well as lesion size, age, and post-stroke period as covariates of no interest. The analysis was restricted to the semantic control network ROI (Jackson, 2021), from which all lesioned voxels were removed (see Figure 2.6A). The results revealed a cluster in the left inferior frontal gyrus (IFG) that was significantly associated with poor semantic performance ($p = 0.05$, corrected for multiple comparisons via non-parametric permutation testing; Figure 2.6B). To understand the nature of this effect, we extracted the gradient values of the left IFG cluster from the simulated post-stroke gradient difference maps and examined the association with semantic deficits. The scatterplot in Figure 2.6C shows that poorer semantic performance was associated with a larger shift toward the unimodal end of Gradient 1. Since left IFG typically falls towards the transmodal end of the principal gradient, a loss of transmodal "identity" in this region is a key predictor of semantic deficits. We focussed this analysis on Gradient 1 because it was simulated with high accuracy in Phase 1 and because changes within the semantic control network for this gradient have been associated with flexible semantic cognition in previous studies (Gao et al., 2022; Wang et al., 2020).

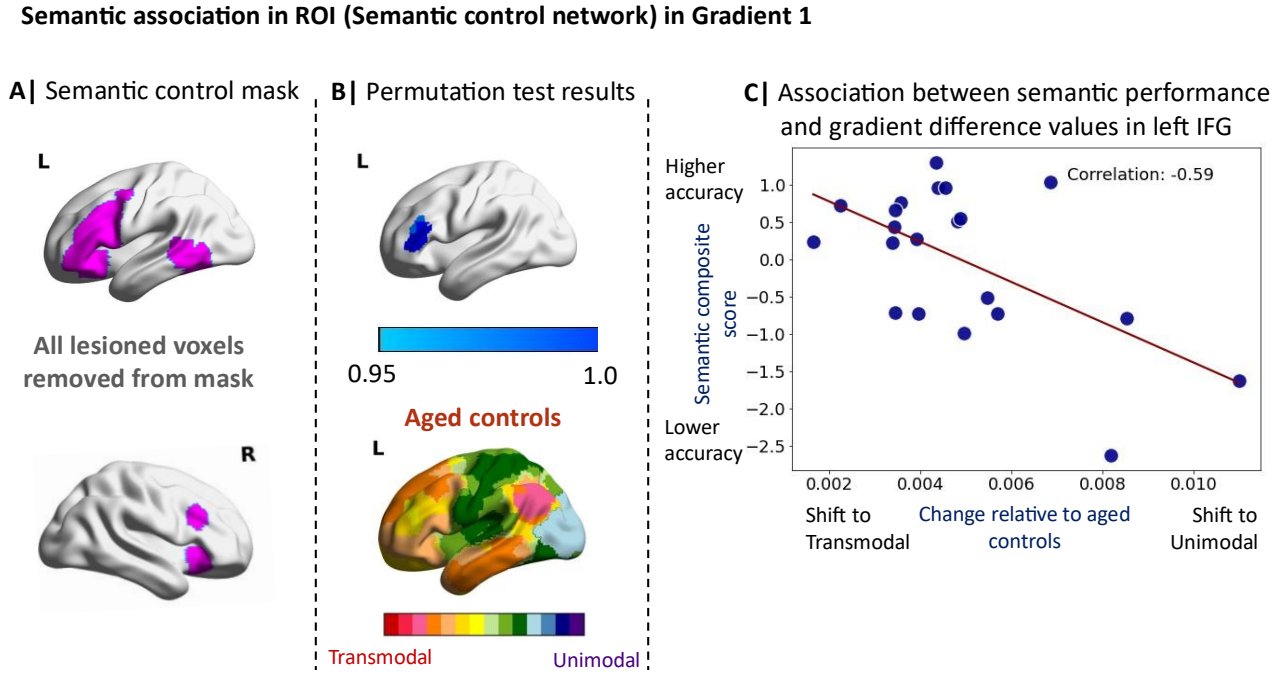

Figure 2.6. Semantic control network ROI analysis. (A) Semantic control network mask used for the ROI analyses, with all lesioned voxels removed. (B) Permutation test results within the semantic control network mask showing a significant cluster in the left inferior frontal gyrus (IFG) associated with poorer semantic performance (top panel). In aged controls (bottom panel), this region is positioned toward the default mode network (DMN) end of the principal gradient. Clusters correspond to thresholded 1 − p images (cut-off = 0.95). (C) Scatter plot showing the association between semantic performance and the direction of shift along the principal gradient in the left IFG cluster.

2.4.7. Phase 2: Whole-brain associations between simulated gradient changes and semantic impairment

We conducted exploratory whole-brain analyses for both Gradients 1 and 2 but no effects were identified. We also performed lesion-symptom mapping to identify lesion locations associated with semantic impairments in the SA group; however, no significant voxels were linked with semantic control deficits. This suggests that, at least in some circumstances, lesion-gradient mapping may be able to recover associations with cognitive outcomes even when lesion-symptom mapping produces null results.

2.5. Discussion

This study suggests that patients with semantic aphasia (SA) have altered functional connectivity gradients compared to age-matched controls, and that these changes predict semantic impairment. Phase 1 compared connectivity gradients extracted from resting-state fMRI with simulated post-stroke gradients derived from structural MRI. These results suggest that stroke-induced shifts in the principal axis of macroscale functional organisation can be approximated from structural lesion data alone. For the majority of participants, simulated changes on Gradient 1 captured the empirical pattern in resting state-fMRI with moderate accuracy, whereas simulations of Gradient 2 changes were less consistently reliable. Phase 2 used lesion-gradient mapping to test whether simulated gradient changes predicted semantic performance. Poorer semantic cognition was associated with left IFG showing more unimodal-like connectivity on Gradient 1, suggesting that impairment occurs when this key site within the semantic control network is shifted away from its transmodal role.

These findings suggest that SA is characterised by large-scale alterations in the distributed networks that support conceptual processing and retrieval. Using connectivity gradients to describe the brain's network architecture, we observed that stroke leads to a "compression" of functional space. Specifically, a structurally intact left IFG shifted its position towards the unimodal pole along the transmodal–unimodal axis, demonstrating gradient space reduction. This shift of the left IFG from the transmodal end towards the unimodal end was associated with semantic control impairment. This finding suggests that multimodal retrieval deficits in SA arise when spared semantic control regions lose their characteristic transmodal "identity" and shift toward a more unimodal-like profile. This movement within the neural state space likely reflects a loss of the functional distance required to generate distinct, context-sensitive patterns of retrieval (cf. Gao et al., 2022). Without this hierarchical separation, semantic cognition may become 'captured' by dominant associations, leading to stereotyped retrieval that lacks the flexibility to prioritise non-dominant features when the context requires it. Consequently, lesion-gradient mapping offers a way to capture how focal damage triggers reduced functional differentiation in remote, structurally preserved tissue.

2.5.1. Functional connectivity gradients capture whole-brain changes post-stroke

The SA patients had infarcts in left frontal and temporal regions, which altered whole-brain patterns of functional connectivity. Previous studies in humans (Bayrak et al., 2019) and macaques (Nashed et al., 2024) show that stroke lesions can cause cortical gradients to 'contract', such that heteromodal and unimodal regions are less differentiated on Gradient 1, and visual and auditory-motor regions are less differentiated on Gradient 2. Phase 1 reproduced this pattern for many regions (although there were some notable exceptions: visual cortex on Gradient 1 became more unimodal following stroke, and motor cortex on Gradient 2 separated further from visual cortex). In this way, SA was associated with reduced separation of DMN from auditory–motor regions specifically. The observation that

unimodal and transmodal cortex become more functionally similar following stroke aligns with previous findings showing that stroke patients do not deactivate the DMN during a motor task (Larivière et al., 2018) and show reduced functional connectivity within the DMN (Tuladhar et al., 2013; Zhu et al., 2019), suggesting less cohesive network functioning. Moreover, since the principal gradient captures the sequence of networks on the cortical surface—from DMN, through frontoparietal control, to attention and then to visual–motor networks—a reduction in the magnitude of the principal gradient following stroke reflects less separation between networks that typically occupy distinct positions along this hierarchy (Margulies et al., 2016), consistent with Carter et al.'s (2010) findings of less distinct network boundaries. Crucially, the observed shift of the left IFG toward the unimodal end of the gradient should not be interpreted as an increase in sensory-motor processing. Instead, it suggests a loss of functional hierarchical distance from unimodal systems. In the healthy brain, this distance allows transmodal hubs to integrate information across domains without being overwhelmed by immediate sensory input (Smallwood et al., 2021); its reduction in SA suggests that stroke weakens the heteromodal control processes required for semantic task demands.

Compared to traditional connectivity measures, the gradient framework offers a more holistic characterization of post-stroke reorganization. While seed-based analysis is often restricted by a priori region selection (Seewoo et al., 2021), and Independent Component Analysis (ICA) typically treats the brain as a set of separate (albeit potentially overlapping) statistical components (Li et al., 2014; Li et al., 2022; Seewoo et al., 2021), gradients capture the continuous functional transitions that define the brain's representational geometry. This allows for the detection of shifts in regions far beyond the primary lesion site, reflecting alterations in the global connectivity landscape rather than isolated edge-level disruptions. Furthermore, the principal gradient shows high reliability and predictive validity for cognitive phenotypes (Hong et al., 2020), supporting its utility as a biologically meaningful biomarker of cortical organization. Gradients are sensitive to individual differences (Serhan et al., 2025) and show systematic associations with cytoarchitectural features of the cortex (Royer et al., 2023), indicating that they capture biologically meaningful aspects of cortical organisation.

Despite these advantages, our focus on cortical gradients provides a partial view of reorganization. Stroke frequently involves subcortical systems, and while gradient methods can be extended to these structures, whole-brain cortical-subcortical integration remains an area for future development. Nevertheless, by capturing the 'collapse' of the functional hierarchy, this approach provides a sensitive window into how focal damage can disrupt the large-scale differentiation required for complex cognition, such as semantic control.

Simulating post-stroke connectivity gradient changes from lesion data: Our study highlights the potential of using lesion characteristics to predict functional changes in connectivity gradients (cf. Aswendt et al., 2021). To our knowledge, this is the first demonstration that simulated connectivity-gradient changes derived from structural lesions can be used to predict specific cognitive deficits. Prior work has shown lesion-induced alterations in gradients (Bayrak et al., 2019), but these were linked to general clinical severity (NIH Stroke Scale), rather than specific cognitive outcomes. By combining lesion topology with normative connectivity data, our approach provides a way to estimate the large-scale functional consequences of stroke across multiple dimensions of cortical organisation without resting-state fMRI, which is rarely collected in routine clinical settings. This suggests potential utility for early post-stroke prognosis, where lesion location could help predict specific cognitive vulnerabilities.

The simulation captured the empirical patterns in Gradient 1 with moderate accuracy; however, the approach also has inherent limitations. Because it estimates disruption using normative connectivity, it models the immediate impact of the lesion on connectivity gradients rather than any subsequent functional reorganisation. Although the simulation is based on lesion location and lesion load, it models each lesioned parcel's connectivity with all other parcels across the cortex using normative functional connectivity, meaning that global patterns of disruption are still represented. This may explain the differences in performance noted in Gradient 1 and Gradient 2. A reasonable explanation for Gradient 2's lower performance in modelling stroke effects could be perhaps because the observed stroke gradient may have reflected Wallerian degeneration, diaschisis and long-term neuroplastic reorganisation comparatively more than the functional disruptions. Furthermore, our model was constrained to cortical grey matter damage. It did not explicitly incorporate white-matter disconnection, which likely contributes to the full extent of functional disruption. (Griffis et al., 2019; Thiebaut De Schotten et al., 2014) Future iterations that incorporate markers of neuroplasticity alongside structural lesion data will likely improve the alignment between simulated and observed gradient alterations.

2.5.2. Role of the left IFG in semantic control

In Phase 2, poorer semantic cognition in SA was associated with changes in Gradient 1 within left anterior LIFG, in structurally intact tissue beyond the posterior LIFG region that was frequently lesioned. Specifically, this anterior cluster showed a connectivity profile that shifted toward the unimodal end of Gradient 1 when semantic performance was more impaired. This pattern is broadly consistent with neuroimaging and brain-stimulation studies in healthy participants that implicate anterior LIFG in semantic control (Jackson, 2021; Jefferies, 2013; Gao et al., 2021; Whitney et al., 2011; Diveica et al., 2021). Within the controlled semantic cognition framework, semantic behaviour reflects the interaction between heteromodal conceptual representations in the anterior temporal lobes and control processes supported by anterior LIFG, posterior temporal cortex and dorsal medial

prefrontal cortex (Lambon Ralph et al., 2017). A shift of anterior LIFG away from its typical transmodal position towards a more unimodal-like connectivity profile may reduce its ability to flexibly integrate conceptual information. This provides a plausible mechanistic account of why SA patients show multimodal semantic control deficits, even when anterior LIFG itself is not directly damaged. Another explanation for this finding is that semantic control regions are involved in the gating of sensory-motor activation during goal-dependent tasks (Eisenhauer et al., 2026; Jackson et al., 2021), and the IFG's shift toward the unimodal end of Gradient 1 may disrupt the capacity to prioritise the modality-specific features needed for context-dependent control.

Regions within the semantic control network, including LIFG, show intrinsic structural and functional connectivity with both the anterior temporal lobe and domain-general executive systems (Davey et al., 2016). They also occupy an intermediate position between the default mode and multiple-demand networks in terms of both functional responses to task difficulty and their location on the cortical surface (Chiou et al., 2021; Wang et al., 2021). LIFG dynamically adjusts its connectivity depending on task demands—for example, coupling with anterior temporal cortex during semantic association tasks and with visual cortex during decisions about the colour, shape or size of concepts (Chiou & Lambon Ralph, 2016). Our findings suggest that while healthy cognition relies on this temporary, task-dependent flexibility, stroke may cause a chronic loss of functional differentiation between these networks. The left IFG cluster identified in this study did not overlap with the multiple-demand network, indicating that the observed effect is specific to semantic control rather than domain-general executive processes.

In healthy brains, Gao et al. (2022) found that LIFG and other regions of the semantic control network alter their functional connectivity along Gradient 1 moment-to-moment as task demands vary. Retrieval of strong associations was associated with increased informational connectivity between the semantic control network and DMN regions at the transmodal apex of this gradient, consistent with cognition largely guided by long-term memory. In contrast, weak associations were associated with increased informational connectivity with the unimodal end of Gradient 1, reflecting higher multivariate pattern similarity between semantic control and attentional/sensory regions when non-dominant features are prioritised during controlled retrieval. While healthy cognition relies on this temporary, task-dependent flexibility, if the semantic control network becomes chronically less differentiated from neighbouring executive and attention systems post-stroke, it may be less able to support these diverse coupling patterns required for context appropriate semantic retrieval. This hypothesis could be tested directly in future work by applying a gradient framework to the analysis of functional connectivity during more automatic and controlled patterns of semantic retrieval in participants with SA.

2.6. Future directions

This study demonstrates the potential of lesion-gradient mapping for understanding cognitive changes following stroke, but given the novelty of our approach, there are many outstanding questions. Further research is needed to verify if Gradients 1 and 2 can be successfully simulated in cohorts with different lesion topologies and distinct cognitive or behavioural impairments. Since simulations of the second gradient were less reliable, future work should explore more complex biophysical models to determine if these can provide more accurate predictions of post-stroke connectivity changes within lower-order axes of variation in functional connectivity. In addition, analyses of longitudinal resting-state fMRI datasets would be valuable; such data could establish the extent to which functional gradients reorganise over time, potentially allowing future simulation models to account for neural plasticity following acute stroke.

While we focussed on SA, future work should consider measures of speech production, hemispatial neglect, apraxia and phonological processing, to examine whether different cognitive consequences of stroke relate to distinct gradient shifts. Furthermore, while semantic cognition is an ideal domain for this approach given its established links to cortical gradients (Gao et al., 2022; Shao et al., 2022; Gonzalez Alam et al., 2021), patients with semantic control deficits frequently present with co-occurring executive impairments (Souter et al., 2022). These domain-general deficits were not separated in the current study; therefore, future research should clarify whether the observed LIFG gradient shifts are specific to semantic control or reflect a broader disruption of executive systems. Finally, our analysis collapsed multimodal semantic deficits into a single composite measure. Examining modality-specific impairments in gradient space remains an important next step, particularly as the second gradient (visual-to-sensory-motor) may be sensitive to distinctions between verbal and non-verbal tasks.

The stroke participants included in this study left formal education at a mean age of 16.3 ± 1.5 years, indicating that the cohort was not highly educated on average. A previous study showed that greater pre-stroke educational attainment is associated with better post-stroke language performance (Roberts et al., 2024). For example, a recent study reported that pre-stroke formal education was positively associated with language performance across a wide range of language assessments in both aphasic and non-aphasic stroke participants. However, this educational advantage was attenuated in older participants with large lesions and severe aphasia. These findings suggest that educational attainment may contribute to individual differences in post-stroke language outcomes. Although the influence of pre-stroke education on functional connectivity gradients remains unclear, educational attainment may affect the brain's resilience to stroke-related network disruption. Future studies should therefore investigate whether pre-stroke educational attainment influences connectivity gradient

organisation and contributes to variability in post-stroke functional reorganisation and behavioural outcomes.

2.7. Conclusion

Our research indicates that structural MRI can be used to simulate key effects of stroke on intrinsic connectivity gradients, and that these simulated changes in functional organisation predict the severity of semantic impairment. The findings provide new insights into semantic cognition, suggesting that the transmodal "identity" of the left IFG—defined by its position at the heteromodal end of Gradient 1—is critical for normal function. Crucially, individual differences in impairment were captured by patient-specific gradient reconfigurations, demonstrating that successful semantic cognition depends on the maintenance of a stable, hierarchical differentiation across cortical systems. More broadly, this work contributes to the themes of multidimensionality, variability, and flexibility by examining how conceptual retrieval is supported by continuous dimensions of brain organisation. By using connectivity gradients as a formal description of the brain's representational geometry, we show that conceptual deficits do not arise from damage to a single module, but from altered positioning within a multidimensional neural state space.

Chapter 3

Reorganisation of functional connectivity gradients in post-stroke aphasia

3.1. Abstract

Aphasia after stroke arises from focal damage to language-relevant cortex but is accompanied by widespread alterations in functional connectivity. In 60 stroke survivors, we related principal component-derived language scores to both lesion location and stroke-related changes in resting-state functional organisation, combining structural lesion-symptom mapping with a gradient-based approach. Structural lesion-symptom mapping identifies which damaged regions are associated with specific language impairments but does not capture how surviving cortex is reconfigured within the brain's large-scale architecture. In contrast, lesion-gradient mapping characterises whole-brain connectivity gradients – data-driven axes that summarise the principal patterns of variation in cortical connectivity – and quantifies how behavioural variation relates to displacement of structurally intact regions along these intrinsic axes. Stroke was associated with altered positioning of cortical regions along the gradient separating default mode and control networks. Notably, the position of the left inferior frontal gyrus along this axis predicted dissociable language outcomes: displacement toward default mode connectivity patterns was associated with better speech but poorer writing performance. This opposing behavioural profile suggests that inferior frontal cortex contributes to language through flexible large-scale coupling, with distinct coupling regimes differentially supporting spoken and written production. These findings indicate that gradient-based mapping provides a mechanistic link between focal tissue damage and distributed behavioural consequences by revealing systematic reorganisation of macroscale functional architecture beyond the lesion site.

3.2. Introduction

Aphasia is a common consequence of stroke, producing heterogeneous impairments across language tasks and other cognitive domains (Jefferies & Lambon Ralph, 2006; Schumacher et al., 2019). Patients may experience difficulties in comprehension, speech, reading, writing, and conversation, with major effects on quality of life (Han et al., 2023; Spaccavento et al., 2013). This variability reflects the fact that language is supported by a distributed neural system spanning multiple cortical and subcortical regions (Wilson & Hula, 2019). Yet, because stroke lesions differ in their size and location, no two patients present with the same profile, making it challenging to predict outcomes and to tailor rehabilitation effectively. Lesion–symptom mapping has been instrumental in linking focal damage to specific deficits, identifying contributions of regions such as the anterior insula, inferior frontal gyrus, and precentral gyrus to speech fluency (Bates et al., 2003; Borovsky et al., 2007; Halai et al., 2017). However, symptoms arise not only from damage to these areas, but also from disruptions to broader networks and disconnection between them (Hope et al., 2024; Zevgolatakou et al., 2022; Bonilha & Fridriksson, 2008). Recovery is equally variable: some patients regain substantial function years after stroke, while others show persistent deficits (Hope et al., 2013; Breitenstein et al., 2017; Wilson & Schneck, 2021). Lesion location and size are important determinants of outcome, but they do not fully explain recovery trajectories, which, among other factors, also depend on functional reorganisation of surviving tissue and remote changes in whole-brain connectivity (Kiran & Thompson, 2019; Thiebaut de Schotten et al., 2020).

Resting-state functional MRI has been widely used to characterise network-level changes after stroke, including connectivity between language regions, interhemispheric interactions between homotopic areas, data-driven identification of large-scale networks, and graph-theoretical measures of network properties such as modularity or hubness (Yourganov et al., 2017; Chen et al., 2021). These methods have been valuable in showing that stroke alters both language-related and domain-general systems, including the default mode, salience, and dorsal attention networks (Falconer et al., 2024; Tsiakiri et al., 2024). However, each approach provides only a partial view: region-of-interest analyses are constrained by prior assumptions, interhemispheric measures capture only one dimension of connectivity, and data-driven techniques such as independent components analysis or graph theory fragment the system into discrete parts. What is missing is a holistic description that situates local and network-level changes within the brain's continuous macroscale organisation (Margulies et al., 2016). Such a perspective may better reveal how distributed functional systems support recovery and how focal lesions induce widespread alterations that shape cognitive and language outcomes.

Connectivity gradients offer a data-driven way to summarise large-scale patterns of functional connectivity across the cortex (Margulies et al., 2016; Huntenburg et al., 2018). Rather than dividing the brain into discrete spatially defined networks, gradients position cortical regions along continuous

axes based on similarities in their whole-brain connectivity profiles, with each brain region occupying a unique position in an abstract gradient space. The principal connectivity gradient reflects the dominant pattern of variation in cortical connectivity and is commonly linked, post hoc, with unimodal sensory–motor connectivity at one pole and transmodal default mode regions at the other, capturing the hierarchy from local specialisation to global integration (Margulies et al., 2016; Wang et al., 2025). Additional higher-order gradients capture further, independent patterns of connectivity variation; for example, the second gradient differentiates between visual and somatomotor profiles, while the third distinguishes patterns typically associated with the control and default mode networks (Wang et al., 2020). Critically, because gradients capture multiple independent components of connectivity, a region may appear normal along one axis but abnormal along another, reflecting different functional roles or task contexts. Language processing depends on coordination across distributed cortical regions including auditory areas for sound processing, temporal regions for word comprehension, and frontal regions for speech planning and production (Hickok & Poeppel, 2007). By situating each region within a continuous, multidimensional connectivity space, gradients provide a nuanced, component-specific characterisation of disrupted connectivity, revealing how stroke-related disruptions to functional connectivity relate to behavioural performance.

Here, we apply a combined lesion–symptom and lesion–gradient symptom mapping approach in a large cohort of stroke survivors from the PLORAS dataset who all had both structural and resting-state functional MRI as well as language and cognitive assessments. We asked three questions: (i) which lesion sites are associated with specific language deficits, (ii) how does stroke disrupt whole-brain functional connectivity as summarised by connectivity gradients, and (iii) how do gradient-based measures capture associations with language outcomes beyond focal lesion effects? By relating principal components of performance on the Comprehensive Aphasia Test to both lesion location and gradient-derived connectivity measures from resting-state fMRI, we aimed to move beyond focal accounts by incorporating large-scale patterns of functional connectivity gradients in the study of aphasia (Fox, 2018; Meier, 2022; Crinion & Price, 2005).

3.3. Methods

3.3.1. Participants

The source dataset included 83 stroke survivors and 86 age-matched control participants from the PLORAS (Predict Language Outcome and Recovery After Stroke) dataset (Seghier et al., 2016). All participants were free from other neurological or psychiatric conditions such as dementia or depression, and were selected to have both a T1-weighted structural scan and resting-state fMRI. Stroke survivors completed an assessment of cognition and language using the Comprehensive

Aphasia Test (CAT) (Swinburn et al., 2004) and provided demographic information (age, gender, handedness, age at stroke onset, date of scanning and CAT). We applied further inclusion criteria to select participants with resting state fMRI scans suitable for functional connectivity analyses: i) a minimum of 70% valid scans; ii) no denoising failure cases; and iii) a mean head motion less than 0.35 mm.

The final sample consisted of 60 stroke survivors (24 females; mean age = 56.86 ± 10.74 years) and 79 age-matched controls (43 females; mean age = 38.23 ± 16.2 years). The mean age at stroke onset was 52.25 ± 11.51 years. All stroke participants were in the chronic phase, with a mean post-stroke duration of 55.31 ± 58.12 months. Among the 60 stroke participants, 36 had left-hemisphere lesions, 7 had right-hemisphere lesions, 15 had bilateral lesions, and 2 had lacunar infarcts. Lesion volume, estimated by the number of affected voxels, averaged 11,590 (SD = 11,320) voxels. Lesions spanned both cortical and subcortical regions, with the greatest overlap in the left superior corona radiata (present in 30 of 60 participants; Figure 3.1. Across the sample, damage extended from frontal and parietal into occipital (visual) regions and portions of the temporal lobe, while sparing the temporal pole, temporal fusiform cortex, and parahippocampal gyrus.

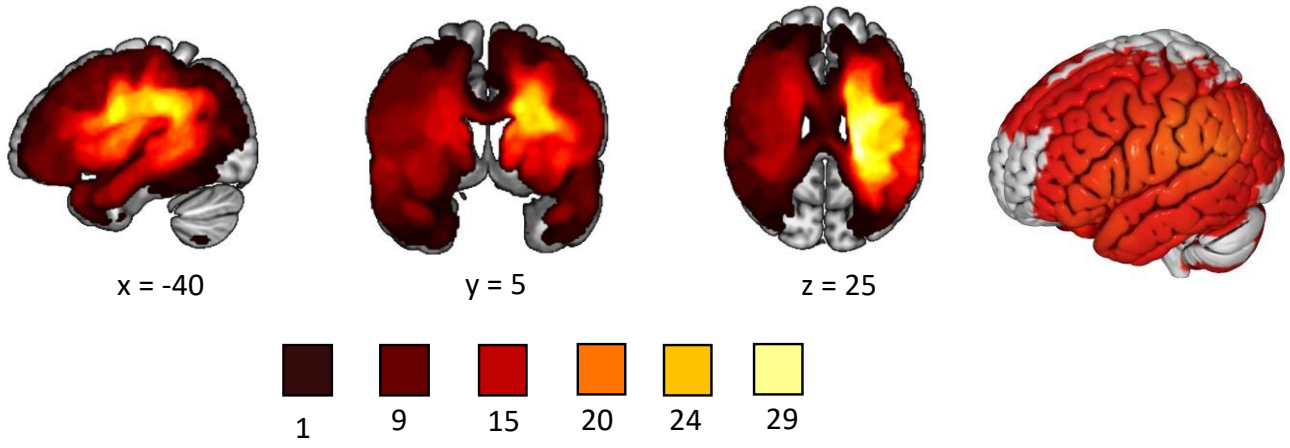

Figure 3.1. Overlap map of stroke lesions (N = 60). Binarised lesion maps were generated using FSLmaths (Jenkinson et al., 2012) and displayed in MNI space with MRIcroGL. Brighter colours indicate greater lesion overlap across stroke participants.

3.3.2. Comprehensive aphasia test

Stroke-induced language dysfunction was examined using the Comprehensive Aphasia Test (CAT; Swinburn et al., 2004). This test provides a broad assessment of aphasic patients' performance in language functions and related cognitive domains. It includes language production tests (repetition, naming, and spoken picture description), as well as comprehension of spoken and written language, reading, writing, and repetition skills. Additional subtests evaluate cognitive domains, including line bisection, semantic memory, word fluency, recognition memory, gesture object use, and arithmetic.

Principal component analysis was performed to reduce these correlated language tests into distinct language domains explaining unique variance. First, we identified which subtests were suitable for inclusion by examining score variability using the interquartile range (IQR). Five subtests with few items and an IQR of zero, indicating that at least 50% of participants received the same score, were excluded (semantic memory, repetition of complex words, writing copy, comprehension of spoken paragraph, and reading functional words). PCA with oblique rotation was then performed on the standardised scores of the remaining subtests using R Studio. Components with eigenvalues greater than 1 were retained, yielding six components. The first four components loaded on multiple assessments and were readily interpretable as broader language domains; the remaining two components captured more task-specific variance and are reported in the Supplementary Materials (Section I).

3.3.3. Lesion segmentation

High-resolution whole-brain T1-weighted structural MRI (1 mm isotropic) was acquired for all participants, at the same time as the resting-state data, using research-dedicated 3T Siemens scanners at the Department of Imaging Neuroscience, UCL. Lesion segmentation was performed using established procedures implemented in SPM (running in MATLAB), in which each T1-weighted image was spatially normalised to MNI space and converted into a continuous lesion map that quantifies structural abnormality at each voxel on a scale from 0 (normal) to 1 (abnormal), relative to normative data from neurologically healthy controls (Seghier et al., 2008). Each lesion map was thresholded at 0.3 to generate binary lesion images. As this procedure has previously been shown to yield robust associations with behavioural outcomes, no other manual edits were applied. Segmented lesion maps were binarised using the fslmaths tool from FSL (FMRIB's Software Library), and lesion–symptom mapping was performed on these maps.

3.3.4. Resting-state fMRI data preprocessing

We used the default resting-state fMRI preprocessing pipeline in CONN (https://www.nitrc.org/projects/conn) (Whitfield-Gabrieli and Nieto-Castanon, 2012), consisting of motion estimation, correction by volume realignment through a six-parameter rigid body transformation, slice time correction, and simultaneous white matter, grey matter, and cerebrospinal

fluid segmentation and normalization to MNI152 stereotactic space (2 mm isotropic). These measures were applied to both functional and structural data. After preprocessing, the following potential confounding variables were statistically controlled for: six motion parameters determined at the previous step and their 1st- and 2nd-order derivatives; volumes with excessive movement (motion greater than 0.5 mm and global signal changes larger than z = 3); linear drifts; and five principal components of the signal from white matter and cerebrospinal fluid (CompCor approach) (Behzadi et al., 2007). Then, a band-pass filter was applied to the data between 0.01 and 0.1 Hz. Global signal regression was not performed.

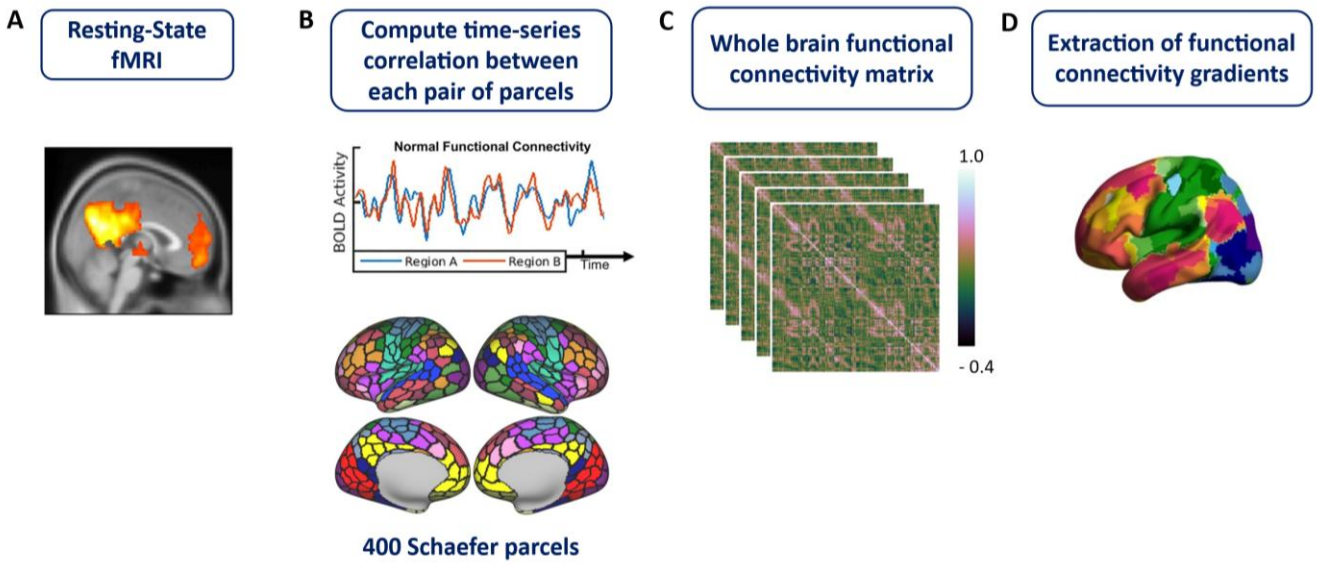

Figure 3.2. Processing pipeline for functional connectivity gradients in stroke participants and aged matched controls. A) Resting-state data of aged matched controls and stroke participants were pre-processed. B) Pearson correlations were computed between the mean time series of each of the 400 ROIs. C) A 400 × 400 functional connectivity matrix was generated for each participant in both groups. D) Functional connectivity gradients were extracted from the functional connectivity matrix for each participant.

3.3.5. Whole-brain functional connectivity

After preprocessing and denoising the resting-state fMRI data for each participant in both groups (stroke and controls), we computed a functional connectivity (FC) matrix (Figure 3.2) and extracted the mean functional time series of each of the 400 cortical parcels, based on the Schaefer parcellation (Schaefer et al., 2018) (https://github.com/ThomasYeoLab/CBIG/tree/master/stable_projects/brain_parcellation/Schaefer2018_LocalGlobal). We then constructed a 400 × 400 FC matrix by calculating pairwise Pearson correlations between the mean time series of all parcels. These FC matrices were then averaged within each group to generate group-level connectivity matrices separately for stroke participants and age-matched controls. Finally, each Schaefer parcel contributing to the functional connectivity matrices was assigned to one of the seven canonical large-scale functional networks defined by Yeo et al. (2011), according to maximum overlap between parcel and network. The Yeo networks were derived from group-level clustering of resting-state functional connectivity in healthy individuals and are labelled: (1) visual, (2) somatomotor, (3) dorsal attention, (4) ventral attention (or salience), (5) limbic, (6) frontoparietal control, and (7) default mode. We used these network assignments purely for interpretive reference. They did not influence the construction of functional connectivity matrices or the estimation of connectivity gradients.

3.3.6. Functional connectivity gradient extraction

Functional connectivity gradients for stroke participants and aged matched controls were extracted from the functional connectivity matrices using the BrainSpace Toolbox (Vos de Wael et al., 2020). Healthy brains are expected to share common dominant axes of functional connectivity variation, with inter-subject variability in the precise positioning of regions along each axis. We focused on the first three gradients (Gradients 1-3), which capture the most dominant sources of variance in functional connectivity and have been linked to cognition in prior work (Margulies et al., 2016; Shao et al., 2022). To estimate Gradients 1–3 in each individual, we first extracted ten gradients from the functional connectivity matrix of each stroke participants and each age-matched control (dimensionality-reduction technique: diffusion embedding; kernel: normalized angle; sparsity: 0.9). The pipeline for gradient extraction is shown in Figure 3.2. Ten gradients were extracted because this allows the first three gradients to achieve a higher fit with canonical group-level gradients (Margulies et al., 2016; Gonzalez Alam et al., 2021; McKeown et al., 2020). Gradients estimated from individual datasets can differ in orientation and ordering. Therefore, we aligned individual gradients for both stroke participants and controls to gradients extracted from the Human Connectome Project (HCP) dataset (n = 217; 122 women; mean ± SD age = 28.5 ± 3.7 years; Vos de Wael et al., 2018) using Procrustes rotation. This procedure translates, rotates, and scales configurations to optimise alignment with the larger group average (Goodall, 1991; Vos de Wael et al., 2020), while preserving the overall shape and structure of the data (Siegel et al., 2017). In other words, this alignment step improves

interpretability by expressing individual gradients in a common coordinate system, facilitating comparison to gradients reported in other studies (Margulies et al., 2016; Gonzalez Alam et al., 2021; McKeown et al., 2020).

3.3.7. Post-stroke gradient differences

Connectivity gradients for stroke participants contained effects of both stroke and aging. To isolate stroke-specific changes in connectivity, we subtracted each post-stroke gradient from the average gradient of age-matched controls included in this study using fslmaths (FMRIB's Software Library). The resulting difference maps illustrate how each brain parcel shifted across the gradients following stroke; statistical analyses were then performed on these post-stroke gradient differences.

3.3.8. Statistical analyses

We conducted lesion–symptom mapping and lesion–gradient mapping. Lesion–gradient mapping was performed to identify probabilistic associations between lesion locations and the four PCA-derived components accounting for the largest sources of variance in language performance on the CAT. To directly compare lesion–symptom results with disruptions to gradient-based functional connectivity, we only examined lesions that damaged the cortex. This excluded 2 participants with lacunar infarcts and 6 with subcortical infarcts, leaving a sample of 52 stroke participants. Lesion–gradient symptom mapping addressed two questions: (1) What are the post-stroke changes in functional connectivity gradients? and (2) Can these changes in connectivity gradients predict language outcomes?

We used non-parametric t-tests in Randomise (Winkler et al., 2014; https://fsl.fmrib.ox.ac.uk/fsl/fslwiki/Randomise/UserGuide), with 5,000 permutations, for both lesion–symptom and lesion–gradient mapping. For lesion–symptom mapping, the general linear model included binarised cortical lesion maps (n = 52) and each stroke participant's language composite scores as covariates of interest, with whole-brain lesion size, age, and post-stroke duration were included as a covariates of no interest. Whole-brain lesion size was included to control for overall lesion burden, because behavioural outcomes reflect the total extent of the damage. Threshold-Free Cluster Enhancement (TFCE) was applied to identify significant, spatially extended lesioned clusters rather than relying solely on voxel-wise statistics (Smith & Nichols, 2009). Family-wise error correction was applied, and each contrast was thresholded at $p < 0.05$ to identify the brain regions significantly associated with each function.

For lesion–gradient mapping (n = 60), a general linear model was used to examine the association between stroke-induced connectivity-gradient changes (difference maps relative to healthy controls) and the four PCA-derived cognitive component scores. The model included the connectivity gradient change maps and the four component scores as covariates of interest, with whole-brain lesion size, age, and post-stroke duration included as covariates of no interest. Contrasts were set up for each PCA-derived component to identify parcels associated with poorer performance (Kiran, 2012). TFCE

was implemented to identify parcels showing statistically significant associations between connectivity-gradient values and language outcomes, accounting for spatial contiguity across neighbouring parcels and correcting for multiple comparisons.

Lesion-gradient analyses were performed across the whole-brain and within the Neurosynth-derived language-network mask. A lesion-overlap map was generated by combining cortical lesion masks from all participants. Voxels damaged in at least 25% of individuals were excluded to ensure analyses focused on connectivity changes in structurally intact tissue. This threshold corresponded to approximately 75% of all lesioned voxels, which were excluded from the whole-brain analysis. The same 25% threshold was applied to remove lesioned voxels from the language-network ROI. For visualisation, statistical maps for each contrast were thresholded at 0.95, corresponding to $p < 0.05$.

3.4. Results

3.4.1. Principal Component Analysis: Comprehensive Aphasia Test

The first four components accounted for 59% of the total variance, while two additional components explained a further 10%, giving a cumulative variance of 69%. The PCA loading matrix of CAT subtests and the scree plot illustrating the eigenvalues of each principal component are reported in Section I of the supplementary material (Supplementary Figure 3.S1). The first component (explaining 36% of the variance) had strong loadings on reading words (0.95), object naming (0.79), reading non-words (0.77), and reading complex words (0.75). The second component (explaining 9% of the variance) had strong loadings on repetition of digit strings (0.77) and sentence repetition (0.68) and was associated with phonology and working memory. The third component (explaining 7% of the variance) had high loadings for written picture naming (0.89) and writing to dictation (0.69) and was associated with writing and visuo-motor capacity. The fourth component (explaining 6% of the variance) showed strong loadings on comprehension of written words (0.82), comprehension of spoken words (0.54), and arithmetic (0.58), suggestive of semantic and broader cognitive difficulties, but was more mixed across tasks and showed more cross-loading with other components. Two further components had eigenvalues exceeding 1 but were dominated by loadings from single tasks assessing recognition memory (0.65) and gesture (0.94), respectively. As such, these components were treated as task-specific variance rather than coherent latent dimensions. They were included as covariates in subsequent brain analyses to account for this variance, but were not interpreted further (results are reported in Section I of the Supplementary Materials). PCA scores for each component were extracted; lower PCA scores reflected greater impairment on the respective component. These language component scores were used in lesion–symptom and lesion–gradient mapping analyses.

3.4.2. Lesion symptom mapping

Lesion–symptom mapping identified significant clusters associated with three language components from the PCA. PCA-2 (associated with poor phonology and working memory) showed the largest significant effect, which included left Heschl's gyrus, parietal operculum, the anterior part of the superior temporal gyrus, the posterior part of the middle temporal gyrus, angular gyrus, supramarginal gyrus, and the superior division of the lateral occipital cortex (Figure 3.3A). PCA-3 (associated with worse visuomotor performance) identified a cluster extending from the temporo-occipital part of the inferior temporal gyrus to the superior and inferior divisions of the lateral occipital cortex, as well as the superior parietal lobule, precuneus, and postcentral gyrus in the right hemisphere (Figure 3.3B). PCA-4 (associated with poor performance on comprehension/arithmetic) identified the left middle temporal gyrus (temporo-occipital part) and the posterior part of the supramarginal gyrus (Figure 3.3C). PCA-1 (associated with speech production) did not identify any significant effects in lesion-symptom mapping.

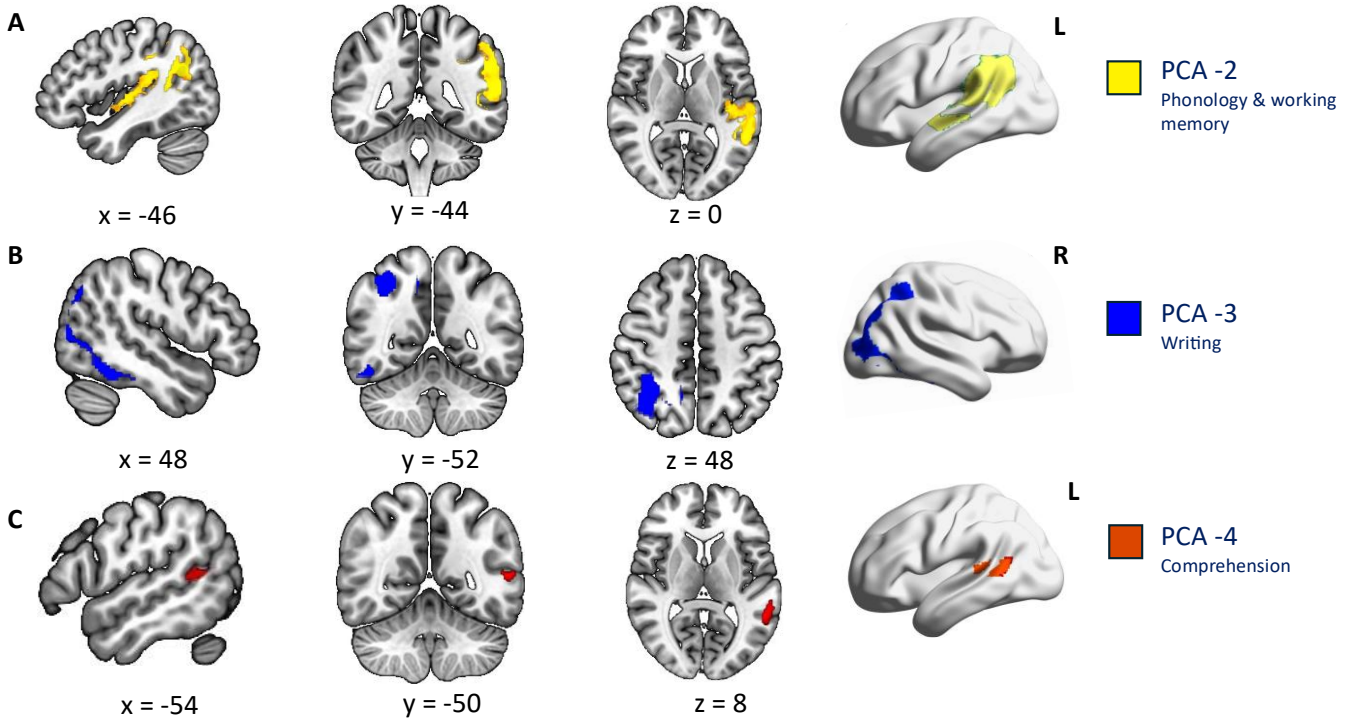

Figure 3.3. Lesion–symptom associations with PCA-derived language outcomes. A) Lesion locations associated with PCA-2 (phonology and working memory). B) Lesion locations associated with PCA-3 (writing and visuomotor capacity). C) Lesion locations associated with PCA-4 (comprehension/control difficulties).

3.4.3. Post-stroke gradient differences

Figure 3.4 shows connectivity gradients for young adults from the HCP dataset, plus the age-matched controls and stroke participants included in this study. Gradients for the young HCP sample, reproduced from Margulies et al. (2016), are displayed using a warm-to-cool colour scale: warm colours indicate higher gradient values, and cool colours indicate lower values. Gradients for the age-matched controls and stroke participants are shown using a purple-to-green colour scale, with darker purple indicating higher values and darker green indicating lower values. Gradient 1 differentiates unimodal (green) from transmodal (purple) regions; Gradient 2 separates motor (green) and visual (purple) regions; and Gradient 3 distinguishes default mode (green) and control networks (purple). Data for the stroke volunteers and controls are plotted on the same scale for each gradient. The maps are interpreted by comparing the colour assigned to each cortical region between these two groups; differences in colour reflect differences in a region's position along the gradient. While both the control and stroke participants show the basic gradient structure identified by Margulies et al. (2016) in the HCP sample, some subtle differences in the magnitude of these gradients are visible – with less bright purple and green shades for the stroke survivors indicating that the magnitude of the connectivity gradients is attenuated following stroke (i.e. the networks that fall at opposite ends of these dimensions of connectivity are less distinct).

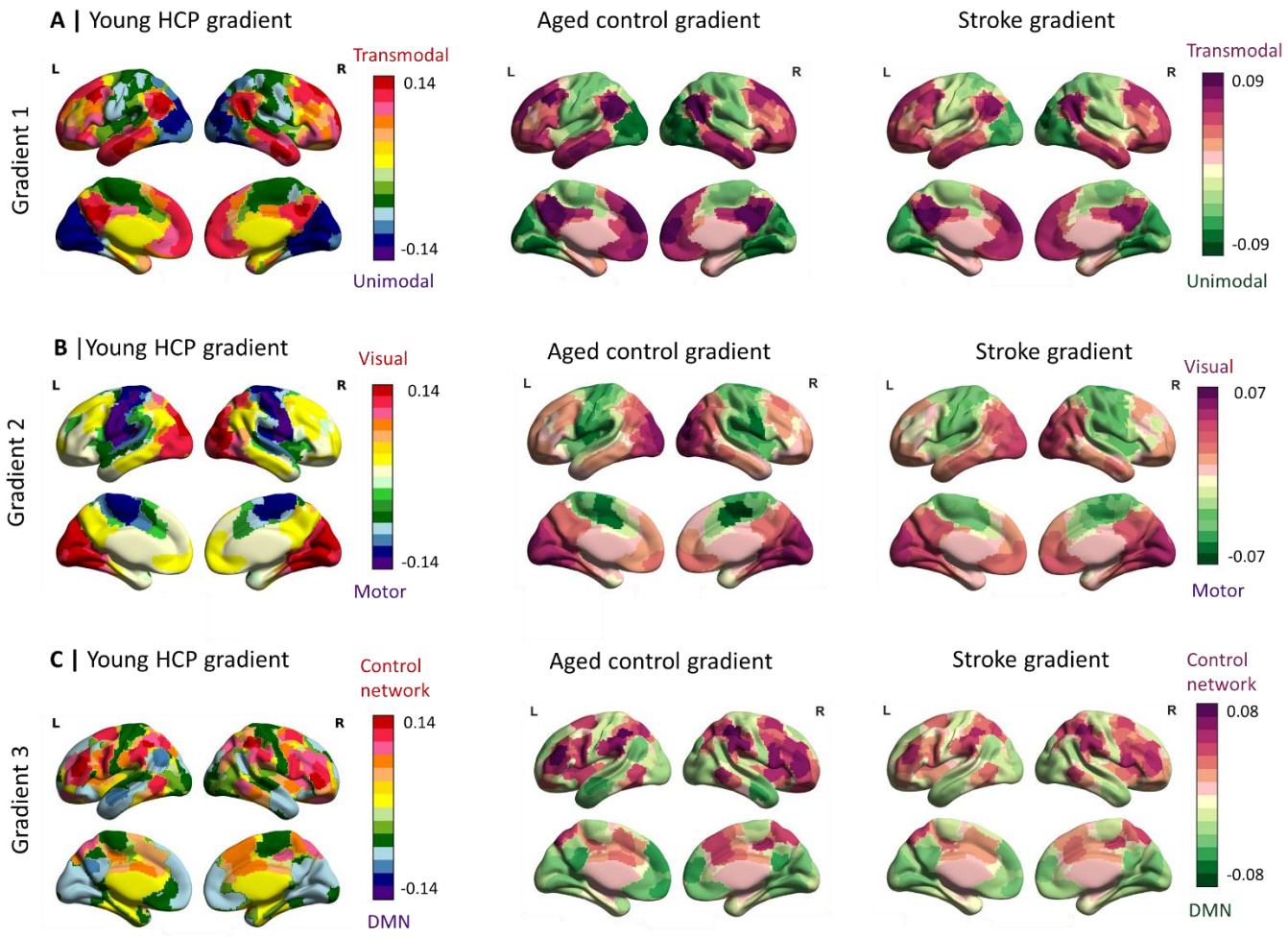

Figure 3.4. Functional connectivity gradients for age-matched controls and stroke participants from the PLORAS dataset, shown alongside canonical gradients from the young HCP sample (from Margulies et al., 2016). In control and stroke participants, darker purple indicates higher gradient values and darker green indicates lower values. Panel A shows Gradient 1, representing the unimodal–to–transmodal axis. Panel B shows Gradient 2, representing the visual–to–motor axis. Panel C shows Gradient 3, distinguishing between the default mode and control networks. Compared with age-matched controls, stroke survivors show reduced gradient differentiation across all three gradients.

To isolate stroke-specific effects, we subtracted each stroke participant's connectivity gradient from the average gradient map of age-matched controls, generating post-stroke difference maps for all three gradients. The average post-stroke difference maps for all three gradients are provided in Section II of the supplementary material (Supplementary Figure 3.S2). A non-parametric t-test with 5,000 permutations was used to determine significant post-stroke changes across the three gradients. Figure 3.5 shows the significant post-stroke changes on the gradients. Gradient 1 (unimodal

vs. transmodal) showed reduced differentiation after stroke, with transmodal regions—including the prefrontal cortex, temporal pole, middle and inferior temporal gyri, and right posterior cingulate—shifting toward the unimodal end of the gradient (Figure 3.5A, warm colours). In contrast, unimodal regions such as the lateral occipital cortex and motor regions shifted toward the transmodal end (Figure 3.5A, cool colours). Gradient 2 (visual vs. motor) also showed significant post-stroke changes: lateral and medial prefrontal regions shifted toward the motor end, while the pre- and postcentral gyri shifted toward the visual end, particularly in the right hemisphere (Figure 3.5B). Gradient 3 (DMN vs. cognitive control) showed the most extensive post-stroke changes. Regions typically belonging to the control network—including the inferior frontal gyrus, frontal pole, supramarginal gyrus, and anterior cingulate cortex—shifted toward the DMN end of the spectrum (Figure 3.5C). In contrast, DMN regions—including the medial prefrontal cortex, left dorsolateral prefrontal cortex, and lateral temporal cortex—as well as regions outside the DMN, such as motor areas, were positioned closer to the control-network end of this gradient axis (Figure 3.5C).

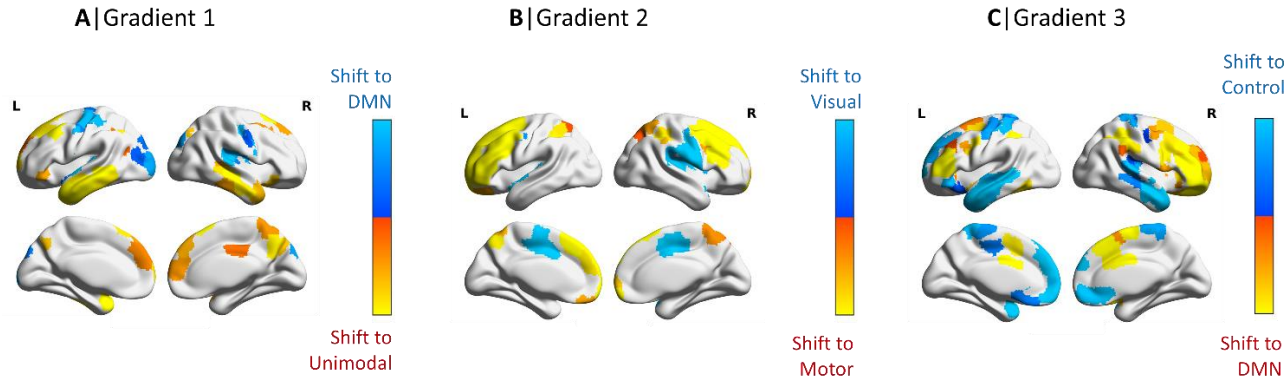

Figure 3.5. Significant post-stroke gradient changes for Gradients 1–3. Panel A shows Gradient 1, panel B shows Gradient 2, and panel C shows Gradient 3. Difference maps were generated by subtracting the mean age-matched control gradient map from each stroke participant's gradient map. Warm-coloured regions indicate areas typically positioned toward the upper end of the gradient that shifted toward the lower end after stroke, whereas cool-coloured regions indicate areas typically positioned toward the lower end that shifted toward the upper end.

3.4.4. Association between post-stroke functional connectivity gradient changes and language outcomes within the language network

We examined how stroke-related changes in functional connectivity gradients within the language network related to PCA-derived language outcomes. We focussed on changes within the language network since the available behavioural data focussed on language assessments; changes in the position of language regions within the brain's connectivity landscape are most likely to relate to these outcomes. To focus on intact tissue, voxels with ≥25% lesion involvement were excluded from the language-network mask (Figure 3.6A).

Significant associations with Gradient 3 were found for PCA-1 (speech production), PCA-3 (writing), and PCA-5 (gesture–object use; reported in Section III of the Supplementary Materials, as PCA-5 loaded on a single task: Supplementary Figure 3.S3). Displacement of the left inferior frontal gyrus (IFG) pars triangularis (Figure 3.6B) toward the DMN end of Gradient 3 was associated with better speech performance in stroke survivors (Figure 3.6C). In healthy controls, this region is typically positioned toward the control network end of Gradient 3; thus, post-stroke movement toward the DMN reflects a relative shift in large-scale coupling. Notably, this same displacement of left IFG along Gradient 3 was associated with poorer writing to dictation (Figure 3.6D), consistent with reduced engagement of control-related connectivity that may be required to coordinate linguistic, visuomotor, and executive processes during written output. These findings indicate that variation in IFG coupling along the DMN–control axis has dissociable behavioural consequences across language domains. A confirmatory permutation analysis found the results were unchanged when two participants who had lesions including this LIFG region were removed from the sample; PCA-1 and PCA-3 showed the same association with Gradient 3 displacement relative to age-matched controls.

To minimise the risk of Type II errors, we also conducted whole-brain lesion–gradient–symptom analyses relating gradient changes to PCA-derived language components, excluding voxels lesioned in ≥25% of participants. Full results are reported in Section IV of the Supplementary Materials (Supplementary Figure 3.S4).

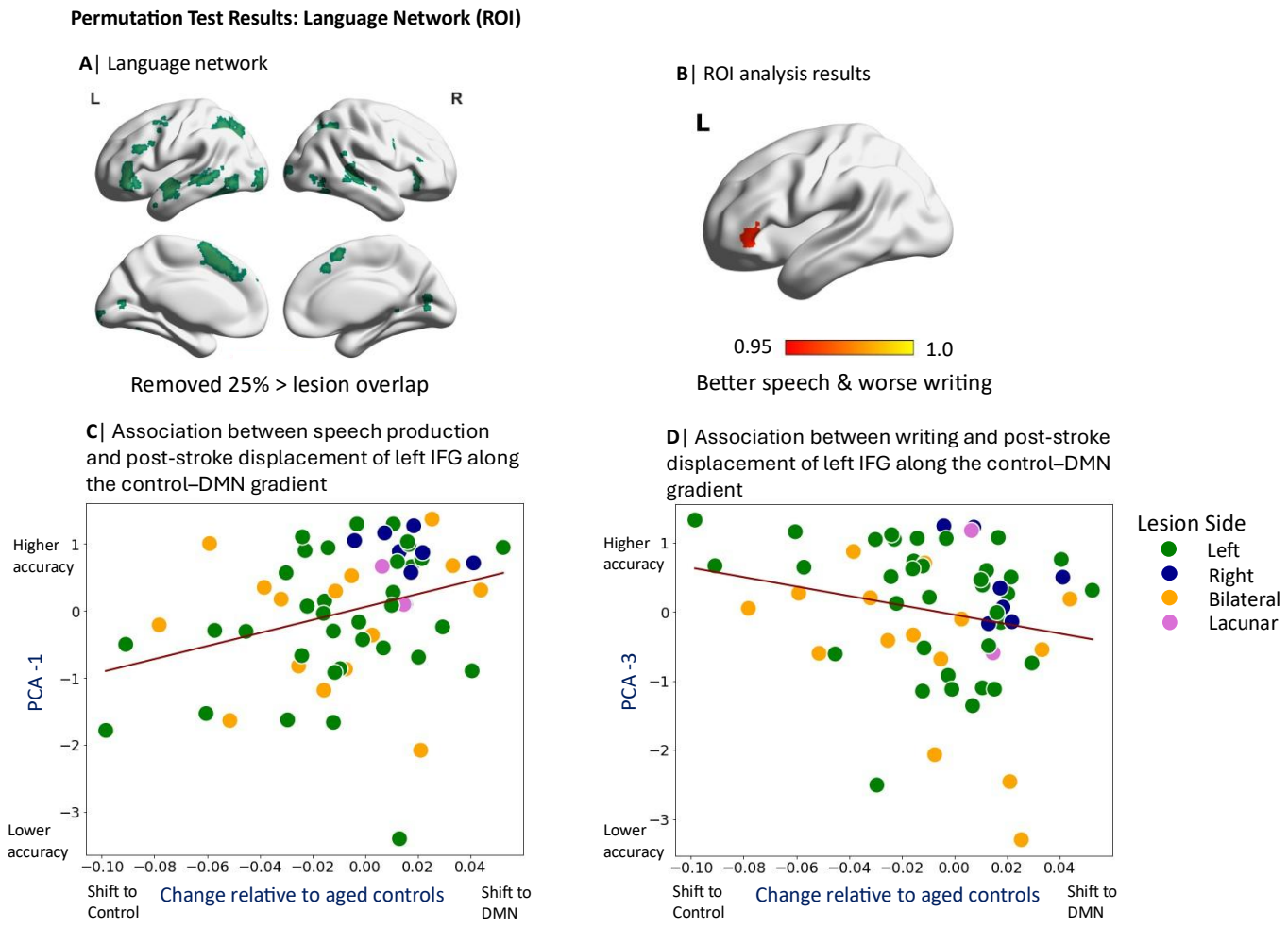

Figure 3.6. Permutation test results within the language ROI. A) Language-network mask used for the ROI analyses after removing lesion voxels. B) A significant cluster in the left inferior frontal gyrus (IFG) showed opposing behavioural associations along Gradient 3 (the default mode–control axis): displacement toward the default mode end (i.e. relatively greater DMN and reduced executive connectivity) was associated with higher PCA-1 scores (better speech production) and lower PCA-3 scores (poorer writing performance). C) Scatterplot showing the relationship between left IFG position along Gradient 3 and PCA-1 scores (speech production). D) Scatterplot showing the relationship between left IFG position along Gradient 3 and PCA-3 scores (writing ability).

3.5. Summary of results

Lesion–symptom mapping highlighted distinct neural substrates for specific language components: left temporoparietal damage was associated with verbal working memory deficits, right intraparietal sulcus lesions were linked to impaired visuo-motor tasks, and left posterior temporal lesions affected a component loading on comprehension and arithmetic, consistent with disruption to representational control processes. Beyond these structural effects, lesion–gradient mapping demonstrated that shifts in functional connectivity along the control–default mode axis (Gradient 3) captured cognitively meaningful aspects of functional reorganisation. Within the language network, left-hemispheric control regions exhibited greater functional affiliation with the DMN: a shift of the left inferior frontal gyrus towards this end of Gradient 3 predicted better speech production but poorer visuo-motor performance, reflecting domain-specific trade-offs in network reorganisation.

3.6. Discussion

This study shows that post-stroke language outcomes reflect both the location of structural damage and systematic variation in large-scale functional organisation captured by connectivity gradients. By integrating lesion–symptom mapping with gradient-based analyses, we provide a unified framework for understanding how focal injuries interact with the brain's intrinsic macroscale architecture to shape behavioural variability after stroke. Lesion mapping identifies regions in which tissue damage is associated with persistent language deficits, whereas gradient analyses quantify how surviving cortex is positioned along principal axes of functional organisation – particularly the axis separating default mode and control networks – and how displacement along these axes relates to language performance. Gradient displacement reflects structured reconfiguration of large-scale coupling patterns whose behavioural consequences depend on task demands. For example, variation in the position of left inferior frontal gyrus along the DMN–control axis was associated with opposing effects on speech and writing, indicating that differences in large-scale embedding of this region constrain distinct language functions. These findings situate post-stroke language variability within the geometry of intrinsic cortical organisation rather than attributing outcomes solely to lesion location.

3.6.1. Interpretation of lesion-symptom mapping

Lesion–symptom mapping was used to relate anatomical damage to behavioural impairment via PCA-derived dimensions of task performance. Our interpretation of these lesion–component associations draws on both the task loadings defining each component and prior evidence linking specific regions to cognitive functions; where these sources converge, the associations provide stronger inference about the functional consequences of focal damage. Convergent lesion evidence was observed for

three PCA components (2, 3 and 4; see below). In contrast, no focal lesion effects were identified for PCA-1, which loaded heavily on speech production tasks. This absence of a localised lesion correlate suggests that variability in speech production in chronic aphasia may be less dependent on damage to a single cortical site and more influenced by distributed or reconfigured network dynamics. Consistent with this interpretation, PCA-1 showed significant associations with displacement along connectivity gradients (reported below), indicating that speech outcomes were better captured by variation in large-scale functional embedding than by focal tissue loss alone.

The strongest lesion effect was observed for the second PCA component. Behaviourally, this component loaded on tasks tapping phonological processing and verbal working memory. Anatomically, it was associated with damage to left posterior perisylvian and temporoparietal cortices. Similar lesions have been linked to repetition deficits in aphasia (Ripamonti et al., 2018; Acharya et al., 2024), consistent with the role of the left superior temporal gyrus and supramarginal gyrus in phoneme identification (Liebenthal et al., 2005; Desai et al., 2008) and phonology (Purcell et al., 2021; Oberhuber et al., 2016) and auditory short-term memory (Ekert et al., 2021).

The fourth PCA component was least specific, at the behavioural level capturing shared variance across spoken and written comprehension and arithmetic – perhaps indexing linguistic or representational control. However, anatomically, the associated lesion pattern involved the left posterior middle temporal gyrus, a region that integrates phonological information with lexical-semantic knowledge (Price, 2012) and acts as a convergence zone bridging DMN and multiple-demand control systems (Davey et al., 2016). In addition, converging evidence has highlighted posterior temporal regions as critical for controlled semantic retrieval and regulation (e.g. Jefferies, 2013), providing a plausible anatomical context for this component despite its diffuse behavioural loadings.

Finally, the third PCA component weighted heavily on writing tasks, and less strongly on the line bisection and arithmetic tasks. The behavioural loadings therefore suggest a broader visuomotor function. It was associated with lesions extending into right occipital, parietal, and ventral temporal cortices. This pattern is consistent with a previous study linking right temporal lesions to writing deficits (Chen et al., 2019) and aligns with accounts emphasising the reliance of writing on visual-motor integration (Goodale et al., 2004; Bonzano et al., 2021). Damage to the superior parietal lobule and precuneus are associated with visuospatial and working memory processes essential for orthographic planning (Koenigs et al., 2009), whereas ventral temporal lesions impair semantic contributions to written output (Fernández et al., 2001). These findings reinforce the principle that persistent deficits on language assessments arise not only from injury to classical language regions but also from damage to multimodal hubs that support integration.

3.6.2. Reorganisation of gradient-based functional connectivity

The connectivity gradient differences between the young HCP cohort and the aged controls were larger than those observed between the aged controls and stroke patients. One explanation is that healthy ageing itself is associated with substantial alterations in the brain's functional hierarchy. Previous studies have shown that ageing is accompanied by reduced functional segregation, less distinct boundaries between large-scale networks, and attenuation of the principal connectivity gradients. Transmodal communities, including the dorsal attention (DAN), ventral attention (VAN), frontoparietal (FPN) and DMN networks, also exhibit greater within-network variability with ageing (e.g. Bethlehem et al., 2020; Wang et al., 2024), partly reflecting changes in long-range functional connectivity. Consequently, the aged control cohort already shows age-related reorganisation relative to young adults. Comparisons between aged controls and stroke patients therefore capture the additional effects of stroke on an already reorganised ageing brain rather than deviations from a young healthy baseline.

Given that stroke often disrupts hub regions and white-matter tracts supporting integration across networks (Li et al., 2025), functional reorganisation is expected to extend beyond damaged tissue. Connectivity gradients revealed stroke-related differences in large-scale functional organisation associated with language outcomes. Gradient 3 represents a continuum between control networks and the default mode network (DMN), providing a quantitative measure of how cortical regions are embedded within these systems. The left inferior frontal gyrus (IFG) pars triangularis occupied a relatively more DMN-weighted position along this axis in some individuals, reflecting comparatively stronger DMN and weaker control-network connectivity. Variation in IFG position along Gradient 3 was associated with better speech production but poorer writing and visuomotor performance, indicating that differences in its large-scale coupling profile relate differentially to distinct behavioural components.

The left IFG is widely regarded as a hub that coordinates distributed processes across cortical systems. Intracranial and neuroimaging evidence implicates this region in speech production (Flinker et al., 2015), and prior work suggests it occupies an intermediate position between control and default mode systems, enabling integration of conceptual representations with top-down control processes (Davey et al., 2016; Chiou et al., 2023; Wang et al., 2024). Within this framework, post-stroke variation in IFG embedding along the DMN–control axis can be interpreted as systematic alteration of large-scale coupling, with distinct consequences for different language and visuomotor demands. In healthy brains, the left IFG sits closer to the DMN than its right-hemisphere homologue, and this asymmetry relates to semantic selection ability (Gonzalez Alam et al., 2021). In stroke survivors with aphasia, retaining or enhancing this DMN alignment may support better speech production by boosting word retrieval and selection mechanisms that underpin fluency (Thompson-Schill et al., 1997; Wagner et al., 2014). However, the same shift toward the DMN was linked to more

impaired writing and visuomotor performance, suggesting a functional trade-off in which tasks requiring stronger control-network engagement are disadvantaged (Labache et al., 2024). Since the right IFG is typically positioned closer to control networks than the left IFG, one possible interpretation of our results is that shifts of left IFG toward the control end of this axis supports visuomotor demands at the expense of language fluency processes.

More broadly, the gradient changes observed within the language network are consistent with prior evidence that functional reorganisation in chronic stroke predominantly involves left-hemisphere language regions and, in some cases, their right-hemisphere homologues (Meinzer et al., 2008; Fridriksson et al., 2012; Jiang et al., 2025). However, earlier studies largely relied on seed-based connectivity analyses, whereas the gradient framework characterises changes in the overall connectivity profile of language-network regions without requiring predefined seed regions. Rather than framing reorganisation as a binary shift between hemispheres, gradients quantify variation along continuous axes of large-scale organisation, revealing systematic alterations in how language regions are embedded within distributed networks. Such variation in large-scale embedding may reflect underlying plasticity processes, including stabilisation of surviving circuits and strengthening of alternative functional pathways when pre-existing networks no longer fully support language function (Billot & Kiran, 2024).

3.6.3. Integrating lesion location and gradient organisation

Taken together, lesion mapping identifies regions in which structural damage constrains language performance, whereas gradient analyses quantify how surviving regions are positioned within large-scale functional organisation. For example, temporoparietal hubs, damaged in many stroke survivors in our sample, typically occupy positions that coordinate interactions between control and default mode systems (Hearne et al., 2017); gradient analyses then capture how other language-relevant regions vary in their large-scale embedding following stroke and how this variation relates to behaviour. Importantly, variation in connectivity along a single gradient axis can show opposing associations with different language components, indicating that the behavioural consequences of reorganisation cannot be reduced to a simple gain or loss of function. Instead, the impact of altered large-scale coupling depends on the specific cognitive demands being considered. This framework situates behavioural variability within a low-dimensional functional architecture, showing how local damage and distributed changes in network embedding jointly shape language outcomes after stroke.

3.7. Future directions

The present study employed a binary lesion-mapping approach, in which each voxel was classified as either lesioned or non-lesioned. This approach provides a clear representation of lesion extent and is widely used in lesion-symptom mapping studies (Bates et al., 2003;Borovsky et al., 2007; Ploner et al., 2005). However, it does not capture graded changes in tissue integrity within structurally preserved regions. An alternative approach is voxel-based morphometry (VBM), which identifies differences in local tissue composition after removing gross anatomical differences between individuals and is fully automated. Unlike binary lesion masks, VBM provides continuous voxel-wise measures of grey matter density, enabling the detection of more subtle structural alterations that may show linear associations with behavioural performance. VBM also involves whole-brain analysis and can detect changes in tissue composition outside the primary lesion. This may be particularly relevant in chronic stroke, where secondary neurodegenerative processes, such as Wallerian degeneration and remote cortical atrophy, may not be captured by binary lesion mapping (Geva et al., 2012). Consequently, incorporating VBM could potentially improve sensitivity to structural changes associated with behavioural impairments and provide complementary information to lesion-based analyses. Future work should therefore compare behavioural associations identified using VBM with those obtained from binary lesion mapping to determine whether incorporating continuous measures of tissue integrity improves the prediction of post-stroke language outcomes.

While this study focused on language function, gradient-based functional organisation is likely to influence other cognitive domains, including executive function, memory, and spatial processing. Richer neuropsychological assessments of these functions would provide greater clarity about the cognitive consequences of gradient changes following stroke. Longitudinal studies are needed to track how connectivity gradients evolve across different stages of recovery, and how compensatory mechanisms develop in relation to structural damage. In addition, spared regions, often unaffected by MCA strokes, for example in anterior prefrontal regions, may play a critical role in supporting recovery through gradient-mediated network reorganisation. Understanding these dynamics could inform targeted therapies designed to boost neuroplasticity in chronic stroke.

3.8. Conclusion

Our findings demonstrate that gradient-based functional connectivity changes are associated with language outcomes after chronic stroke. Lesion–symptom mapping identified both classical perisylvian language regions and additional parietal, temporal, and occipital areas as critical for verbal working memory, comprehension, and writing. Connectivity gradient analyses revealed how surviving regions shift along DMN–control axes, capturing associations with both better performance (speech production via left IFG integration with DMN) and impaired performance (poorer writing following the same connectivity changes). Together, these complementary approaches provide a framework for understanding how focal lesions co-occur with distributed network dynamics, offering a new method for understanding the effects of stroke on behaviour.

Chapter 4
A Connectivity-gradient simulation model captures stroke reorganisation and language outcomes

4.1. Abstract

Stroke causes both local tissue damage and remote disruption across networks, producing whole-brain functional disturbances that extend beyond the focal injury. Attempts to model the functional impact of stroke typically remove nodes or edges, or rely on lesion topology to approximate network-wide effects. We introduce a connectivity-gradient–based stroke simulation model that uses intact-tissue information from structural MRI to model graded network disturbances in connectivity-gradient space. Using structural and resting-state fMRI data from chronic stroke participants in the PLORAS dataset, we evaluate, within the same individuals, the extent to which lesion-derived simulations capture empirically observed post-stroke reorganisation of connectivity gradients, and whether these effects relate to language outcome (Comprehensive Aphasia Test). This direct comparison between simulated and observed gradient changes has rarely if ever been deployed in lesion-modelling studies. The simulation showed moderate similarity with stroke-induced functional reorganisation along the transmodal–unimodal and visuo-motor axes of functional brain organisation. The model reproduced stroke-related shifts in Gradient 1 within the default mode and dorsal-attention networks, and captured frontoparietal network changes along Gradient 2. Simulated changes in cortex-wide functional connectivity gradients were associated with language performance and two of these patterns were verified in observed resting-state fMRI data collected for the same patients: (i) right inferior frontal gyrus showed more motor connectivity on the visuomotor axis, in participants with better phonology and working memory, while left supplementary motor area and paracingulate cortex showed increased motor-related connectivity along the same axis in participants with more severe speech difficulties. These findings suggest that outcome-relevant connectivity patterns are partially recoverable from lesion information, and that connectivity gradients provide a useful framework for linking lesion-driven changes in large-scale functional organisation to behavioural performance.

4.2. Introduction

Stroke causes local damage to brain tissue, disrupting the functional and structural integrity of affected regions (Griffis et al., 2020; Tsiakiri et al., 2024). However, focal lesion location does not

fully account for the range and co-occurrence of behavioural deficits observed after stroke, with similar symptom profiles arising from anatomically distinct lesion sites (Siddiqi et al., 2022). Advances in neuroimaging have supported a shift from a localisation-based account to a network-based understanding of stroke, emphasising that symptoms arise not only from the site of damage but from how that region is embedded within a highly interconnected and dynamic brain network (Veldsman & Brodtmann, 2019; Siddiqi et al., 2022). Functional connectivity studies show that stroke leads to widespread network interruptions, including reductions in (i) interhemispheric integration, (ii) segregation of ipsilesional networks, and (iii) overall network modularity (Griffis et al., 2019). These effects extend to regions that are structurally intact but functionally connected to the lesion site, demonstrating remote disruptions in large-scale organisation (Carrera et al., 2014). Together, these findings support a view of stroke as a network disorder (Guggisberg et al., 2019). Lesions affecting "connector hub" regions, which interact with multiple functional networks, produce particularly widespread disruptions in connectivity and are associated with more severe neurological deficits (Gratton et al., 2012). Such network-level disruptions are clinically meaningful, with lesion-affected networks showing distinct changes in functional connectivity relative to unaffected systems (Ovadia-Caro et al., 2013).

To understand the causal mechanisms underlying stroke-induced brain network disruptions, a range of lesion simulation approaches have been developed (Drost et al., 2025; Gratton et al., 2012; Honey & Sporns, 2008; Van Assche et al., 2022; Alstott et al., 2009; Schmidt et al., 2015; Tao & Rapp, 2021). Early influential work demonstrated that virtual lesions produce systematic patterns of remote functional disruption, with hub and midline lesions in particular leading to widespread bilateral effects (Alstott et al., 2009). Subsequent studies have extended this framework to examine questions such as network resilience and reorganisation following repeated lesions, suggesting that pre-existing connectivity structure can modulate vulnerability and recovery (Van Assche et al., 2022). Together, these approaches establish simulation as a useful tool for probing aspects of network disruption that are difficult to access empirically.

Most stroke simulation studies have relied on either virtual lesioning of brain networks or topology-informed modulation of connectivity. In graph-theoretical approaches, brain regions are represented as nodes and their interactions as edges, allowing lesion effects to be modelled through node or edge removal within an intact connectome (Almeida et al., 2022; Miraglia et al., 2022). Network properties of the resulting system are then quantified using summary metrics such as clustering coefficient, path length, modularity, and global efficiency. While these measures provide useful characterisations of global organisation, they reduce complex spatially distributed changes to single network-level values and assume fixed node definitions for each network (Solo et al., 2018; Bassett et al., 2018). This limits their ability to capture graded regional changes or overlapping patterns of disruption across systems. More fundamentally, lesion simulation based on node or edge

removal treats stroke as a binary disconnection process, whereas connectivity is often weakened rather than eliminated in stroke, and perilesional tissue typically remains active (Carter et al., 2010; Dijkhuizen et al., 2012).

An alternative class of approaches incorporates lesion topology into connectivity models by scaling or decaying connectivity strengths based on proximity to the lesion core (Alstott et al., 2009; Honey & Sporns, 2008; Kuceyeski et al., 2013). These methods introduce graded effects but remain fundamentally lesion-centred, in that they propagate disruption outward from the lesion without explicitly modelling how large-scale network organisation constrains or shapes these effects. Across both classes of approach, a common limitation is that they characterise stroke-induced disruption primarily as a local perturbation that propagates through predefined edges, without fully capturing changes in the organisation of intact whole-brain connectivity. In addition, relatively few studies have directly compared simulated lesion effects with empirically observed functional reorganisation in the same patients (Tao & Rapp, 2021), and it remains largely untested whether simulation-derived predictions generalise to behavioural outcomes in clinical stroke datasets.

To address these limitations, we propose a connectivity-gradient-based stroke simulation model that uses lesion data to computationally simulate lesion effects at three levels: (i) focal lesion effects, (ii) distant effects in regions connected to the lesion core, and (iii) distributed network-wide changes that extend beyond directly lesion-linked connections. This approach models disruption within the spared connectome, allowing lesion effects to be expressed as graded changes in functional organisation rather than binary disconnection.

Connectivity gradients provide a framework for modelling these effects in a continuous, low-dimensional space. Unlike graph-theoretical approaches, which represent networks as discrete nodes and edges, gradients capture smooth variations in connectivity profiles across cortex, such that regions with similar connectivity are located near one another (Margulies et al., 2016; Wang et al., 2020; Bernhardt et al., 2022). The principal gradient reflects the transition from unimodal sensory–motor systems to transmodal regions involved in higher cognition, while additional gradients capture other large-scale axes of organisation, such as the distinction between visual and auditory-motor cortex (Wang et al., 2020). This representation allows stroke-related changes to be characterised as shifts in position within a continuous functional architecture, rather than as loss of discrete network components.

Our simulation approach uses lesion information to estimate the proportion of intact tissue within each parcel of the Schaefer atlas (Schaefer et al., 2018), and applies this information to normative functional connectivity matrices derived from age-matched controls. Connectivity strengths are reduced proportionally to the amount of intact tissue, preserving graded functional integrity. These effects are then propagated across the connectome using an iterative diffusion-inspired procedure (cf.

Raj et al., 2012), allowing local tissue loss to influence both directly connected regions and more distant areas that depend on affected inputs. This propagation step is intended to capture diaschisis-like effects within an intact network architecture. The resulting patterns of disruption are then projected into connectivity-gradient space to obtain low-dimensional representations of large-scale functional reorganisation.

We evaluated the performance of this iterative-propagation simulation using the Predicting Language Outcome and Recovery After Stroke (PLORAS) dataset (Seghier et al., 2016), which includes structural MRI, resting-state fMRI, and detailed behavioural assessments. This enables direct comparison between simulated gradient changes derived from lesions and empirically observed gradient reorganisation within the same individuals. Language performance was assessed using the Comprehensive Aphasia Test (CAT). We addressed three questions: (i) to what extent can lesion-based simulations of stroke-related changes reproduce observed changes in connectivity gradients? (ii) whether simulated and observed gradients capture similar patterns of large-scale functional disruption; and (iii) whether regions identified by the simulation as behaviourally relevant show corresponding associations with language outcomes in the empirical data. Linking simulation-derived gradient changes to behavioural outcomes provides a means of assessing whether the model captures functionally meaningful aspects of network disruption. Language impairments after stroke are not confined to classical language regions but involve distributed networks, including domain-general control systems (Hope et al., 2024; Zevgolatakou et al., 2022). The CAT assesses multiple language domains (comprehension, speech, reading, writing) that depend on these distributed systems (Swinburn et al., 2012**)**. Convergence between simulated and observed gradient–behaviour relationships would therefore indicate that the model captures behaviourally relevant patterns of large-scale functional reorganisation rather than purely local effects.

4.3. Methods

4.3.1. Participants

We included 86 age-matched control participants and 83 chronic stroke survivors from the PLORAS (Predict Language Outcome and Recovery After Stroke) dataset (Seghier et al., 2016). None of the stroke participants had additional neurological or psychiatric conditions such as dementia or depression. All selected stroke participants had both T1-weighted structural scans and resting-state fMRI. We applied specific inclusion criteria for resting-state fMRI required for functional connectivity analyses: (1) at least 70% valid scans; (2) no denoising failure; and (3) mean head motion below 0.35 mm. Based on these criteria, we excluded 23 stroke patients and 7 age-matched

controls. The final sample included 60 stroke individuals (24 females; mean age = 56.86 ± 10.74 years) and 79 age-matched controls (43 females; mean age = 38.23 ± 16.2 years). The stroke participants' mean age at stroke onset was 52.25 ± 11.51 years, and their mean post-stroke duration was 55.31 ± 58.12 months. Although the available control group was younger than the stroke cohort, the analyses below focus on within-subject comparisons between simulated and observed gradients; normative connectivity patterns were used primarily as a baseline for modelling stroke-related changes in simulated and real functional connectivity data.

4.3.2. Comprehensive Aphasia Test

The Comprehensive Aphasia Test (CAT; Swinburn et al., 2004) assesses language dysfunction in stroke. This test provides a broad assessment of performance in language functions and language-related cognitive domains in patients with aphasia. The test consists of language production tests (repetition, naming, and spoken picture description), comprehension of spoken and written language, reading, writing, and repetition skills. There are additional subtests that examine cognitive domains: line bisection, semantic memory, word fluency, recognition memory, gesture-object use, and arithmetic. All stroke participants included in this study completed the CAT. We performed principal component analysis (PCA) on the CAT subtests to reduce these correlated language subtests into distinct language domains that explained unique variance. Before performing PCA on these tests, we first identified suitable subtests by examining score variability using the interquartile range (IQR). Five subtests had few items and an IQR of zero, indicating that at least 50% of individuals received the same score, and were excluded (semantic memory, repetition of complex words, writing copy, comprehension of spoken paragraph, and reading functional words) from the PCA. PCA with oblique rotation was conducted on the standardised Z-scores of the remaining subtests using R Studio. The language components with eigenvalues greater than 1 were included, resulting in six components. The first four components loaded on multiple subtests and were readily explainable as broader language domains; the fifth and sixth components captured more task-specific variance and are reported in the Supplementary Materials (Supplementary Figure 4.S1).

4.3.3. Lesion segmentation

For all participants in the stroke cohort, whole-brain T1-weighted structural MRI was acquired during the same session as the resting-state data, using research-dedicated 3T Siemens scanners at the Department of Imaging Neuroscience, UCL. We segmented the lesions using established procedures implemented in SPM (running in MATLAB). First, T1 weighted image was spatially normalised to MNI space and then converted into a continuous lesion map which quantified structural abnormality at each voxel on a scale from 0 (normal) to 1 (abnormal), comparing with normative data from neurologically healthy controls (Seghier et al., 2008). To generate binary lesion images, each lesion map was thresholded at 0.3. This procedure has previously been shown to provide robust associations

with behavioural outcomes; therefore, no further manual edits were applied. We used the fslmaths tool from FSL (FMRIB's Software Library) to binarise the segmented lesions maps. These lesion maps were instrumental in deriving simulated lesion connectivity matrix.

4.3.4. Resting-state fMRI data preprocessing

The CONN toolbox was used for preprocessing the resting-state functional magnetic resonance imaging (fMRI) of age-matched controls and stroke patients (v.22b; Whitfield-Gabrieli and Nieto-Castanon, 2012), implemented in MATLAB R2023a. The default preprocessing pipeline in CONN included motion estimation; correction by volume realignment using a six-parameter rigid-body transformation; slice-timing correction; and simultaneous segmentation of white matter, grey matter, and cerebrospinal fluid, followed by normalisation to MNI152 stereotactic space (2 mm isotropic voxel size) performed for both functional and structural MRI. The following potential confounding variables were statistically controlled after preprocessing: six motion parameters estimated in the previous step and their first- and second-order derivatives; volumes with excessive movement (motion > 0.5 mm or global signal change > z = 3); linear drifts; and five principal components of signals from white matter and cerebrospinal fluid (CompCor approach; Behzadi et al., 2007). Finally, a band-pass filter (0.01–0.1 Hz) was applied to the data, and global signal regression was not performed.

4.3.5. Whole-brain functional connectivity

We constructed a functional connectivity (FC) matrix for each individual in both groups after preprocessing and denoising the resting-state fMRI data. First, we extracted the mean functional time series of each of the 400 cortical parcels based on the Schaefer parcellation (Schaefer et al., 2018) (https://github.com/ThomasYeoLab/CBIG/tree/master/stable_projects/brain_parcellation/Schaefer2018_LocalGlobal). Next, we estimated pairwise Pearson correlations between the mean time series of all parcels, resulting in a 400 × 400 FC matrix for each individual. The Schaefer parcels were aligned to the seven canonical networks from the Yeo parcellation (Yeo et al., 2011) based on spatial overlap. Lesioned parcels were not removed at this stage because we assumed that they do not influence the variance explained by the functional connectivity patterns and therefore would not affect the gradient structure. However, lesioned parcels were removed in the spatial correlation analyses, and these parcels were masked out in analyses focusing on associations between language outcomes and post-stroke gradient changes, from simulation and observed data. Finally, group-level matrices were generated separately for the stroke group and the age-matched control group by averaging the individual FC matrices within each group.

4.3.6. Functional connectivity gradient extraction

The BrainSpace Toolbox was used to extract ten gradients from the functional connectivity matrix generated from the resting-state data of each stroke patient and each age-matched control

(dimension-reduction technique = diffusion embedding, kernel = normalized angle, sparsity = 0.9). We also derived ten gradients from the simulated lesion connectivity matrix. Details on the generation of the simulated lesion connectivity matrix are provided in Section 4.3.7. Extracting ten gradients allows the first three gradients to achieve a greater fit with canonical group-level gradients (Margulies et al., 2016; Gonzalez Alam et al., 2021; McKeown et al., 2020). We mainly focused on the first three gradients, as they explain the greatest variance in functional connectivity and have been used to characterise functional relationships between brain regions. Procrustes rotation is a critical step in the process of gradient extraction, as it increases the agreement between individual canonical gradients and the group-level solutions, improving the interpretability of gradient analysis (Margulies et al., 2016; Gonzalez Alam et al., 2021; McKeown et al., 2020). The individual-level gradients for age-matched controls and stroke patients were aligned using Procrustes rotation to gradients extracted from a subsample of the Human Connectome Project (HCP) dataset (n = 217; 122 women; mean ± SD age = 28.5 ± 3.7 years; for more information on subject selection, see Vos de Wael et al., 2018), which is embedded within the BrainSpace Toolbox (Vos de Wael et al., 2020). This procedure translates, rotates, and scales configurations to optimise alignment with the larger group average (Goodall, 1991; Vos de Wael et al., 2020), while preserving the overall shape and structure of the data (Siegel et al., 2017), ensuring that gradients for individuals can be interpreted within a common space. Similarly, group-level gradients for age-matched controls were also aligned to the HCP gradients using Procrustes rotation.

4.3.7. Simulated lesion functional connectivity

We simulated the direct and indirect effects of lesions on the normative functional connectivity (FC) of aged controls using an iterative propagation model. This model is conceptually similar to the well-established lesion network mapping approach, where network disruption is examined by estimating the lesion's connectivity with the rest of the brain using a normative connectome to generate a disconnection map (e.g., Fox, 2018; Boes et al., 2015). We used lesion data derived from stroke individuals' structural MRI scans to simulate post-stroke changes in FC. The simulation approach consisted of two parts. The first part focused on modelling the focal and lesion-linked remote effects by proportionately reducing the FC matrix of aged controls. A lesion matrix was constructed using lesion information from the structural images to scale functional connections according to the proportion of intact tissue. The second part involved propagating lesion-induced effects across the cortex by constructing an edge-wise scaling matrix and superimposing these reductions onto the lesion-modelled matrix from the first part to produce whole-brain network-level disruption. The propagation concept was inspired by Raj and colleagues' (2012) network diffusion model, used to simulate dementia-related network alterations. In our framework, the first part models the direct effects of stroke by proportionately reducing connections associated with the affected parcels in the FC matrix—that is, applying reductions to the specific rows and columns corresponding

to lesioned parcels. The subsequent propagation step allows lesion effects to spread across the cortex by reducing connectivity across all edges, enabling simulation of indirect and remote disruptions and capturing whole-brain network disturbance beyond the lesion's immediate neighbourhood (Figure 4.1).

Focal lesion effects were simulated by constructing a lesion matrix that represented the pairwise association of intact tissue between cortical parcels. Segmented lesion maps were derived from T1-weighted images. Each binarised lesion map was multiplied by the Schaefer 400-parcel template (aligned to the 7 Yeo networks; Yeo et al., 2011) to map the lesion maps to this atlas template using FSL's *fslmaths* tool. This step identified affected parcels and estimated the proportion of each parcel that was lesioned (lesion load). The proportion of intact tissue in each parcel was calculated as the complement of lesion load, yielding 400 parcel-wise values. A 400 × 400 lesion matrix was then constructed by computing the pairwise products of all intact parcel values, such that each matrix entry represented the estimated fraction of connectivity preserved between two parcels based on the amount of intact tissue in both. The underlying assumption is that a fully intact parcel maintains its typical level of functional connectivity with the rest of the brain. If a parcel retains 60% intact tissue, then all of its functional connections to other regions are scaled according to that 60% integrity, rather than being removed or uniformly set to zero. To simulate the direct impact of stroke on functional connectivity, each lesion matrix was multiplied element-wise with the corresponding aged control FC matrix. This operation proportionately reduced the strength of functional connections according to intact tissue, thereby modelling immediate post-stroke connectivity loss, such that

$$FC_{\text{lesioned}} = FC_{\text{aged control}} \times \text{Lesion Matrix.}$$

Indirect effects of stroke were then modelled using an edge-based propagation approach, which introduces functional disruptions across the cortex. This results in larger connectivity reductions for parcels directly affected by stroke and comparatively smaller reductions in structurally intact parcels relative to the aged-control baseline. Together, these effects produce distributed network-level disruptions across the cortex. Lesion-induced functional disruption was propagated across the cortex through the construction of an edge-wise connectivity loss matrix. These calculations were performed separately for each aged-control functional connectivity matrix, thereby simulating 79 lesion-specific FC perturbations per lesion. This step allowed us to model how focal tissue loss cascades through the preserved connectome to generate indirect and remote effects beyond the lesion's immediate neighbourhood. For each pair of parcels, fractional connectivity loss was estimated by comparing the functional connection strength in the lesioned FC matrix with the corresponding connection in the aged control FC matrix. In other words, the ratio between the

lesioned and baseline connectivity values was calculated, and the proportional reduction in connectivity strength was defined as one minus this ratio:

$$loss_{ij} = 1 - \frac{| FC_{lesioned,ij} |}{| FC_{control,ij} |}$$

This formulation directly quantifies the fractional reduction in connectivity strength for each functional connection relative to the aged control baseline. Each edge in the FC matrix represents a connection between a pair of parcels. This edge-wise loss was converted into a scaling factor using the equation

$$scale_{ij} = (1 - \alpha \cdot loss_{ij})^{\gamma}$$

where α represents propagation strength and γ represents nonlinearity. Different combinations of these parameters were applied to model variability in how strongly and nonlinearly lesion effects propagated across the cortex. Propagation strength (α) was set to {0.1, 0.3, 0.5, 0.8, 1.0}, reflecting the magnitude at which local connectivity loss spreads globally across the functional network. Higher α values (e.g., 0.8 or 1.0) produced stronger propagation of stroke effects beyond directly damaged regions, modelling more extensive network-level disruption, whereas lower values constrained effects more locally around lesioned parcels. Nonlinearity (γ) was set to {1.0, 0.8, 0.3}, controlling the sensitivity of scaling to connectivity loss. Higher γ values resulted in approximately linear, proportionate reductions, whereas lower values introduced softer, more conservative scaling and reduced excessive global propagation of lesion effects. The edge-wise scaling factors for each connection were then organised into a scaling matrix representing the propagated connectivity disruption across all parcel pairs. This procedure was iterated three times to allow progressively stronger propagation of lesion-induced disruption through the brain network. The multi-step iteration was designed to capture both direct lesion effects (iteration 1) and higher-order remote network effects in structurally intact parcels that depend on indirect inputs from the damaged region (iterations 2 and 3), following the principles of network-based propagation models (Iturria-Medina et al., 2014; Pandya et al., 2019; Raj et al., 2012).

The scaling matrix obtained after the third iteration was then multiplied element-wise with the lesioned FC matrix to generate the final simulated FC matrix. The final simulated FC matrix for each lesion was generated by performing element-wise multiplication between the scaling matrix and the lesioned FC matrix.

$$FC_{\text{simulated lesion}} = FC_{\text{lesioned}} \times \text{Scaling Matrix.}$$

For each lesion, this procedure produced one simulated functional connectivity matrix per aged control for each α–γ parameter combination. These simulated matrices were then averaged across controls to obtain a single ensemble simulated FC matrix per lesion for each α–γ parameter combination. The resulting matrix is a robust overall estimate of the lesion's impact on functional connectivity. This step yielded one simulated (propagated) functional connectivity matrix per lesion for each α–γ parameter combination, capturing both direct and remote (network-level) effects of the lesion. We used five different lesion propagation strengths by setting α to 0.1, 0.3, 0.5, 0.8, and 1.0. Each α value was then modelled with three different γ values {1.0, 0.8, 0.3}, resulting in 15 combinations of α–γ parameters. Different propagation strengths and levels of nonlinearity were tested to identify which α–γ parameter combination produced gradients that were closer to the observed post-stroke gradients. Finally, connectivity gradients were extracted from the simulated FC matrices for each lesion and for each α–γ parameter combination. We also extracted connectivity gradients from the lesioned FC matrices for each lesion, which represent the direct effects of stroke without propagation. This comparison allows evaluation of how propagation modelling captures distributed network disruptions beyond the focal lesion effects.

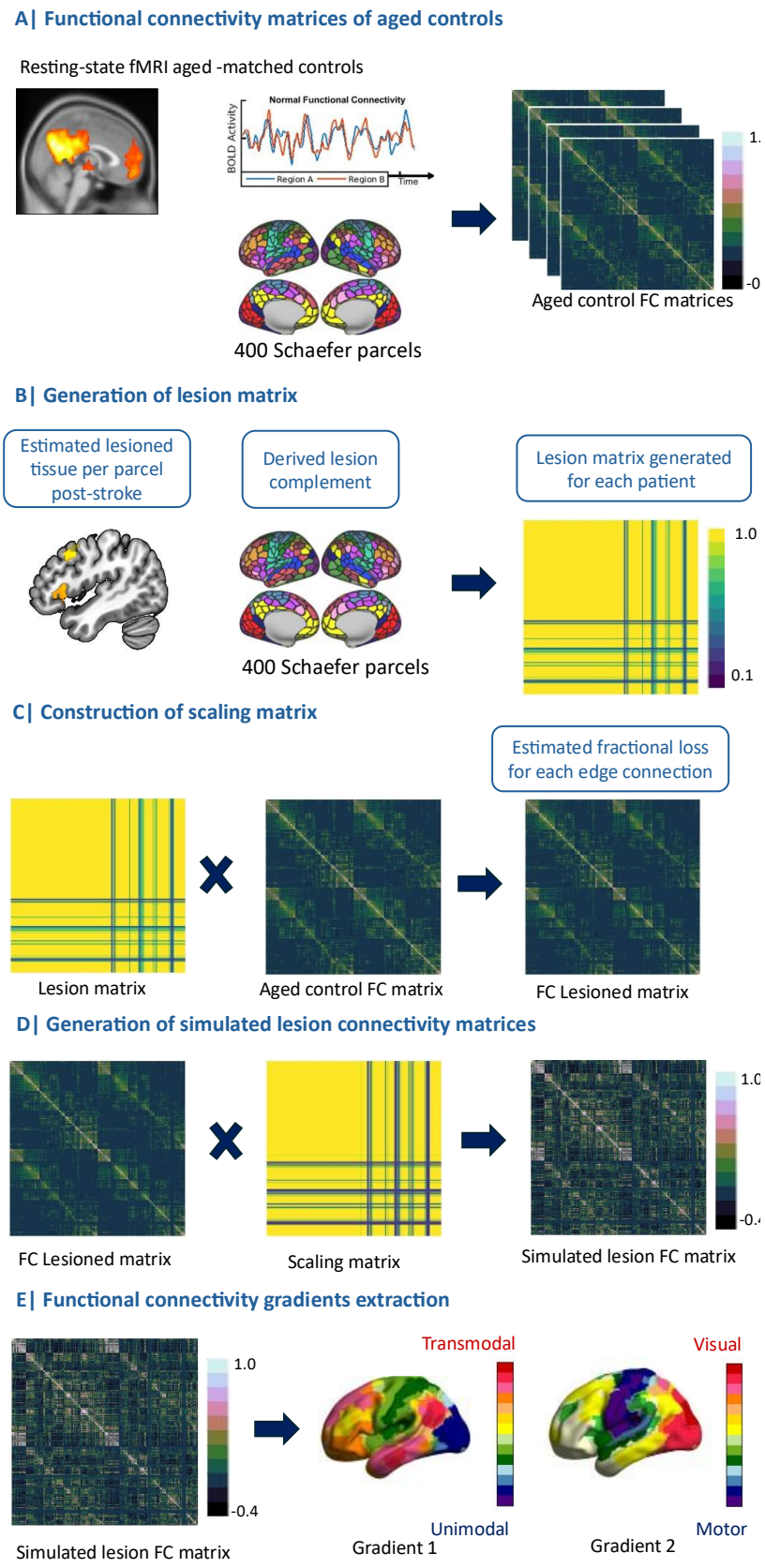

Figure 4.1. Processing pipeline for simulated post-stroke gradients for each lesion using the iterative propagation model. A) A connectivity matrix for each control was generated by

computing the Pearson correlation between the mean time series of each of the 400 ROIs, resulting in a 400 × 400 connectivity matrix per participant. B) The T1-weighted brain map for each lesion was multiplied by the Schaefer parcellation (400 parcels) to identify lesioned parcels. Lesion complements were then estimated from the lesioned parcels for each lesion and these values were used to generate lesion matrices. C) Each lesion matrix was element-wise multiplied with the 79 individual functional connectivity matrices from the aged control group, yielding 79 FC lesioned matrices per lesion. D) Fractional connectivity loss was estimated for each FC lesioned matrix relative to each aged control matrix, and scaling matrices were constructed using α–γ parameter combinations (this step was iterated three times). E) Each FC lesioned matrix was then multiplied element-wise with the scaling matrix, resulting in simulated functional connectivity matrices for each control, introducing network-wide disruptions. F) Simulated post-stroke gradients were then extracted for each lesion from the ensemble-averaged simulated functional connectivity matrix obtained by averaging across the control-specific simulations.

4.3.8. Post-stroke gradient differences

To capture stroke-related gradient differences relative to the age-matched controls, we generated gradient difference maps for both the observed and simulated stroke gradients. These gradient difference maps highlight the specific effects related to stroke by showing each parcel's displacement across the gradient axes. The gradient difference maps for both observed and simulated stroke gradients were derived by subtracting each stroke gradient from the corresponding aged control gradient using the fslmaths tool from FSL (FMRIB's Software Library) for the first three gradients. Gradient difference maps were generated for simulated stroke gradients obtained from all α–γ parameter combinations. In addition, gradient difference maps were also generated for the focal-effect simulations derived from the lesioned FC matrices (without propagation) to characterise the gradient changes associated with direct lesion effects alone.

4.3.9. Highest-correlation α–γ parameter

We extracted connectivity gradients for all α–γ parameter combinations used to simulate stroke effects beyond the focal lesion impact. We also derived connectivity gradients for aged controls and for the stroke participants from their resting-state fMRI scans. Stroke-related gradient changes were captured by subtracting each stroke gradient from the average aged-control gradient. These post-stroke gradient difference maps were generated for both the observed data and all α–γ simulation parameter combinations. All statistical analyses were performed on these difference maps, as they reflect each parcel's displacement along the gradient axes relative to the normative control organisation. The similarity between post-stroke difference gradients derived from resting-state fMRI

in observed stroke and simulations derived from lesion data of the same individual was estimated using spatial correlation analysis. For each lesion, spatial correlations were computed between the observed gradient difference map and the simulated gradient difference maps from all α–γ parameter combinations using spin permutation testing. We then identified which α–γ parameter combinations yielded the highest correlations for each lesion. The spatial correlation values showed minimal variation across α–γ parameter combinations, differing only slightly in magnitude. For each lesion, the parameter combination producing the highest correlation is reported in the Supplementary Materials (Supplementary Figures 4.S2 and 4.S3).

Across lesions, the parameter combination $\alpha = 0.1$ and $\gamma = 0.8$ most frequently yielded the highest correspondence between simulated and observed gradients. For each α–γ parameter, the number of stroke cases for which it produced the highest correlation between the simulated and observed gradients is shown in the bar plot in Supplementary Figure 4.S4. This pattern suggests that, within our propagation framework, the lowest propagation strength with approximately linear scaling of connectivity loss ($\gamma = 0.8$) best captures post-stroke gradient reorganisation, consistent with the idea that lesions alter, but do not fully collapse, whole-brain network structure. All statistical analyses reported in the following sections are based on the $\alpha = 0.1$, $\gamma = 0.8$ parameter combination. Using these fixed parameters allowed all lesions to be tested under the same propagation parameter space, enabling comparable results and identification of cases for which the simulations worked well.

4.4. Statistical analyses

4.4.1. Spatial correlation analyses

We performed spin permutation testing to estimate the spatial similarity between post-stroke gradient differences captured by the observed and simulated lesion effects. We computed spatial correlations for all α–γ parameter combinations to identify which parameter combinations captured the highest spatial correspondence across stroke cases. Additionally, spatial correspondence of post-stroke changes was estimated between the observed gradients and the simulations for each stroke case. Spin permutation testing for spatial correlation accounts for spatial autocorrelation, which is an inherent property of brain imaging data where neighbouring regions display greater similarity than remote regions (Alexander-Bloch et al., 2018; White et al., 2022). We conducted spin permutation tests on post-stroke gradient difference maps by comparing each lesion's observed gradient difference map with the simulated gradient difference maps generated from each α–γ parameter combination. For this analysis, we used the Neuromaps Python library (Markello et al., 2022). First, post-stroke difference maps were converted from MNI152 volumetric space to cortical surface space using Neuromaps. Then, a set of $N = 5000$ randomly rotated versions of the simulated gradient maps were generated by

applying spherical rotations ("spins") to the data, resulting in a null distribution of simulated gradient maps that retain spatial autocorrelation, while the observed gradient difference map was kept fixed. For each permuted simulated map, the Pearson correlation with the observed gradient difference map was computed to generate a null distribution of correlation coefficients. The correlation between the simulated and observed maps was then compared against this null distribution to derive a p-value, allowing the statistical significance of their correspondence to be evaluated while accounting for spatial autocorrelation.

4.4.2. Lesion–gradient symptom mapping

We examined whether the simulated stroke gradient changes from the best alpha–gamma parameter combinations were associated with the language outcomes from the PCA in a similar manner to the observed post-stroke gradient changes. This was tested in two phases: first, identifying significant simulated gradient parcels linked to language outcomes using lesion–gradient symptom mapping; second, validating these simulation-identified effects in observed stroke gradients (see section 4.4.3). We performed lesion–gradient symptom mapping on simulated gradients, focusing on the following questions: what stroke-related changes are captured by the simulated gradients, and are there any associations between the PCA-derived language components and simulated post-stroke gradients? A general linear model was used to examine the associations between simulated stroke gradient changes (using gradient difference maps with baseline aged-control gradient effects removed) and the PCA-derived language components as covariates of interest. We also entered whole-brain lesion size as a covariate of no interest.

We set up contrasts for each PCA-derived language component to identify parcels where simulated stroke gradient differences relative to the average aged controls were linked to language outcomes. For each component, two contrasts were included: better and worse performance, as functional reorganisation may underlie both of these effects. Lesion–gradient symptom mapping was implemented using nonparametric t-tests in Randomise (Winkler et al., 2014, https://fsl.fmrib.ox.ac.uk/fsl/fslwiki/Randomise/UserGuide), with 5000 permutations performed. Threshold-free cluster enhancement was applied to identify significant parcels where differences in simulated stroke gradient values were statistically associated with PCA-derived language components. Family-wise error (FWE) correction was applied to control for multiple comparisons. A Language network mask from Neurosynth was used as the search space for this analysis. Damaged voxels in at least 25% of stroke survivors were identified and excluded, ensuring that analyses focused on connectivity gradient changes in structurally intact tissue. This threshold represented 75% of all lesioned voxels, which were excluded from the whole-brain and the language network region of interest (ROI) analysis. For visualisation, the statistical maps generated for each contrast were thresholded at 0.95, reflecting significant values in the TFCE-corrected 1–p maps. We also performed the lesion gradient symptom mapping using the same approach on the

observed stroke difference gradient maps to examine whether the same clusters, or neighbouring clusters, identified in the observed gradients were replicated by the simulation.

4.4.3. Validation of lesion–gradient symptom mapping of simulation

To validate our findings, we extracted real post-stroke connectivity values (from Chapter 3) specifically from the brain clusters identified in our current simulations, and tested whether these real values were associated with the same language components found in the simulation analyses. The clusters associated with simulated stroke gradient changes and PCA-derived language components were identified using lesion–gradient symptom mapping (see Section 4.4.2). We employed robust linear regression (M-estimator) to detect true effects in the observed gradients that might otherwise have been missed. The robust regression analyses were designed to match the original simulation's GLM. For each model, the predictor was the observed difference-gradient value extracted from the significant simulation clusters, and the outcome variable was the corresponding language component score. Lesion size and the remaining PCA-derived language components were included as nuisance variables to control for their effects. Freedman–Lane permutation included recomputing the regression slope for each permutation and bootstrapped confidence intervals. Directional (one-tailed) permutation tests were used to evaluate significance in the expected direction defined by simulation-based contrasts (for example negative contrast in randomise test negative slope only). Benjamini–Hochberg FDR correction ($q < 0.05$) was applied to control for multiple comparisons within each component-specific parcel. The empirical p-value was computed as the proportion of permuted slopes more extreme than the observed slope (one-tailed, based on the hypothesised direction).

4.5. Results

4.5.1. Lesion analysis

Of the 60 stroke participants, we excluded 2 cases with lacunar infarcts and 6 cases with lesions confined entirely to subcortical regions, as cortical damage is essential for simulating lesion effects on functional organisation. The final sample comprised 52 individuals with stroke (19 females; mean age = 57.04 ± 10.57 years). Within this cohort, 31 had left-hemispheric lesions, 6 had right-hemispheric lesions, and 15 had bilateral lesions. Lesion volume was calculated as the number of stroke-affected voxels, with a mean of 13,277 (SD = 11,355). Lesions involved both cortical and subcortical regions, with the greatest overlap observed in the left anterior thalamic radiation and corticospinal tract, affecting 30 of the 52 participants (Figure 4.2A). Cortical involvement extended across frontal, parietal, and occipital regions, with some temporal areas affected, whereas the frontal pole, temporal fusiform cortex, and parahippocampal gyrus were spared.

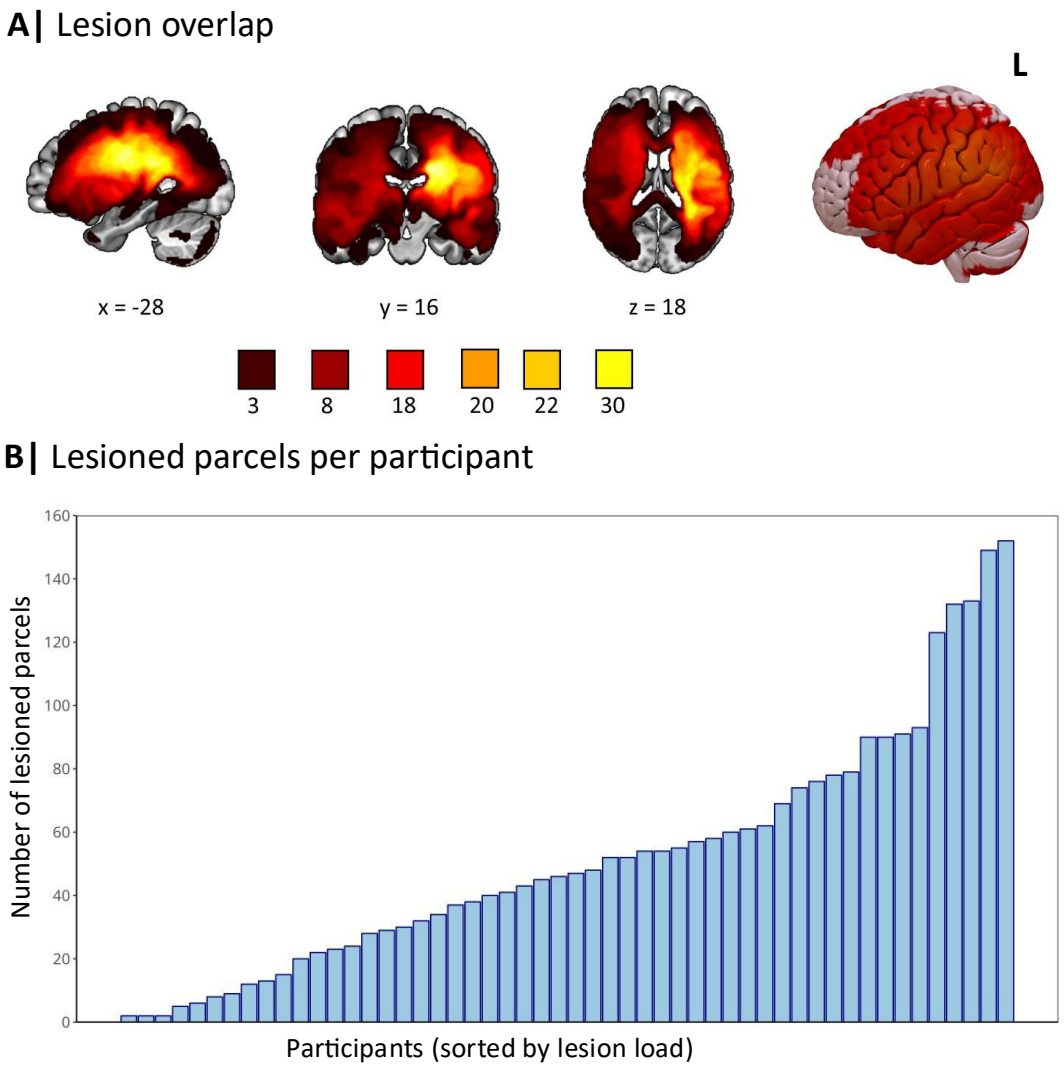

Figure 4.2. Lesion distribution across the stroke cohort. (A) Lesion overlap map for the 52 stroke patients. Binary lesion masks were generated using FSLmaths (Jenkinson et al., 2012) and visualised in MNI space with MRIcroGL. Brighter colours indicate greater lesion overlap across patients. (B) Bar plot showing the number of lesioned parcels for each participant.

Our simulation framework is based on parcel-wise lesion information, hence we characterised the distribution and extent of lesioned parcels across stroke participants (Figure 4.2B). We tested this approach in a sample with a broad range of lesioned profiles, allowing us to test the model across various lesion loads in diverse locations. The number of lesioned parcels was estimated by mapping the lesion maps to the Schaefer 400-parcel template (aligned to the 7 Yeo networks; Yeo et al., 2011) and then estimating the number of affected parcels using the fslstats tool from FSL (FMRIB's Software Library). The smallest cortical lesion involved 2 parcels and the largest cortical lesion affected 152 parcels (mean = 51.8 ± 37.9 lesioned parcels). The lesion complement (intact tissue per

parcel) derived from these lesioned parcels formed the basis of the lesion matrices used in our simulations of stroke effects on connectivity gradients.

4.5.2. Principal Component Analysis: Comprehensive Aphasia Test

The first four components explained 59% of the total variance, with two additional components accounting for a further 10%, giving a cumulative variance of 69%. The PCA loading matrix for all CAT subtests and the scree plot of eigenvalues are provided in the Supplementary Materials (Supplementary Figure 4.S1). The first component (36% variance) showed strong loadings for reading words (0.95), object naming (0.79), reading non-words (0.77), and reading complex words (0.75). The second component (9% variance) loaded highly on digit-string repetition (0.77) and sentence repetition (0.68) and reflected phonology and verbal working memory. The third component (7% variance) showed high loadings for written picture naming (0.89) and writing to dictation (0.69), capturing writing and visuomotor abilities. The fourth component (6% variance) loaded on written word comprehension (0.82), spoken word comprehension (0.54), and arithmetic (0.58), suggesting semantic and broader cognitive demands, although this component showed more cross-loadings and was less clearly defined. Two additional components had eigenvalues >1 but were dominated by single tasks—recognition memory (0.65) and gesture (0.94)—and were therefore treated as task-specific variance rather than meaningful latent dimensions. These components were included as covariates in subsequent analyses but were not interpreted further (see Supplementary Figure 4.S1). PCA scores were extracted for each component, with lower scores indicating greater impairment. Although PCA was conducted on the full stroke sample (n = 60) in Chapter 3, lesion–gradient mapping analyses used component scores only from the 52 individuals with usable fMRI data and cortical lesions, as the simulation approach required cortical lesion maps (the remaining eight participants had subcortical lesions).

4.5.3. Single-case illustration of the lesion simulation model

In Figure 4.3, we show an example of how closely the simulation model reproduced lesion-related effects for an individual case. A moderate level of similarity is evident between the observed and simulated post-stroke FC matrices (Figure 4.3A–B). In the top panel, the spatial correlation between the observed and simulated stroke gradients was 0.63 ($p = 0.0002$) for Gradient 1, which captures the transmodal–unimodal axis. Transmodal regions in the simulation—including the temporal pole, angular gyrus, precuneus, and right prefrontal cortex—as well as unimodal regions such as the postcentral gyrus and visual cortex—occupied positions closely matching those in the observed Gradient 1 maps (Figure 4.3C–D). In the bottom panel, Gradient 2 illustrates the visual–motor axis, where the simulation similarly reproduced the broad spatial organisation observed in the empirical data ($r = 0.77$, $p = 0.0002$). In particular, the medial prefrontal cortex and portions of the motor and visual cortices showed spatial positions closely aligned with those in the observed Gradient 2.

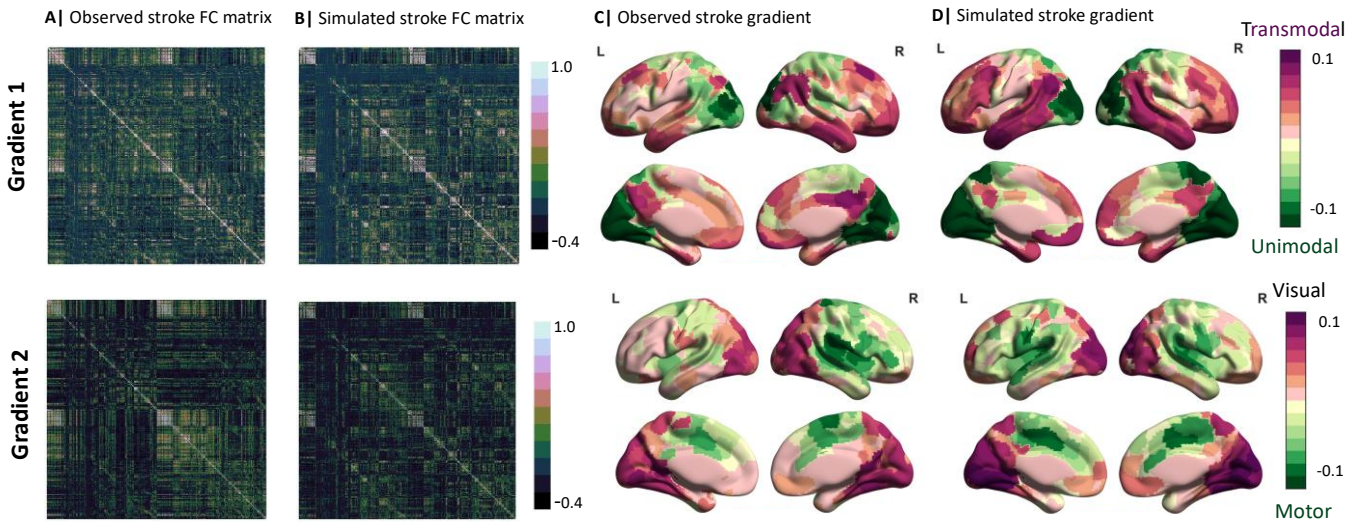

Figure 4.3. Visual correspondence between observed and simulated stroke connectivity. (A) Observed stroke functional-connectivity (FC) matrix. (B) Simulated stroke FC matrix. (C) Observed stroke gradients. (D) Simulated stroke gradients. Gradients for the observed and simulated stroke are shown using a purple-to-green colour scale, where transmodal regions are represented by shades of purple and unimodal regions by shades of green. Gradient 1 captures the transmodal–unimodal axis of functional organisation, and Gradient 2 captures the visual–motor axis. The individual case that showed the highest spatial correlation between observed and simulated gradients for both Gradient 1 and Gradient 2 is displayed.

4.5.4. Spatial correlation: Focal effects simulation vs. iterative propagation simulation

We identified the parameter setting $\alpha = 0.1$ and $\gamma = 0.8$ as producing the highest correlation for the maximum number of lesions when comparing the iterative-propagation–based simulation with the observed stroke gradients (Section 4.3.8). We then compared the iterative propagation model with the direct lesion effects simulation to determine which approach more closely replicated the post-stroke connectivity gradient changes observed in resting-state data. All analyses were performed on the gradient-difference maps. Spatial correlations were computed between the observed post-stroke gradient differences and the simulated gradient differences for both the iterative propagation model and the direct lesion effects simulation (without propagation). For each lesion, spatial correlations were estimated using spin permutation. For Gradient 1, the iterative propagation model yielded significant correspondence in 41 of 52 lesions ($r = 0.25–0.63$ per individual; group mean = 0.40, SD = ±0.09). The direct lesion effects simulation showed significant similarity in 30 of 52 lesions ($r = 0.33–0.57$ per individual; group mean = 0.34, SD = ±0.11). In addition, 32 lesions in the iterative

propagation model exceeded a correlation of 0.3, indicating that incorporating the α–γ parameters captured meaningful aspects of the observed gradient alterations.

For Gradient 2, the iterative-propagation model showed significant spatial correspondence in 42 lesions (r = 0.24–0.58 per individual; group mean = 0.43, SD = ±0.06), whereas the focal lesion simulation produced significant similarity in 23 lesions (r = 0.30–0.63 per individual; group mean = 0.30, SD = ±0.15). Of the 42 significant cases in the iterative-propagation model, 41 exceeded a correlation of 0.3, suggesting that the model captured a substantial proportion of the observed Gradient 2 changes. The distribution of spatial correlation values for the iterative propagation and direct lesion-effects simulations is shown in Figure 4.6, illustrating how the iterative propagation model achieved higher correspondence with the observed stroke gradients across both Gradient 1 and Gradient 2.

For Gradient 3, correspondence was weak: the iterative-propagation model produced significant correlations in only 14 lesions (r = 0.10–0.20), and the direct lesion-effects simulation performed even less effectively. Given the limited ability of these two approaches to reproduce Gradient 3, subsequent statistical analyses focused on Gradients 1 and 2.

The Fisher z-transformed correlation values between the observed gradient-difference maps and the simulated gradient-difference maps for both simulation approaches, for Gradient 1 and Gradient 2, are reported in Table 4.S1 in the supplementary material. Wilcoxon signed-rank tests were used to compare the performance of the two simulation methods. For this analysis, Fisher z-transformed spatial correlations between the observed gradient difference maps and the simulated gradient difference maps were compared on a lesion-by-lesion basis. For Gradient 1, the iterative model produced a slightly higher mean Fisher z value than the direct simulation (0.388 vs 0.360), but this difference was not statistically significant (W = 764, p = 0.247). The iterative model yielded higher correlations in 27 of the 52 lesions. For Gradient 2, the iterative model showed stronger correspondence with the observed gradients than the direct simulation. The mean Fisher z value was 0.323 for the direct simulation and 0.409 for the iterative model, and this improvement was statistically significant (W = 1034, p = 0.00084). In total, 38 of the 52 lesions showed higher correlations following iterative propagation. These findings suggest that the iterative propagation step can improve the reproduction of observed stroke-related gradient alterations, particularly for Gradient 2, where propagation significantly increased correspondence with the observed gradients.

4.5.5. Post-stroke connectivity gradients

Connectivity gradients for aged controls, observed stroke, and simulated stroke are shown in Figure 4. 4. All gradients are displayed using the same purple-to-green colour scale, where dark purple indicates higher gradient values and dark green indicates lower values. Gradient 1 differentiates transmodal (purple) from unimodal (green) regions, and Gradient 2 separates visual (purple) from

motor (green) regions. Aged-control maps show clear separation between regions occupying the extreme poles of Gradients 1 and 2 (Figure 4. 4A). The observed stroke gradients show attenuated functional separation along both the transmodal–unimodal and visual–motor axes, revealed by less intense colours (Figure 4.4B). The simulated gradients broadly reproduced this attenuation. For Gradient 1, transmodal regions—including prefrontal cortex, precuneus, and intraparietal lobule—and unimodal motor regions occupied similar positions to those in the observed stroke gradients along the transmodal–unimodal axis. For Gradient 2, the simulation captured some overall compression of the visual–motor axis, particularly within motor regions, consistent with the observed gradients, but visual areas did not show the same degree of attenuation as the observed stroke gradients (Figure 4.4C).

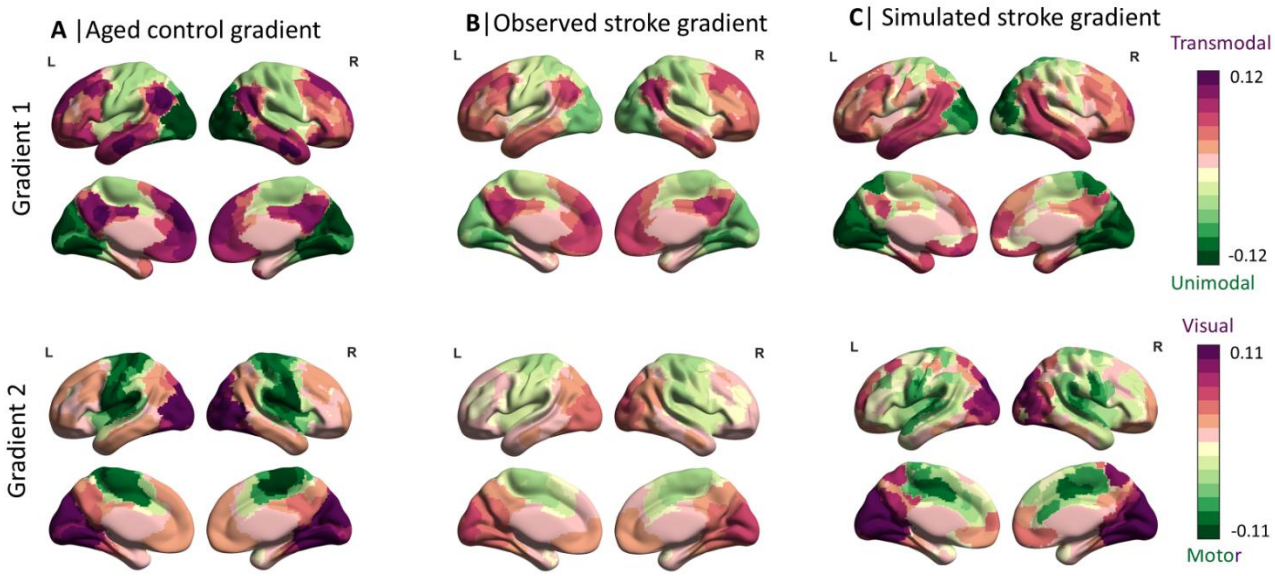

Figure 4.4. Functional connectivity gradients for age-matched controls, observed stroke, and simulated stroke. Darker purple indicates higher gradient values and darker green indicates lower values. A) Aged-control gradients. B) Observed stroke gradients. C) Simulated stroke gradients. The top row shows Gradient 1, representing the unimodal–to–transmodal axis, and the bottom row shows Gradient 2, representing the visual–to–motor axis. Compared with age-matched controls, the simulated and observed stroke gradients showed a reduction in gradient differentiation.

We then examined whether the simulation's replication accuracy depended on lesioned hemisphere or lesion size, and found that it was not influenced by either factor. Spatial correlation values between observed and simulation for each case, based on lesion category (left hemispheric, right hemispheric,

and bilateral infarcts), are reported in Supplementary Figure 4.S5 in the supplementary material. Associations between lesion size and simulation performance, assessed through spatial correlation estimates, are also reported in the supplementary material (supplementary Figure 4.S6).

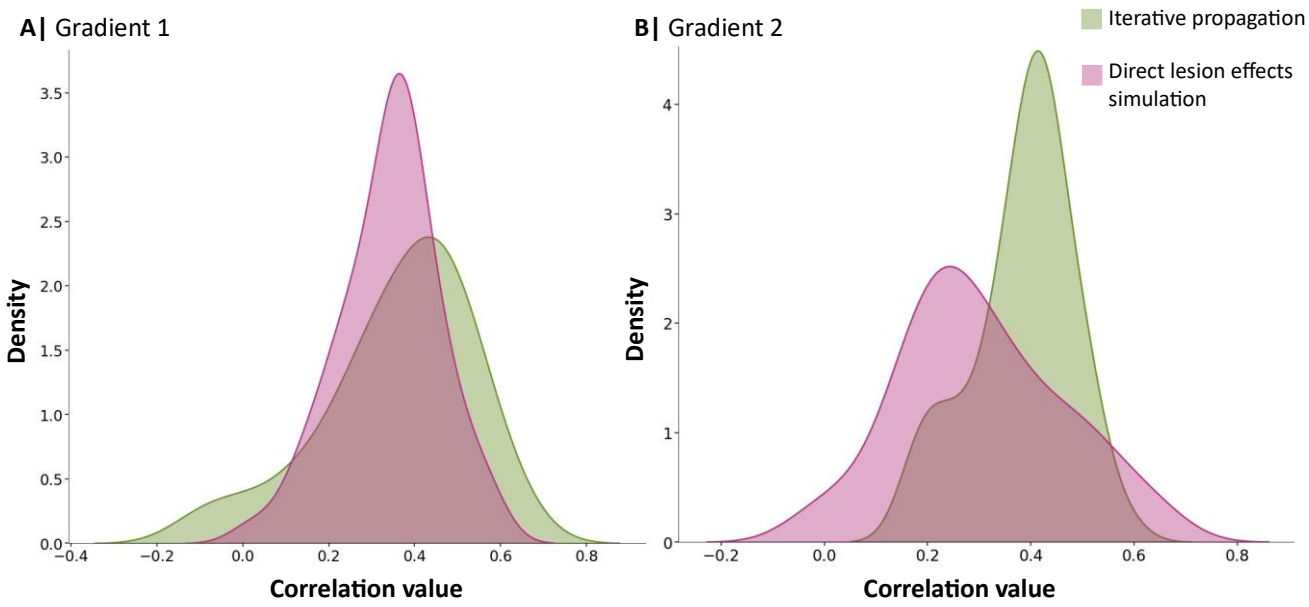

Figure 4.5. Distribution of correlation values for iterative propagation and direct lesion effects simulation. Density plots show the distribution of spatial correlation values between observed post-stroke gradient difference maps and simulated gradient difference maps for each simulation approach. Higher correlation values reflecting greater correspondence between simulated and observed post-stroke gradient changes. A) Gradient 1 and B) Gradient 2 illustrate the comparison between the iterative propagation model (green) and the direct lesion-effects simulation (pink).

4.5.6. Post-stroke connectivity gradient changes: observed versus simulated gradients from the iterative propagation model

Next, we compared stroke-specific effects between the observed gradients and those simulated using the iterative propagation model. For this analysis, we generated difference maps by subtracting each lesion gradient from the average aged-control gradient. These maps were created for both the observed gradients and the simulated gradients derived from the iterative propagation method. The average difference-gradient maps for the observed and simulated data are provided in the supplementary material (supplementary Figure 4.S7).Whole-brain non-parametric tests were conducted separately for the observed and simulated gradients, and we then assessed how closely the significant post-stroke changes from simulation matched the significant changes in the observed

gradients, which reflect the real effects of stroke on connectivity gradients. We quantified how well the simulation captured the real pattern of post-stroke disruption by first estimating the spatial correlation between the group-level significant post-stroke changes in the observed and simulated gradients. The simulation reproduced the observed pattern at a moderate to strong level ($r = 0.692$, $p = 0.0003$).

Figure 4.6 shows the significant post-stroke gradient changes for both the observed and simulated gradients. Regions in warm colours indicate significant shifts toward the bottom end of the gradient, whereas regions in cool colours indicate significant shifts toward the top end. In Gradient 1, the observed stroke group showed transmodal regions—including prefrontal cortex, cingulate cortex, anterior temporal pole, middle temporal gyrus, inferior temporal gyrus, precuneus, and angular gyrus—shifting toward the unimodal end (Figure 4. 6A, top left panel). The simulation reproduced most of these transmodal shifts, except for the anterior temporal pole (Figure 4.6B, top right panel). Along the same axis, the observed stroke group also showed visuo-motor regions shifting toward the opposite transmodal pole. The simulation captured most of these effects, although medial visual regions such as the calcarine sulcus did not follow this pattern and instead shifted further in the same direction.

For Gradient 2, the spatial correlation between the observed and simulated significant changes indicated that the simulation reproduced the pattern at a moderately strong level ($r = 0.6130$, $p = 0.0003$). In the observed data, both motor and visual regions were less differentiated along this axis (Figure 4.6A, bottom left panel). The simulation captured most of this reduction in differentiation, but medial visual regions—including the calcarine sulcus, cuneus, lingual gyrus, and posterior parieto-occipital cortex—shifted in the same direction rather than toward the motor end (Figure 4.6B, top right panel). Overall, both axes showed a reduction in gradient space, reflecting stroke-related changes in functional reorganisation.

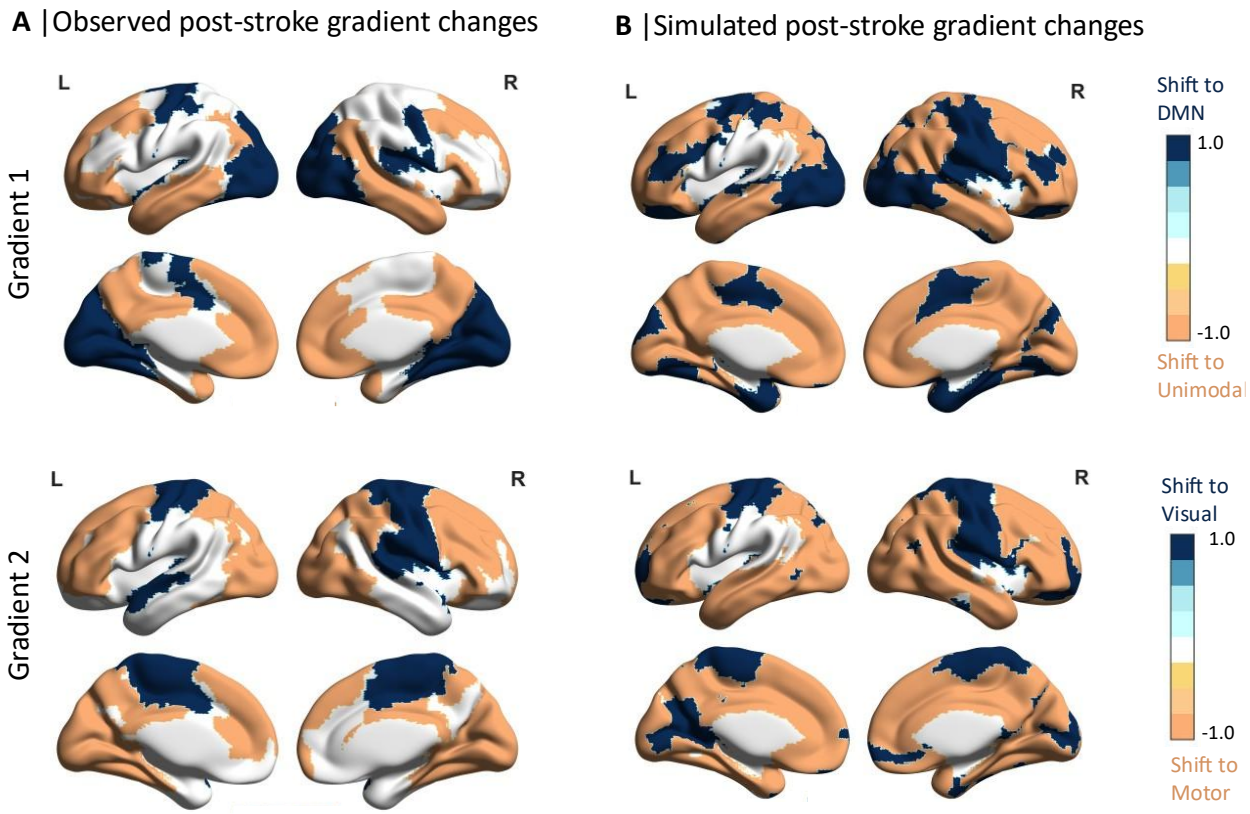

Figure 4.6. Comparisons of significant post-stroke functional changes between observed and simulated gradients from permutation tests. Difference maps reflect post-stroke gradient changes, created by subtracting each lesion gradient from the average aged-control gradients. A) Significant post-stroke changes in observed Gradients 1 and 2. B) Significant post-stroke changes in simulated Gradients 1 and 2. Warm colours indicate significant shifts toward the lower end of each gradient following stroke, whereas cool colours indicate significant shifts toward the upper end.

4.5.7. Comparisons of network organisation in gradients between observed and stimulated stroke

Next, we compared the network-wise organisation of the simulated stroke gradients with the observed stroke gradients in the first two gradient axes. In Gradient 1, networks were arranged from DMN and frontoparietal networks through ventral and dorsal attention networks, ending with unimodal somatomotor and visual networks. In Gradient 2, the organisation progressed from visual to somatomotor networks. A figure illustrating network organisation in simulated and observed post-stroke gradients across these axes is provided in the supplementary material (Section II, supplementary Figure 4.S8).

To assess how accurately the simulation captured stroke-induced changes at the network level, we examined whether shifts in gradient space relative to age-matched controls differed between observed and simulated stroke across networks. All analyses were performed on gradient difference maps computed by subtracting each lesion gradient from the average age-matched control gradient, thereby isolating stroke-specific network shifts in gradient organization. While spatial correlation analyses of these difference maps (using spin permutation) quantified overall similarity between observed and simulated stroke effects, they did not provide information about network-specific agreement. To address this, we performed a repeated-measures analysis of variance (ANOVA) on network-level gradient values, where each subject contributed one value per network. The dependent variable was the gradient difference value, and fixed effects included Network, Group (Observed Stroke vs Simulation), and their interaction. This approach allowed us to determine whether the deviation between observed and simulated stroke effects varied across networks (Network × Group interaction) and to quantify the extent of these deviations. From the ANOVA analyses, significant interactions between Network and Group were observed for both gradients (Gradient 1: $F(13,1428) = 56.956$, $p < .001$; Gradient 2: $F(13,1428) = 109.5329$, $p < .001$), indicating that differences between real and simulated gradient values depended on brain network. We also found significant main effects of Network in Gradient 1 ($F(13,1428) = 301.313$, $p < .001$) and Gradient 2 ($F(13,1428) = 592.5153$, $p < .001$). Significant main effects of Group were found only for Gradient 1 ($F(1,1428) = 34.669$, $p < .001$) and not for Gradient 2. Individual data points for the difference-gradient values displayed in the box–scatter plots for both the observed stroke and simulation conditions are presented in Supplementary Figure 4.S9.

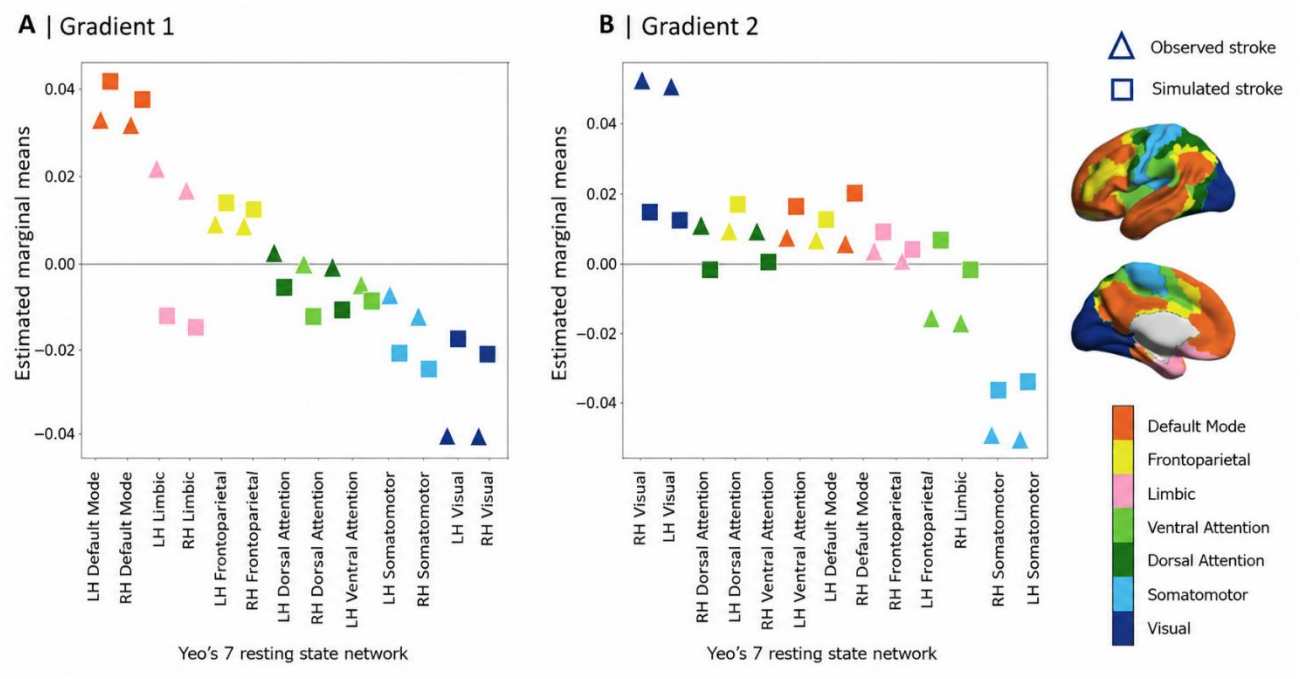

Figure 4.7. Network-level shifts of observed and simulated stroke in gradient space. Difference-gradient values extracted for each network are displayed as estimated marginal means. Triangles represent observed stroke, and squares represent simulated stroke. Points indicate the estimated marginal means for each network, illustrating the extent to which the simulation captures stroke-related shifts in gradient space relative to the observed stroke data. Brain maps depict the spatial topology of Yeo's seven resting-state networks, and the plots show their relative positions along the two principal gradients. (A) Network shifts along the transmodal–unimodal axis (Gradient 1). (B) Network shifts along the visuomotor axis (Gradient 2).

Post hoc pairwise comparisons were conducted within each network using estimated marginal means derived from the ANOVA, with Bonferroni correction applied for multiple comparisons. Contrasts were defined as Observed Stroke − Simulation, where values close to zero indicate close correspondence between observed and simulated stroke effects, whereas larger positive or negative values indicate greater divergence. Post hoc analyses revealed significant group differences across multiple networks for both gradients. Figure 4.7A–B displays the estimated marginal means for observed and simulated stroke, illustrating the position of each network along the two gradient axes. The separation between the observed and simulated values provides a visual indication of the magnitude and direction of the deviations, with networks showing greater overlap indicating closer correspondence between the simulated and observed stroke effects. This pattern of separation is consistent with the post hoc comparison results.

For Gradient 1, the smallest differences were observed in the frontoparietal and ventral attention networks, which did not show significant group differences, reflecting very close correspondence between simulated and observed stroke effects. Among networks showing significant differences, the smallest deviations were observed in the dorsal attention and default mode networks ($|\Delta| \approx 0.006–0.010$), reflecting relatively close alignment. Moderate differences were observed in somatomotor and ventral attention networks ($|\Delta| \approx 0.011–0.015$), indicating moderate deviation. In contrast, the largest discrepancies were found in visual and limbic networks ($|\Delta| > 0.02$), indicating substantial divergence between simulated and observed stroke effects. For Gradient 2, the smallest difference was observed in the right limbic network, which did not show a significant group difference, indicating very close correspondence between simulated and observed stroke effects. Among networks showing significant differences, the smallest deviations were observed in limbic and frontoparietal networks ($|\Delta| \approx 0.004–0.006$), followed by default mode and dorsal attention networks ($|\Delta| \approx 0.007–0.009$), indicating relatively close alignment. Moderate differences were observed in right hemisphere default mode, dorsal attention, somatomotor, and ventral attention networks ($|\Delta| \approx 0.012–0.014$). Larger deviations were evident in left somatomotor and ventral attention networks ($|\Delta| \approx 0.017–0.022$). In contrast, the largest discrepancies were observed in visual networks ($|\Delta| > 0.03$), indicating substantial divergence between simulated and observed stroke effects.

For Gradient 1, the smallest differences were observed in the default mode and dorsal attention networks, with the frontoparietal network also showing very close correspondence between simulated and observed effects. For Gradient 2, the frontoparietal network showed the smallest differences, indicating relatively good simulation performance for this network. In contrast, visual networks consistently exhibited the largest deviations across the gradients, indicating poor correspondence between simulated and observed stroke effects.

4.5.8. Validation of simulated post-stroke gradient–language outcome associations in observed stroke gradients

We performed lesion–gradient mapping to identify associations between simulated post-stroke gradient changes from the iterative propagation model (derived from the difference-gradient maps) and PCA-derived language components. For this analysis, we focused on gradient changes within the language network, as functional connectivity alterations in these regions are directly relevant to the language outcomes assessed using the CAT. Voxels with ≥25% lesion involvement were excluded from the language network mask to ensure that gradient changes were examined only in spared language regions from direct lesion damage. We then tested whether these simulation-based associations were also present in the observed stroke gradients. To do this, we extracted gradient values from the observed data for the significant clusters identified in the simulation and used robust

linear regression to examine whether the observed gradients showed comparable associations with the PCA-derived language components.

The simulation-based lesion–symptom mapping identified six significant effects; of these, only the associations linked with worse speech and better phonology were recovered in the observed post-stroke gradients. In the worse-speech contrast, the left paracingulate cortex and supplementary motor area (Figure 4.8A) showed greater displacement toward the motor end of the visuomotor axis (Gradient 2). In the observed gradients, motor-region parcels typically showed displacement toward the visual end as part of functional reorganisation; however, deviations in the opposite direction were associated with poorer speech performance (Figure 4.8B), consistent with the simulation findings (Figure 4.8C). The observed and simulated gradient–speech associations showed similar trends, indicating good correspondence between the two. For phonology and working memory (PCA 2), the simulation also identified a significant cluster in the right inferior frontal gyrus (IFG) (Figure 4. 8D). This region typically occupies a position closer to the visual end of Gradient 2 in normative organisation, but in the simulation it shifted toward the motor end (Figure 4.8F), and this displacement was associated with better phonology and working-memory performance. The same directional shift and behavioural association were recovered in the observed gradients (Figure 4.8E), indicating convergence between simulated and empirical reorganisation patterns. Scatterplots show that associations between difference-gradient values in the paracingulate cortex, supplementary motor area, and right IFG and their corresponding PCA components follow similar trends in both the simulated and observed data. The significant clusters that were not recovered in the observed gradients are reported in the supplementary materials (Supplementary Figure 4.S10).

We performed lesion–gradient symptom mapping on the observed stroke difference-gradient maps to examine whether the same clusters or neighbouring clusters identified in the observed gradients were replicated by the simulation. Observed stroke gradient changes showed no significant clusters in Gradient 1 and Gradient 2. However, the PCA-3 (writing) language component was associated with the left IFG in Gradient 3 in the observed stroke. Since the iterative propagation approach poorly replicated the real effects of stroke, we did not attempt to validate the observed stroke gradient's language association in the simulation gradient.

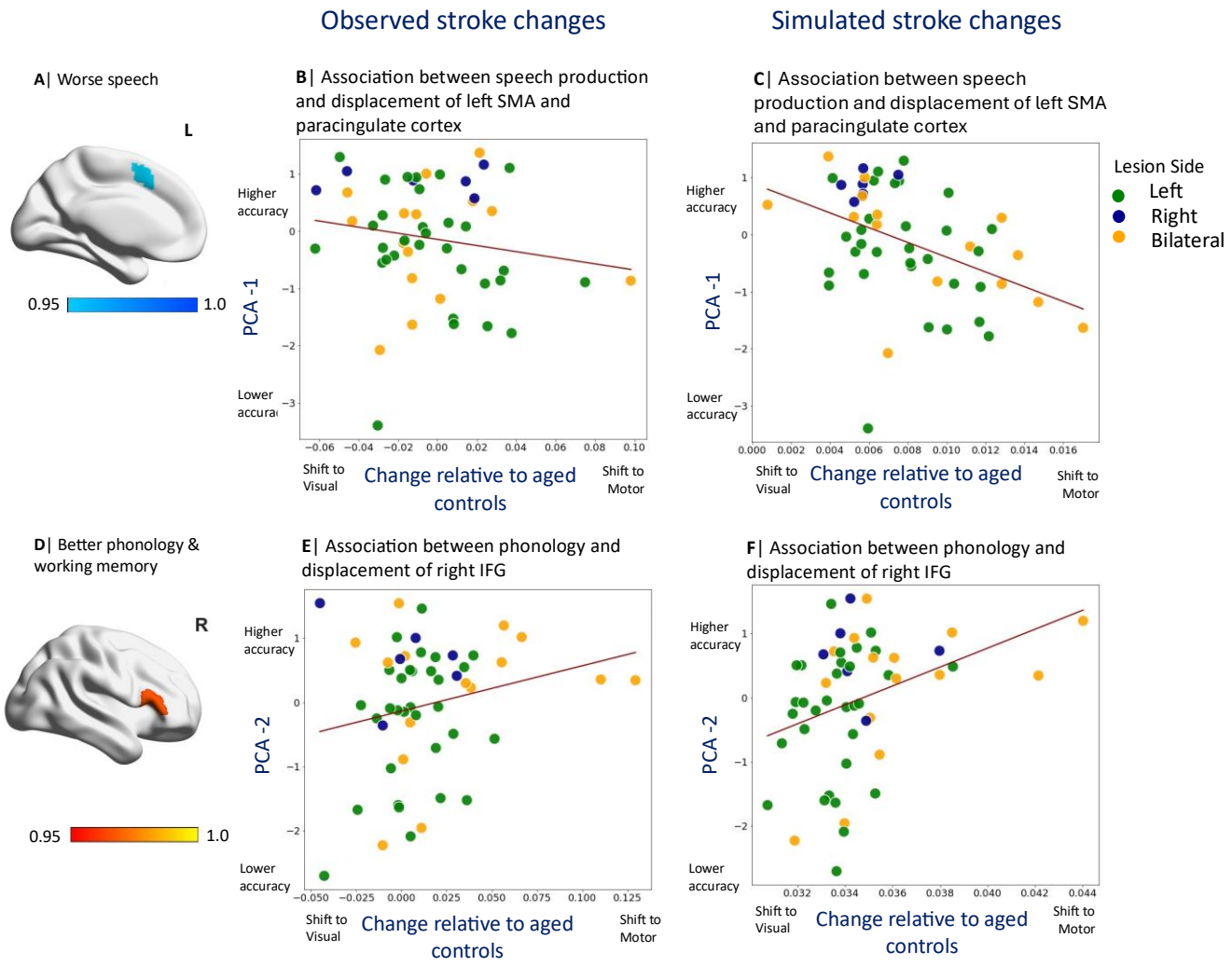

Figure 4.8. Permutation test results within the language ROI. A) Significant cluster associated with worse speech (PCA-1) within the language network ROI. B) Association between speech production and observed post-stroke displacement of left supplementary motor area and paracingulate cortex along Gradient 2 (visual–to–motor axis). C) Association between speech production and simulated post-stroke displacement of the same medial regions along Gradient 2. D) Significant cluster associated with better phonology and working memory (PCA-2) in the right inferior frontal gyrus (IFG). E) Association between phonology and observed post-stroke displacement of right IFG along Gradient 2. F) Association between phonology and simulated post-stroke displacement of right IFG along Gradient 2.

4.6. Discussion

This study demonstrates that simulating both direct and indirect stroke-related changes within intact gradient space can moderately reproduce the empirical alterations observed after stroke, particularly along Gradients 1 and 2. The iterative-propagation model provided a closer approximation to the observed stroke gradients than the direct proportionate-reduction approach, highlighting the importance of modelling how focal damage spreads through the preserved functional architecture, especially for Gradient 2. Both observed and simulated gradients showed reduced functional separation along the transmodal–unimodal and visual–motor axes, consistent with the widespread attenuation of large-scale organisation noted in observed stroke gradients. We also found that two simulated associations with language outcomes were recovered in the observed gradients, particularly along the visuomotor axis for two PCA-derived language components. A cluster in right IFG was linked to better phonology and working memory (PCA-2) when its connectivity was shifted toward the motor end of the visuomotor axis (Gradient 2). The left paracingulate cortex was also associated with poorer spoken language in participants with more motor-like connectivity on the same gradient. These convergent patterns across methods suggest that the simulation captures behaviourally meaningful aspects of lesion-induced reorganisation; however, this approach might also be associated with some false positives (findings not verified by observed gradients derived from resting-state fMRI), suggesting there is a need for caution in the application of this approach, and in further refinement of this method.

4.6.1. Iterative propagation approach to model lesion effects on cortical gradients

Both lesion simulation (Alstott et al., 2009; He et al., 2009; Tao & Rapp, 2021) and lesion network studies (Fox, 2018; Jimenez Marin et al., 2022; van den Heuvel et al., 2026) use lesion data to examine stroke-induced functional disruption. Our approach is conceptually similar to these studies, using lesion data to model stroke impact on the normative connectome. However, we focus on functional reorganisation in spared cortical tissue. Existing approaches provide a binary view of network damage (connected vs. disconnected) and are limited in their ability to capture whole-brain changes, resulting in a predominantly unidirectional lesion-linked network perspective. Although perilesional regions may undergo changes (Kiran & Thompson, 2019; Alia et al., 2017), these methods do not incorporate such changes and may therefore oversimplify by treating affected regions as fully disconnected. This limitation has been demonstrated empirically: Tao and Rapp (2021) compared network properties between the real functional connectomes of chronic stroke patients and simulated lesion connectomes generated by removing lesioned nodes in aged controls. They found that discrepancies between simulated and empirical network effects were driven by long-range

functional reorganisation in chronic stroke, which the simulation could not model (Tao & Rapp, 2021).

We introduce a lesion simulation method that combines proportional reduction of connectivity with an iterative propagation step, allowing lesion effects to spread through preserved cortex rather than being limited to lesion-centred disruption. This approach extends beyond focal and lesion-linked remote effects, influencing connectivity throughout the connectome. In doing so, it models how reduced drive from damaged regions influences structurally intact networks, capturing global alterations that arise from interregional connectivity dependencies across the cortex.In this framework, applying lesion effects to the normative functional connectome captures only the direct impact of the lesion on connections involving the damaged region. This includes both nearby and distant regions that are directly connected to the lesion site, but it does not capture effects on regions that are indirectly connected through multi-step pathways. These broader network-level consequences are instead approximated by the iterative propagation stage, which allows lesion-related disruption to extend beyond directly connected parcels. To our knowledge, this is the first simulation framework to incorporate the indirect effects of stroke across the whole connectome alongside direct lesion impacts. Prior lesion-topology models were restricted to disruptions in networks directly connected to the lesion and did not account for these broader system-level consequences.

We attempted to address this limitation by modelling the graded functional changes in spared tissue and projecting these changes onto the gradient space. The direct lesion simulation without propagation captured some of the observed stroke-related gradient changes, but scaling lesion effects in functional connectivity space produced simulated gradients that more closely matched the observed stroke gradients and the relative arrangement of regions along those gradients. We observed that lower propagation strength ($\alpha = 0.1$) combined with near-linear scaling of connectivity loss ($\gamma = 0.8$) produced simulated gradients that more closely resembled the observed stroke gradients. This suggests that this specific parameter combination is sufficient to approximate the distributed gradient alterations seen after stroke. The largest source of variation in simulation success was individual differences, rather than lesion size, lesion laterality, or the type of language impairment. Introducing these two forms of disruption into the gradients leads to observable gradient reorganisation. Because the simulation method operates in connectivity-gradient space, it captures graded changes along major functional axes, revealing both each region's shift in connectivity profile and the broader system-level pattern in which functionally similar regions move together. In contrast, node- or edge-removal models and the graph-theory metrics derived from them provide only numerical summary values and therefore cannot represent these continuous pattern-level changes in connectivity organisation. A key advantage of projecting lesion effects into gradient space is that it offers interpretable dimensions

linked to cognition. This may help explain how introducing lesions into an aged normative connectome alters gradient dimensions and influences behaviour.

The proposed iterative propagation approach is consistent with the widely accepted view that focal brain lesions lead to distributed functional network alterations (Carrera & Tononi, 2014). Our simulation framework builds on this concept by using lesion topology to drive changes in functional connectivity patterns, which subsequently alter the organisation of connectivity gradients. This interpretation is supported by previous studies showing that structural brain lesions can disrupt resting-state functional connectivity across distributed brain networks (Eldaief et al., 2016; Gratton et al., 2012; Nomura et al., 2010). This design is consistent with network-based accounts of cognition in which cognitive functions emerge from system-wide topology and global communication efficiency across the entire connectome (Friston, 2011; Mohr et al., 2016; Tompson et al., 2018). Importantly, the method uses structural MRI alone, providing a practical alternative when resting-state fMRI is not clinically available.

4.6.2. Post-stroke connectivity gradients

However, not all aspects of post-stroke gradient changes were reproduced effectively by the simulations. In Gradient 1, the simulation failed to reproduce the medial visual region's shift towards the transmodal end. Likewise, in Gradient 2, the simulation failed to capture the medial visual region's shift toward the motor end. This discrepancy may have occurred because the simulation approach did not sufficiently alter connectivity in these regions to reproduce the observed gradient shifts.

4.6.3. Simulation captured functional reorganisation changes associated with language outcomes

The average post-stroke period for individuals in this study was more than four years, meaning that the resting-state data used to extract connectivity gradients may have reflected long-term functional reorganisation, residual functional disruption, and stroke-related degenerative changes. This context is important because, unlike previous simulation studies that modelled only lesion-driven disconnection (Alstott et al., 2009; He et al., 2009; Tao & Rapp, 2021; Fox, 2018; Jimenez Marin et al., 2022; van den Heuvel et al., 2026), our approach was evaluated against gradients that would have captured broad functional changes driven by these different dynamics, and the simulation moderately reproduced these patterns. This also helps explain why the simulation did not reproduce stroke-specific gradient shifts in some cases, as those empirical changes may have been strongly shaped by long-term neurodegenerative processes. Some of the effects that did not replicate may

reflect acute lesion-driven changes that are no longer present in the chronic phase, having been reduced or compensated for through common patterns of long-term reorganisation.

We found that the right IFG shift toward a motor like connectivity profile in Gradient 2 was associated with better performance in phonology and working memory (PCA 2). This pattern may represent compensatory functional changes that support phonological processing. Importantly, this simulation derived association was also present in the observed stroke gradients, indicating that the model captured aspects of functional reorganisation beyond lesion driven disruption. The right IFG is known to support phonological working memory and the maintenance of verbal information (Hartwigsen et al., 2010; Nucci et al., 2026). Evidence from developmental dyslexia shows that right IFG hyperactivity compensates for left hemisphere impairment during reading (Sinha et al., 2024), and right IFG involvement has also been reported in aphasia recovery following left hemisphere stroke (van Oers et al., 2010). Aphasic patients have been shown to employ right IFG and dorsolateral prefrontal cortex as domain general compensatory regions for difficult language tasks. This upregulation of the cognitive control network increases with higher language processing demands and functions as a facilitator for communication recovery (Geranmayeh et al., 2014). The right IFG additionally contributes to inhibitory control and motor monitoring, which aligns with its functional links to primary motor cortex (Hinton et al., 2018; Neubert et al., 2010). These findings suggest that a right IFG shift toward the motor end of Gradient 2 supports phonology and working memory recovery in stroke.

Left paracingulate gyrus and supplementary motor cortex shifting further toward the motor end of Gradient 2 was linked with impaired speech (PCA 1). The permutation tests showed that the dominant stroke related change in Gradient 2 was a shift of motor regions toward the visual end, reflecting reduced modularity. In contrast to this general compression pattern, these medial frontal regions involved in speech control deviated from the overall trend, and this deviation was associated with poorer speech performance. These regions form part of the medial frontal network supporting speech initiation and monitoring (Tremblay and Gracco, 2010). The supplementary motor area contributes to initiating and timing voluntary speech (Bullock et al., 2024; Hertrich et al., 2016), while the paracingulate cortex supports error monitoring and affective prosody (Gennari et al., 2018; Barrett et al., 2004). The gradient based association between these regions and impaired speech aligns with evidence showing reduced functional connectivity between medial frontal regions and cognitive control or salience networks after stroke, which has been linked to deficits in motor and speech initiation, even in individuals who appear functionally recovered (Liu et al., 2020).

4.7. Future directions

Our iterative propagation approach captured Gradient 1 and Gradient 2 changes with moderate accuracy and their associations with language outcomes, but did not fully model Gradient 3 alterations involving higher-order networks. Incorporating mechanisms that better approximate the reorganised functional architecture of chronic stroke may improve the simulation of this axis. Gradient 3 changes were associated with language outcomes in the observed data, suggesting that more accurate modelling of higher-order network reorganisation could enhance clinical relevance. In this study, lesion-induced connectivity loss was propagated across all edges for three iterations; whether additional iterations (e.g., four or five) would yield greater correspondence with the observed stroke gradients, including for lower-order gradients, remains to be explored.

The simulation approach was also confined to stroke-specific functional changes in the cortex and did not model functional changes in subcortical regions. Future work should examine both cortical and subcortical functional changes. It is also worth exploring whether the proportion of lesion involving grey matter and white-matter tracts influences the simulation's ability to reproduce observed stroke effects. Larger simulation-derived clusters linked to behaviour warrant cautious interpretation and replication in independent datasets. Further validation should extend the approach to additional behavioural domains such as executive function, motor performance, and visuospatial attention to test generalisability, and systematically assess performance across strategic lesion locations, including hubs and rich-club nodes, to understand how these influence gradient organisation. Longitudinal datasets would also allow modelling of acute-to-chronic gradient trajectories, providing a more complete picture of how lesion-driven disruption evolves into long-term reorganisation. Future work should also simulate lesions targeted to unimodal versus transmodal regions to test how damage to different points along the cortical hierarchy affects gradient organisation. This would clarify whether gradient alterations primarily reflect hierarchical position, lesion topology, or their interaction. From a methodological perspective, although the healthy control cohort in this study was not closely matched to the stroke cohort with respect to age or sex, the control data were used primarily as a normative reference for the simulation framework. Future studies should include age- and sex-matched healthy controls to further validate and extend these findings.

4.8. Conclusions

This study demonstrates that modelling stroke effects in connectivity-gradient space provides a framework for capturing both direct lesion-driven disruptions and longer-term functional reorganisation. The iterative propagation approach, which integrates lesion topology with graded reductions in functional connectivity, replicated observed post-stroke gradients with greater precision than a direct lesion-effect simulation model. Both simulated and observed gradients showed reduced functional differentiation along the transmodal–unimodal and visual–motor axes, consistent with broader evidence of decreased modularity and increased cross-network coupling after stroke. Importantly, the simulation also recovered behaviourally relevant reorganisational patterns: a compensatory right IFG shift supporting phonology and working memory, and medial frontal shifts linked with impaired speech. These findings highlight connectivity gradients as a sensitive framework for characterising distributed stroke effects and demonstrate that lesion-derived simulations can approximate meaningful patterns of functional reorganisation years after injury.

Chapter 5
General Discussion

5.1. Scope and aims of the thesis

Stroke produces widely distributed effects that extend beyond the focal lesion, disrupting the broader architecture of functional networks. Connectivity gradients provide a low dimensional framework for characterising large-scale functional organisation and offer a principled way to capture these system level changes and relate them to behavioural outcomes.

The primary aims of this thesis were to (1) characterise how stroke alters connectivity gradients, and (2) determine whether gradient changes are associated with semantic control and language outcomes. A further aim was to evaluate whether clinically available structural imaging can be used to model post-stroke functional reorganisation in the absence of resting-state fMRI. These aims have clinical relevance for understanding the brain reorganisation linked with specific impairments and for evaluating whether routinely acquired scan data can be used to model functional changes in the stroke affected brain. Because semantic control and language depend on long range interactions across distributed networks, these domains provide useful test cases for assessing how stroke related gradient changes relate to preserved and impaired cognitive function. To address these aims, the thesis examined both empirical changes in connectivity gradients derived from resting-state fMRI and lesion impact simulations based on structural MRI. Two simulation approaches were compared: a direct lesion effects simulation, which modelled all connections linked to the lesioned parcel, and an iterative propagation simulation, which modelled both direct and indirect effects across the cortex. The following sections summarise the main findings of the empirical chapters, and common themes across chapters are synthesised in the general discussion.

5.2. Summary of empirical chapters

5.2.1. Chapter 2: Lesion-gradient mapping in semantic aphasia: comparisons of observed and simulated effects of stroke on connectivity gradients

This study aimed to answer three questions related to simulated connectivity gradients in a group of stroke survivors with semantic aphasia, with difficulties controlling semantic retrieval such that it is appropriate for the task or context (Jefferies & Lambon Ralph, 2006; Thompson et al., 2015): (I) as a proof-of-concept, the study asked whether lesion maps transferred into connectivity gradient space

could reproduce post-stroke connectivity changes observed seen in resting-state fMRI data in a small sample, (II) next, in a larger sample, the study considered what stroke-specific connectivity gradient changes are expected in semantic aphasia, and (III) whether simulated connectivity gradients are related to semantic impairments in this group. Lesion maps from structural MRIs of 21 semantic aphasia patients were used to simulate the effects of stroke on the brain's functional landscape. Lesions were left-hemispheric, extending into the insular, prefrontal and lateral occipital cortices, with maximum overlap in the left middle frontal gyrus. A subset of patients (N = 8) had resting-state fMRI data, allowing comparison between simulated and observed gradient changes. Binarised lesion maps were aligned to the Schaefer 400-parcel template, and lesion-complement values were used to construct lesion matrices that were applied to an aged-control normative functional-connectivity matrix. Connectivity gradients were then extracted from the simulated lesion connectivity matrices. Analyses focused on Gradient 1 (transmodal–unimodal axis) and Gradient 2 (visual–motor axis) given the modest sample size. Stroke-specific effects were estimated by subtracting each simulated post-stroke gradient from the averaged aged-control gradient to generate difference maps. Spatial correlation analyses using spin-permutation tests compared observed and simulated maps in the subset of eight patients. In Gradient 1, seven of the eight cases showed significant spatial correlations between observed and simulated post-stroke changes (individual r values = 0.20–0.62; group mean = 0.423; SD = 0.145). Six of these cases had correlation values greater than 0.30. For Gradient 2, only five of the eight cases showed significant spatial correlations, and the overall correspondence was weaker (individual r values = –0.33–0.42; group mean = 0.153; SD = 0.218). These results indicate that the simulation captured most of the empirical post-stroke changes in Gradient 1, but only some aspects of the changes observed in Gradient 2.

Semantic performance in the stroke survivors was assessed using the Camel and Cactus test (word and picture versions) and an ambiguous word decision task. These measures were combined using principal component analysis to derive a single semantic score. Lesion-gradient mapping examined associations between simulated post-stroke gradient changes and these scores. Simulated gradients irrespective of performance showed attenuation along both axes relative to age-matched controls. Lesion-gradient mapping identified the left inferior frontal gyrus (IFG) as associated with semantic deficits when it showed stronger unimodal connectivity on Gradient 1, deviating from its typical transmodal position. This is a relatively novel approach to simulate stroke effects in connectivity-gradient space by using structural MRI, which is more clinically available than resting-state fMRI data. No other studies have examined stroke-induced semantic deficits in relation to connectivity gradients or considered the connectivity profile changes expected in semantic aphasia. Although the accuracy of the simulation was evaluated against only eight lesion cases, the study identified that left IFG shifts toward a unimodal-like connectivity profile might be associated with context-dependent retrieval difficulties in these patients.

5.2.2. Chapter 3: Reorganisation of functional connectivity gradients in post-stroke aphasia

This study focused on the importance of cortical lesion location and cortical connectivity gradients in stroke and their association with language dysfunction. Three principal questions answered were: I) What is the critical lesion location associated with specific language subdomains? II) What stroke-induced cortical functional connectivity changes are characterised by connectivity gradient analyses? III) Which changes in connectivity gradients are associated with language outcomes beyond the effects of focal lesions? To answer these questions, the PLORAS (Predict Language Outcome and Recovery After Stroke) dataset was used, as it includes structural and resting-state functional MRI along with language and cognitive assessments. Chronic stroke individuals (N = 60) with diverse lesion profiles were included (left, right, bilateral, and lacunar infarcts). The Comprehensive Aphasia Test was administered to assess language subdomains. To reduce dimensionality, derive more robust measures of specific language processes, and address multicollinearity stemming from shared underlying processes, a principal component analysis (PCA) was used to identify six functionally distinct language components.

Two symptom-mapping approaches were used: (i) lesion-symptom mapping using cortical lesion location from structural images to identify critical loci associated with the language-derived components; (ii) lesion-gradient mapping to examine functional reorganisation in the unlesioned brain linked to language outcomes. Lesion-symptom mapping implicated left temporoparietal regions (including Heschl's gyrus, parietal operculum, angular and supramarginal gyri) and the superior division of the lateral occipital cortex in phonological and working-memory difficulties. Worse visuomotor performance was associated with lesions extending from the temporo-occipital portion of the inferior temporal gyrus to the lateral occipital cortex in the right hemisphere. The visuomotor PCA component showed strong loadings for writing to dictation, writing picture description, and written naming, consistent with its interpretation as reflecting visually guided motor output. However, the significant cluster in the right hemisphere should be interpreted cautiously, as the sample included 46 left-hemispheric, 2 bilateral, and only 12 right-hemispheric infarcts. This means that the visuomotor finding is driven by a relatively small subset of right-hemisphere lesions (n = 14), and therefore may not generalise to new samples of stroke survivors. Poor comprehension and arithmetic performance were associated with damage to the left middle temporal gyrus (temporo-occipital part) and the posterior supramarginal gyrus.

There was a clear distinction between the aged-control and stroke gradients. Stroke gradients showed attenuation across the three functional axes compared with aged controls: the transmodal–unimodal axis, the visual-motor axis, and the control–default-mode-network (DMN) axis. These findings indicate that stroke reduces functional differentiation between large-scale functional systems. A shift of the left inferior frontal gyrus (IFG) along the control–DMN axis was associated with better speech but poorer visuomotor performance, as revealed by lesion-gradient mapping. The novel

findings of this study help to reveal how post-stroke functional reorganisation along connectivity gradients within the unlesioned brain relates to language function. Although dimensional changes were observed across all gradient axes, shifts in heteromodal network positions, particularly along the control–DMN axis, may reflect compensatory re-embedding of surviving regions that support language function. These gradient shifts provide a low-dimensional, behaviourally relevant account of how local damage and distributed reorganisation jointly shape language outcomes after stroke.

5.2.3. Chapter 4: A connectivity-gradient simulation model captures stroke reorganisation and language outcomes

The final empirical chapter of this thesis further developed and evaluated simulations of post-stroke gradient connectivity changes in a larger sample. The primary research questions were: (I) To what extent can lesion topography simulate the impact of stroke on connectivity gradients? (II) To determine whether modelling lesion effects across all edges in the functional connectivity matrix (iterative propagation) improves simulation accuracy relative to a direct lesion effects simulation. (III) Do observed stroke gradients show similar associations with language outcomes as simulated gradient changes? This study included PLORAS participants with both structural and resting-state fMRI, which allowed us to compare simulated gradient changes with empirical resting-state gradients. The language and cognitive functions of the stroke individuals were again assessed using the Comprehensive Aphasia Test, with scores for different language components extracted using PCA. Unlike previous lesion-simulation studies, an iterative-propagation simulation model introduced stroke-specific changes at three levels: (i) direct effects on damaged parcels; (ii) remote effects on regions connected to the lesion core; and (iii) global, network-wide disruption of edges across the unlesioned brain. These levels were modelled to capture local, diaschisis-like, and whole-network consequences of stroke, and were validated by comparing simulated gradients with empirical resting-state gradients from the PLORAS sample.

Lesion effects were simulated using a normative, aged-control connectome and projected onto functional connectivity gradients. For each lesion, spatial correlations assessed the similarity between simulated and observed stroke gradients, comparing direct lesion effects simulation with the iterative-propagation simulation to determine which approach better reproduced the chronic stroke changes observed in the empirical data. Although the iterative-propagation simulation produced higher correlation values than the direct lesion-effects simulation for both Gradient 1 and Gradient 2, statistical testing showed that the iterative step significantly improved the accuracy of modelling real stroke effects only for Gradient 2. Iterative-propagation–based simulation moderately reproduced post-stroke functional reorganisation along the transmodal–unimodal and visuomotor axes. Lesion-gradient mapping was used to examine associations between simulated post-stroke gradient changes and the PCA-derived language components; significant clusters from the simulation analyses were validated against the empirical stroke gradients. The simulation lesion-gradient mapping

identified six significant clusters linked to PCA-derived language performance. Of these six clusters, the empirical gradients recovered only two clusters for Gradient 2 (visuomotor axis), suggesting the simulation approach may generate false positives. The two verified effects suggested that a shift in the right inferior frontal gyrus (right IFG) towards the motor end of Gradient 2 was associated with better phonology and working memory after stroke. A similar shift in left supplementary motor area and paracingulate cortex also towards the motor end of Gradient 2 was associated with impaired speech.

This was, to our knowledge, the first study to investigate both the accuracy and the behavioural relevance of gradient simulations using empirical stroke data, thereby assessing the extent to which the simulation's associations with language outcomes were reliable. The results suggest that simulations based on lesion information alone show moderate correlations with real gradient changes, especially for higher-order gradients; however, the approach requires further refinement, as it was not possible to recover the observed Gradient 3 stroke effects reported in Chapter 3, and not all simulation-derived findings from Chapter 4 were replicated in the empirical data.

5.3. Key Themes from the Empirical Chapters

The remainder of the General Discussion is divided into two parts. The first part provides a methodological rationale for the analytical choices made across Chapters 2–4, outlining the conceptual and biological foundations underlying the use of connectivity gradients to characterise stroke-induced functional changes, and discussing the consequences of these choices for how the findings should be interpreted. Because this thesis applies gradient based methods in a novel way, it is important to consider both the rationale for these approaches and the implications of the assumptions that underpin them. The second part synthesises the common themes that emerged across the three empirical chapters, integrating the results to explain how focal lesions and distributed reorganisation jointly shape semantic control and language outcomes after stroke.

5.3.1. Methodological rationale for connectivity gradients

Functional-connectivity gradients were the primary method used to characterise cortical organisation across the three empirical chapters. Across the thesis, gradients were applied in three complementary ways: Chapter 2 simulated the direct impact of focal lesions on functional connectivity; Chapter 3 examined post-stroke functional reorganisation in aphasia; and Chapter 4 introduced an iterative propagation model to capture how lesion effects might spread across the functional connectome. Together, these applications demonstrate how low-dimensional gradient axes capture both focal

damage and distributed reorganisation, and how these changes relate to behavioural outcomes after stroke.

The brain's functioning depends on efficient information transfer between distinct functional units. Its anatomical foundation enables functional coordination, communication, and integration through the connectome, the structural scaffold that supports large-scale organisation (Sporns et al., 2005). Building on this scaffold, the cortical landscape is characterised as a network composed of multiple system-level organisations that support perceptual, cognitive, and motor processes (Van den Heuvel & Fornito, 2014). Importantly, neurocognitive network topology highlights the key organisational principles that govern this architecture (van den Heuvel & Sporns, 2019). These principles provide the theoretical basis for interpreting how stroke alters functional organisation when examined in connectivity-gradient space across the empirical chapters. Connectivity gradients capture central organising principles of the cortex, reflecting how each brain region supports cognition and perception through a set of intrinsic functional dimensions (Boring et al., 2024; Huntenburg et al., 2018). These gradients capture transitions in functional connectivity across the cortex, indicating that large-scale spatial organisation is a prominent feature of cortical architecture (Hong et al., 2020). Connectivity gradient dimensions are useful because they position brain regions along meaningful axes that correspond to cognitive demands, and these axes are functionally interpretable (Huntenburg et al., 2018). Different dimensions of connectivity gradients capture distinct functional systems linked to large-scale cortical differentiation. The dimensional axes exhibit functional properties of regions that are maximally dissimilar at their opposing ends (Dohmatob et al., 2021; Margulies et al., 2016). The principal gradient (Gradient 1) separates unimodal from transmodal regions and is associated with cognition driven more by memory-based than sensory processes (Murphy et al., 2018, 2019). Gradients 2 and 3 refine the organisation within these extremes, providing a more targeted view of how unimodal and transmodal hierarchies are structured. Gradient 2 spans motor to visual regions, whereas Gradient 3 differentiates the default-mode and control networks.

Individual differences in gradient space have been shown to predict cognitive performance (Shao et al., 2022; Bethlehem et al., 2020; Sun et al., 2025), and this association has been examined using several methodological approaches. Some studies treat each gradient as a single global parameter, relating overall gradient strength or dispersion to behavioural outcomes. Others extract gradient values from specific regions, such as parcels corresponding to a lesion site, to test whether local embedding shifts relate to impairment. A further set of studies examines spatially distributed changes across the whole gradient map, identifying where in the cortex gradient alterations are associated with the effect of interest. This thesis adopts the latter approach, which is well suited to stroke, where lesions are typically large and heterogeneous and their effects extend beyond the lesion site. As a result, approaches based on global metrics or regional sampling would capture different and potentially incomplete aspects of individual variation, leading to different interpretations of the

relationship between connectivity gradients and behaviour. Such individual variation in gradient organisation arises because heteromodal networks show substantial dispersion in their gradient values, producing distinctive connectivity signatures for each person (Serhan et al., 2025). Recent work has also shown that Procrustes alignment improves the comparability of gradient embeddings across participants, particularly when aligning multidimensional gradient subspaces (Sasse et al., 2026). Together, these findings highlight the methodological consequences of how connectivity gradients are quantified and compared. Although gradients capture meaningful individual differences, the specific features that are emphasised depend on the analytical choices made, and these choices shape the inferences that can be drawn about post-stroke cognition.

The empirical work in this thesis focuses on functional connectivity at rest, which is a well-established marker of cognition given the strong convergence between resting-state and task-based network organisation (Nickerson, 2018). Structural and functional connectivity are closely related but not equivalent: white matter pathways constrain large-scale neural communication (O'Donnell & Westin, 2011; Madden et al., 2011), yet diffusion tractography can underestimate long-range or complex fibre architecture (Bennett & Rypma, 2013). Functional connectivity, by contrast, reflects the combined influence of anatomical pathways, cortical topography, and common functional recruitment, and therefore captures both direct and indirect interactions that may not map cleanly onto structural connections (Deco et al., 2014; Demirtas et al., 2019; Kristanto et al., 2023; Shine et al., 2021; Sporns et al., 2021). This distinction is important for interpreting the findings of this thesis, because white matter disconnection is likely to contribute to the gradient reorganisation observed after stroke, alongside changes occurring within structurally intact cortex. The present work does not quantify how much variance is attributable to structural versus functional sources. Understanding this limitation clarifies the scope of the conclusions: the thesis characterises functional reorganisation at the systems level, but does not disentangle the relative contributions of structural damage, diaschisis, and altered functional recruitment. This represents an important direction for future work.

In this thesis, atlas based parcellation was used to provide functionally meaningful and reproducible units of analysis for estimating connectivity gradients. A voxelwise approach was avoided because it produces extremely high dimensional correlation matrices with substantial spatial redundancy, making gradient estimation unstable in the presence of lesions (Faria et al., 2012; Craddock et al., 2011). Parcellation reduces this redundancy and offers a stable representational space in which gradients can be compared across individuals. Importantly, connectivity gradients are highly robust across different parcellation schemes (Vos de Wael et al., 2020; Margulies et al., 2016), indicating that the large-scale organisational patterns identified in Chapters 2 to 4 are not driven by atlas choice.

Whole-brain functional connectivity matrices were used to characterise large-scale network organisation, providing a representation of how all cortical regions interact rather than restricting analyses to predefined networks (de Reus & van den Heuvel, 2013). This whole connectome approach is well suited to connectivity gradient analysis, which depends on the similarity structure across regions and benefits from preserving both strong and weak connections (Hahn et al., 2018). Although some studies threshold weak links to reduce noise, this can disproportionately remove long range or low magnitude connections and alter network topology (Boschi et al., 2021). Across the empirical chapters, stroke effects were distributed rather than confined to isolated networks, making it essential to retain the full correlation structure to capture large-scale changes in functional architecture. Importantly, multiple studies demonstrate that weak functional connections carry meaningful information, supporting the decision to preserve them. For example, chronic stroke patients show abnormally low connectivity in the naming network, and these weaker connections increase following therapy (Johnson et al., 2021). Similarly, in autism spectrum disorder, reduced connectivity has been observed between medial prefrontal cortex and precuneus/posterior cingulate cortex, as well as the temporal pole (Chen et al., 2018; Yerys et al., 2015). Together, these findings indicate that weak connections capture important disturbances in network architecture related to pathology, and that discarding them risks losing critical information.

ROIs served a distinct and limited role in this thesis. Gradients were always derived from whole-brain connectomes to preserve the distributed organisation of the cortex. ROIs were introduced only after gradient extraction to focus interpretation on networks relevant to the research questions, such as the semantic control and language networks. In this context, ROIs narrowed the interpretive search space rather than defining connectivity structure. This differs from conventional ROI to ROI analyses, which restrict inference to a small set of predefined connections and risk overlooking broader system level organisation. The present approach therefore enabled network specific interpretation while preserving the whole-brain perspective.

Pearson correlation was used to estimate functional connectivity prior to extracting connectivity gradients in all empirical chapters. Because the focus was on large-scale organisation rather than fine grained nonlinear interactions, Pearson correlation provided a stable and interpretable foundation for the analyses. Although it assumes linear dependence between BOLD signals, recent work suggests that this limitation has minimal impact on large-scale connectivity structure. Jin and colleagues (2025) compared Pearson correlation with multiscale graph correlation, a method designed to capture both linear and nonlinear statistical relationships across multiple scales. Across datasets collected under different experimental conditions, they found that Pearson correlation recovered similar cortical connectivity patterns and showed higher reliability. These findings support its use as an adequate and robust measure of functional connectivity for the purposes of the present analyses.

Raw functional connectivity was used in all three empirical chapters in line with the standard approach in Brainspace. Raw connectivity matrices preserve the full correlation structure, providing an undistorted representation of large-scale organisation. Although thresholding and weighted graphs are often motivated by concerns about spurious correlations, these issues are better addressed during preprocessing, before pairwise correlations are computed. The CONN pipeline targets motion, physiological noise, outliers, and other artefacts during preprocessing and denoising (Whitfield-Gabrieli & Nieto-Castanon, 2012), meaning that weak connections that remain are more likely to be biologically meaningful rather than noise. In Chapters 2 and 4, simulated stroke effects were applied to aged-control functional connectivity matrices, which represented the raw functional links. Lesion effects were modelled by systematically reducing the strength of these connections, allowing the simulations to reflect how focal damage propagates through the intact connectome and alters large-scale organisation captured by connectivity gradients.

Another key question concerns the number of gradients that should be extracted and interpreted. Previous studies have typically linked behavioural variation or impairment to Gradient 1, with fewer examining associations in Gradient 2 (Bayrak et al., 2019; Bethlehem et al., 2020; Hong et al., 2020; Rene del Jesus Gonzalez Alam et al., 2022). Far less attention has been given to Gradient 3, partly because higher-order gradients often capture more subtle or context-dependent aspects of functional organisation. In this thesis, we extended prior work by examining relationships between behaviour and all three principal gradients. The simulation studies in Chapters 2 and 4 focused on the first two gradient dimensions, modelling how focal lesions propagate through the functional connectome. These simulations were driven by the structural extent of cortical damage and were designed to capture lesion-related alterations in long-range connectivity. In contrast, the empirical analyses in Chapter 3 examined the first three gradients in chronic stroke participants, enabling a more detailed characterisation of how stroke alters large-scale organisation across multiple functional axes. The limited accuracy of the simulations above Gradient 2 raises an important interpretive issue: higher-order gradients may reflect aspects of functional organisation that are less tightly constrained by lesion topology and more sensitive to experience, task history, or long-term reorganisation. This interpretation is consistent with the findings in Chapter 3, which suggest that Gradient 3 is particularly sensitive to the dynamic reorganisation of transmodal systems that support language outcomes in the chronic phase. Together, these results highlight a methodological consequence of gradient selection: restricting analyses to the first two gradients may overlook behaviourally relevant reorganisation in higher-order functional axes, whereas including additional gradients requires careful consideration of what these dimensions represent and how they relate to structural damage.

Huntenburg et al. (2021) noted that neuroanatomical studies reveal gradient like frameworks in cortical microstructure and connectivity across species, suggesting that these patterns reflect the trajectory of cortical evolution. According to the dual origin theory, the neocortex evolved from two

allocortical sources, the archicortex which includes the hippocampus and the paleocortex which includes the piriform cortex, with evolutionarily newer regions emerging furthest from these origins and forming spatial gradients that mirror neocortical expansion (Abbie, 1942; Kaas, 2013). This organisation is evident in gradients of microstructural differentiation, where newly evolved areas show reduced laminar differentiation (Huntenburg et al., 2021). Extending this point, the principal gradient shows broad correspondence with these microstructural patterns. Primary sensory and motor cortex exhibits strong laminar differentiation, whereas heteromodal regions such as prefrontal cortex show comparatively reduced differentiation (García Cabezas et al., 2019; Vázquez Rodríguez et al., 2019). This aligns with Mountcastle's proposal that a shared cortical microcircuit underpins a unifying computational principle across the cortex (Edelman & Mountcastle, 1978; Rao, 2024), providing a mechanistic basis for why large-scale gradients emerge from common laminar and microcircuit motifs. Recent evidence further demonstrates that the principal gradient is associated with layer specific gene expression, mesoscopic cortical layer thickness and geometric representations of cytoarchitecture (Meng et al., 2022). Together, these findings counter the criticism that connectivity gradients are purely mathematical constructs and show that they correspond closely to biological features of cortical organisation and evolution.

Hong et al. (2020) evaluated the suitability of connectivity gradients for biomarker development by assessing reliability, reproducibility and predictive validity in a large sample ($n = 209$). They reported high reproducibility and reliability, and showed that gradients achieved greater predictive accuracy than traditional edge-based connectivity measures, indicating that a low dimensional, multivariate gradient approach offers advantages over conventional methods. Further evidence from ageing research demonstrates that global gradient range shows robust associations with age across multiple datasets (Knodt et al., 2023), supporting the stability of large-scale gradient structure. The gradients extracted in Chapters 3 and 4 showed highly similar large-scale organisation across both aged controls and stroke participants. This observation is consistent with previous evidence that connectivity gradients capture stable, low dimensional features of cortical organisation that are preserved across populations, even in the presence of neurological damage. The similarity of gradient architecture across groups therefore supports the interpretation that the large-scale patterns identified in this thesis reflect fundamental aspects of cortical organisation rather than idiosyncratic features of a particular sample.

All three empirical chapters extracted connectivity gradients from functional connectivity matrices computed from time series correlations for both aged controls and stroke individuals. The aged controls were age matched, and the average aged control gradients were used to quantify how stroke gradients differed along the three principal axes. Stroke specific positional shifts were estimated by applying a subtraction step, in which each patient's gradient was contrasted with the averaged aged control gradient. Most existing stroke gradient studies align patients to a healthy

control gradient template and quantify deviation using distance based metrics (Bayrak et al., 2019; Chen et al., 2026; Koba et al., 2025). In contrast, this thesis applied a subtraction approach, removing the aged control gradient structure from each patient's embedding to isolate stroke specific effects. Subtraction based contrasts are widely used in functional neuroimaging, for example in pre versus post therapy connectivity analyses (Johnson et al., 2021), patient versus control comparisons (Yerys et al., 2015), and task based condition contrasts (Smith et al., 2009).

An alternative approach would have been to perform direct group comparisons between stroke participants and aged controls. Such analyses are useful for establishing whether group level gradient changes differ significantly from age related variation. However, they provide limited information about individual differences within the stroke cohort and are less well suited to relating gradient alterations to behavioural outcomes that are typically assessed only in patients. The subtraction approach adopted here therefore provided a complementary perspective, enabling stroke related deviations from normative organisation to be quantified at the individual level and linked to cognitive performance.

5.3.2. Global attenuation of connectivity gradients after stroke

This section first considers the common, group-level pattern of gradient attenuation observed after stroke, and the subsequent sections examine the IFG's typical position along the three gradient axes and how stroke alters that position. Across this thesis, two stroke samples were examined to characterise restingstate functional connectivity gradients following stroke. The first was a smaller group of twenty-one individuals with semantic aphasia, all with left hemisphere infarcts; a subset of these participants had resting-state fMRI data from which connectivity gradients were extracted in Chapter 2. The second was a larger and more heterogeneous cohort of sixty stroke survivors with diverse lesion profiles, used in Chapters 3 and 4. Importantly, the findings discussed in this section refer only to the resting state–derived gradients from these two samples and not based on the simulated post-stroke gradients. Despite differences in lesion location and behavioural phenotype, both samples showed a consistent global pattern of gradient attenuation. In the semantic aphasia group, the first two gradients were compressed, reducing the separation between transmodal and unimodal regions. In the larger cohort, the first three gradients were similarly reduced relative to age matched controls. Across both samples, transmodal and unimodal regions moved toward the centre of Gradient 1, visual and motor regions shifted toward the centre of Gradient 2, and control network and default mode regions converged toward the midpoint of Gradient 3. Together, these findings indicate a common global signature of stroke in which dimensional hierarchy is less differentiated.

Focal lesions disrupt the brain's small-world organisation by altering the balance between local clustering and long-range integration (Grefkes & Fink, 2011). Stroke alters network organisation in both the ipsilesional and contralesional hemispheres, producing widespread changes in regions far from the lesion site (Wang et al., 2010; Sagues et al., 2025). This global compression of gradient space aligns with classical and contemporary accounts of diaschisis, in which focal lesions produce widespread functional disturbances in structurally intact regions through the disruption of long-range connections (Carrera & Tononi, 2014). In gradient space, these distributed effects appear as parcels shifting toward the centre of the axes. However, this shift may reflect not only a loss of differentiation in functional connectivity profiles, but also changes in connectivity that are associated with the support of particular functions (Latifi et al., 2020). For example, in Chapter 3, left IFG's stronger DMN connectivity supported better speech production. Thus, reductions in gradient separation may reflect both the loss of a region's typical functional role and its movement toward a new position in gradient space that supports reorganisation. This interpretation is consistent with evidence that network disturbances caused by stroke elicit new or strengthened connections, which may be linked to impairment but also support recovery, a process commonly referred to as functional reorganisation (Latifi et al., 2020; Latifi & Carmichael, 2024).

5.3.3. Gradient-specific shifts of the inferior frontal gyrus after stroke

Interpreting the IFG's position in connectivity gradients

Across the three empirical chapters, the inferior frontal gyrus (IFG) emerged as a region that reorganised in different ways across the principal gradients, with each pattern linked to distinct language outcomes and to different large-scale control networks (Figure 5.1). In Chapter 2, the left IFG showed a shift toward a more unimodal connectivity profile along Gradient 1, and the significant cluster overlapped primarily with the semantic control network but also extended into the frontoparietal network. In Chapter 3, the left IFG moved from the control network end toward the default mode end of Gradient 3, and this cluster aligned with the semantic control network without overlap with the multiple demand or frontoparietal networks. In Chapter 4, the right IFG showed a more motor like connectivity profile along Gradient 2, and the corresponding cluster aligned with the frontoparietal network, consistent with its connections to premotor and motor cortices. Together, these findings show that left and right IFG reorganise along distinct gradient axes and within different functional networks, providing a mechanistic account of how these regions contribute to recovery of semantic control, speech, phonology and working memory after stroke.

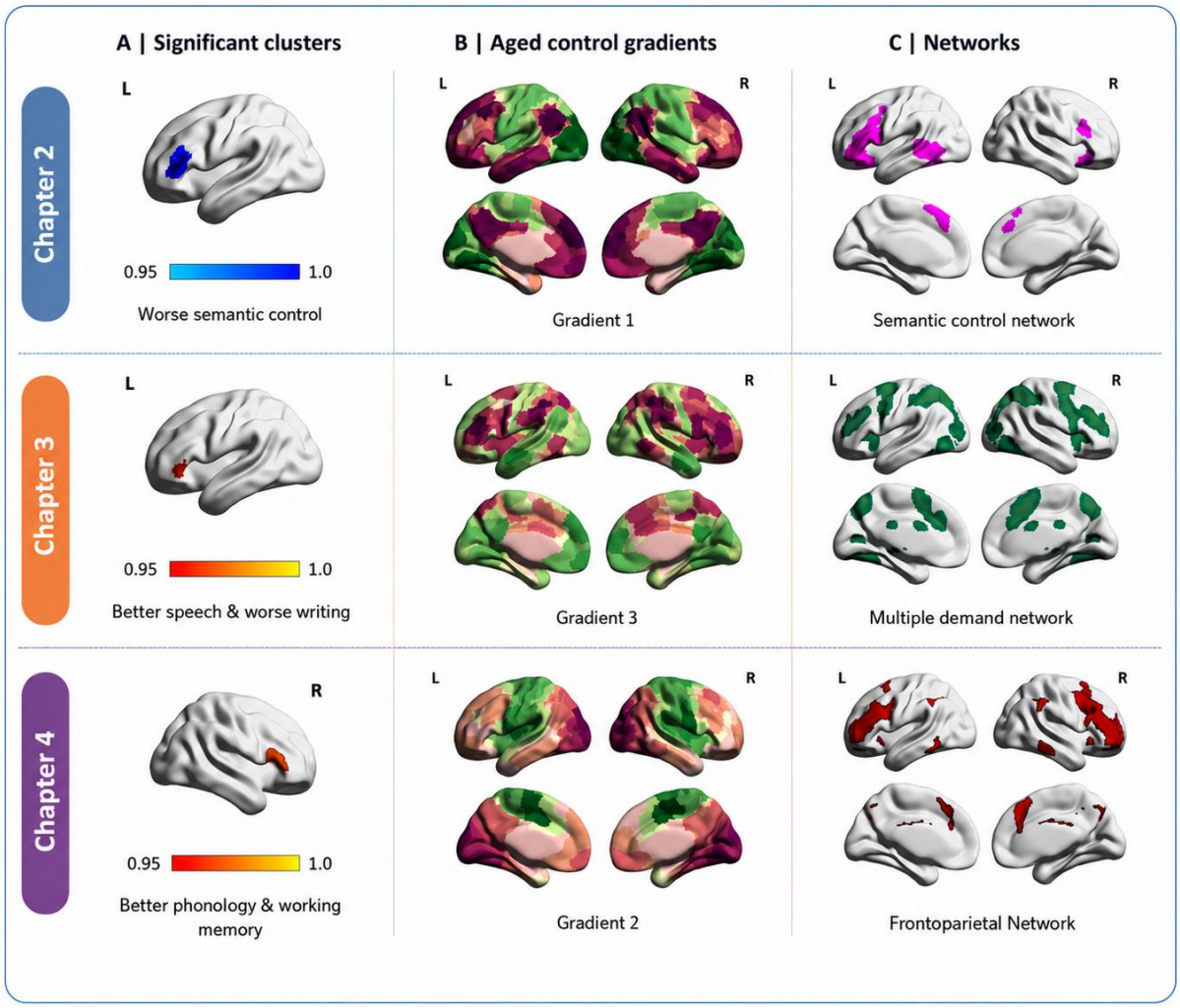

Figure 5.1. Behaviourally significant IFG clusters identified across the three empirical chapters, their positions in gradient space, and their relation to large-scale control networks. A) Significant clusters associated with behaviour in each chapter. From top to bottom, the rows show the left IFG cluster from Chapter 2 associated with poor semantic control in Gradient 1, the left IFG cluster from Chapter 3 in Gradient 3 linked with speech and writing, and the right IFG cluster from Chapter 4 in Gradient 2 linked with phonology and working memory. B) The three aged control gradients derived from the PLORAS sample. C) The networks associated with each cluster, shown with the semantic control network (SCN), multiple demand network (MDN), and frontoparietal network (FPN). The Chapter 2 left IFG cluster overlaps primarily with the SCN but also extends into the FPN, the Chapter 3 left IFG cluster aligns with the SCN, and the Chapter 4 right IFG cluster aligns with the FPN.

This section first outlines the IFG's anatomical location, functional role, and position within connectivity gradients, before interpreting its shifts along the gradient axes and their relationship to post-stroke cognition. The IFG occupies a prominent region on the ventrolateral surface of the prefrontal cortex (Petrides & Pandya, 2004). It is divided in a caudorostral direction into three

subregions—pars opercularis, pars triangularis, and pars orbitalis (Briggs et al., 2019)—each showing distinct patterns of functional connectivity. Anterior IFG is associated with higher-order networks, whereas posterior IFG is linked to primary and sensorimotor systems (Diveica et al., 2023; Rauschecker, 2010). This anatomical variation corresponds to specialised functional roles.

A recent study characterised this organisation using connectivity gradients, identifying an anterior–posterior gradient spanning from high-level control networks to perceptually driven networks, and a dorsal–ventral gradient differentiating domain-general control regions dorsally from ventral regions anchored in the semantic control network (Diveica et al., 2023). The IFG participates in several large-scale networks involved in language, executive control, and semantic control (Gratton et al., 2017; Hagoort, 2014; Underwood et al., 2021; Whitney et al., 2011). It has also been described as a connector hub due to its strategic position at the intersection of functional systems including the salience, frontoparietal, and default mode networks (Das & Menon, 2024; Gordon et al., 2018). Such hubs are critical for coordinating interactions between control and representational systems (Bertolero et al., 2017; Mesulam, 1990). Across this thesis, the IFG showed systematic shifts along the principal gradient axes, and these shifts were closely related to semantic control and language outcomes after stroke. These findings indicate that the IFG undergoes measurable functional reorganisation in gradient space, and that its altered position along these axes may serve as a sensitive marker of post-stroke changes in higher-order cognition.

Across the three gradients, the IFG occupies consistent positions in young adults: it lies toward the transmodal end of the unimodal–transmodal axis (Gradient 1), toward the visual end of the visuomotor axis (Gradient 2), and along the control–DMN axis (Gradient 3). These positional descriptions are based on gradients derived from the young HCP dataset. In the empirical chapters, two different aged-control samples were used, and the IFG showed the same relative positions along each gradient, although the overall spread of gradient space was reduced in ageing. Because the stroke participants in this thesis were between 55 and 80 years old, aged-control gradients provided the appropriate baseline for comparison. Establishing the IFG's position in ageing individuals is therefore essential for interpreting stroke-related shifts in gradient space. The IFG's positions along the three gradients reflect established connectivity patterns rather than arbitrary placements in gradient space. The position of the inferior frontal gyrus near the transmodal end of Gradient 1 is consistent with the broad organisation captured by the principal gradient, which separates sensory regions from higher association cortex. This organisation draws parallels with accounts in which complex language functions rely on the interaction of memory, unification and control processes (Hagoort, 2013), supported by prefrontal and temporoparietal regions that sit toward the transmodal end of this hierarchy. The IFG's position toward the visual end of the visuomotor axis (Gradient 2) aligns with evidence that the executive-control network is engaged during visual working-memory tasks, which require interactions between frontal regions and visual cortex (Jiayu et al., 2025). The IFG is also a

node of the control network, and its role in maintaining and flexibly using information according to contextual demands reflects its contribution to top-down cognitive control (Badre et al., 2005; Das & Menon, 2024). This is captured in its position along the control–DMN axis (Gradient 3), which represents the contrast between task-positive control regions and the task-negative DMN, and the IFG's placement toward the control-network end is consistent with its established role in cognitive control (Smallwood et al., 2021). At the same time, the IFG is a core region of the semantic control network and occupies an intermediate position between DMN and MDN, suggesting that its role on Gradient 3 is not fixed but flexible, allowing it to shift between internally oriented, DMN-related semantic processes and externally oriented, MDN-related controlled processing depending on task demands (Chiou et al., 2023).

5.3.4. Functional reorganisation of the inferior frontal gyrus across connectivity gradients

Although the findings from the empirical chapters can be interpreted individually, they collectively suggest that the inferior frontal gyrus undergoes multiple forms of functional reorganisation that are captured by different connectivity gradients. This diversity likely reflects the position of the inferior frontal gyrus at the intersection of several large-scale systems, where default mode, control, and sensorimotor influences converge. Because the inferior frontal gyrus bridges the default mode and control networks in the Yeo parcellation (Yeo et al., 2011) and occupies transmodal positions along several cortical gradients, it is well placed to shape how long-range conceptual representations interact with task-relevant control and sensorimotor features. This integrative role is consistent with accounts of semantic control, in which the inferior frontal gyrus guides conceptual activation according to current goals (Jackson, 2021; Gao et al., 2023). Consequently, even modest shifts in its position within gradient space may alter how different sources of information are integrated during language processing. The following subsections examine how these distinct patterns of reorganisation emerged across individual gradients and how they related to specific behavioural outcomes in the stroke cohort.

Left IFG shift toward unimodal connectivity in semantic aphasia

The left IFG is a core region of the semantic control network, and the stroke participants in Chapter 2 showed semantic control impairments characteristic of semantic aphasia—a multimodal deficit in which the ability to flexibly shape conceptual knowledge is disrupted across modalities. As shown in Fig. 1, a key finding in Chapter 2 was that the left IFG shifted towards the unimodal end of Gradient 1, despite typically occupying a transmodal position. This shift was correlated with poorer semantic control performance. Within the Controlled Semantic Cognition framework, semantic control refers to the processes that shape conceptual activation according to task demands. Conceptual

knowledge is represented in heteromodal hub regions, where information from different modalities is integrated into coherent semantic representations. Accessing this knowledge in a context-appropriate way requires control processes supported by the left IFG, which bias activation within semantic memory to retrieve only the information relevant to current goals (Jefferies et al., 2019). Lesion–symptom studies have consistently linked frontal lobe damage with semantic control deficits. In our sample, however, the left IFG was structurally spared, yet its altered functional organisation was still associated with semantic control difficulties, suggesting that network-level functional reorganisation in structurally intact regions may contribute to behavioural impairments

Recent work has identified a cortical mosaic for conceptual integration across posterior temporal and inferior frontal regions, recruited during controlled semantic retrieval (Murphy et al., 2023). The semantic aphasia group in Chapter 2 showed maximal lesion overlap in the insular cortex. Given that the anterior insula connects strongly with prefrontal regions and the posterior insula with posterior temporal cortex, a plausible explanation is that damage to this bridging structure disrupted functional integration between IFG and posterior temporal regions. One possible interpretation is that displacement of the IFG from its typical transmodal position toward a more unimodal connectivity profile reduced its capacity to support goal-directed semantic retrieval.

Left IFG's shift along the control–DMN axis and its impact on expressive language

In Chapter 3, the left IFG showed a dissociation in expressive language outcomes: speech production was stronger, whereas writing performance was weaker, in individuals whose IFG was positioned closer to the default mode network rather than its typical control-network affiliation along the control–DMN axis. Understanding the IFG's classical contributions to speech and writing provides essential context for interpreting how this reorganisation relates to expressive outcomes in the stroke group. Broca's area, situated within the IFG, has long been recognised as a key region for expressive language, supporting both spoken and written output (Foundas et al., 2014; Johns, 2014). Contemporary speech motor control models clarify how the IFG contributes to speech production. In the dual stream model, the left dorsal stream contains posterior IFG, premotor cortex and the parietal–temporal junction, and supports the transformation of phonological representations into articulatory plans through interactions with sensorimotor cortex (Hickok, 2012; Hickok & Poeppel, 2007). Neuroimaging studies show that the left IFG is engaged during motor planning and programming of speech, which aligns with this framework (Memarian et al., 2012; Pützer et al., 2019; Silva et al., 2022). Lesions affecting Broca's region and neighbouring frontal areas typically result in Broca's aphasia, which is characterised by effortful and non-fluent speech (Andrews et al., 2022; Gajardo-Vidal et al., 2021). In the Chapter 3 sample, the left IFG was structurally spared despite frontal involvement elsewhere. A systematic review of post-stroke language outcomes shows that increased activation in perilesional and spared left-hemisphere regions (Fridriksson et al., 2012;

Meinzer et al., 2008; Van Hees et al., 2014), including increased activation of left IFG, is associated with better naming after anomia therapy (Simic et al., 2023). This evidence highlights the importance of the IFG for supporting expressive language after stroke, and other studies suggest that activity within the default mode network is also linked to improved language function (Dreyer et al., 2020; Geranmayeh et al., 2016). Our findings connect these two strands of evidence by showing that the IFG's position within large-scale connectivity gradients is behaviourally relevant. A shift of the left IFG toward the DMN end of the control–DMN axis was associated with better speech production. Evidence for interaction between the control network and the DMN comes from work by Gordon and colleagues (2018), who identified a set of control–default connector hubs that interface between the frontoparietal network and the DMN. These hubs are thought to support the regulation of internally generated processes such as memory, planning and conceptual retrieval (Andrews-Hanna et al., 2014; Dixon et al., 2018; Spreng and Schacter, 2012). This organisational principle makes it plausible that regions within the control network, including the IFG, can shift toward more DMN-like connectivity patterns along the control–DMN gradient (Dixon et al., 2018; Gordon et al., 2020).

The DMN is not a purely task-negative system but contributes to episodic memory, working memory, divergent thinking and semantic processing, including individual word meaning, sentence-level integration and discourse comprehension (Benedek et al., 2016; Konishi et al., 2015; Krieger-Redwood et al., 2016; Murphy et al., 2018; Smallwood et al., 2021; Fernandino & Binder, 2024). In this context, a shift of the left IFG toward the DMN end of the control–DMN gradient may enhance internally guided semantic and memory access that supports speech production. In contrast, writing relies more heavily on externally directed, controlled processing (Planton et al., 2013) and typically requires down-regulation of DMN activity (Čeko et al., 2015; Thomason et al., 2008). The same DMN-ward shift that benefits speech may therefore disadvantage writing, reflecting a functional dichotomy in how the IFG engages with DMN-related versus control-related processes.

Writing is a complex cognitive process that integrates linguistic and motor components. Cognitive models propose two routes for converting linguistic input into written output: a phonological route that supports sound-to-letter mapping, and a lexical route that converts semantic information into orthographic forms. The writing component identified in the principal component analysis, which loaded on written picture naming and writing to dictation, reflects demands on both routes (Chen et al., 2023; Roeltgen et al., 1985). Lesion–symptom mapping in Chapter 3 showed that damage to superior and middle temporal gyri was associated with phonological and working memory deficits, whereas premotor and primary motor cortices were largely spared, suggesting that the writing difficulties observed in this cohort are unlikely to reflect motor impairment. Instead, writing relies heavily on externally directed, controlled processing, including orthographic retrieval and the sequencing of grapheme-to-motor plans, processes that are typically supported by control-network engagement rather than DMN involvement. Although the left inferior frontal gyrus contributes to

writing, a shift toward more default-mode-like connectivity may reduce its ability to support these control-dependent linguistic processes, particularly in the context of weakened phonological and lexical inputs from temporal-lobe regions. However, alternative interpretations are possible. The PCA component associated with writing loaded on written dictation, written picture description and written naming, tasks that require the flexible coupling of control, orthographic and semantic processes. From this perspective, the observed shift could reflect reduced engagement of control mechanisms, increased integration with default-mode processes, or a loss of flexibility in how the region couples with orthographic and semantic systems (Fedorenko & Thompson-Schill, 2014; Hertrich et al., 2020; Jefferies et al., 2020) during visually guided writing. These accounts each provide a plausible explanation for why a more default-mode-like connectivity profile in the left inferior frontal gyrus was associated with poorer writing performance.

Right IFG's visuomotor shift and phonology

In Chapter 4, for the first time we introduced a simulation model that incorporated multiple layers of stroke impact: focal effects, distant effects and global changes in structurally intact regions. All of these effects were modelled from a cortical, lesion-centred perspective, with reductions explicitly propagated across the unlesioned connectome. This framework allowed us to examine how lesion-driven disruptions might alter large-scale functional organisation beyond the site of damage. One of the key findings was that the right inferior frontal gyrus shifted toward the motor end of Gradient 2, the visuomotor axis, and this pattern was associated with better phonology and working memory (Fig. 3). Simulated post-stroke gradient maps generated using the iterative propagation method were used to characterise how lesion-driven changes in gradient space relate to language outcomes. A lesion–gradient mapping analysis conducted on these simulated maps identified a right inferior frontal gyrus cluster linked to the phonology and working-memory component. A follow-up analysis then tested whether the same region showed a comparable association in the observed stroke gradients, and it demonstrated the same directional relationship. The right IFG acts as an integrative hub supporting phonology-related functions such as phonetic monitoring, mismatch detection and phonological decision-making (Hartwigsen et al., 2010; Nucci et al., 2026). Several left-hemisphere regions also contribute to phonological processing, including the left IFG, frontal operculum, insula, anterior cingulate cortex, cerebellum and thalamus, while the left inferior and superior temporal gyri, precentral gyrus and supplementary motor area are additionally engaged during phonological processing in tasks such as picture naming (Lacey et al., 2017; Price et al., 2005).

The phonological loop from Baddeley and Hitch's working-memory model aligns closely with the phonological component identified in the principal component analysis reported in Chapter 4, which showed strong loadings on digit-string repetition and sentence repetition (Baddeley & Hitch, 1974). These subtests from the Comprehensive Aphasia Test require the temporary maintenance of phonological information. The model proposes a specialised system for holding speech-based

material, comprising a phonological store that briefly retains verbal input and an articulatory rehearsal process that refreshes these representations through subvocal repetition (Hughes, 2024). The articulatory component has been linked to the left inferior frontal cortex, supplementary motor area, premotor cortex and insula (Emch et al., 2019), while verbal working memory more broadly engages prefrontal regions (Lara & Wallis, 2015; Narayanan et al., 2005).

Lesions to dorsal stream regions such as the supramarginal gyrus, inferior postcentral gyrus, precentral gyrus and premotor cortex are known to impair phonological production, but these areas were largely spared in most participants included in Chapter 4. Of the 52 stroke survivors, 44 had left hemisphere infarcts that extended into parts of the left IFG, and the lesion–gradient mapping therefore examined functional reorganisation in unlesioned language network regions, including right hemisphere areas. Previous work has shown that the right IFG pars triangularis can support naming improvements following phonological cueing therapy (Abel et al., 2014; Harvey et al., 2019), and mechanistic accounts of post-stroke recovery propose that damage to the left hemisphere language network may lead to recruitment of right hemisphere homologues and residual non-linguistic networks. These ideas support the finding in Chapter 4 that better phonology and working memory performance were associated with the right IFG, suggesting that this engagement may reflect increased recruitment of contralesional frontal regions when left hemisphere language areas are compromised. The gradient-based analysis clarified not only which region was associated with behaviour but also how its functional embedding changed. The right IFG shifted toward the motor end of the visuomotor axis, a plausible pattern given its connections with premotor and motor cortices. The novelty lies in showing that the behavioural improvement corresponds to a specific reorganisation in gradient space rather than a general increase in right hemisphere involvement.

There are several possible interpretations of this right hemisphere involvement. One possibility is that phonological and working memory processes are supported by bilateral networks, and that these functions may reorganise to rely more on right hemisphere regions when left hemisphere areas are damaged (Xing et al., 2015). Another interpretation is that increased right hemisphere engagement reflects greater task demands. Geranmayeh et al., (2014) have argued that increased right hemisphere activation after stroke can arise from heightened processing difficulty, and similar patterns can be observed in healthy individuals when speech input is degraded (Wild et al., 2012). The present findings are consistent with both accounts. The right IFG may be recruited because it can support phonological and working memory processes when left hemisphere regions are compromised, but its engagement may also reflect the increased cognitive effort required to perform these tasks after stroke. The gradient-based analysis adds specificity by showing that this involvement corresponds to a shift toward a more motor-like connectivity profile.

Chapter 4 used a subset of the PLORAS dataset analysed in Chapter 3. The reduced sample reflected the requirement for cortical lesions in the simulation model. Because the two chapters draw on largely the same participants, the patterns observed across them relate meaningfully to one another. In Chapter 3, the left IFG was associated with better speech production when its connectivity shifted toward the DMN end of the control–DMN axis. In Chapter 4, the right IFG was associated with better phonology and working memory when its connectivity shifted toward the motor end of the visuomotor axis. Together, these findings show how homologous regions contribute to related language functions and demonstrate that two different functional axes provide a mechanistic explanation for how left and right IFG reorganise to support recovery of speech, phonology and working memory after stroke. These patterns align with evidence that physiological connectivity can be restored during the chronic phase of stroke (Tao & Rapp, 2020).

The empirical chapters show that connectivity gradient shifts capture behaviourally meaningful reorganisation in both left and right IFG, and that different gradient dimensions explain why some aspects of language improve while others decline. An alternative account is that stroke-related changes reflect a broader loss of modular organisation, sometimes referred to as network randomisation. In other neuropathologies such as brain tumour, severe traumatic brain injury and Alzheimer's disease, this term has been used to describe shifts towards more random-like connectivity patterns associated with reduced small-world organisation (Bartolomei et al., 2006; Gerloff and Hallett, 2010; Nakamura et al., 2009; Stam et al., 2007). However, the concept lacks a universally agreed definition and remains difficult to operationalise (Tscherpel et al., 2025). The present findings instead indicate that stroke-related changes are organised along specific gradient dimensions and linked to distinct behavioural outcomes, which suggests that reorganisation is structured rather than uniformly distributed across the cortex.

The IFG shifts observed in this thesis were directional and linked with behaviour, which indicates that reorganisation in this region has functional consequences rather than simply reflecting a non-specific loss of network organisation. The prefrontal cortex coordinates cognitive control across large-scale networks including the frontoparietal, salience, cingulo-opercular, default mode and attention systems (Menon and D'Esposito, 2021). The IFG contributes to this control architecture by supporting inhibition, selection and goal-directed behaviour. All behavioural associations observed in this thesis, including semantic control, speech, writing, phonology and working memory, involve control-related demands. Therefore, the IFG's involvement in these functions is not unexpected. What is novel is that its connectivity pattern changes in gradient space in ways that are associated with both preserved and impaired cognitive performance after stroke. These findings suggest selective reconfiguration of the IFG within the surviving network architecture.

These findings also have potential clinical implications. Connectivity gradients provide information beyond lesion location by identifying how transmodal regions have been repositioned within the brain's functional hierarchy after stroke. Because the direction of IFG reorganisation was associated with different behavioural outcomes, gradient position may offer a framework for identifying the functional changes linked with specific impairments. Rather than targeting the lesion itself, rehabilitation could ultimately aim to influence the functional embedding of surviving transmodal regions, encouraging shifts toward positions within gradient space that are associated with improved behavioural performance. In this way, connectivity gradients could provide a quantitative basis for designing and monitoring personalised rehabilitation strategies. Although this thesis cannot determine whether therapy can induce such shifts, it establishes an association between the position of transmodal regions within gradient space and behavioural performance, providing a rationale for future longitudinal intervention studies.

Further validation is required, but gradient-based measures may contribute to future biomarkers of reorganisation for domains such as semantic control, phonology and speech production. Identifying whether a region has shifted toward a connectivity profile that supports or hinders a specific language function may help stratify patients, refine prognostic models and guide therapy selection. Specific positional changes in gradient space that are linked with improvements in semantic cognition and language could, in principle, serve as indicators of therapy responsiveness, although this remains to be tested. The present results therefore provide an initial mechanistic framework that could inform the development of targeted interventions, while recognising that translation into clinical practice will require larger samples, longitudinal designs and replication across independent cohorts.

5.4. Future directions

This thesis opens the door to further exploration of connectivity gradients in stroke. We observed that the IFG's shifts along different gradient dimensions influenced post-stroke cognitive outcomes. The next step is to identify what drives these shifts: lesion location, preserved white-matter pathways, or behavioural factors such as repeated task practice that reshape connectivity. Future work should develop statistical models that link lesion characteristics to gradient changes and, in turn, to cognitive outcomes, providing a mechanistic account of how structural damage leads to functional reorganisation. It will also be important to determine whether gradient shifts are driven primarily by grey-matter damage or by white-matter tract disconnection, as understanding their proportional contributions may clarify which mechanisms lead to greater severity or facilitate maximal recovery. A further, more exploratory direction is to test whether experience-dependent factors, such as therapy or repeated task practice, also reshape gradient positions over time.

Another important direction is to extend analyses to whole-brain gradients that include subcortical structures (Lucas et al., 2023; Yang et al., 2020). Regions such as the thalamus and basal ganglia form integrative loops with frontal and parietal cortices and play established roles in language and cognitive control (Greene et al., 2020; Hamker et al., 2025; Hwang & D'Esposito, 2022; Kawabata et al., 2021). Including these structures may reveal how subcortical regions are positioned within post-stroke gradient dimensions, capturing aspects of reorganisation that cortical gradients alone cannot detect.

This thesis identified a key finding: the left IFG showed a shift toward a DMN-like connectivity profile that was associated with better speech production. A valuable next step is to determine whether the left IFG shows increased functional connectivity with DMN regions during speech in healthy ageing, given that the DMN, although often described as task-negative, also supports internally guided and semantic processes. Future work could test whether this interaction is a pre-existing but weak feature linked with speech, whether stroke amplifies it as a compensatory mechanism, or whether it emerges specifically in response to damage.

A further avenue is to broaden both the behavioural and neural scope of gradient analyses. Executive-control impairments frequently co-occur with semantic and language deficits, yet they were not assessed here; future studies should incorporate broader neuropsychological batteries to determine how executive processes contribute to gradient reorganisation. The language assessments were also limited to CAT subtests, and richer measures of discourse, apraxia of speech, and visuospatial abilities would allow a more complete characterisation of how different cognitive domains relate to gradient changes. Methodologically, the analyses focused on the first two gradients (and Gradient 3 in one chapter), but higher-order gradients often capture hemispheric asymmetries (Rene del Jesus Gonzalez Alam et al., 2022); examining these could clarify how lateralised systems reorganise after stroke. It will also be important to compare ipsilesional and contralesional gradient attenuation directly, to test whether differences in gradient reduction across hemispheres relate to compensatory recruitment in the intact hemisphere. Together, these extensions would provide a more comprehensive account of how focal damage and distributed reorganisation jointly shape post-stroke cognition.

Integrating temporal variability with gradient-based approaches also represents a promising direction. Moment-to-moment variability in the BOLD signal has been linked to the dynamical properties of large-scale networks and their ability to transition between functional states (Pincus, 1994; Baracchini et al., 2021). In this thesis, connectivity gradients were extracted from resting-state fMRI of stroke individuals and aged controls across all three empirical chapters, but the analyses were based on static connectivity estimates. Combining temporal variability with gradient methods may reveal how stroke disrupts transitions between network states, potentially contributing to altered

occupancy of specific positions along a gradient dimension. Future work could test whether disrupted variability contributes to impairments in semantic control and language outcomes after stroke.

Finally, comparing gradient-based changes across different patient groups and aetiologies may clarify whether distinct pathologies produce characteristic patterns in gradient space. Conducting gradient analyses in primary progressive aphasia would help distinguish lesion-induced gradient changes from neurodegenerative alterations. In the same way, gradient changes following stroke, traumatic brain injury, and network-level disorders such as Alzheimer's disease could be examined to determine whether any features are shared across conditions or whether each pathology produces a characteristic pattern. Identifying such distinctions may eventually have clinical relevance, as pathology-specific gradient signatures could contribute to developing network-level biomarkers for diagnosis or prognosis.

5.5. Conclusions

This thesis applied the relatively new paradigm of connectivity gradients to examine post-stroke functional reorganisation and to test whether these continuous axes provide a deeper understanding of how cognitive performance relates to changes in functional organisation. Connectivity gradients revealed clear differences in functional organisation between aged controls and stroke survivors. They also showed a global stroke pattern in which all three functional axes were compressed, with gradient poles moving toward the centre. The thesis then examined how these alterations relate to behaviour. Each gradient axis captures a dimension defined by diametrically opposite functional profiles, and each brain region occupies a position along these axes that reflects its role within large-scale cortical organisation. Stroke disrupts these positional patterns, and the direction of displacement along an axis provides insight into whether reorganisation supports or hinders cognitive performance. For the first time, the gradient framework demonstrated how a connectivity profile defined by continuous functional axes, rather than within-network or between-network measures, can explain variation in cognitive outcomes. These findings show that shifts in gradient space capture meaningful reorganisation linked with both improvement and impairment across different cognitive domains.

Across the three empirical chapters, behavioural outcomes were not determined by lesion location alone. Instead, dynamic reorganisation in structurally intact regions accounted for stroke outcomes through network-level changes beyond the lesion site. Patterns of improvement and impairment reflected how surviving regions repositioned themselves within large-scale cortical gradients that capture transmodal to unimodal, control to DMN and visuomotor dimensions of brain organisation. In semantic control, the left IFG shifted toward a more unimodal profile along Gradient 1, and this displacement was associated with poorer performance despite structural sparing.

This demonstrates that functional disorganisation in intact tissue can produce semantic control deficits characteristic of semantic aphasia.

In expressive language, the left IFG's position along the control–DMN axis explained a dissociation between speech and writing: a shift toward the DMN supported speech production but was linked to poorer writing, reflecting their different cognitive demands. This finding provides a new perspective by showing that writing difficulties are not solely a motor control problem but reflect a broader, multifaceted disruption of control-related processes. In phonology and working memory, the right IFG shifted toward the motor end of the visuomotor axis, and this reorganisation was associated with better performance, highlighting the compensatory contribution of right-hemisphere homologues when left-hemisphere language regions are compromised. The multidimensional perspective offered by gradients moves beyond traditional lesion-based approaches and provides a richer explanation for why some functions improve while others decline. The results also have potential clinical relevance. Connectivity-gradient shifts captured meaningful reorganisation in both hemispheres. Although further validation is required, gradient-based measures show promise as biomarkers of reorganisation across semantic control, phonology, speech production and writing. Identifying supportive or limiting connectivity profiles may help refine prognosis and guide therapy.

Overall, this thesis provides a mechanistic framework for understanding post-stroke language outcomes, showing that reorganisation is shaped not only by where damage occurs but by how the surviving system reorganises across multiple functional axes. These insights lay the groundwork for future translational work aimed at developing targeted interventions and gradient-informed biomarkers, with the long-term goal of improving personalised rehabilitation after stroke.

Supplementary materials

Chapter 2 supplementary materials

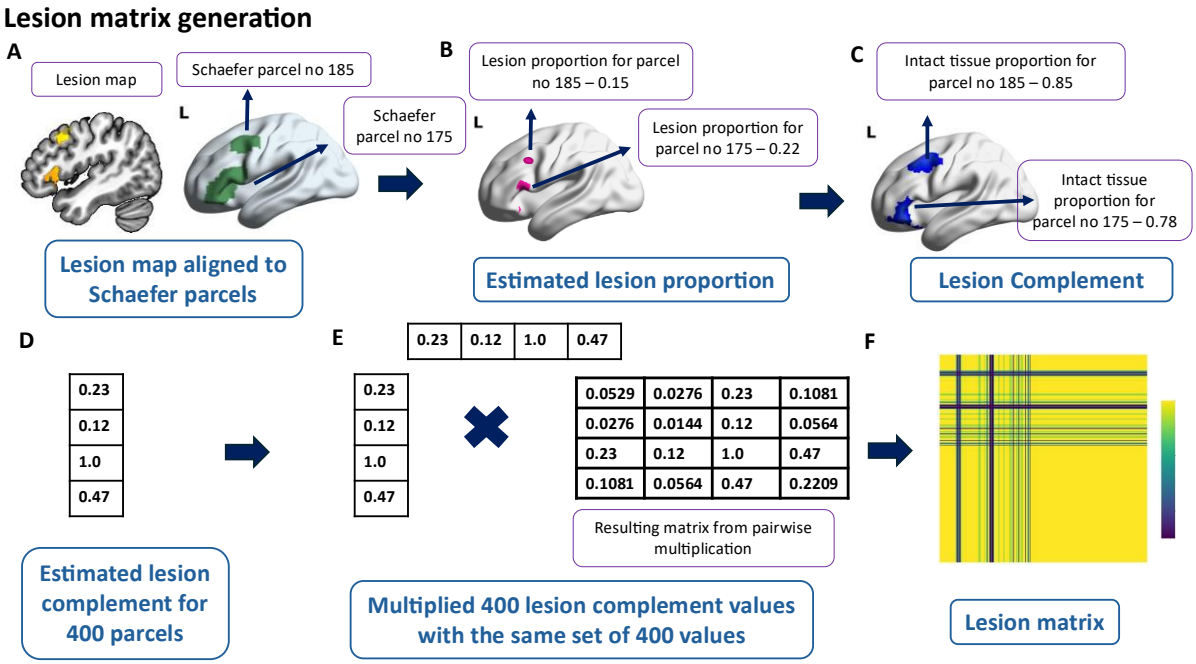

Supplementary Figure 2.S1. Steps followed for generating the lesion matrix: A) The lesion map was aligned to the Schaefer parcellation. B) The lesion proportion was estimated for each parcel. C) For each lesion, the lesion complement (spared tissue) per parcel was calculated from the lesion proportion. D) For each lesion, lesion complements were estimated for all 400 parcels. E) The 400 lesion complement values were multiplied by the same set of 400 values, resulting in a 400 x 400 lesion matrix (Example values from the matrix shown). F) Lesion matrix generated.

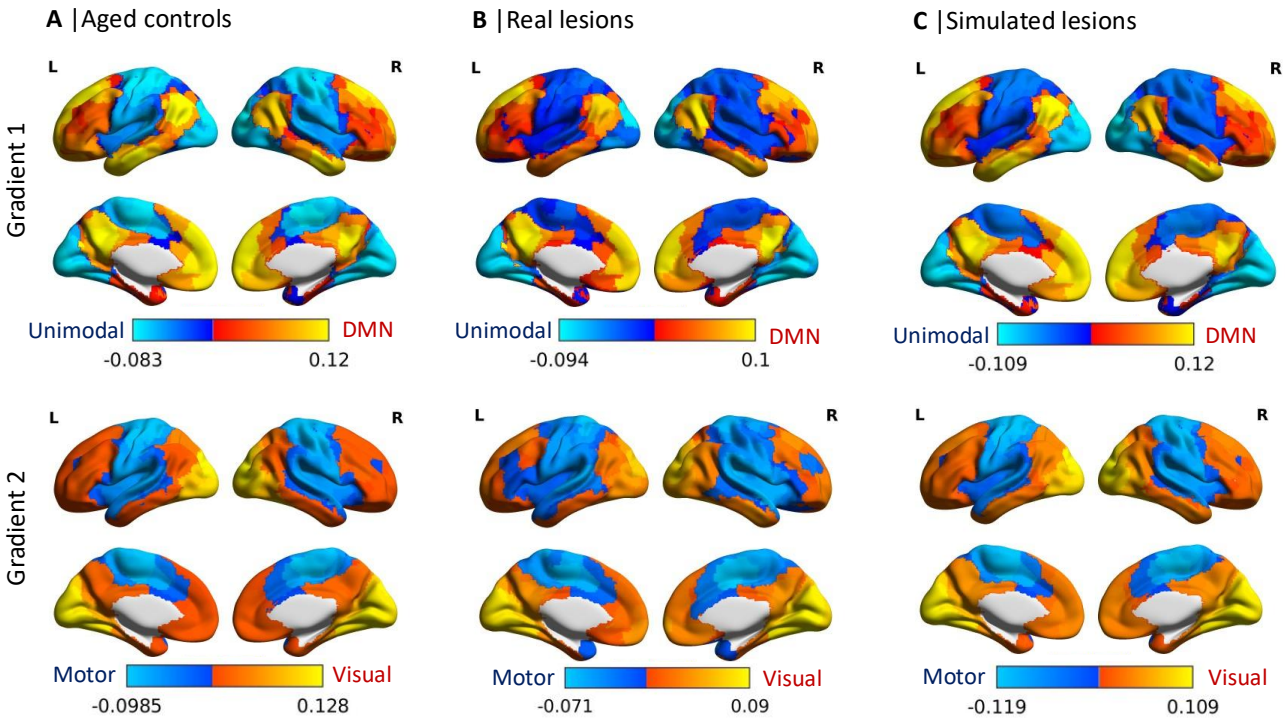

Supplementary Figure 2.S2. Topographic organisation of connectivity gradients. (A) Topographic functional organisation of each gradient in aged controls. (B) and (C) Topographic cortical organisation of the observed and simulated functional gradients derived from resting-state fMRI and structural lesion data, respectively. For Gradients 1 and 2, regions located at the lower end of the gradient are shown in cool colours, whereas regions positioned toward the upper end of the gradient are shown in warm colours.

Supplementary Table 2.S1. Lesion location and lesion size. Lesion volume is reported in terms of the number of voxels (1 × 1 × 1 mm3).

ID	Hemisphere	Lesion location	Lesion volume (voxels)
01	Left	Lateral occipital cortex; Occipital cortex; Insular cortex	4039
02	Left	Inferior frontal gyrus (IFG); Lateral occipital cortex; Temporal fusiform cortex	8766
03	Left	Intracalcarine cortex; Parahippocampal cortex	168
04	Left	Lateral occipital cortex; Motor cortex; Lateral prefrontal cortex; IFG	13463
05	Left	Lateral occipital cortex; Precuneus; Posterior cingulate cortex	2596
06	Left	Insular cortex; Motor cortex; Frontal pole; IFG	6943
07	Left	Lateral occipital cortex; Precuneus; Posterior cingulate cortex	8317
08	Left	Insular cortex; IFG; Middle frontal gyrus; Temporal cortex; Supramarginal gyrus	13907
09	Left	Middle frontal gyrus; Angular gyrus; Lateral occipital cortex	762
10	Left	Middle frontal gyrus; IFG; Insular cortex; Lateral occipital cortex; Postcentral gyrus; Temporal cortex	14491
11	Left	IFG; Temporal pole; Insular cortex; Supramarginal gyrus	7318
12	Left	IFG; Middle frontal gyrus; Frontal orbital cortex; Insular cortex; Temporal lobe	7190
13	Left	Frontal orbital cortex; Insular cortex; Postcentral gyrus	4307
14	Left	Insular cortex	16
15	Left	Insular cortex; Temporal pole	2286
16	Left	IFG; Lateral occipital cortex; Angular gyrus; Supramarginal gyrus; Postcentral gyrus; Temporal cortex	8809
17	Left	Middle frontal gyrus; Lateral occipital cortex	592
18	Left	IFG; Frontal orbital cortex; Insular cortex; Temporal pole	3700
19	Left	Superior frontal gyrus; Middle frontal gyrus; IFG; Motor cortex; Insular cortex; Temporal pole; Supramarginal gyrus	16807
20	Left	Superior frontal gyrus; Middle frontal gyrus; IFG; Insular cortex; Motor cortex	6590
21	Left	Angular gyrus; Postcentral gyrus	597

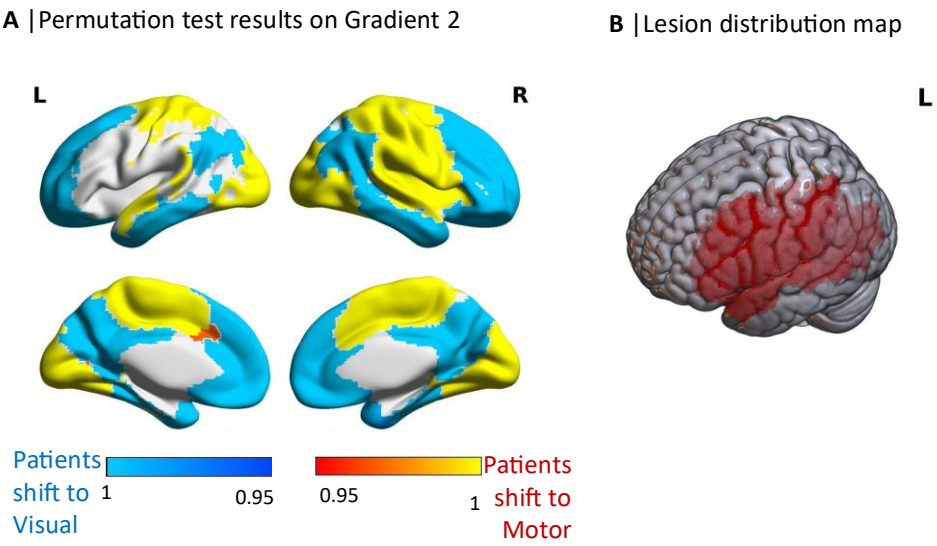

Supplementary Figure 2.S3. Permutation test results for Gradient 2 and lesion distribution. (A) Regions showing significant post-stroke changes in Gradient 2. Warm colours indicate areas where patients had significantly higher gradient values than controls, corresponding to shifts toward the motor end of the gradient, whereas cool colours indicate areas where patients had significantly lower values, corresponding to shifts toward the visual end. Clusters correspond to thresholded 1 − p images (cut-off = 0.95). (B) Lesion distribution map showing all lesioned voxels across the 21 semantic aphasia (SA) patients.

Chapter 3 supplementary materials

Section I: PCA Results for the Comprehensive Aphasia Test

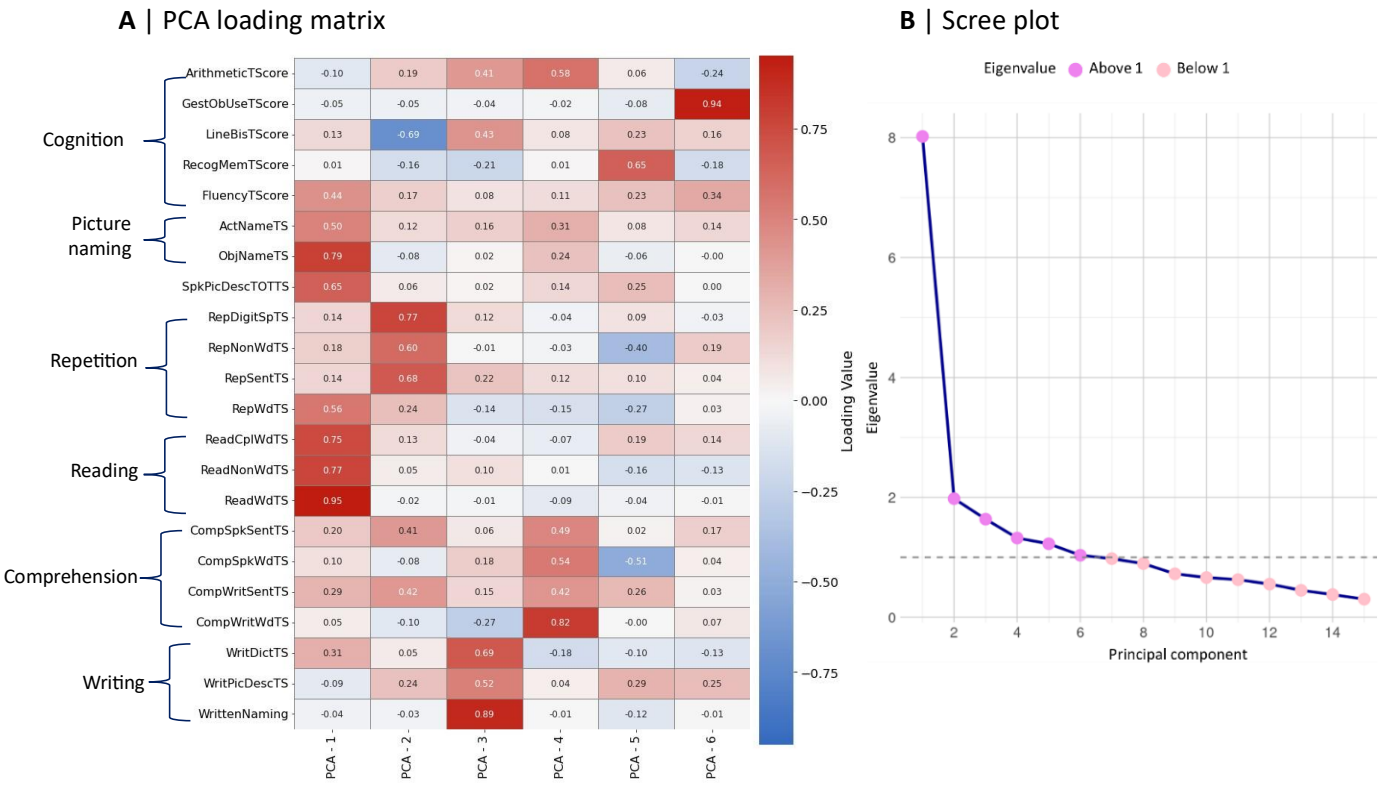

Supplementary Figure 3. S1. Principal component analysis results of the CAT. A) PCA loading matrix of CAT subtests. PCA-1 is associated with speech; PCA-2 with phonology and working memory; PCA-3 with writing and visuomotor capacity; PCA-4 with comprehension and arithmetic; PCA-5 with recognition memory; and PCA-6 with gesture–object use. B) Scree plot showing the eigenvalues for each principal component.

Section II: Post-stroke difference gradients

We subtracted each stroke patient's connectivity gradient from the average gradient map of age-matched controls to focus only on stroke-specific effects, generating post-stroke difference maps for all three gradients. Figure 3.S2 shows the average post-stroke difference maps for all three gradients (Figure 3.S2A–C). Positive values (red–yellow) in the difference maps indicate parcels with

lower gradient values in patients than in age-matched controls, whereas negative values (green–blue) indicate parcels with higher gradient values in patients compared to controls.

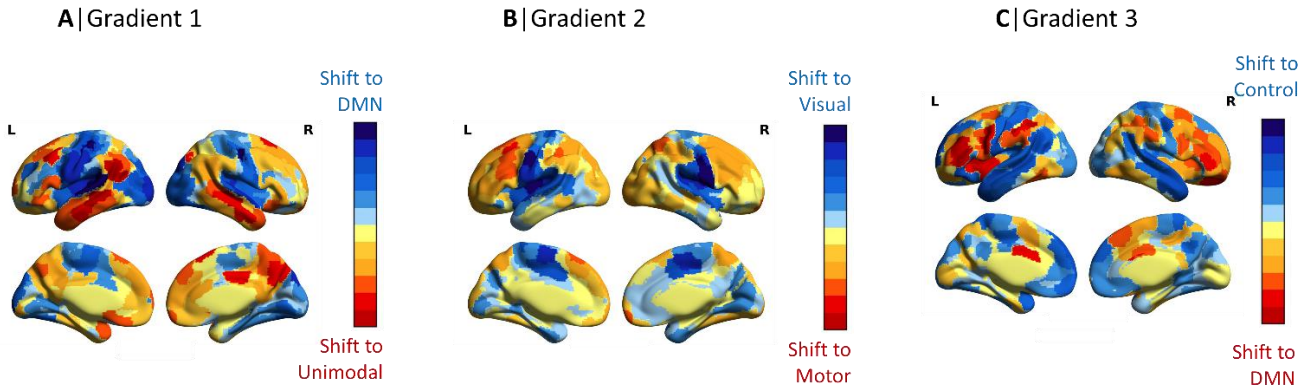

Supplementary Figure 3.S2. Post-stroke functional connectivity differences after removing aging effects. Average connectivity maps from age-matched controls were subtracted from each stroke patient's connectivity map, revealing positional shifts of brain regions across gradients. Top panel: A) shows stroke-related connectivity changes in Gradient 1, with shifts in both default mode network (DMN) and unimodal regions. B) shows connectivity changes in Gradient 2, involving shifts between visual and motor regions. C) shows connectivity changes in Gradient 3, with positional shifts in DMN regions and the control network. Warm colours indicate areas where patients had lower values than controls, while cool colours indicate areas where patients had higher values.

Section III: Association between post-stroke functional connectivity gradient changes and language outcomes within the language network

We explored how post-stroke changes in functional connectivity gradients within the language network were associated with PCA-derived language outcomes. To focus on intact tissue, voxels with ≥25% lesion involvement were excluded from the language network mask (Figure 3.S3A). Results for PCA components 1-4 are in the main text. We additionally found worse performance in gesture–object use (PCA component 6) was associated with gradient changes in the left superior frontal gyrus, paracingulate gyrus, and juxtapositional lobule cortex (Figure 3.S3B). These regions, normally anchored toward the control end of Gradient 3, showed a shift in functional alignment toward the DMN, and this shift was linked to poorer gesture–object use (Figure 3.S3C).

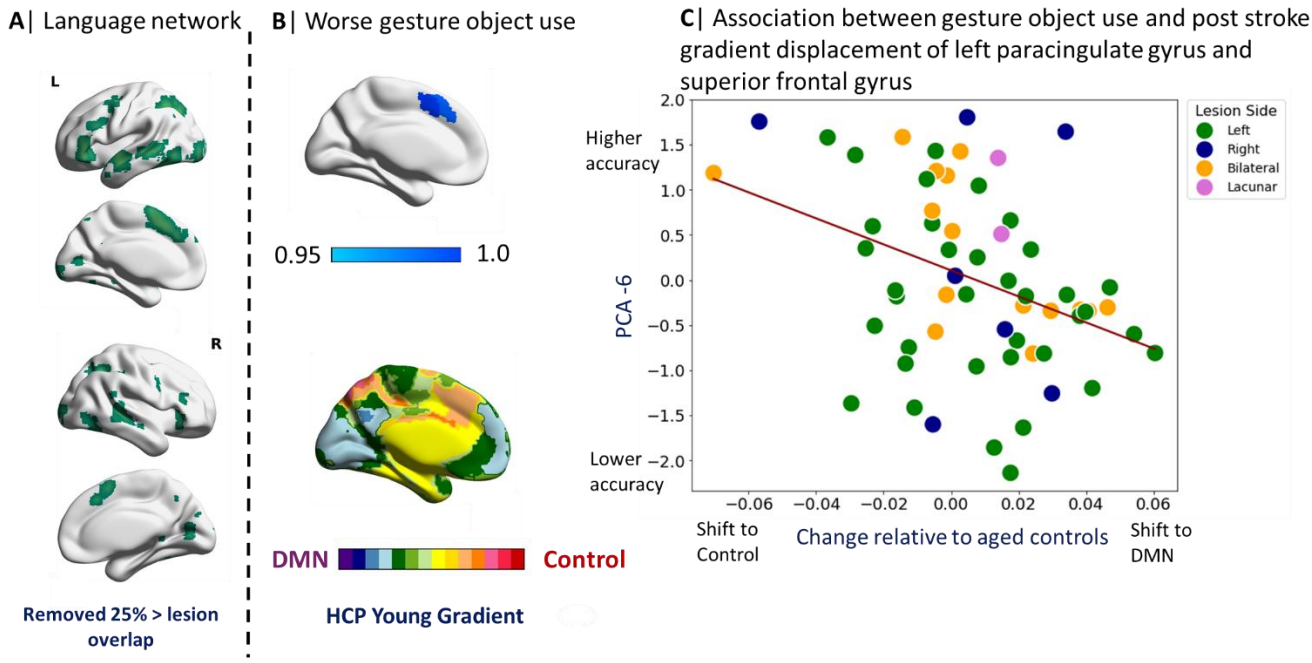

Supplementary Figure 3.S3. Permutation test results within the language ROI. A) Language network mask used after removing lesion voxels for the ROI analyses. B) Poorer gesture–object use was associated with the left paracingulate and superior frontal gyri, regions normally aligned with the control-network end of Gradient 3. C) Scatterplot showing the relationship between shifts in these regions along Gradient 3 and gesture–object use performance.

Section IV: Whole-brain associations between post-stroke functional connectivity gradient changes and language outcomes

We investigated the association between changes in functional connectivity gradients in aphasia patients and PCA-derived language components by conducting lesion–gradient symptom mapping within largely intact brain regions (removing voxels lesioned in ≥25%) across the whole-brain, to reduce the risk of type II errors. Nonparametric two-sample t-tests, using FSL's Randomise, with 5000 permutations were performed. Gradient 3 in whole-brain analysis showed clusters for both PCA component 5 (recognition memory) and component 6 (gesture-object use). Right frontal medial cortex, paracingulate cortex, and subcallosal cortex were associated with worse recognition memory (Figure 3.S4A) while the bilateral anterior cingulate cortex and juxtapositional cortex were associated with worse gesture-object use (Figure 3.S4C). We further examined these regions' functional affiliation with the default mode network (DMN) and control network end: to visualise these associations, we plotted gradient values for these clusters from the post-stroke difference gradient maps against task performance. Figure 3.S4B shows that in aphasia patients, a shift of the right frontal medial, paracingulate, and subcallosal cortices toward the default mode network (DMN) was associated with poorer recognition memory. These regions normally occupy an intermediate position

along Gradient 3. A similar pattern was observed in the anterior cingulate and juxtapositional lobule cortices, which are typically located nearer the control-network end of this gradient. In stroke patients, these areas also shifted toward the DMN pole, and this shift was linked to poorer performance on gesture-object use (Figure 3.S4D).

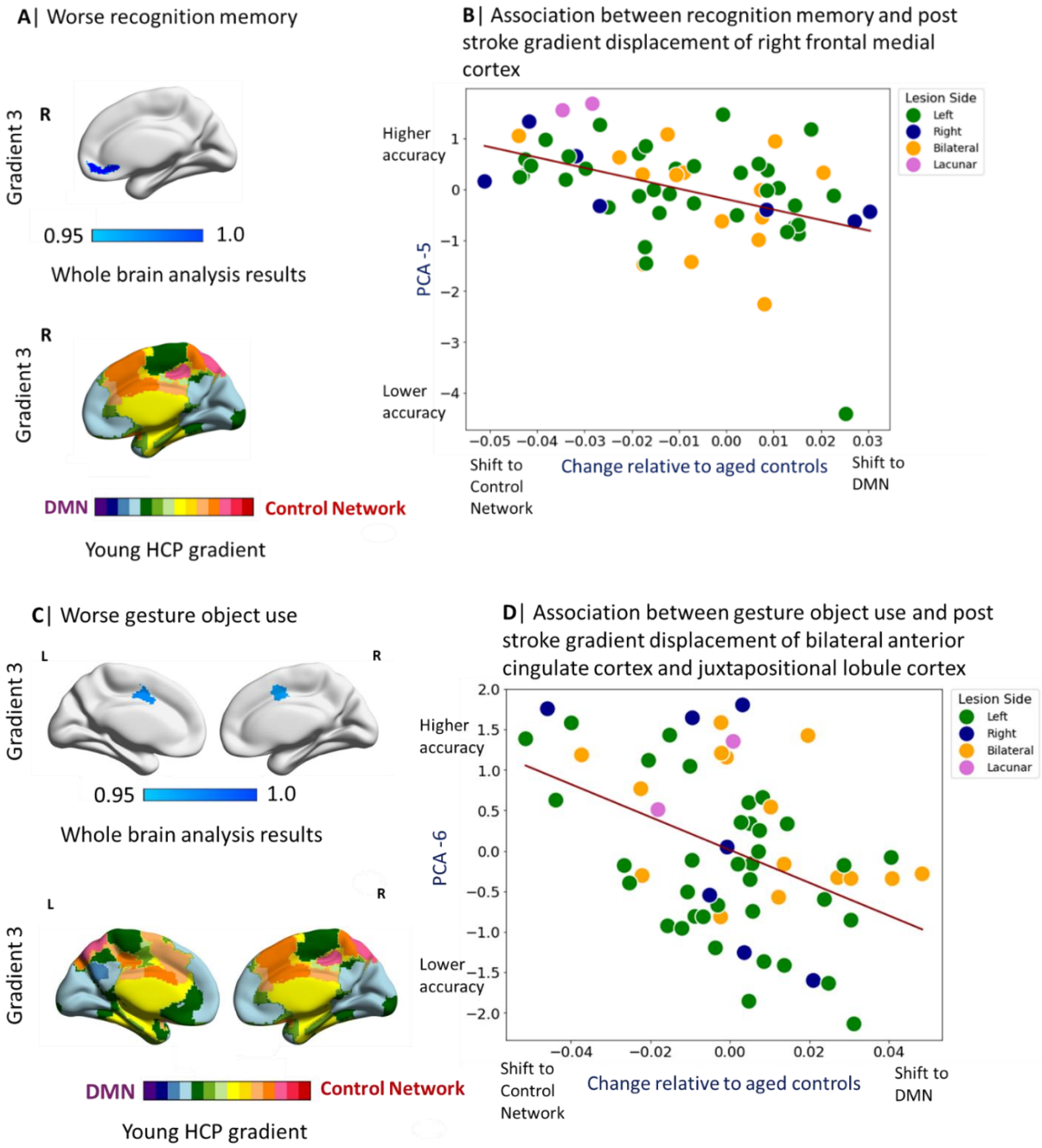

Supplementary Figure 3.S4. Permutation test results at the whole-brain level. A) A significant cluster in the right frontal medial cortex was associated with poorer recognition memory performance (top left panel) along Gradient 3. This region normally occupies an intermediate position on this gradient. B) Scatterplot showing the association between the right frontal medial cortex's position along Gradient 3 and recognition memory performance (top right panel). C) Poorer gesture–object use was associated with bilateral anterior cingulate and juxtapositional lobule cortices (bottom left panel), regions typically located toward the control-network end of Gradient 3. D) Scatterplot showing the relationship between shifts in these bilateral regions along Gradient 3 and gesture–object use performance (bottom right panel).

Chapter 4 supplementary materials

Section I: PCA Results for the Comprehensive Aphasia Test

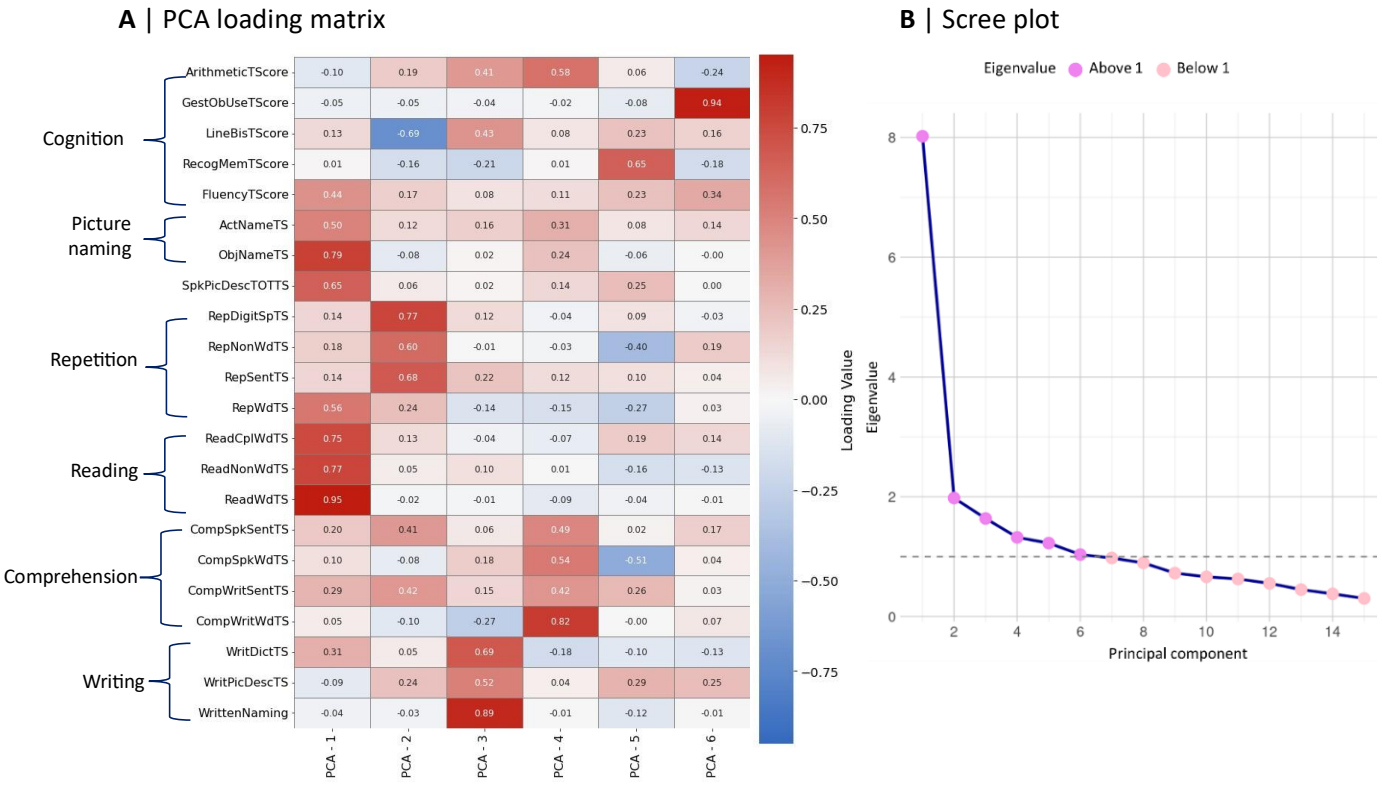

Supplementary Figure 4.S1. Principal component analysis results of the CAT. A) PCA loading matrix of CAT subtests. PCA-1 is associated with speech; PCA-2 with phonology and working memory; PCA-3 with writing and visuomotor capacity; PCA-4 with comprehension and arithmetic; PCA-5 with recognition memory; and PCA-6 with gesture–object use. B) Scree plot showing the eigenvalues for each principal component.

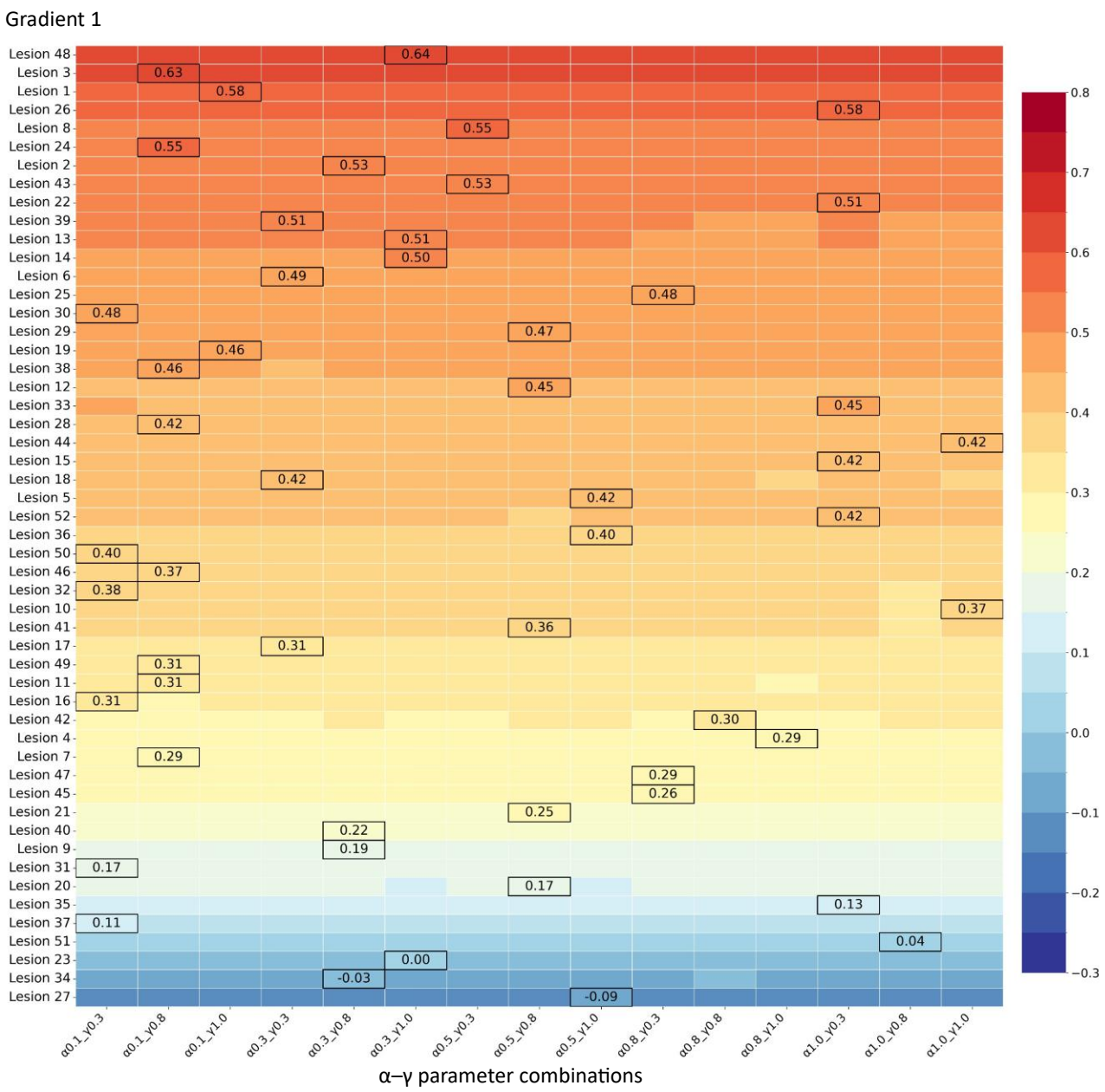

Supplementary Figure 4.S2. Heatmap showing spatial correlations between the observed and simulated Gradient 1 maps across α–γ parameter combinations. Each row corresponds to a stroke case, and each column represents an α–γ parameter pair. The parameter combination yielding the highest spatial correlation for each case is highlighted in black.

Gradient 2

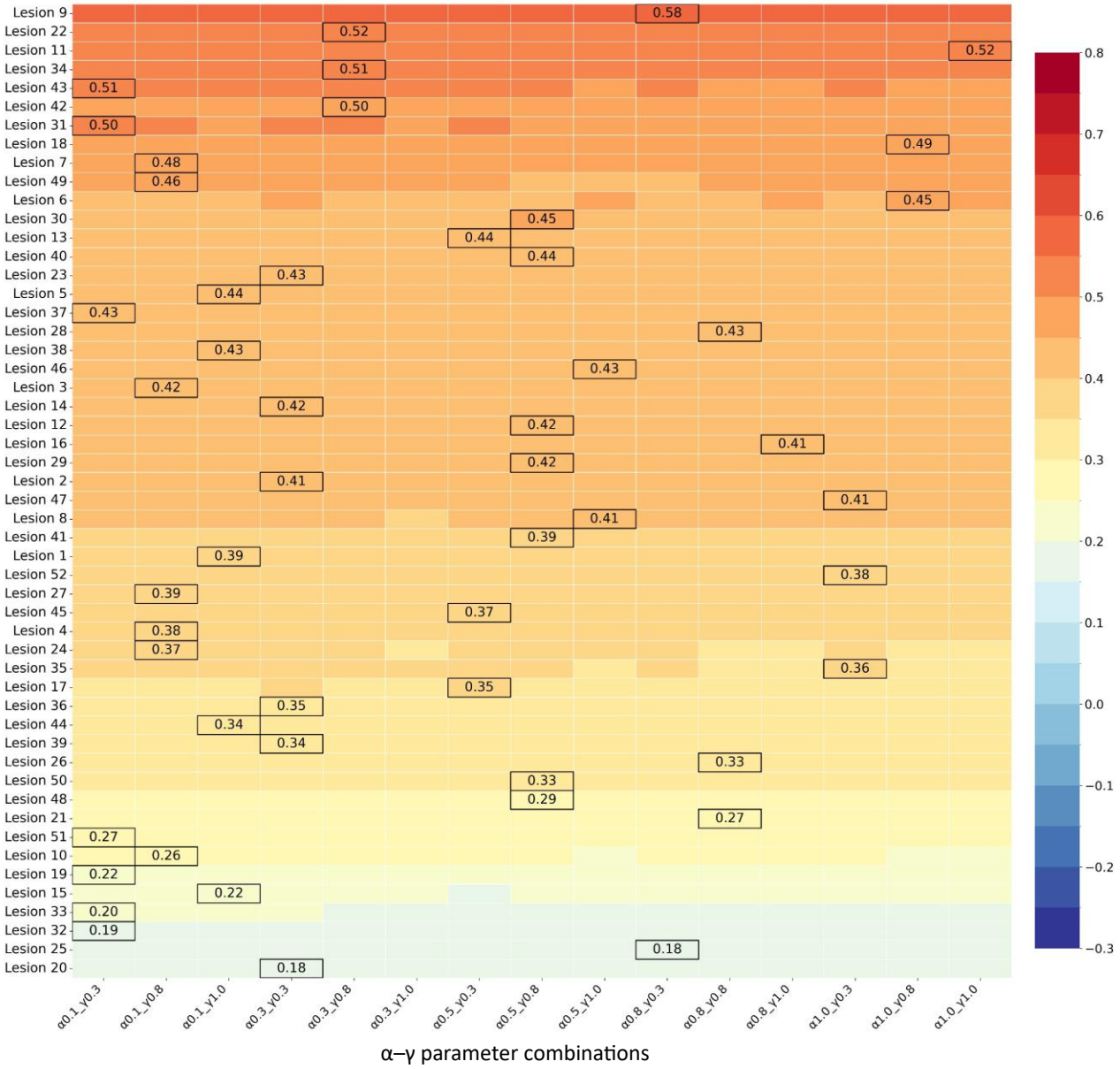

Supplementary Figure 4.S3. Heatmap showing spatial correlations between the observed and simulated Gradient 2 maps across α–γ parameter combinations. Each row corresponds to a stroke case, and each column represents an α–γ parameter pair. The parameter combination yielding the highest spatial correlation for each case is highlighted in black.

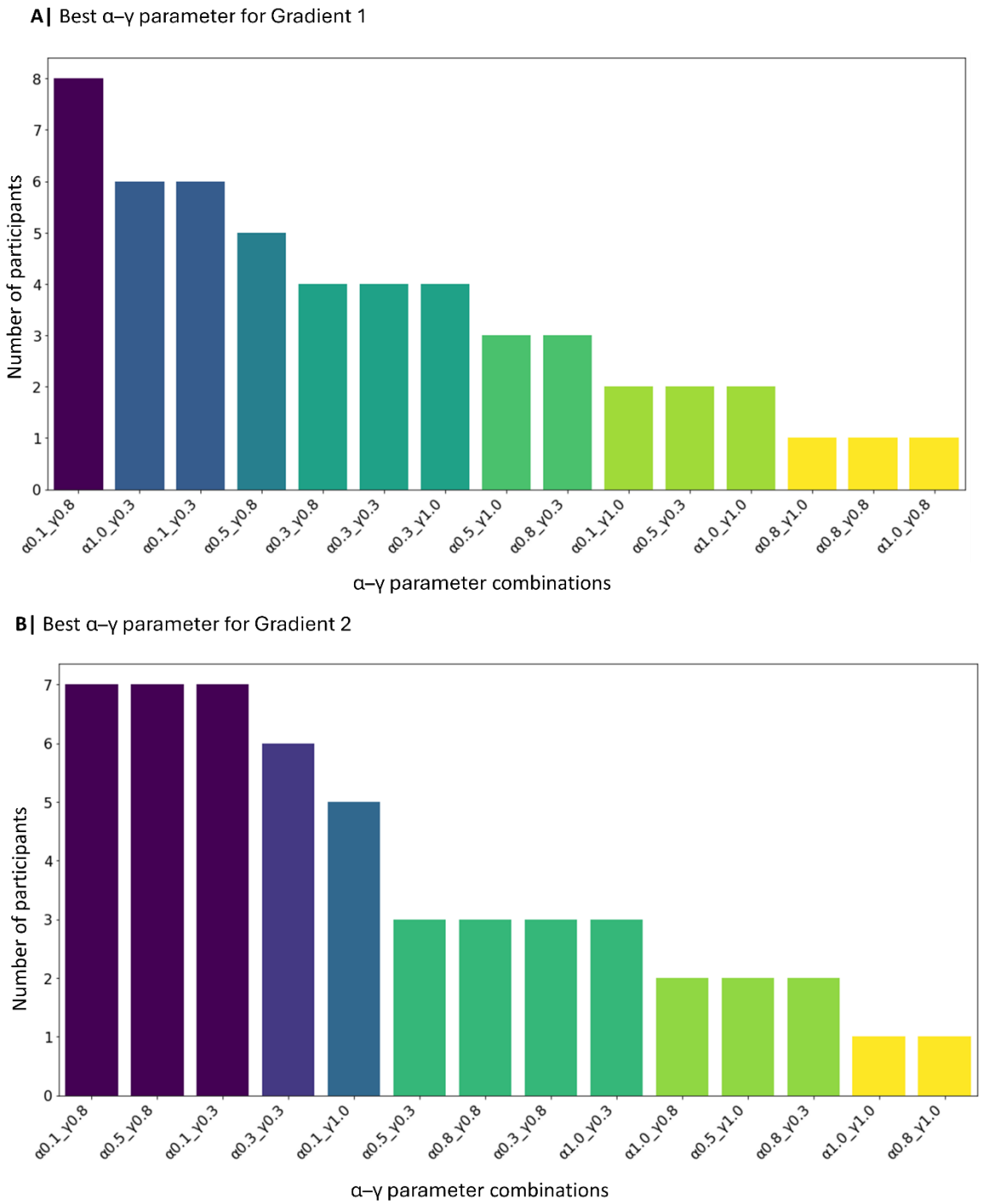

Supplementary Figure 4.S4. Bar plots showing the α–γ parameter combinations that produced the highest correlation between simulated and observed stroke gradients. A) Best α–γ combinations for Gradient 1. B) Best α–γ combinations for Gradient 2. Bars indicate the number of participants for whom each α–γ parameter pair yielded the highest spatial correlation between the simulated and observed post-stroke connectivity gradients.

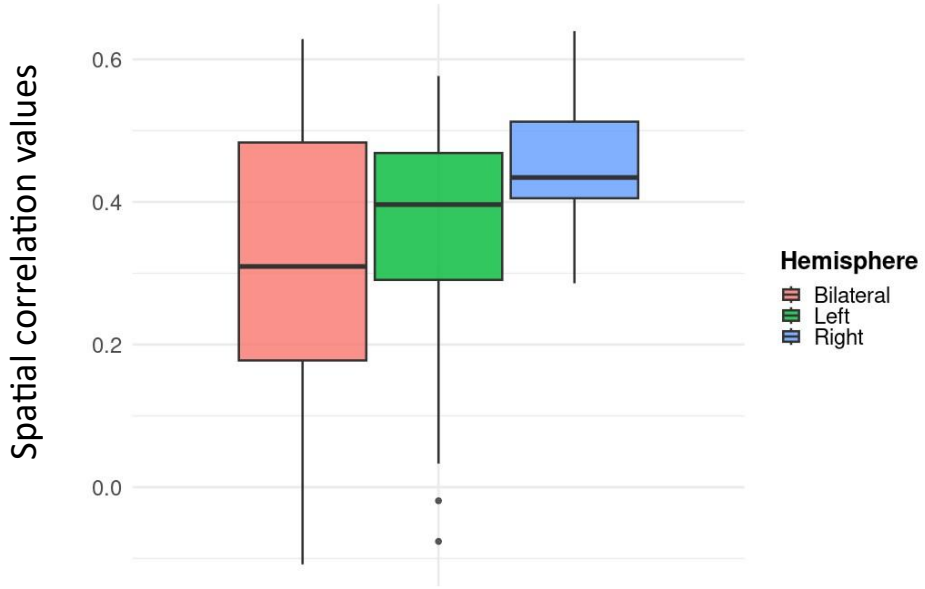

Supplementary Figure 4.S5. Relationship between lesion hemisphere and simulation accuracy. Box plots showing spatial correlation values between observed and simulated post-stroke gradient changes, grouped by the lesioned hemisphere (left, right, and bilateral lesions). Each box represents the distribution of spatial correlation values within that category. Median spatial correlation values did not vary across lesion groups, and no systematic differences were observed.

Supplementary Table 4.S1. Spatial correlations between observed and simulated post-stroke gradient changes for each lesion.

Lesion	Iterative model (G1)	Direct simulation (G1)	Iterative model (G2)	Direct simulation (G2)
Lesion 1	0.657390229	0.296658450	0.407615319	0.215697604
Lesion 2	0.589004145	0.370557224	0.438035802	0.210674288
Lesion 3	0.738865113	0.238896683	0.450326072	0.321150243
Lesion 4	0.300190570	0.361641096	0.398822503	0.277402611
Lesion 5	0.430413717	0.395064916	0.458372713	0.286906593
Lesion 6	0.530569109	0.363057002	0.482224039	0.270427797
Lesion 7	0.298357738	0.346445934	0.525891143	0.190336881
Lesion 8	0.615152637	0.401390764	0.428630306	0.292671230
Lesion 9	0.188795603	0.278141683	0.661861651	0.597688085
Lesion 10	0.379267311	0.386318518	0.269238375	0.551441238
Lesion 11	0.321487160	0.434147273	0.570806051	0.281817400
Lesion 12	0.476303091	0.372826340	0.444171239	0.120553305
Lesion 13	0.552174259	0.510757874	0.473194755	0.242084837
Lesion 14	0.544899845	0.198309930	0.450553650	0.226382582
Lesion 15	0.435224219	0.224797047	0.216625061	0.488849440
Lesion 16	0.300342483	0.281844314	0.440534029	0.716859433
Lesion 17	0.320041008	0.519701419	0.361081167	0.010339930
Lesion 18	0.433665425	0.275313611	0.531796308	0.388758462
Lesion 19	0.498122092	0.641605371	0.223317757	0.008434081
Lesion 20	0.166635401	0.398611183	0.182274147	0.178491343
Lesion 21	0.242396433	0.510379190	0.272391796	0.252448391
Lesion 22	0.561264450	0.156808109	0.579645880	0.515748332
Lesion 23	-0.019052305	0.437008240	0.462193148	0.575945713
Lesion 24	0.619158707	0.370128564	0.385793283	0.209968620
Lesion 25	0.515082801	0.611526523	0.182129447	0.169136270
Lesion 26	0.655440375	0.397322596	0.339413846	0.505725329
Lesion 27	-0.108650528	0.322579248	0.406220682	0.173320284
Lesion 28	0.451267093	0.169797423	0.450783707	0.336941701
Lesion 29	0.501610770	0.127542030	0.434655954	0.385525772
Lesion 30	0.510178159	0.346447141	0.472790218	0.239453457
Lesion 31	0.170496059	0.273666413	0.551111775	0.378489438
Lesion 32	0.379913103	0.542018501	0.184428995	0.344160545
Lesion 33	0.483033816	0.502196505	0.205908539	0.219317452
Lesion 34	-0.076213218	0.119748225	0.553987778	0.607614436
Lesion 35	0.117935758	0.388762641	0.376679115	0.138302052
Lesion 36	0.419242397	0.415614699	0.359964767	-0.014958413
Lesion 37	0.080323300	0.365748358	0.457366001	0.372172772
Lesion 38	0.501018784	0.427853644	0.455053359	0.486922283
Lesion 39	0.552459118	0.449097339	0.346172769	0.273569598
Lesion 40	0.212603363	0.410960281	0.469644460	0.223719387
Lesion 41	0.368351562	0.413132096	0.409689493	0.155528017
Lesion 42	0.304194010	0.331215996	0.540000044	0.553153121
Lesion 43	0.587130922	0.238794478	0.555957623	0.255620533
Lesion 44	0.447040186	0.644506556	0.354060869	0.141457796
Lesion 45	0.265841373	0.505509798	0.379545851	0.365817353
Lesion 46	0.393137635	0.359778102	0.451547231	0.107561095
Lesion 47	0.294038939	0.302198368	0.434634333	0.402922791

Lesion 48	0.757618387	0.222084653	0.292878471	0.232337124
Lesion 49	0.323628349	0.222440115	0.493390144	0.770077894
Lesion 50	0.420060027	0.367561845	0.337942155	0.432816996
Lesion 51	0.033169159	0.450344572	0.271469847	0.392417304
Lesion 52	0.429662241	0.023185656	0.399441516	0.724063938

Table 4.S1 shows the Fisher z-transformed spatial correlations between the observed post-stroke gradient difference maps and the simulated gradient difference maps, estimated for both the iterative propagation model and the direct lesion effects simulation (without propagation) for Gradient 1 and Gradient 2.

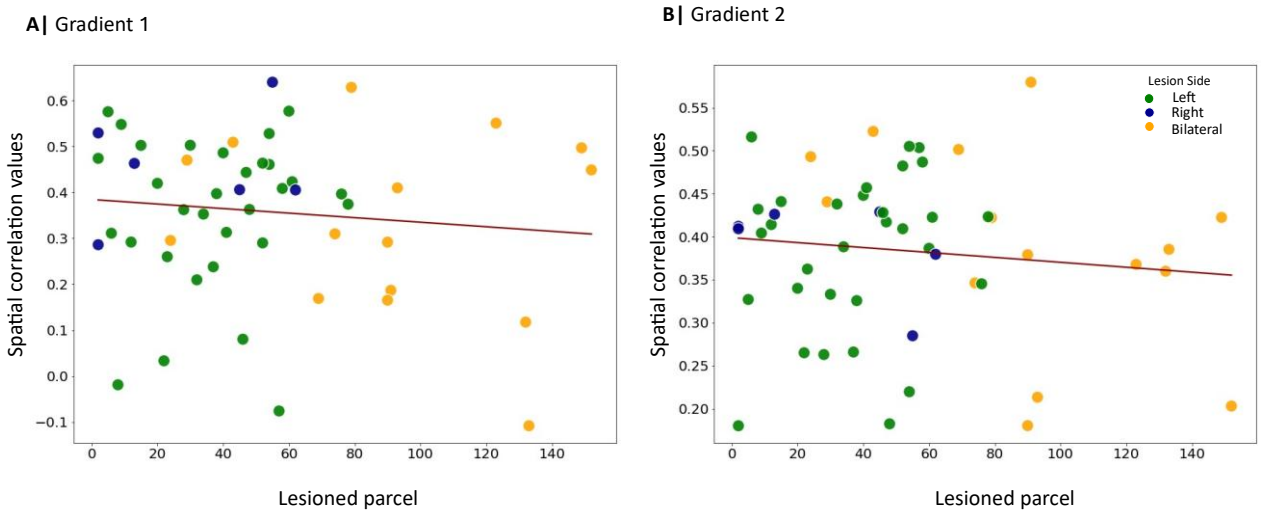

Supplementary Figure 4.S6. Relationship between lesion size and simulation accuracy for Gradient 1 and Gradient 2. A) Scatter plot showing the association between lesion size (number of lesioned parcels) and spatial correlation values between observed and simulated post-stroke gradient changes for Gradient 1. The red line indicates the fitted regression slope, showing no meaningful relationship between lesion size and simulation accuracy. B) Scatter plot showing the association between lesion size and spatial correlation values for Gradient 2.

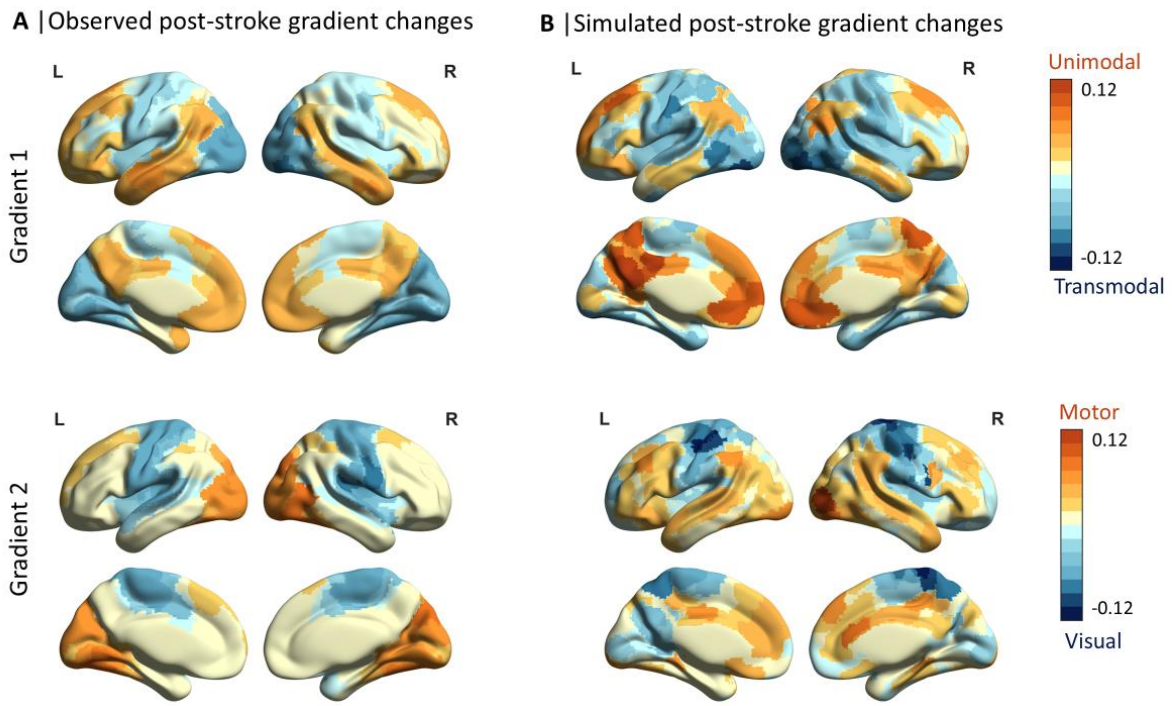

Supplementary Figure 4.S7. Comparison of post-stroke gradient changes between observed resting-state gradients and simulated gradients from the iterative propagation model. A) Observed effects of stroke on Gradients 1 and 2. B) Simulated effects of stroke on Gradients 1 and 2. Warm colours indicate regions where patients had lower gradient values than controls, and cool colours indicate regions where patients had higher values than control.

Section II: Post-stroke connectivity gradient changes: observed versus simulated gradients from the iterative propagation model

We compared post-stroke changes between the observed gradients and those simulated using the iterative propagation model (Figure 4.S7). A warm–cool colour scale indicates each brain region's shift along the gradient axes. Warm colours mark regions where patients had lower gradient values than controls, reflecting a shift toward the top end of the gradient. Cool colours mark regions where patients had higher values than controls, reflecting a shift toward the bottom end of the gradient.

In Gradient 1, observed post-stroke changes showed large portions of the default mode and frontoparietal networks shifting toward the unimodal end, whereas visuomotor regions shifted toward the transmodal end (Figure 4. S7A, top left). The simulation broadly captured both the direction and approximate magnitude of these displacements, although temporal and occipital pole regions showed mismatches in the direction of shift relative to the observed gradients (Figure 4.S7B, top right). In Gradient 2, the observed gradient showed visual regions shifting toward the motor end and motor

regions shifting toward the visual end (Figure 4.S7A, bottom left). The simulation captured the motor-region shifts relatively well, although some visual regions did not shift toward the motor end to the same extent as in the observed gradient (Figure 4.S7B, bottom right).

Section III: Network organisation in gradients between observed and stimulated stroke

Connectivity gradients were aligned to Yeo's network parcellation (Yeo et al., 2011), and average gradient values were computed for each network in both the observed and simulated stroke groups. Figure 4.S8 illustrates the relative positioning of each network along the transmodal–unimodal axis (Gradient 1) and the visuo–motor axis (Gradient 2) for both groups. For Gradient 1, the observed stroke showed a hierarchical ordering of networks: higher-order systems (DMN and frontoparietal) were positioned at the transmodal end, followed by the ventral and dorsal attention networks, and finally the unimodal somatomotor and visual networks at the opposite end (Figure 4.S8A). The simulated stroke broadly recapitulated this organisation. The DMN and frontoparietal networks occupied similar positions to those in the observed data, and the ventral attention, dorsal attention, and somatomotor networks were also placed in comparable positions in gradient space (Figure 4.S8A). The main deviation was the limbic and visual networks, for which the simulation did not fully capture the observed positioning. On Gradient 2, visual and somatomotor networks were positioned at the extreme ends in the observed stroke. Most of the networks in the simulation occupied comparable positions, except the visual network, which was positioned much higher than the observed visual network (Figure 4.S8B).

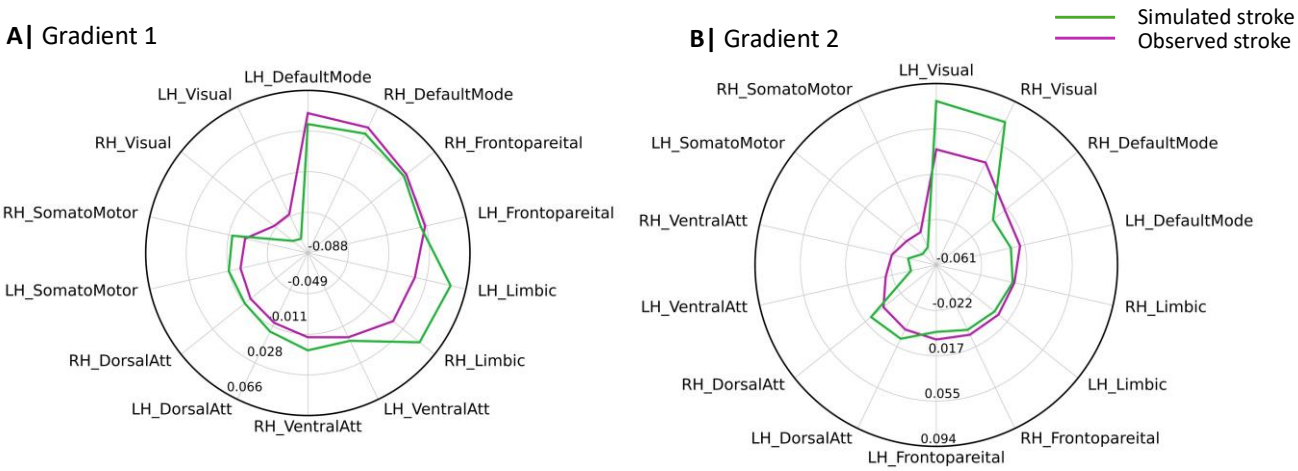

Supplementary Figure 4.S8. Network-level comparisons between observed and simulated stroke across connectivity gradients. A) Radar plot showing network positions along Gradient 1 for observed stroke (magenta) and simulated stroke (green). B) Radar plot showing average network positions along Gradient 2 for observed stroke (magenta) and simulated stroke (green). Values represent mean gradient coordinates for each Yeo network in the left and right hemispheres.

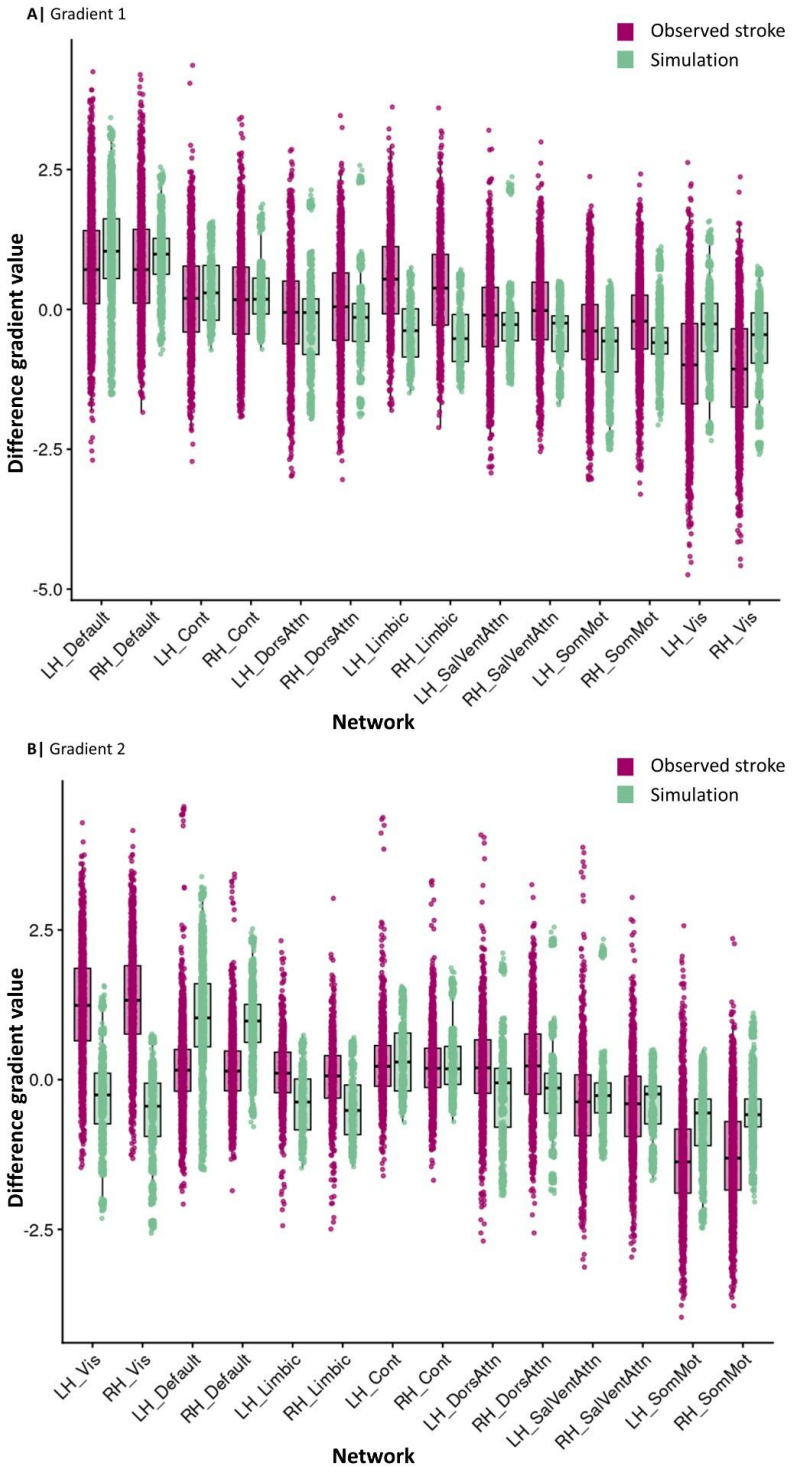

Supplementary Figure 4.S9. Comparison of observed and simulated stroke-related gradient differences across functional networks. Box-and-scatter plots show the distribution of difference-gradient values (difference between aged controls and stroke participants) for both the observed stroke data (magenta) and the simulation model (green). (A) Gradient 1 and (B) Gradient 2 illustrate network-wise displacement patterns. Individual data points are plotted to show variability within networks.

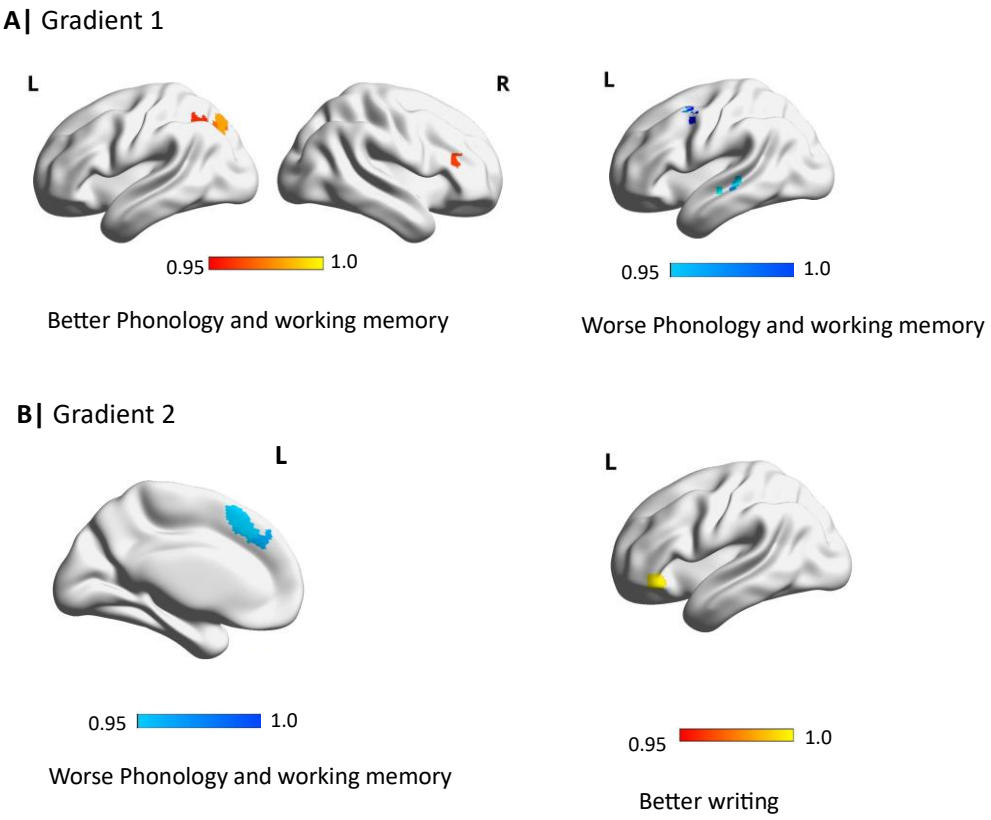

Supplementary Figure 4.S10. Significant clusters from lesion–symptom mapping conducted on the simulation. Panels show cortical regions where simulated lesion–symptom mapping revealed significant associations between gradient changes and behavioural performance (A) Gradient 1: Clusters associated with better phonology and working memory (orange–red) and worse phonology and working memory (blue). (B) Gradient 2: Clusters associated with worse phonology and working memory (blue) and better writing performance (yellow–red). Colour bars indicate 1 – p values, where higher values reflect stronger statistical significance.

References

Abel, S., Weiller, C., Huber, W., & Willmes, K. (2014). Neural underpinnings for model-oriented therapy of aphasic word production. *Neuropsychologia*, *57*(1), 154–165. https://doi.org/10.1016/J.NEUROPSYCHOLOGIA.2014.03.010

Acharya, A. B., Lui, F., & Maani, C. V. (2024). Conduction Aphasia. StatPearls. https://www.ncbi.nlm.nih.gov/books/NBK537006/

Adlam, A. L. R., Patterson, K., Bozeat, S., & Hodges, J. R. (2010). The Cambridge Semantic Memory Test Battery: Detection of semantic deficits in semantic dementia and Alzheimer's disease. Neurocase, 16(3), 193–207. https://doi.org/10.1080/13554790903405693

Ahrens, K., Liu, H. L., Lee, C. Y., Gong, S. P., Fang, S. Y., & Hsu, Y. Y. (2022). Impact of motor stroke on novel and conventional action metaphor comprehension. *Brain and Language*, *226*(2), 105081. https://doi.org/10.1016/j.bandl.2005.10.004

Akinina, Y., Dragoy, O., Ivanova, M. V., Iskra, E. V., Soloukhina, O. A., Petryshevsky, A. G., Fedina, O. N., Turken, A. U., Shklovsky, V. M., & Dronkers, N. F. (2022). Structural disconnections associated with language impairments in chronic post-stroke aphasia using disconnectome maps. *Cortex*, *155*, 90–106. https://doi.org/10.1016/j.neuropsychologia.2019.05.015

Alexander-Bloch, A. F., Shou, H., Liu, S., Satterthwaite, T. D., Glahn, D. C., Shinohara, R. T., Vandekar, S. N., Raznahan, A., & Alexander-Bloch, A. F. (2018). On testing for spatial correspondence between maps of human brain structure and function. https://doi.org/10.1016/j.neuroimage.2018.05.070

Alyahya, R. S. W., Lambon Ralph, M. A., Halai, A., & Hoffman, P. (2022). The cognitive and neural underpinnings of discourse coherence in post-stroke aphasia. Brain Communications, 4(3), fcac147. https://doi.org/10.1093/BRAINCOMMS/FCAC147

Alia, C., Spalletti, C., Lai, S., Panarese, A., Lamola, G., Bertolucci, F., Vallone, F., Di Garbo, A., Chisari, C., Micera, S., & Caleo, M. (2017). Neuroplastic Changes Following Brain Ischemia and their Contribution to Stroke Recovery: Novel Approaches in Neurorehabilitation. *Frontiers in Cellular Neuroscience*, *11*, 76. https://doi.org/10.3389/fncel.2017.00076

Almeida, S. R. M., Filho, C. A. S., Vicentini, J., Novi, S. L., Mesquita, R. C., Castellano, G., & Li, L. M. (2022). Modeling functional network topology following stroke through graph theory: functional reorganization and motor recovery prediction. *Brazilian Journal of Medical and Biological Research*, *55*, e12036. https://doi.org/10.1590/1414-431X2022e12036

Aminoff, E. M., Kveraga, K., & Bar, M. (2013). The role of the parahippocampal cortex in cognition. Trends in Cognitive Sciences, 17(8), 379. https://doi.org/10.1016/J.TICS.2013.06.009

Andrews, J. P., Cahn, N., Speidel, B. A., Chung, J. E., Levy, D. F., Wilson, S. M., Berger, M. S., & Chang, E. F. (2022). Dissociation of Broca's area from Broca's aphasia in patients undergoing neurosurgical resections. *Journal of Neurosurgery*, *138*(3), 847–857. https://doi.org/10.3171/2022.6.JNS2297

Asan, A. S., McIntosh, J. R., & Carmel, J. B. (2022). Targeting Sensory and Motor Integration for Recovery of Movement After CNS Injury. *Frontiers in Neuroscience*, *15*, 791824. https://doi.org/10.3389/fnins.2021.791824

Aswendt, M., Pallast, N., Wieters, F., Baues, M., Hoehn, M., & Fink, G. R. (2021). Lesion Size- and Location-Dependent Recruitment of Contralesional Thalamus and Motor Cortex Facilitates Recovery after Stroke in Mice. Translational Stroke Research, 12(1), 87–97. https://doi.org/10.1007/S12975-020-00802-3/FIGURES/4

Athale, R. A., & Lee, J. N. (1984). Optical Processing Using Outer-Product Concepts. Proceedings of the IEEE, 72(7), 931–941. https://doi.org/10.1109/PROC.1984.12949

Avants, B. B., Tustison, N. J., Song, G., Cook, P. A., Klein, A., & Gee, J. C. (2011). A Reproducible Evaluation of ANTs Similarity Metric Performance in Brain Image Registration. NeuroImage, 54(3), 2033. https://doi.org/10.1016/J.NEUROIMAGE.2010.09.025

Avants, B. B., Tustison, N. J., Stauffer, M., Song, G., Wu, B., & Gee, J. C. (2014). The Insight ToolKit image registration framework. Frontiers in Neuroinformatics, 8(APR). https://doi.org/10.3389/FNINF.2014.00044

Aziz, M., Baig, S., Hai, W., Ali, A., Majid, A., & Su, L. (2025). Systematic review: Resting state functional MRI as a biomarker for non-invasive brain stimulation in upper limb recovery post-stroke. *Neurological Sciences*, *46*(9), 4233. https://doi.org/10.1007/S10072-025-08224-5

Baddeley, A. D., & Hitch, G. (1974). Working Memory. *Psychology of Learning and Motivation - Advances in Research and Theory*, *8*(C), 47–89. https://doi.org/10.1016/S0079-7421(08)60452-1

Badre, D. (2008). Cognitive control, hierarchy, and the rostro–caudal organization of the frontal lobes. *Trends in Cognitive Sciences*, *12*(5), 193–200. https://doi.org/10.1016/j.tics.2008.02.004

Badre, D., Hoffman, J., Cooney, J. W., & D'Esposito, M. (2009). Hierarchical cognitive control deficits following damage to the human frontal lobe. *Nature Neuroscience*, *12*(4), 515. https://doi.org/10.1038/nn.2277

Badre, D., Poldrack, R. A., Paré-Blagoev, E. J., Insler, R. Z., & Wagner, A. D. (2005). Dissociable Controlled Retrieval and Generalized Selection Mechanisms in Ventrolateral Prefrontal Cortex. *Neuron*, *47*(6), 907–918. https://doi.org/10.1016/J.NEURON.2005.07.023

Bar, M., Aminoff, E., & Ishai, A. (2008). Famous Faces Activate Contextual Associations in the Parahippocampal Cortex. Cerebral Cortex, 18(6), 1233–1238. https://doi.org/10.1093/CERCOR/BHM170

Barrett, J., Pike, G. B., & Paus, T. (2004). The role of the anterior cingulate cortex in pitch variation during sad affect. *The European Journal of Neuroscience*, *19*(2), 458–464. https://doi.org/10.1111/j.0953-816X.2003.03113.x

Bartolo, A., Cubelli, R., Sala, S. Della, & Drei, S. (2003). Pantomimes are special gestures which rely on working memory. Brain and Cognition, 53(3), 483–494. https://doi.org/10.1016/S0278-2626(03)00209-4

Bartolomei, F., Bosma, I., Klein, M., Baayen, J. C., Reijneveld, J. C., Postma, T. J., Heimans, J. J., van Dijk, B. W., de Munck, J. C., de Jongh, A., Cover, K. S., & Stam, C. J. (2006). Disturbed functional connectivity in brain tumour patients: Evaluation by graph analysis of synchronization matrices. *Clinical Neurophysiology*, *117*(9), 2039–2049. https://doi.org/10.1016/J.CLINPH.2006.05.018

Bartolomeo, P. (2011). The quest for the 'critical lesion site' in cognitive deficits: Problems and perspectives. *Cortex*, *47*(8), 1010–1012. https://doi.org/10.1016/J.CORTEX.2010.11.007

Bartolomeo, P., Thiebaut De Schotten, M., & Doricchi, F. (2007). Left Unilateral Neglect as a Disconnection Syndrome. *Cerebral Cortex*, *17*(11), 2479–2490. https://doi.org/10.1093/cercor/bhl181

Bassett, D. S., Zurn, P., & Gold, J. I. (2018). On the nature and use of models in network neuroscience. *Nature Reviews Neuroscience*, *19*(9), 566–578. https://doi.org/10.1038/s41583-018-0038-8

Bates, E., Wilson, S. M., Saygin, A. P., Dick, F., Sereno, M. I., Knight, R. T., & Dronker, N. F. (2003). Voxel-based lesion-symptom mapping. Nature Neuroscience, 6(5), 448–450. https://doi.org/10.1038/NN1050;KWRD=BIOMEDICINE

Batista-García-Ramó, K., & Fernández-Verdecia, C. I. (2018). What We Know About the Brain Structure-Function Relationship. Behavioral Sciences (Basel, Switzerland), 8(4). https://doi.org/10.3390/BS8040039

Bayrak, Ş., Khalil, A. A., Villringer, K., Fiebach, J. B., Villringer, A., Margulies, D. S., & Ovadia-Caro, S. (2019). The impact of ischemic stroke on connectivity gradients. *NeuroImage : Clinical*, *24*, 101947. https://doi.org/10.1016/j.nicl.2019.101947

Bègue, I., Nicholson, T. R., Kozlowska, K., Lafrance, W. C., Levenson, J. L., Rapaport, M. H., Carson, A. J., & Perez, D. L. (2025). Functional Connectivity Gradients Reveal Altered

Hierarchical Cortical Organization in Functional Neurological Disorder. *Biological Psychiatry: Cognitive Neuroscience and Neuroimaging*, *51*(12), 1961–1963. https://doi.org/10.1017/S0033291721002038

Behzadi, Y., Restom, K., Liau, J., & Liu, T. T. (2007). A Component Based Noise Correction Method (CompCor) for BOLD and Perfusion Based fMRI. NeuroImage, 37(1), 90. https://doi.org/10.1016/J.NEUROIMAGE.2007.04.042

Benedek, M., Jauk, E., Beaty, R. E., Fink, A., Koschutnig, K., & Neubauer, A. C. (2016). Brain mechanisms associated with internally directed attention and self-generated thought. *Scientific Reports 2016 6:1*, *6*(1), 22959-. https://doi.org/10.1038/srep22959

Bennett, I. J., & Rypma, B. (2013). Advances in Functional Neuroanatomy: A Review of Combined DTI and fMRI Studies in Healthy Younger and Older Adults. *Neuroscience and Biobehavioral Reviews*, *37*(7), 1201. https://doi.org/10.1016/J.NEUBIOREV.2013.04.008

Bernhardt, B. C., Smallwood, J., Keilholz, S., & Margulies, D. S. (2022). Gradients in brain organization. *NeuroImage*, *251*(6506), 118987. https://doi.org/10.1016/j.neuroimage.2022.118987

Bertolero, M. A., Yeo, B. T. T., & D'Esposito, M. (2017). The diverse club. *Nature Communications 2017 8:1*, *8*(1), 1277-. https://doi.org/10.1038/s41467-017-01189-w

Bethlehem, R. A. I., Paquola, C., Seidlitz, J., Ronan, L., Bernhardt, B., Consortium, C. C. A. N., & Tsvetanov, K. A. (2020). Dispersion of functional gradients across the adult lifespan. *Neuroimage*, *222*. https://doi.org/10.1016/J.NEUROIMAGE.2020.117299

Betzel, R., Puxeddu, M. G., Seguin, C., Bazinet, V., Luppi, A., Podschun, A., Singleton, S. P., Faskowitz, J., Parakkattu, V., Misic, B., Markett, S., Kuceyeski, A., & Parkes, L. (2026). Controlling the human connectome with spatially diffuse input signals. *Communications Biology 2026*. https://doi.org/10.1038/s42003-026-09560-8

Billot, A., & Kiran, S. (2024). Disentangling Neuroplasticity Mechanisms in Post-Stroke Language Recovery. Brain and Language, 251, 105381. https://doi.org/10.1016/J.BANDL.2024.105381

Biswal, B., Zerrin Yetkin, F., Haughton, V. M., & Hyde, J. S. (1995). Functional connectivity in the motor cortex of resting human brain using echo-planar mri. *Magnetic Resonance in Medicine*, *34*(4), 537–541. https://doi.org/10.1002/MRM.1910340409

Blom-Smink, M., Verly, M., Spielmann, K., Smits, M., Ribbers, G. M., & van de Sandt-Koenderman, M. W. M. E. (2020). Change in Right Inferior Longitudinal Fasciculus Integrity Is Associated With Naming Recovery in Subacute Poststroke Aphasia. *Neurorehabilitation and Neural Repair*, *34*(9), 784–794. https://doi.org/10.1177/1545968320940982

Bo Lee, K., Hoon Lim, S., Hoon Kim, K., Jeon Kim, K., Rae Kim, Y., Nam Chang, W., Woo Yeom, J., Dong Kim, Y., & Yong Hwang, B. (2015). Six-month functional recovery of stroke patients: a multi-time-point study. https://doi.org/10.1097/MRR.0000000000000108

Boes, A. D. (2021). Lesion network mapping: where do we go from here? Brain, 144(1), e5–e5. https://doi.org/10.1093/BRAIN/AWAA350

Boes, A. D., Prasad, S., Liu, H., Liu, Q., Pascual-Leone, A., Caviness, V. S., & Fox, M. D. (2015). Network localization of neurological symptoms from focal brain lesions. Brain : A Journal of Neurology, 138(Pt 10), 3061–3075. https://doi.org/10.1093/BRAIN/AWV228

Bolognini, N., Russo, C., & Edwards, D. J. (2016). The sensory side of post-stroke motor rehabilitation. *Restorative Neurology and Neuroscience*, *34*(4), 571. https://doi.org/10.3233/RNN-150606

Bonakdarpour, B., Beeson, P. M., DeMarco, A. T., & Rapcsak, S. Z. (2015). Variability in blood oxygen level dependent (BOLD) signal in patients with stroke-induced and primary progressive aphasia. *NeuroImage: Clinical*, *8*, 87–94. https://doi.org/10.1016/j.nicl.2015.03.014

Bonilha, L., & Fridriksson, J. (2008). Subcortical damage and white matter disconnection associated with non-fluent speech. Brain, 132(6), e108. https://doi.org/10.1093/BRAIN/AWN200

Bonilha, L., Nesland, T., Rorden, C., Fillmore, P., Ratnayake, R. P., & Fridriksson, J. (2014). Mapping Remote Subcortical Ramifications of Injury after Ischemic Strokes. *Behavioural Neurology*, *2014*. https://doi.org/10.1155/2014/215380

Bonkhoff, A. K., Rehme, A. K., Hensel, L., Tscherpel, C., Volz, L. J., Espinoza, F. A., Gazula, H., Vergara, V. M., Fink, G. R., Calhoun, V. D., Rost, N. S., & Grefkes, C. (2021). Dynamic connectivity predicts acute motor impairment and recovery post-stroke. *Brain Communications*, *3*(4). https://doi.org/10.1093/braincomms/fcab227

Bonner, M. F., & Price, A. R. (2013). Where Is the Anterior Temporal Lobe and What Does It Do? Journal of Neuroscience, 33(10), 4213–4215. https://doi.org/10.1523/JNEUROSCI.0041-13.2013

Bonzano, L., Bisio, A., Pedullà, L., Brichetto, G., & Bove, M. (2021). Right Inferior Parietal Lobule Activity Is Associated With Handwriting Spontaneous Tempo. Frontiers in Neuroscience, 15, 656856. https://doi.org/10.3389/FNINS.2021.656856/FULL

Boring, M. J., Richardson, R. M., & Ghuman, A. S. (2024). Interacting ventral temporal gradients of timescales and functional connectivity and their relationships to visual behavior. *IScience*, *27*(6), 110003. https://doi.org/10.1016/J.ISCI.2024.110003

Borovsky, A., Saygin, A. P., Bates, E., & Dronkers, N. (2007). Lesion correlates of conversational speech production deficits. Neuropsychologia, 45(11), 2525. https://doi.org/10.1016/J.NEUROPSYCHOLOGIA.2007.03.023

Boschi, A., Brofiga, M., & Massobrio, P. (2021). Thresholding Functional Connectivity Matrices to Recover the Topological Properties of Large-Scale Neuronal Networks. *Frontiers in Neuroscience*, *15*, 705103. https://doi.org/10.3389/FNINS.2021.705103/TEXT

Bouzigues, A., Godefroy, V., Le Du, V., Russell, L. L., Houot, M., Le Ber, I., Batrancourt, B., Levy, R., Warren, J. D., Rohrer, J. D., Margulies, D. S., & Migliaccio, R. (2024). Disruption of macroscale functional network organisation in patients with frontotemporal dementia. *Molecular Psychiatry 2024 30:6*, *30*(6), 2436–2447. https://doi.org/10.1038/s41380-024-02847-4

Bowren, M., Bruss, J., Manzel, K., Edwards, D., Liu, C., Corbetta, M., Tranel, D., & Boes, A. D. (2022). Post-stroke outcomes predicted from multivariate lesion-behaviour and lesion network mapping. *Brain*, *145*(4), 1338–1353. https://doi.org/10.1093/brain/awac010

Braaß, H., Gutgesell, L., Backhaus, W., Higgen, F. L., Quandt, F., Choe, C. un, Gerloff, C., & Schulz, R. (2023). Early functional connectivity alterations in contralesional motor networks influence outcome after severe stroke: a preliminary analysis. Scientific Reports 2023 13:1, 13(1), 1–8. https://doi.org/10.1038/s41598-023-38066-0

Braban, A., Leech, R., Murphy, K., & Geranmayeh, F. (2023). Cerebrovascular reactivity has negligible contribution to haemodynamic lag after stroke: implications for fMRI studies. *Stroke*, *54*(4), 1066. https://doi.org/10.1161/STROKEAHA.122.041880

Braun, E. J., Billot, A., Meier, E. L., Pan, Y., Parrish, T. B., Kurani, A. S., & Kiran, S. (2022). White matter microstructural integrity pre- and post-treatment in individuals with chronic post-stroke aphasia. *Brain and Language*, *232*, 105163. https://doi.org/10.1016/j.bandl.2022.105163

Braunlich, K., Gomez-Lavin, J., & Seger, C. A. (2014). Frontoparietal networks involved in categorization and item working memory. *NeuroImage*, *107*, 146. https://doi.org/10.1016/j.neuroimage.2014.11.051

Breitenstein, C., Grewe, T., Flöel, A., Ziegler, W., Springer, L., Martus, P., Huber, W., Willmes, K., Ringelstein, E. B., Haeusler, K. G., Abel, S., Glindemann, R., Domahs, F., Regenbrecht, F., Schlenck, K. J., Thomas, M., Obrig, H., de Langen, E., Rocker, R., … Bamborschke, S. (2017). Intensive speech and language therapy in patients with chronic aphasia after stroke: a randomised, open-label, blinded-endpoint, controlled trial in a health-care setting. The Lancet, 389(10078), 1528–1538. https://doi.org/10.1016/S0140-6736(17)30067-3

Briggs, R. G., Chakraborty, A. R., Anderson, C. D., Abraham, C. J., Palejwala, A. H., Conner, A. K., Pelargos, P. E., O'Donoghue, D. L., Glenn, C. A., & Sughrue, M. E. (2019). Anatomy and white matter connections of the inferior frontal gyrus. *Clinical Anatomy*, *32*(4), 546–556. https://doi.org/10.1002/CA.23349

Broca P. Nouvelle observation d'aphémie produite par une lésion de la moitié postérieure des deuxième et troisième circonvolutions frontales. Bulletins de la Société Anatomique de Paris 1861a; 36: 398–407.

Buckner, R. L., & Yeo, B. T. T. (2014). Borders, map clusters, and supra-areal organization in visual cortex. *NeuroImage*, *93*(P1), 292–297. https://doi.org/10.1016/j.neuroimage.2013.12.036

Bullmore, E., & Sporns, O. (2009). Complex brain networks: graph theoretical analysis of structural and functional systems. *Nature Reviews Neuroscience 2009 10:3*, *10*(3), 186–198. https://doi.org/10.1038/nrn2575

Bullock, L., Forseth, K. J., Woolnough, O., Rollo, P. S., & Tandon, N. (2024). Supplementary motor area in speech initiation: A large-scale intracranial EEG evaluation of stereotyped word articulation. *IScience*, *28*(1), 111531. https://doi.org/10.1016/j.isci.2024.111531

Camargo, A., Mauro, G. Del, Wang, Z., & Initiative, for the A. D. N. (2026). Cross entropy gradient analysis for Alzheimer's disease assessment. *Journal of Alzheimer's Disease*, *111*(1), 301–311. https://doi.org/10.1177/13872877261431317

Campos, B., Choi, H., DeMarco, A. T., Seydell-Greenwald, A., Hussain, S. J., Joy, M. T., Turkeltaub, P. E., & Zeiger, W. (2023). Rethinking Remapping: Circuit Mechanisms of Recovery after Stroke. *The Journal of Neuroscience : The Official Journal of the Society for Neuroscience*, *43*(45), 7489–7500. https://doi.org/10.1523/JNEUROSCI.1425-23.2023

Carmichael, S. T. (2015). The 3 Rs of Stroke Biology: Radial, Relayed, and Regenerative. Neurotherapeutics, 13(2), 348. https://doi.org/10.1007/S13311-015-0408-0

Carrera, E., & Tononi, G. (2014). Diaschisis: past, present, future. *Brain*, *137*(9), 2408–2422. https://doi.org/10.1093/BRAIN/AWU101

Carter, A. R., Astafiev, S. V., Lang, C. E., Connor, L. T., Rengachary, J., Strube, M. J., Pope, D. L. W., Shulman, G. L., & Corbetta, M. (2010). Resting Inter-hemispheric fMRI Connectivity Predicts Performance after Stroke. Annals of Neurology, 67(3), 365. https://doi.org/10.1002/ANA.21905

Catani, M., & Ffytche, D. H. (2005). The rises and falls of disconnection syndromes. Brain, 128(10), 2224–2239. https://doi.org/10.1093/brain/awh622

Čeko, M., Gracely, J. L., Fitzcharles, M. A., Seminowicz, D. A., Schweinhardt, P., & Bushnell, M. C. (2015). Is a Responsive Default Mode Network Required for Successful Working Memory Task Performance? *Journal of Neuroscience*, *35*(33), 11595–11605. https://doi.org/10.1523/JNEUROSCI.0264-15.2015

Chan, M. Y., Park, D. C., Savalia, N. K., Petersen, S. E., & Wig, G. S. (2014). Decreased segregation of brain systems across the healthy adult lifespan. *Proceedings of the National Academy of Sciences of the United States of America*, *111*(46), E4997–E5006. https://doi.org/10.1073/PNAS.1415122111

Chapman, C. A., Hasan, O., Schulz, P. E., & Martin, R. C. (2020). Evaluating the distinction between semantic knowledge and semantic access: Evidence from semantic dementia and comprehension-impaired stroke aphasia. *Psychonomic Bulletin and Review*, *27*(4), 607–639. https://doi.org/10.3758/S13423-019-01706-6/FIGURES/2

Chechlacz, M., Rotshtein, P., & Humphreys, G. W. (2012). Neuro-anatomical dissections of unilateral visual neglect symptoms: ALE meta-analysis of lesion-symptom mapping. *Frontiers in Human Neuroscience*, *6*(JULY), 23518. https://doi.org/10.3389/fnhum.2012.00230

Chen, A. C., Oathes, D. J., Chang, C., Bradley, T., Zhou, Z. W., Williamsa, L. M., Glover, G. H., Deisseroth, K., & Etkin, A. (2013). Causal interactions between fronto-parietal central executive and default-mode networks in humans. *Proceedings of the National Academy of Sciences of the United States of America*, *110*(49), 19944–19949. https://doi.org/10.1073/pnas.1311772110

Chen, H., Pan, X., Bickerton, W. L., Lau, J. K., Zhou, J., Zhou, B., Harris, L., & Rotshtein, P. (2019). Delineating the cognitive-neural substrates of writing: a large scale behavioral and voxel based morphometry study. Scientific Reports, 9(1), 1–19. https://doi.org/10.1038/S41598-019-55129-3

Chen, H., Wang, J., Uddin, L. Q., Wang, X., Guo, X., Lu, F., Duan, X., Wu, L., & Chen, H. (2018). Aberrant functional connectivity of neural circuits associated with social and sensorimotor deficits in young children with autism spectrum disorder. *Autism Research : Official Journal of the International Society for Autism Research*, *11*(12), 1643. https://doi.org/10.1002/AUR.2029

Chen, H., Yu, S., Pan, X., Chen, Y., Zhang, T., Li, Z., Zhou, J., Hu, J., Bickerton, W. L., Lau, J. K., Guo, A., Kong, A. P. H., & Rotshtein, P. (2023). The Cognitive Makeup of Writing: Multivariate Analysis of Writing Impairments Following Stroke. *Cognitive Computation 2023 15:1*, *15*(1), 220–237. https://doi.org/10.1007/S12559-023-10111-0

Chen, Q., Zhong, T., Liu, J., Yan, D., & Gao, H. (2026). Dynamic reorganization of functional connectome gradients reveals time-specific recovery patterns after stroke. *NeuroImage*, *325*(18), 121653. https://doi.org/10.1016/j.neuroimage.2025.121653

Chen, X., Chen, L., Zheng, S., Wang, H., Dai, Y., Chen, Z., & Huang, R. (2021). Disrupted Brain Connectivity Networks in Aphasia Revealed by Resting-State fMRI. Frontiers in Aging Neuroscience, 13, 666301. https://doi.org/10.3389/FNAGI.2021.666301/BIBTEX

Chiou, R., & Lambon Ralph, M. A. (2016). The anterior temporal cortex is a primary semantic source of top-down influences on object recognition. Cortex; a Journal Devoted to the Study of the Nervous System and Behavior, 79, 75. https://doi.org/10.1016/J.CORTEX.2016.03.007

Chiou, R., Humphreys, G. F., Jung, J. Y., & Lambon Ralph, M. A. (2018). Controlled semantic cognition relies upon dynamic and flexible interactions between the executive 'semantic control' and hub-and-spoke 'semantic representation' systems. Cortex, 103, 100–116. https://doi.org/10.1016/J.CORTEX.2018.02.018

Chiou, R., Jefferies, E., Duncan, J., Humphreys, G. F., & Lambon Ralph, M. A. (2022). A middle ground where executive control meets semantics: the neural substrates of semantic control are topographically sandwiched between the multiple-demand and default-mode systems. *Cerebral Cortex (New York, NY)*, *33*(8), 4512. https://doi.org/10.1093/CERCOR/BHAC358

Chiou, R., Jefferies, E., Duncan, J., Humphreys, G. F., & Lambon Ralph, M. A. (2023). A middle ground where executive control meets semantics: the neural substrates of semantic control are topographically sandwiched between the multiple-demand and default-mode systems. Cerebral Cortex, 33(8), 4512–4526. https://doi.org/10.1093/CERCOR/BHAC358

Christidi, F., Orgianelis, I., Merkouris, E., Koutsokostas, C., Tsiptsios, D., Karavasilis, E., Psatha, E. A., Tsiakiri, A., Serdari, A., Aggelousis, N., & Vadikolias, K. (2024). A Comprehensive Review on the Role of Resting-State Functional Magnetic Resonance Imaging in Predicting Post-Stroke Motor and Sensory Outcomes. *Neurology International*, *16*(1), 189–201. https://doi.org/10.3390/NEUROLINT16010012/S1

Cohen, A. L., Soussand, L., Corrow, S. L., Martinaud, O., Barton, J. J. S., & Fox, M. D. (2019). Looking beyond the face area: lesion network mapping of prosopagnosia. Brain, 142(12), 3975. https://doi.org/10.1093/BRAIN/AWZ332

Cohen, Y. E., & Andersen, R. A. (2004). Multimodal Spatial Representations in the Primate Parietal Lobe. *Crossmodal Space and Crossmodal Attention*. https://doi.org/10.1093/acprof:oso/9780198524861.003.0005

Cole, M. W., Reynolds, J. R., Power, J. D., Repovs, G., Anticevic, A., & Braver, T. S. (2013). Multi-task connectivity reveals flexible hubs for adaptive task control. *Nature Neuroscience 2013 16:9*, *16*(9), 1348–1355. https://doi.org/10.1038/nn.3470

Cookson, S. L., & D'Esposito, M. (2022). Evaluating the reliability, validity, and utility of overlapping networks: Implications for network theories of cognition. *Human Brain Mapping*, *44*(3), 1030. https://doi.org/10.1002/hbm.26134

Corbett, F., Jefferies, E., & Lambon Ralph, M. A. (2009). Exploring multimodal semantic control impairments in semantic aphasia: Evidence from naturalistic object use. Neuropsychologia, 47(13), 2721–2731. https://doi.org/10.1016/J.NEUROPSYCHOLOGIA.2009.05.020

Corbett, F., Jefferies, E., Ehsan, S., & Ralph, M. A. L. (2009). Different impairments of semantic cognition in semantic dementia and semantic aphasia: evidence from the non-verbal domain. *Brain*, *132*(9), 2593. https://doi.org/10.1093/BRAIN/AWP146

Corbett, F., Jefferies, E., & Lambon Ralph, M. A. (2011). Deregulated Semantic Cognition Follows Prefrontal and Temporo-parietal Damage: Evidence from the Impact of Task Constraint on Nonverbal Object Use. Journal of Cognitive Neuroscience, 23(5), 1125–1135. https://doi.org/10.1162/JOCN.2010.21539

Corbetta, M., & Shulman, G. L. (2011). SPATIAL NEGLECT AND ATTENTION NETWORKS. *Annual Review of Neuroscience*, *34*, 569. https://doi.org/10.1146/annurev-neuro-061010-113731

Corbetta, M. (2012). Functional connectivity and neurological recovery. Developmental Psychobiology, 54(3), 239–253. https://doi.org/10.1002/DEV.20507

Corbetta, M., Ramsey, L., Callejas, A., Baldassarre, A., Hacker, C. D., Siegel, J. S., Astafiev, S. V., Rengachary, J., Zinn, K., Lang, C. E., Connor, L. T., Fucetola, R., Strube, M., Carter, A. R., & Shulman, G. L. (2015). Common behavioral clusters and subcortical anatomy in stroke. *Neuron*, *85*(5), 927–941. https://doi.org/10.1016/j.neuron.2015.02.027

Corbetta, M., Siegel, J. S., & Shulman, G. L. (2018). On the low dimensionality of behavioral deficits and alterations of brain network connectivity after focal injury. *Cortex*, *107*(4), 229–237. https://doi.org/10.1016/j.cortex.2017.12.017

Craddock, R. C., James, G. A., Holtzheimer, P. E., Hu, X. P., & Mayberg, H. S. (2011). A whole brain fMRI atlas generated via spatially constrained spectral clustering. *Human Brain Mapping*, *33*(8), 10.1002/hbm.21333. https://doi.org/10.1002/HBM.21333

Crinion, J., & Price, C. J. (2005). Right anterior superior temporal activation predicts auditory sentence comprehension following aphasic stroke. *Brain : A Journal of Neurology*, *128*(Pt 12), 2858–2871. https://doi.org/10.1093/brain/awh659

Cui, F., Zhao, L., Lu, M., Liu, R., Lv, Q., Lin, D., Li, K., Zhang, Y., Wang, Y., Wang, Y., Wang, L., Tan, Z., Tu, Y., & Zou, Y. (2023). Functional and structural brain reorganization in patients with ischemic stroke: a multimodality MRI fusion study. *Cerebral Cortex*, *33*(19), 10453–10462. https://doi.org/10.1093/cercor/bhad295

Dahms, C., Noll, A., Wagner, F., Schmidt, A., Brodoehl, S., & Klingner, C. M. (2024). Connecting the dots: Motor and default mode network crossroads in post-stroke motor learning deficits. *NeuroImage : Clinical*, *42*, 103601. https://doi.org/10.1016/j.nicl.2024.103601

Das, A., & Menon, V. (2024). Electrophysiological dynamics of salience, default mode, and frontoparietal networks during episodic memory formation and recall revealed through multi-experiment iEEG replication. *ELife*, *13*, RP99018. https://doi.org/10.7554/ELIFE.99018

Davey, J., Rueschemeyer, S. A., Costigan, A., Murphy, N., Krieger-Redwood, K., Hallam, G., & Jefferies, E. (2015). Shared neural processes support semantic control and action understanding. Brain and Language, 142, 24. https://doi.org/10.1016/J.BANDL.2015.01.002

Davey, J., Thompson, H. E., Hallam, G., Karapanagiotidis, T., Murphy, C., De Caso, I., Krieger-Redwood, K., Bernhardt, B. C., Smallwood, J., & Jefferies, E. (2016). Exploring the role of the posterior middle temporal gyrus in semantic cognition: Integration of anterior temporal lobe with executive processes. Neuroimage, 137, 165. https://doi.org/10.1016/J.NEUROIMAGE

de Reus, M. A., & van den Heuvel, M. P. (2013). The parcellation-based connectome: Limitations and extensions. *NeuroImage*, *80*, 397–404. https://doi.org/10.1016/j.neuroimage.2013.03.053

De Rosa, A. P., d'Ambrosio, A., Bisecco, A., Altieri, M., Cirillo, M., Gallo, A., & Esposito, F. (2024). Functional gradients reveal cortical hierarchy changes in multiple sclerosis. *Human Brain Mapping*, *45*(6), e26678. https://doi.org/10.1002/hbm.26678

Deco, G., Ponce-Alvarez, A., Hagmann, P., Romani, G. L., Mantini, D., & Corbetta, M. (2014). How Local Excitation–Inhibition Ratio Impacts the Whole Brain Dynamics. *Journal of Neuroscience*, *34*(23), 7886–7898. https://doi.org/10.1523/JNEUROSCI.5068-13.2014

Demirtaş, M., Burt, J. B., Helmer, M., Ji, J. L., Adkinson, B. D., Glasser, M. F., Van Essen, D. C., Sotiropoulos, S. N., Anticevic, A., & Murray, J. D. (2019). Hierarchical Heterogeneity across Human Cortex Shapes Large-Scale Neural Dynamics. *Neuron*, *101*(6), 1181-1194.e13. https://doi.org/10.1016/J.NEURON.2019.01.017

den Ouden, D. B., Malyutina, S., Basilakos, A., Bonilha, L., Gleichgerrcht, E., Yourganov, G., Hillis, A. E., Hickok, G., Rorden, C., & Fridriksson, J. (2019). Cortical and structural-connectivity damage correlated with impaired syntactic processing in aphasia. *Human Brain Mapping*, *40*(7), 2153. https://doi.org/10.1002/hbm.24514

Desai, R. H., Binder, J. R., Conant, L. L., & Seidenberg, M. S. (2009). Activation of Sensory–Motor Areas in Sentence Comprehension. *Cerebral Cortex (New York, NY)*, *20*(2), 468. https://doi.org/10.1093/cercor/bhp115

Desai, R., Liebenthal, E., Waldron, E., & Binder, J. R. (2008). Left Posterior Temporal Regions are Sensitive to Auditory Categorization. Journal of Cognitive Neuroscience, 20(7), 1174. https://doi.org/10.1162/JOCN.2008.20081

Dijkhuizen, R. M., van der Marel, K., Otte, W. M., Hoff, E. I., van der Zijden, J. P., van der Toorn, A., & van Meer, M. P. A. (2012). Functional MRI and Diffusion Tensor Imaging of Brain Reorganization After Experimental Stroke. *Translational Stroke Research 2012 3:1*, *3*(1), 36–43. https://doi.org/10.1007/s12975-011-0143-8

Dimyan, M. A., & Cohen, L. G. (2011). Neuroplasticity in the context of motor rehabilitation after stroke. *Nature Reviews Neurology 2011 7:2*, *7*(2), 76–85. https://doi.org/10.1038/nrneurol.2010.200

Ding, J., Thye, M., Edmondson-Stait, A. J., Szaflarski, J. P., & Mirman, D. (2024). Metric comparison of connectome-based lesion-symptom mapping in post-stroke aphasia. *Brain Communications*, *6*(5). https://doi.org/10.1093/braincomms/fcae313

Ding, L., Liu, H., Jing, J., Jiang, Y., Meng, X., Chen, Y., Zhao, X., Niu, H., Liu, T., Wang, Y., & Li, Z. (2023). Lesion Network Mapping for Neurological Deficit in Acute Ischemic Stroke. Annals of Neurology, 94(3), 572–584. https://doi.org/10.1002/ANA.26721

Dipasquale, O., & Cercignani, M. (2017). Network functional connectivity and whole-brain functional connectomics to investigate cognitive decline in neurodegenerative conditions. *Functional Neurology*, *31*(4), 191. https://doi.org/10.11138/FNEUR/2016.31.4.191

Diveica, V., Koldewyn, K., & Binney, R. J. (2021). Establishing a role of the semantic control network in social cognitive processing: A meta-analysis of functional neuroimaging studies. NeuroImage, 245, 118702. https://doi.org/10.1016/J.NEUROIMAGE.2021.118702

Diveica, V., Riedel, M. C., Salo, T., Laird, A. R., Jackson, R. L., & Binney, R. J. (2023). Graded functional organization in the left inferior frontal gyrus: evidence from task-free and task-based functional connectivity. *Cerebral Cortex (New York, NY)*, *33*(23), 11384. https://doi.org/10.1093/CERCOR/BHAD373

Dixon, M. L., De La Vega, A., Mills, C., Andrews-Hanna, J., Spreng, R. N., Cole, M. W., & Christoff, K. (2018). Heterogeneity within the frontoparietal control network and its relationship to the default and dorsal attention networks. *Proceedings of the National Academy of Sciences of the United States of America*, *115*(7), E1598–E1607. https://doi.org/10.1073/PNAS.1715766115/-/DCSUPPLEMENTAL

Dohmatob, E., Richard, H., Pinho, A. L., & Thirion, B. (2021). Brain topography beyond parcellations: Local gradients of functional maps. *NeuroImage*, *229*, 117706. https://doi.org/10.1016/J.NEUROIMAGE.2020.117706

Domin, M., Hordacre, B., Hok, P., Boyd, L. A., Conforto, A. B., Andrushko, J. W., Borich, M. R., Craddock, R. C., Donnelly, M. R., Dula, A. N., Warach, S. J., Kautz, S. A., Lo, B. P., Schranz, C., Seo, N. J., Srivastava, S., Wong, K. A., Zavaliangos-Petropulu, A., Thompson, P. M., … Lotze, M. (2023). White Matter Integrity and Chronic Poststroke Upper Limb Function: An ENIGMA Stroke Recovery Analysis. *Stroke*, *54*(9), 2438–2441. https://doi.org/10.1161/STROKEAHA.123.043713

Domin, M., Liew, S. L., Hordacre, B., Boyd, L. A., Conforto, A. B., Andrushko, J. W., Borich, M. R., Craddock, R. C., Donnelly, M. R., Dula, A. N., Warach, S. J., Kautz, S. A., Tavenner, B. P., Seo, N. J., Srivastava, S., Wong, K. A., Zavaliangos-Petropulu, A., Thompson, P. M., & Lotze, M. (2025). Comparison of post-stroke white matter assessment using disconnectome-symptom mapping versus quantitative diffusion MRI. *NeuroImage*, *317*(5), 121347. https://doi.org/10.1016/j.neuroimage.2025.121347

Doricchi, F., Thiebaut de Schotten, M., Tomaiuolo, F., & Bartolomeo, P. (2008). White matter (dis)connections and gray matter (dys)functions in visual neglect: Gaining insights into the brain networks of spatial awareness. Cortex, 44(8), 983–995. https://doi.org/10.1016/j.cortex.2008.03.006

Dreyer, F. R., Doppelbauer, L., Büscher, V., Arndt, V., Stahl, B., Lucchese, G., Hauk, O., Mohr, B., & Pulvermüller, F. (2020). Increased Recruitment of Domain-General Neural Networks in Language Processing Following Intensive Language-Action Therapy: fMRI Evidence From People With Chronic Aphasia. *American Journal of Speech-Language Pathology*, *30*(1 Suppl), 455. https://doi.org/10.1044/2020_AJSLP-19-00150

Duncan, J., & Owen, A. M. (2000). Common regions of the human frontal lobe recruited by diverse cognitive demands. Trends in Neurosciences, 23(10), 475–483. https://doi.org/10.1016/S0166-2236(00)01633-7

Duncan, J. (2010). The multiple-demand (MD) system of the primate brain: mental programs for intelligent behaviour. *Trends in Cognitive Sciences*, *14*(4), 172–179. https://doi.org/10.1016/j.tics.2010.01.004

Edelman, G. M. ., & Mountcastle, V. B. . (19821978). *The mindful brain : cortical organization and the group-selective theory of higher brain function*. 100.

Eickhoff, S. B., Constable, R. T., & Yeo, B. T. T. (2018). Topographic organization of the cerebral cortex and brain cartography. *NeuroImage*, *170*, 332–347. https://doi.org/10.1016/j.neuroimage.2017.02.018

Einstad, M. S., Saltvedt, I., Lydersen, S., Ursin, M. H., Munthe-Kaas, R., Ihle-Hansen, H., Knapskog, A. B., Askim, T., Beyer, M. K., Næss, H., Seljeseth, Y. M., Ellekjær, H., & Thingstad, P. (2021). Associations between post-stroke motor and cognitive function: a cross-sectional study. *BMC Geriatrics*, *21*(1), 103. https://doi.org/10.1186/s12877-021-02055-7

Eisenhauer, S., Zhang, M., Krieger-Redwood, K., Aveyard, R., Jackson, R. L., Cornelissen, P. L., Smallwood, J., & Jefferies, E. (2026). Controlled Retrieval Relies on Directed Interactions between Semantic Control Regions and Visual Cortex: MEG Evidence from Oscillatory Dynamics. *Journal of Neuroscience*, *46*(11), 271252026. https://doi.org/10.1523/JNEUROSCI.0271-25.2026

Ekert, J. O., Lorca-Puls, D. L., Gajardo-Vidal, A., Crinion, J. T., Hope, T. M. H., Green, D. W., & Price, C. J. (2021). A functional dissociation of the left frontal regions that contribute to single word production tasks. *NeuroImage*, *245*. https://doi.org/10.1016/j.neuroimage.2021.118734

Element wise Operations | EN 1.0.0-M2.1 | Deeplearning4j. (n.d.). Retrieved March 31, 2024, from https://deeplearning4j.konduit.ai/nd4j/how-to-guides/element-wise-operations

Embrechts, E., Van Criekinge, T., Schröder, J., Nijboer, T., Lafosse, C., Truijen, S., & Saeys, W. (2021). The association between visuospatial neglect and balance and mobility post-stroke onset: A systematic review. *Annals of Physical and Rehabilitation Medicine*, *64*(4), 101449. https://doi.org/10.1016/j.rehab.2020.10.003

Emch, M., von Bastian, C. C., & Koch, K. (2019). Neural correlates of verbal working memory: An fMRI meta-analysis. *Frontiers in Human Neuroscience*, *13*, 180. https://doi.org/10.3389/FNHUM.2019.00180/FULL

Esser, F., Paul, T., Rizor, E., Binder, E., Hensel, L., Rehme, A. K., Ringmaier, C., Schönberger, A., Tscherpel, C., Vossel, S., Garcea, F. E., Grefkes, C., Fink, G. R., Grafton, S. T., & Volz, L. J. (2025). Distinct Disconnection Patterns Explain Task-Specific Motor Impairment and Outcome After Stroke. *Stroke*, *56*(8), 2210–2221. https://doi.org/10.1161/STROKEAHA.125.050929

Falaschi, D., Stagg, C., & Sel, A. (2025). Promoting motor recovery after stroke using cortico-cortical paired associative stimulation. *EClinicalMedicine*, *88*, 103473. https://doi.org/10.1016/j.eclinm.2025.103473

Falconer, I., Varkanitsa, M., & Kiran, S. (2024). Resting-state brain network connectivity is an independent predictor of responsiveness to language therapy in chronic post-stroke aphasia. Cortex, 173, 296–312. https://doi.org/10.1016/J.CORTEX.2023.11.022

Fan, Y. T., Wu, C. Y., Liu, H. L., Lin, K. C., Wai, Y. Y., & Chen, Y. L. (2015). Neuroplastic changes in resting-state functional connectivity after stroke rehabilitation. *Frontiers in Human Neuroscience*, *9*(OCT), 148968. https://doi.org/10.3389/FNHUM.2015.00546/TEXT

Fang, Y., Chao, X., Lu, Z., Huang, H., Shi, R., Yin, D., Chen, H., Lu, Y., Wang, J., Wang, P., Liu, X., & Sun, W. (2025). Mechanisms underlying the spontaneous reorganization of depression network after stroke. *NeuroImage: Clinical*, *45*, 103723. https://doi.org/10.1016/J.NICL.2024.103723

Faria, A. V., Joel, S. E., Zhang, Y., Oishi, K., van Zjil, P. C. M., Miller, M. I., Pekar, J. J., & Mori, S. (2012). Atlas-Based Analysis of Resting-State Functional Connectivity: Evaluation for Reproducibility and Multi-Modal Anatomy-Function Correlation Studies. *Neuroimage*, *61*(3), 613. https://doi.org/10.1016/J.NEUROIMAGE.2012.03.078

Fedorenko, E., & Thompson-Schill, S. L. (2014). Reworking the language network. *Trends in Cognitive Sciences*, *18*(3), 120–126. https://doi.org/10.1016/J.TICS.2013.12.006

Fedorenko, E., Duncan, J., & Kanwisher, N. (2013). Broad domain generality in focal regions of frontal and parietal cortex. *Proceedings of the National Academy of Sciences of the United States of America*, *110*(41), 16616–16621. https://doi.org/10.1073/pnas.1315235110

Feng, W., Wang, J., Chhatbar, P. Y., Doughty, C., Landsittel, D., Lioutas, V. A., Kautz, S. A., & Schlaug, G. (2015). Corticospinal Tract Lesion Load - A Potential Imaging Biomarker for Stroke Motor Outcomes. Annals of Neurology, 78(6), 860. https://doi.org/10.1002/ANA.24510

Fernández, G., Heitkemper, P., Grunwald, T., Van Roost, D., Urbach, H., Pezer, N., Lehnertz, K., & Elger, C. E. (2001). Inferior temporal stream for word processing with integrated mnemonic function. Human Brain Mapping, 14(4), 251. https://doi.org/10.1002/HBM.1057

Fernandino, L., & Binder, J. R. (2024). How Does the "Default Mode" Network Contribute to Semantic Cognition? *Brain and Language*, *252*, 105405. https://doi.org/10.1016/J.BANDL.2024.105405

Filippi, M., Bar-Or, A., Piehl, F., Preziosa, P., Solari, A., Vukusic, S., & Rocca, M. A. (2018). Multiple sclerosis. *Nature Reviews. Disease Primers*, *4*(1). https://doi.org/10.1038/s41572-018-0041-4

Finger, S. (2009). Chapter 51 Recovery of function: Redundancy and vicariation theories. *Handbook of Clinical Neurology*, *95*(C), 833–841. https://doi.org/10.1016/S0072-9752(08)02151-9

Flinker, A., Korzeniewska, A., Shestyuk, A. Y., Franaszczuk, P. J., Dronkers, N. F., Knight, R. T., & Crone, N. E. (2015). Redefining the role of Broca's area in speech. Proceedings of the National Academy of Sciences, 112(9), 2871–2875. https://doi.org/10.1073/PNAS.1414491112

Forkel, S. J., & Catani, M. (2018). Lesion mapping in acute stroke aphasia and its implications for recovery. Neuropsychologia, 115, 88. https://doi.org/10.1016/J.NEUROPSYCHOLOGIA.2018.03.036

Fox, M. D. (2018). Mapping Symptoms to Brain Networks with the Human Connectome. *New England Journal of Medicine*, *379*(23), 2237–2245. https://doi.org/10.1056/nejmra1706158

Fox, M. D., & Raichle, M. E. (2007). Spontaneous fluctuations in brain activity observed with functional magnetic resonance imaging. *Nature Reviews Neuroscience 2007 8:9*, *8*(9), 700–711. https://doi.org/10.1038/nrn2201

Freire, I. S., Lopes, T. S., Afonso, S. G., & Pereira, D. J. (2024). From images to insights: a neuroradiologist's practical guide on white matter fiber tract anatomy and DTI patterns for pre-surgical planning. *Neuroradiology 2024 66:8*, *66*(8), 1251–1265. https://doi.org/10.1007/s00234-024-03362-7

Frías, I., Starrs, F., Gisiger, T., Minuk, J., Thiel, A., & Paquette, C. (2018). Interhemispheric connectivity of primary sensory cortex is associated with motor impairment after stroke. Scientific Reports 2018 8:1, 8(1), 12601-. https://doi.org/10.1038/s41598-018-29751-6

Fridman, E. A., Hanakawa, T., Chung, M., Hummel, F., Leiguarda, R. C., & Cohen, L. G. (2004). Reorganization of the human ipsilesional premotor cortex after stroke. *Brain*, *127*(4), 747–758. https://doi.org/10.1093/brain/awh082

Fridriksson, J., Hubbard, H. I., Hudspeth, S. G., Holland, A. L., Bonilha, L., Fromm, D., & Rorden, C. (2012). Speech entrainment enables patients with Broca's aphasia to produce fluent speech. Brain, 135(12), 3815–3829. https://doi.org/10.1093/BRAIN/AWS301

Fridriksson, J., Den Ouden, D. B., Hillis, A. E., Hickok, G., Rorden, C., Basilakos, A., Yourganov, G., & Bonilha, L. (2018). Anatomy of aphasia revisited. Brain, 141(3), 848–862. https://doi.org/10.1093/BRAIN/AWX363

Friston, K. J. (2011). Functional and effective connectivity: a review. *Brain Connectivity*, *1*(1), 13–36. https://doi.org/10.1089/BRAIN.2011.0008

Fruhwirth, V., Berger, L., Gattringer, T., Fandler-Höfler, S., Kneihsl, M., Eppinger, S., Ropele, S., Fink, A., Deutschmann, H., Reishofer, G., Enzinger, C., & Pinter, D. (2024). White matter integrity and functional connectivity of the default mode network in acute stroke are associated with cognitive outcome three months post-stroke. *Journal of the Neurological Sciences*, *462*(1), 123071. https://doi.org/10.1016/j.jns.2024.123071

Funahashi, S., & Andreau, J. M. (2013). Prefrontal cortex and neural mechanisms of executive function. *Journal of Physiology-Paris*, *107*(6), 471–482. https://doi.org/10.1016/J.JPHYSPARIS.2013.05.001

Gajardo-Vidal, A., Lorca-Puls, D. L., Hope, T. M. H., Parker Jones, O., Seghier, M. L., Prejawa, S., Crinion, J. T., Leff, A. P., Green, D. W., & Price, C. J. (2018). How right hemisphere damage after stroke can impair speech comprehension. *Brain*, *141*(12), 3389–3404. https://doi.org/10.1093/brain/awy270

Gajardo-Vidal, A., Lorca-Puls, D. L., Warner, H., Pshdary, B., Crinion, J. T., Leff, A. P., Hope, T. M. H., Geva, S., Seghier, M. L., Green, D. W., Bowman, H., & Price, C. J. (2021). Damage to Broca's area does not contribute to long-term speech production outcome after stroke. Brain, 144(3), 817–832. https://doi.org/10.1093/BRAIN/AWAA460

Gallos, L. K., Makse, H. A., & Sigman, M. (2012). A small world of weak ties provides optimal global integration of self-similar modules in functional brain networks. *Proceedings of the National Academy of Sciences of the United States of America*, *109*(8), 2825–2830. https://doi.org/10.1073/PNAS.1106612109

Gao, Z., Zheng, L., Chiou, R., Gouws, A., Krieger-Redwood, K., Wang, X., Varga, D., Ralph, M. A. L., Smallwood, J., & Jefferies, E. (2021). Distinct and common neural coding of semantic and non-semantic control demands. Neuroimage, 236, 118230. https://doi.org/10.1016/J.NEUROIMAGE.2021.118230

Gao, Z., Zheng, L., Krieger-Redwood, K., Halai, A., Margulies, D. S., Smallwood, J., & Jefferies, E. (2022). Flexing the principal gradient of the cerebral cortex to suit changing semantic task demands. *ELife*, *11*. https://doi.org/10.7554/eLife.80368

Garrett, D. D., Epp, S. M., Perry, A., & Lindenberger, U. (2018). Local temporal variability reflects functional integration in the human brain. *NeuroImage*, *183*, 776–787. https://doi.org/10.1016/J.NEUROIMAGE.2018.08.019

Gennari, S. P., Millman, R. E., Hymers, M., & Mattys, S. L. (2018). Anterior paracingulate and cingulate cortex mediates the effects of cognitive load on speech sound discrimination. *NeuroImage*, *178*(8), 735–743. https://doi.org/10.1016/j.neuroimage.2018.06.035

Geranmayeh, F., Brownsett, S. L. E., & Wise, R. J. S. (2014). Task-induced brain activity in aphasic stroke patients: what is driving recovery? *Brain : A Journal of Neurology*, *137*(Pt 10), 2632–2648. https://doi.org/10.1093/BRAIN/AWU163

Geranmayeh, F., Leech, R., & Wise, R. J. S. (2016). Network dysfunction predicts speech production after left hemisphere stroke. *Neurology*, *86*(14), 1296. https://doi.org/10.1212/WNL.0000000000002537

Gerloff, C., & Hallett, M. (2010). Big news from small world networks after stroke. *Brain*, *133*(4), 952–955. https://doi.org/10.1093/BRAIN/AWQ062

Geva, S., Baron, J. C., Jones, P. S., Price, C. J., & Warburton, E. A. (2012). A comparison of VLSM and VBM in a cohort of patients with post-stroke aphasia. *NeuroImage: Clinical*, *1*(1), 37–47. https://doi.org/10.1016/J.NICL.2012.08.003

Glasser, M. F., Coalson, T. S., Robinson, E. C., Hacker, C. D., Harwell, J., Yacoub, E., Ugurbil, K., Andersson, J., Beckmann, C. F., Jenkinson, M., Smith, S. M., & Van Essen, D. C. (2016). A multi-modal parcellation of human cerebral cortex. *Nature*, *536*(7615), 171–178. https://doi.org/10.1038/NATURE18933

Godbout, L., Grenier, M. C., Braun, C. M. J., & Gagnon, S. (2005). Cognitive structure of executive deficits in patients with frontal lesions performing activities of daily living. *Brain Injury*, *19*(5), 337–348. https://doi.org/10.1080/02699050400005093

Gonzalez Alam, T. R. del J., Mckeown, B. L. A., Gao, Z., Bernhardt, B., Vos de Wael, R., Margulies, D. S., Smallwood, J., & Jefferies, E. (2021). A tale of two gradients: differences between the left and right hemispheres predict semantic cognition. Brain Structure and Function 2021 227:2, 227(2), 631–654. https://doi.org/10.1007/S00429-021-02374-W

Goodale, M. A., Westwood, D. A., & Milner, A. D. (2004). Two distinct modes of control for object-directed action. Progress in Brain Research, 144, 131–144. https://doi.org/10.1016/S0079-6123(03)14409-3

Goodall, C. (1991). Procrustes Methods in the Statistical Analysis of Shape. Journal of the Royal Statistical Society: Series B (Methodological), 53(2), 285–321. https://doi.org/10.1111/J.2517-6161.1991.TB01825.X

Gordon, E. M., Laumann, T. O., Adeyemo, B., Huckins, J. F., Kelley, W. M., & Petersen, S. E. (2016). Generation and Evaluation of a Cortical Area Parcellation from Resting-State Correlations. *Cerebral Cortex (New York, N.Y. : 1991)*, *26*(1), 288–303. https://doi.org/10.1093/CERCOR/BHU239

Gordon, E. M., Laumann, T. O., Marek, S., Raut, R. V., Gratton, C., Newbold, D. J., Greene, D. J., Coalson, R. S., Snyder, A. Z., Schlaggar, B. L., Petersen, S. E., Dosenbach, N. U. F., & Nelson, S. M. (2020). Default-mode network streams for coupling to language and control systems. *Proceedings of the National Academy of Sciences*, *117*(29), 17308–17319. https://doi.org/10.1073/PNAS.2005238117

Gordon, E. M., Lynch, C. J., Gratton, C., Laumann, T. O., Gilmore, A. W., Greene, D. J., Ortega, M., Nguyen, A. L., Schlaggar, B. L., Petersen, S. E., Dosenbach, N. U. F., & Nelson, S. M. (2018). Three Distinct Sets of Connector Hubs Integrate Human Brain Function. *Cell Reports*, *24*(7), 1687-1695.e4. https://doi.org/10.1016/J.CELREP.2018.07.050

Gratton, C., Nomura, E. M., Pérez, F., & D'Esposito, M. (2012). Focal Brain Lesions to Critical Locations Cause Widespread Disruption of the Modular Organization of the Brain. Journal of Cognitive Neuroscience, 24(6), 1275. https://doi.org/10.1162/JOCN_A_00222

Gratton, C., Sun, H., & Petersen, S. E. (2017). Control Networks and Hubs. *Psychophysiology*, *55*(3), 10.1111/psyp.13032. https://doi.org/10.1111/PSYP.13032

Greene, D. J., Marek, S., Gordon, E. M., Siegel, J. S., Gratton, C., Laumann, T. O., Gilmore, A. W., Berg, J. J., Nguyen, A. L., Dierker, D., Van, A. N., Ortega, M., Newbold, D. J., Hampton, J. M., Nielsen, A. N., McDermott, K. B., Roland, J. L., Norris, S. A., Nelson, S. M., … Dosenbach, N. U. F. (2020a). Integrative and Network-Specific Connectivity of the Basal Ganglia and Thalamus Defined in Individuals. *Neuron*, *105*(4), 742-758.e6. https://doi.org/10.1016/J.NEURON.2019.11.012

Grefkes, C., & Fink, G. R. (2011). Reorganization of cerebral networks after stroke: new insights from neuroimaging with connectivity approaches. *Brain : A Journal of Neurology*, *134*(Pt 5), 1264–1276. https://doi.org/10.1093/BRAIN/AWR033

Grefkes, C., Grefkes, C., Fink, G. R., & Fink, G. R. (2020). Recovery from stroke: current concepts and future perspectives. *Neurological Research and Practice*, *2*(1), 17. https://doi.org/10.1186/S42466-020-00060-6

Griffis, J. C., Metcalf, N. V., Corbetta, M., & Shulman, G. L. (2019). Structural Disconnections Explain Brain Network Dysfunction after Stroke. *Cell Reports*, *28*(10), 2527-2540.e9. https://doi.org/10.1016/J.CELREP.2019.07.100

Griffis, J. C., Metcalf, N. V., Corbetta, M., & Shulman, G. L. (2020). Damage to the shortest structural paths between brain regions is associated with disruptions of resting-state functional connectivity after stroke. *NeuroImage*, *210*. https://doi.org/10.1016/j.neuroimage.2020.116589

Guggisberg, A. G., Koch, P. J., Hummel, F. C., & Buetefisch, C. M. (2019). Brain networks and their relevance for stroke rehabilitation. Clinical Neurophysiology : Official Journal of the International Federation of Clinical Neurophysiology, 130(7), 1098. https://doi.org/10.1016/J.CLINPH.2019.04.004

Hagoort, P. (2013). MUC (Memory, Unification, Control) and beyond. *Frontiers in Psychology*, *4*(JUL), 416. https://doi.org/10.3389/FPSYG.2013.00416

Hagoort, P. (2014). Nodes and networks in the neural architecture for language: Broca's region and beyond. *Current Opinion in Neurobiology*, *28*, 136–141. https://doi.org/10.1016/j.conb.2014.07.013

Hahn, A., Lanzenberger, R., & Kasper, S. (2018). Making Sense of Connectivity. *International Journal of Neuropsychopharmacology*, *22*(3), 194. https://doi.org/10.1093/IJNP/PYY100

Halai, A. D., Woollams, A. M., & Lambon Ralph, M. A. (2017). Using principal component analysis to capture individual differences within a unified neuropsychological model of chronic post-stroke aphasia: Revealing the unique neural correlates of speech fluency, phonology and semantics. Cortex; a Journal Devoted to the Study of the Nervous System and Behavior, 86, 275. https://doi.org/10.1016/J.CORTEX.2016.04.016

Hallam, G. P., Thompson, H. E., Hymers, M., Millman, R. E., Rodd, J. M., Lambon Ralph, M. A., Smallwood, J., & Jefferies, E. (2018). Task-based and resting-state fMRI reveal compensatory network changes following damage to left inferior frontal gyrus. *Cortex*, *99*, 150–165. https://doi.org/10.1016/J.CORTEX.2017.10.004

Hallam, G. P., Whitney, C., Hymers, M., Gouws, A. D., & Jefferies, E. (2016). Charting the effects of TMS with fMRI: Modulation of cortical recruitment within the distributed network supporting semantic control. *Neuropsychologia*, *93*(Pt A), 40–52. https://doi.org/10.1016/j.neuropsychologia.2016.09.012

Hamker, F. H., Baladron, J., & Janssen, L. K. (2025). Interacting cortico-basal ganglia-thalamocortical loops shape behavioral control through cognitive maps and shortcuts. *Trends in Neurosciences*, *48*(11), 841–852. https://doi.org/10.1016/J.TINS.2025.09.006

Han, L., Ke, J., Zhang, D., Ni, B., Tao, Y., Zhou, Q., Zhu, H., & Fang, Q. (2023). Altered functional connectivity in language and non-language brain networks in patients diagnosed with acute

post-stroke aphasia. Clinical Neurology and Neurosurgery, 235, 108044. https://doi.org/10.1016/J.CLINEURO.2023.108044

Hannan, J., Wilmskoetter, J., Fridriksson, J., Hillis, A. E., Bonilha, L., & Busby, N. (2023). Brain health imaging markers, post-stroke aphasia and Cognition: A scoping review. NeuroImage. Clinical, 39. https://doi.org/10.1016/J.NICL.2023.103480

Hartwigsen, G., Price, C. J., Baumgaertner, A., Geiss, G., Koehnke, M., Ulmer, S., & Siebner, H. R. (2010). The right posterior inferior frontal gyrus contributes to phonological word decisions in the healthy brain: Evidence from dual-site TMS. *Neuropsychologia*, *48*(10), 3155–3163. https://doi.org/10.1016/j.neuropsychologia.2010.06.032

Harvey, D. Y., Mass, J. A., Shah-Basak, P. P., Wurzman, R., Faseyitan, O., Sacchetti, D. L., DeLoretta, L., & Hamilton, R. H. (2019). Continuous theta burst stimulation over right pars triangularis facilitates naming abilities in chronic post-stroke aphasia by enhancing phonological access. *Brain and Language*, *192*, 25. https://doi.org/10.1016/J.BANDL.2019.02.005

He, Y., Li, Q., Fu, Z., Zeng, D., Han, Y., & Li, S. (2023). Functional gradients reveal altered functional segregation in patients with amnestic mild cognitive impairment and Alzheimer's disease. *Cerebral Cortex*, *33*(21), 10836–10847. https://doi.org/10.1093/cercor/bhad328

He, Y., Wang, J., Wang, L., Chen, Z. J., Yan, C., Yang, H., Tang, H., Zhu, C., Gong, Q., Zang, Y., & Evans, A. C. (2009). Uncovering Intrinsic Modular Organization of Spontaneous Brain Activity in Humans. *PLOS ONE*, *4*(4), e5226. https://doi.org/10.1371/journal.pone.0005226

Head H (1926) Aphasia and kindred disorders of speech, vol II. Cambridge University Press, New York

Head H. Aphasia and kindred disorders of speech. London: CUP; 1926

Hearne, L. J., Cocchi, L., Zalesky, A., & Mattingley, J. B. (2017). Reconfiguration of Brain Network Architectures between Resting-State and Complexity-Dependent Cognitive Reasoning. *The Journal of Neuroscience*, *37*(35), 8399. https://doi.org/10.1523/JNEUROSCI.0485-17.2017

Hebscher, M., Barkan-Abramski, M., Goldsmith, M., Aharon-Peretz, J., & Gilboa, A. (2016). Memory, Decision-Making, and the Ventromedial Prefrontal Cortex (vmPFC): The Roles of Subcallosal and Posterior Orbitofrontal Cortices in Monitoring and Control Processes. Cerebral Cortex, 26(12), 4590–4601. https://doi.org/10.1093/CERCOR/BHV220

Heiss, W. D., & Kidwell, C. S. (2014). Imaging for Prediction of Functional Outcome and Assessment of Recovery in Ischemic Stroke. Stroke; a Journal of Cerebral Circulation, 45(4), 1195. https://doi.org/10.1161/STROKEAHA.113.003611

Heiss, W. D., & Thiel, A. (2006). A proposed regional hierarchy in recovery of post-stroke aphasia. *Brain and Language*, *98*(1), 118–123. https://doi.org/10.1016/j.bandl.2006.02.002

Herbet, G., Lafargue, G., & Duffau, H. (2015). Rethinking voxel-wise lesion-deficit analysis: A new challenge for computational neuropsychology. *Cortex*, *64*(4), 413–416. https://doi.org/10.1016/j.cortex.2014.10.021

Hertrich, I., Dietrich, S., & Ackermann, H. (2016). The role of the supplementary motor area for speech and language processing. *Neuroscience & Biobehavioral Reviews*, *68*(1), 602–610. https://doi.org/10.1016/j.neubiorev.2016.06.030

Hertrich, I., Dietrich, S., & Ackermann, H. (2020). The Margins of the Language Network in the Brain. *Frontiers in Communication*, *5*, 519955. https://doi.org/10.3389/FCOMM.2020.519955/FULL

Hickok, G. (2012). Computational neuroanatomy of speech production. *Nature Reviews. Neuroscience*, *13*(2), 135–145. https://doi.org/10.1038/NRN3158

Hickok, G., & Poeppel, D. (2007). The cortical organization of speech processing. *Nature Reviews Neuroscience*, *8*(5), 393–402. https://doi.org/10.1038/NRN2113;KWRD

Hinton, K. E., Lahey, B. B., Villalta-Gil, V., Boyd, B. D., Yvernault, B. C., Werts, K. B., Plassard, A. J., Applegate, B., Woodward, N. D., Landman, B. A., & Zald, D. H. (2018). Right Fronto-Subcortical White Matter Microstructure Predicts Cognitive Control Ability on the Go/No-go Task in a Community Sample. *Frontiers in Human Neuroscience*, *12*, 127. https://doi.org/10.3389/fnhum.2018.00127

Honey, C. J., & Sporns, O. (2008). Dynamical consequences of lesions in cortical networks. *Human Brain Mapping*, *29*(7), 802–809. https://doi.org/10.1002/hbm.20579

Hong, S. J., de Wael, R. V., Bethlehem, R. A. I., Lariviere, S., Paquola, C., Valk, S. L., Milham, M. P., Di Martino, A., Margulies, D. S., Smallwood, J., & Bernhardt, B. C. (2019). Atypical functional connectome hierarchy in autism. *Nature Communications 2019 10:1*, *10*(1), 1–13. https://doi.org/10.1038/s41467-019-08944-1

Hong, S. J., Xu, T., Nikolaidis, A., Smallwood, J., Margulies, D. S., Bernhardt, B., Vogelstein, J., & Milham, M. P. (2020). Toward a connectivity gradient-based framework for reproducible biomarker discovery. *NeuroImage*, *223*, 117322. https://doi.org/10.1016/J.NEUROIMAGE.2020.117322

Hope, T. M. H., Seghier, M. L., Leff, A. P., & Price, C. J. (2013). Predicting outcome and recovery after stroke with lesions extracted from MRI images. NeuroImage : Clinical, 2(1), 424. https://doi.org/10.1016/J.NICL.2013.03.005

Hope, T. M. H., Leff, A. P., Prejawa, S., Bruce, R., Haigh, Z., Lim, L., Ramsden, S., Oberhuber, M., Ludersdorfer, P., Crinion, J., Seghier, M. L., & Price, C. J. (2017). Right hemisphere structural adaptation and changing language skills years after left hemisphere stroke. Brain : A Journal of Neurology, 140(6), 1718–1728. https://doi.org/10.1093/BRAIN/AWX086

Hope, T. M. H., Leff, A. P., & Price, C. J. (2018). Predicting language outcomes after stroke: Is structural disconnection a useful predictor? NeuroImage: Clinical, 19, 22–29. https://doi.org/10.1016/J.NICL.2018.03.037

Hope, T. M. H., Neville, D., Talozzi, L., Foulon, C., Forkel, S. J., De Schotten, M. T., & Price, C. J. (2024). Testing the disconnectome symptom discoverer model on out-of-sample post-stroke language outcomes. Brain, 147(2), e11–e13. https://doi.org/10.1093/BRAIN/AWAD352

Hughes, R. W. (2024). The phonological store of working memory: A critique and an alternative, perceptual-motor, approach to verbal short-term memory. *Quarterly Journal of Experimental Psychology (2006)*, *78*(2), 240. https://doi.org/10.1177/17470218241257885

Huntenburg, J. M., Bazin, P. L., & Margulies, D. S. (2018). Large-Scale Gradients in Human Cortical Organization. Trends in Cognitive Sciences, 22(1), 21–31. https://doi.org/10.1016/j.tics.2017.11.002

Huo, T., Xia, Y., Zhuang, K., Chen, Q., Sun, J., Yang, W., & Qiu, J. (2022). Linking functional connectome gradient to individual creativity. *Cerebral Cortex*, *32*(23), 5273–5284. https://doi.org/10.1093/cercor/bhac013

Husain, M., & Nachev, P. (2007). Space and the parietal cortex. *Trends in Cognitive Sciences*, *11*(1), 30–36. https://doi.org/10.1016/j.tics.2006.10.011

Hwang, K., & D'esposito, M. (2022). The Thalamus in Cognitive Control. *The Thalamus*, 307–323. https://doi.org/10.1017/9781108674287.017

Iturria-Medina, Y., Sotero, R. C., Toussaint, P. J., & Evans, A. C. (2014). Epidemic Spreading Model to Characterize Misfolded Proteins Propagation in Aging and Associated Neurodegenerative Disorders. *PLOS Computational Biology*, *10*(11), e1003956. https://doi.org/10.1371/JOURNAL.PCBI.1003956

J. N. M. Drost, B., Sharma, V., & Tiesinga, P. (2025). From computational models to clinical practice: Whole brain modelling in stroke research. *Open Research Europe*, *5*, 280. https://doi.org/10.12688/openreseurope.21294.1

Jackson, R. L. (2021). The neural correlates of semantic control revisited. *NeuroImage*, *224*(7), 117444. https://doi.org/10.1016/j.neuroimage.2020.117444

Jackson, R. L., Rogers, T. T., & Lambon Ralph, M. A. (2021). Reverse-engineering the cortical architecture for controlled semantic cognition. *Nature Human Behaviour 2021 5:6*, *5*(6), 774–786. https://doi.org/10.1038/s41562-020-01034-z

Jang, S. H. (2013). Diffusion tensor imaging studies on arcuate fasciculus in stroke patients: A review. *Frontiers in Human Neuroscience*, *7*(NOV), 749. https://doi.org/10.3389/FNHUM.2013.00749/BIBTEX

Jaywant, A., DelPonte, L., Kanellopoulos, D., O'Dell, M. W., & Gunning, F. M. (2022). The Structural and Functional Neuroanatomy of Post-Stroke Depression and Executive Dysfunction: A Review of Neuroimaging Findings and Implications for Treatment. Journal of Geriatric Psychiatry and Neurology, 35(1), 3–11. https://doi.org/10.1177/0891988720968270;PAGEGROUP:STRING:PUBLICATION

Jefferies, E., & Lambon Ralph, M. A. (2006). Semantic impairment in stroke aphasia versus semantic dementia: a case-series comparison. Brain, 129(8), 2132–2147. https://doi.org/10.1093/BRAIN/AWL153

Jefferies, E., Patterson, K., & Ralph, M. A. L. (2008). Deficits of knowledge vs. executive control in semantic cognition: Insights from cued naming. Neuropsychologia, 46(2), 649. https://doi.org/10.1016/J.NEUROPSYCHOLOGIA.2007.09.007

Jefferies, E. (2013). The neural basis of semantic cognition: Converging evidence from neuropsychology, neuroimaging and TMS. Cortex, 49(3), 611–625. https://doi.org/10.1016/J.CORTEX.2012.10.008

Jefferies, E., & Lambon Ralph, M. A. (2006). Semantic impairment in stroke aphasia versus semantic dementia: a case-series comparison. *Brain*, *129*(8), 2132–2147. https://doi.org/10.1093/brain/awl153

Jefferies, E., & Smallwood, J. (2025). A state-space perspective on the role of the default mode network in semantic cognition. *Current Opinion in Behavioral Sciences*, *66*, 101616. https://doi.org/10.1016/j.cobeha.2025.101616

Jefferies, E., Thompson, H., Cornelissen, P., & Smallwood, J. (2020). The neurocognitive basis of knowledge about object identity and events: dissociations reflect opposing effects of semantic coherence and control. Philosophical Transactions of the Royal Society B: Biological Sciences, 375(1791). https://doi.org/10.1098/RSTB.2019.0300

Jefferies, E., Thompson, H., Cornelissen, P., & Smallwood, J. (2019). The neurocognitive basis of knowledge about object identity and events: dissociations reflect opposing effects of semantic coherence and control. *Philosophical Transactions of the Royal Society B: Biological Sciences*, *375*(1791), 20190300. https://doi.org/10.1098/RSTB.2019.0300

Jenkinson, M., Beckmann, C. F., Behrens, T. E. J., Woolrich, M. W., & Smith, S. M. (2012). FSL. NeuroImage, 62(2), 782–790. https://doi.org/10.1016/J.NEUROIMAGE.2011.09.015

Jiang, J., Bruss, J., Lee, W. T., Tranel, D., & Boes, A. D. (2023). White matter disconnection of left multiple demand network is associated with post-lesion deficits in cognitive control. Nature Communications, 14(1), 1740. https://doi.org/10.1038/S41467-023-37330-1

Jiang, Z., Kuhnke, P., Stockert, A., Wawrzyniak, M., Halai, A., Saur, D., & Hartwigsen, G. (2025). Dynamic reorganization of task-related network interactions in post-stroke aphasia recovery. *Brain*, *148*(10), 3563–3575. https://doi.org/10.1093/brain/awaf036

Jiayu, L., Qiuzhu, Z., Wenjuan, L., Junjun, Z., Zhenlan, J., & Ling, L. (2025). Neural structural underlying audiovisual working memory and visual dominance under cognitive load. *Scientific Reports 2025 15:1*, *15*(1), 32778-. https://doi.org/10.1038/s41598-025-16286-w

Jimenez-Marin, A., De Bruyn, N., Gooijers, J., Llera, A., Meyer, S., Alaerts, K., Verheyden, G., Swinnen, S. P., & Cortes, J. M. (2022). Multimodal and multidomain lesion network mapping enhances prediction of sensorimotor behavior in stroke patients. *Scientific Reports 2022 12:1*, *12*(1), 22400-. https://doi.org/10.1038/s41598-022-26945-x

Jin, H., Ramirez, J. S. B., Byeon, K., Russ, B. E., Falchier, A., Linn, G., Kiar, G., Schroeder, C. E., Vogelstein, J. T., Milham, M. P., & Xu, T. (2025). Is Pearson's correlation coefficient enough for functional connectivity in fMRI? *Imaging Neuroscience*, *3*, IMAG.a.1052. https://doi.org/10.1162/IMAG.A.1052

Joel, S. E., Caffo, B. S., Van Zijl, P. C., & Pekar, J. J. (2011). On the relationship between seed-based and ICA-based measures of functional connectivity. Magnetic Resonance in Medicine, 66(3), 644-657. https://doi.org/10.1002/mrm.22818

Johnson, J. P., Meier, E. L., Pan, Y., & Kiran, S. (2021). Abnormally weak functional connections get stronger in chronic stroke patients who benefit from naming therapy. *Brain and Language*, *223*, 105042. https://doi.org/10.1016/J.BANDL.2021.105042

Jones, D.K., 2009. Chapter 3 – Gaussian Modeling of the Diffusion Signal. In H. Johansen-Berg & T. E. J. B. T.-. D. M. R. I. Behrens (Eds.), Diffusion MRI: From quantitative measurement to in vivo neuroanatomy (pp. 37–54). Academic Press. 10.1016/B978-0-12-374709-9.00003-1.

Jones, T. A., & Adkins, D. L. (2015). Motor System Reorganization After Stroke: Stimulating and Training Toward Perfection. *Physiology (Bethesda, Md.)*, *30*(5), 358–370. https://doi.org/10.1152/physiol.00014.2015

Jung, J., & Lambon Ralph, M. A. (2023). Distinct but cooperating brain networks supporting semantic cognition. Cerebral Cortex, 33(5), 2021–2036. https://doi.org/10.1093/CERCOR/BHAC190

Kaiser, R. H., Andrews-Hanna, J. R., Wager, T. D., & Pizzagalli, D. A. (2015). Large-Scale Network Dysfunction in Major Depressive Disorder: A Meta-analysis of Resting-State Functional Connectivity. *JAMA Psychiatry*, *72*(6), 603–611. https://doi.org/10.1001/JAMAPSYCHIATRY.2015.0071

Karabanov, A. N., Chillemi, G., Madsen, K. H., & Siebner, H. R. (2023). Dynamic involvement of premotor and supplementary motor areas in bimanual pinch force control. NeuroImage, 276, 120203. https://doi.org/10.1016/J.NEUROIMAGE.2023.120203

Katsumi, Y., Zhang, J., Chen, D., Kamona, N., Bunce, J. G., Hutchinson, J. B., Yarossi, M., Tunik, E., Dickerson, B. C., Quigley, K. S., & Barrett, L. F. (2023). Correspondence of functional connectivity gradients across human isocortex, cerebellum, and hippocampus. *Communications Biology*, *6*(1), 401. https://doi.org/10.1038/s42003-023-04796-0

Kawabata, K., Bagarinao, E., Watanabe, H., Maesawa, S., Mori, D., Hara, K., Ohdake, R., Masuda, M., Ogura, A., Kato, T., Koyama, S., Katsuno, M., Wakabayashi, T., Kuzuya, M., Hoshiyama, M., Isoda, H., Naganawa, S., Ozaki, N., & Sobue, G. (2021). Bridging large-scale cortical networks: Integrative and function-specific hubs in the thalamus. *IScience*, *24*(10), 103106. https://doi.org/10.1016/j.isci.2021.103106

Keser, Z., Sebastian, R., Hasan, K. M., & Hillis, A. E. (2020). Right Hemispheric Homologous Language Pathways Negatively Predicts Poststroke Naming Recovery. *Stroke*, *51*(3), 1002–1005. https://doi.org/10.1161/STROKEAHA.119.028293

Kessner, S. S., Schlemm, E., Cheng, B., Bingel, U., Fiehler, J., Gerloff, C., & Thomalla, G. (2019). Somatosensory Deficits After Ischemic Stroke: Time Course and Association With Infarct Location. *Stroke*, *50*(5), 1116–1123. https://doi.org/10.1161/STROKEAHA.118.023750

Khalilian, M., Roussel, M., Godefroy, O., & Aarabi, A. (2024). Predicting functional impairments with lesion-derived disconnectome mapping: Validation in stroke patients with motor deficits. *European Journal of Neuroscience*, *59*(11), 3074–3092. https://doi.org/10.1111/ejn.16334

Kiran, S. (2012). What Is the Nature of Poststroke Language Recovery and Reorganization? ISRN Neurology, 2012, 786872. https://doi.org/10.5402/2012/786872

Kiran, S., & Thompson, C. K. (2019). Neuroplasticity of language networks in aphasia: Advances, updates, and future challenges. Frontiers in Neurology, 10(APR), 423206. https://doi.org/10.3389/FNEUR.2019.00295/XML

Kiran, S., Meier, E. L., & Johnson, J. P. (2019). Neuroplasticity in Aphasia: A Proposed Framework of Language Recovery. *Journal of Speech, Language, and Hearing Research : JSLHR*, *62*(11), 3973. https://doi.org/10.1044/2019_JSLHR-L-RSNP-19-0054

Knodt, A. R., Elliott, M. L., Whitman, E. T., Winn, A., Addae, A., Ireland, D., Poulton, R., Ramrakha, S., Caspi, A., Moffitt, T. E., & Hariri, A. R. (2023). Test–retest reliability and predictive utility of a macroscale principal functional connectivity gradient. *Human Brain Mapping*, *44*(18), 6399. https://doi.org/10.1002/HBM.26517

Koba, C., Falcó-Roget, J., & Crimi, A. (2025). Reshaped functional connectivity gradients in acute ischemic stroke. *NeuroImage : Clinical*, *45*, 103755. https://doi.org/10.1016/J.NICL.2025.103755

Koch, M. A., Norris, D. G., & Hund-Georgiadis, M. (2002). An investigation of functional and anatomical connectivity using magnetic resonance imaging. *NeuroImage*, *16*(1), 241–250. https://doi.org/10.1006/nimg.2001.1052

Koch, P., Schulz, R., & Hummel, F. C. (2016). Structural connectivity analyses in motor recovery research after stroke. *Annals of Clinical and Translational Neurology*, *3*(3), 233–244. https://doi.org/10.1002/ACN3.278

Koenigs, M., Barbey, A. K., Postle, B. R., & Grafman, J. (2009). Superior Parietal Cortex Is Critical for the Manipulation of Information in Working Memory. The Journal of Neuroscience, 29(47), 14980. https://doi.org/10.1523/JNEUROSCI.3706-09.2009

Koller, M. (2016). robustlmm: An R Package for Robust Estimation of Linear Mixed-Effects Models. Journal of Statistical Software, 75(1), 1–24. https://doi.org/10.18637/JSS.V075.I06

Kolskår, K. K., Ulrichsen, K. M., Richard, G., Dørum, E. S., de Schotten, M. T., Rokicki, J., Monereo-Sánchez, J., Engvig, A., Hansen, H. I., Nordvik, J. E., Westlye, L. T., & Alnæs, D. (2022). Structural disconnectome mapping of cognitive function in poststroke patients. *Brain and Behavior*, *12*(8), e2707. https://doi.org/10.1002/brb3.2707

Kong, R., Yang, Q., Gordon, E., Xue, A., Yan, X., Orban, C., Zuo, X. N., Spreng, N., Ge, T., Holmes, A., Eickhoff, S., & Yeo, B. T. T. (2021). Individual-Specific Areal-Level Parcellations Improve Functional Connectivity Prediction of Behavior. *Cerebral Cortex (New York, NY)*, *31*(10), 4477. https://doi.org/10.1093/CERCOR/BHAB101

Kong, T. S., Gratton, C., Low, K. A., Tan, C. H., Chiarelli, A., Fletcher, M. A., Zimmerman, B., Maclin, E. L., Sutton, B. P., Gratton, G., & Fabiani, M. (2020). Age-related differences in functional brain network segregation are consistent with a cascade of cerebrovascular, structural, and cognitive effects. *Network Neuroscience*, *4*(1), 89. https://doi.org/10.1162/NETN_A_00110

Konishi, M., McLaren, D. G., Engen, H., & Smallwood, J. (2015). Shaped by the Past: The Default Mode Network Supports Cognition that Is Independent of Immediate Perceptual Input. *PLoS ONE*, *10*(6), e0132209. https://doi.org/10.1371/JOURNAL.PONE.0132209

Krieger-Redwood, K., Teige, C., Davey, J., Hymers, M., & Jefferies, E. (2015). Conceptual control across modalities: graded specialisation for pictures and words in inferior frontal and posterior temporal cortex. Neuropsychologia, 76, 92. https://doi.org/10.1016/J.NEUROPSYCHOLOGIA.2015.02.030

Krieger-Redwood, K., Jefferies, E., Karapanagiotidis, T., Seymour, R., Nunes, A., Ang, J. W. A., Majernikova, V., Mollo, G., & Smallwood, J. (2016). Down but not out in posterior cingulate cortex: Deactivation yet functional coupling with prefrontal cortex during demanding semantic cognition. *NeuroImage*, *141*, 366–377. https://doi.org/10.1016/J.NEUROIMAGE.2016.07.060

Krieger-Redwood, K., Wang, X., Souter, N., Gonzalez Alam, T. R. del J., Smallwood, J., Jackson, R. L., & Jefferies, E. (2024). Graded and sharp transitions in semantic function in left temporal lobe. Brain and Language, 251, 105402. https://doi.org/10.1016/J.BANDL.2024.105402

Kristanto, D., Hildebrandt, A., Sommer, W., & Zhou, C. (2023). Cognitive abilities are associated with specific conjunctions of structural and functional neural subnetworks. *NeuroImage*, *279*, 120304. https://doi.org/10.1016/J.NEUROIMAGE.2023.120304

Kuceyeski, A., Maruta, J., Relkin, N., & Raj, A. (2013). The Network Modification (NeMo) Tool: elucidating the effect of white matter integrity changes on cortical and subcortical structural connectivity. *Brain Connectivity*, *3*(5), 451–463. https://doi.org/10.1089/brain.2013.0147

Labache, L., Petit, L., Joliot, M., & Zago, L. (2024). Atlas for the Lateralized Visuospatial Attention Networks (ALANs): Insights from fMRI and network analyses. Imaging Neuroscience, 2, 1–22. https://doi.org/10.1162/IMAG_A_00208

Labar, K. S., Gitelman, D. R., Parrish, T. B., & Mesulam, M. M. (1999). Neuroanatomic Overlap of Working Memory and Spatial Attention Networks: A Functional MRI Comparison within Subjects. *NeuroImage*, *10*(6), 695–704. https://doi.org/10.1006/nimg.1999.0503

Lacey, E. H., Skipper-Kallal, L. M., Xing, S., Fama, M. E., & Turkeltaub, P. E. (2017). Mapping Common Aphasia Assessments to Underlying Cognitive Processes and Their Neural Substrates. *Neurorehabilitation and Neural Repair*, *31*(5), 442–450. https://doi.org/10.1177/1545968316688797

Lambon Ralph MA, Jefferies E, Patterson K, Rogers TT (2017) The neural and computational bases of semantic cognition. Nat Rev Neurosci 18(1):42–55. https://doi.org/10.1038/nrn.2016.150

Lambon Ralph, M. A., Lowe, C., & Rogers, T. T. (2007). Neural basis of category-specific semantic deficits for living things: evidence from semantic dementia, HSVE and a neural network model. Brain, 130(4), 1127–1137. https://doi.org/10.1093/BRAIN/AWM025

Lanzoni, L., Thompson, H., Beintari, D., Berwick, K., Demnitz-King, H., Raspin, H., Taha, M., Stampacchia, S., Smallwood, J., & Jefferies, E. (2019). Emotion and location cues bias conceptual retrieval in people with deficient semantic control. Neuropsychologia, 131, 294–305. https://doi.org/10.1016/J.NEUROPSYCHOLOGIA.2019.05.030

Lara, A. H., & Wallis, J. D. (2015). The Role of Prefrontal Cortex in Working Memory: A Mini Review. *Frontiers in Systems Neuroscience*, *9*(DEC), 173. https://doi.org/10.3389/FNSYS.2015.00173

Laredo, C., Zhao, Y., Rudilosso, S., Renú, A., Pariente, J. C., Chamorro, Á., & Urra, X. (2018). Prognostic Significance of Infarct Size and Location: The Case of Insular Stroke. Scientific Reports 2018 8:1, 8(1), 1–10. https://doi.org/10.1038/s41598-018-27883-3

Larivière, S., Ward, N. S., & Boudrias, M. H. (2018). Disrupted functional network integrity and flexibility after stroke: Relation to motor impairments. NeuroImage : Clinical, 19, 883. https://doi.org/10.1016/J.NICL.2018.06.010

Latifi, S., Mitchell, S., Habibey, R., Hosseini, F., Donzis, E., Estrada-Sanchez, A. M., Rezaei Nejad, H., Levine, M., Golshani, P., & Thomas Carmichael, S. (2020). Neuronal Network Topology Indicates Distinct Recovery Processes after Stroke. *Cerebral Cortex (New York, N.Y. : 1991)*, *30*(12), 6363–6375. https://doi.org/10.1093/CERCOR/BHAA191

Latifi, S., & Carmichael, S. T. (2024). The emergence of multiscale connectomics-based approaches in stroke recovery. *Trends in Neurosciences*, *47*(4), 303–318. https://doi.org/10.1016/J.TINS.2024.01.003

Laumann, T. O., Snyder, A. Z., Mitra, A., Gordon, E. M., Gratton, C., Adeyemo, B., Gilmore, A. W., Nelson, S. M., Berg, J. J., Greene, D. J., McCarthy, J. E., Tagliazucchi, E., Laufs, H., Schlaggar, B. L., Dosenbach, N. U. F., & Petersen, S. E. (2017). On the Stability of BOLD fMRI Correlations. *Cerebral Cortex*, *27*(10), 4719–4732. https://doi.org/10.1093/CERCOR/BHW265

Leff, A., Crinion, J., Scott, S., Turkheimer, F., Howard, D., & Wise, R. (2002). A physiological change in the homotopic cortex following left posterior temporal lobe infarction. *Annals of Neurology*, *51*(5), 553–558. https://doi.org/10.1002/ana.10181

Levy, D. F., Entrup, J. L., Schneck, S. M., Onuscheck, C. F., Rahman, M., Kasdan, A., Casilio, M., Willey, E., Davis, L. T., de Riesthal, M., Kirshner, H. S., & Wilson, S. M. (2023). Multivariate lesion symptom mapping for predicting trajectories of recovery from aphasia. Brain Communications, 6(1). https://doi.org/10.1093/BRAINCOMMS/FCAE024

Li, J., Chen, H., & Liao, W. (2025). Mapping the white-matter functional connectome: a personal perspective. *Psychoradiology*, *5*. https://doi.org/10.1093/psyrad/kkaf028

Li, K., & Malhotra, P. A. (2015). Spatial neglect. *Practical Neurology*, *15*(5), 333–339. https://doi.org/10.1136/practneurol-2015-001115

Li, L., Dannenfelser, R., Zhu, Y., Hejduk, N., Segarra, S., & Yao, V. (2023). Joint embedding of biological networks for cross-species functional alignment. Bioinformatics, 39(9). https://doi.org/10.1093/BIOINFORMATICS/BTAD529

Li, M., Lu, S., & Zhong, N. (2016). The Parahippocampal Cortex Mediates Contextual Associative Memory: Evidence from an fMRI Study. BioMed Research International, 2016. https://doi.org/10.1155/2016/9860604

Li, W., Li, Y., Zhu, W., & Chen, X. (2014). Changes in brain functional network connectivity after stroke. Neural Regeneration Research, 9(1), 51. https://doi.org/10.4103/1673-5374.125330

Li, X., Bu, S., Pang, H., Yu, H., Zhao, M., Wang, J., Liu, Y., & Fan, G. (2025). Mapping striatal functional gradients and associated gene expression in Parkinson's disease with continuous cognitive impairment. *Npj Parkinson's Disease 2025 11:1*, *11*(1), 138-. https://doi.org/10.1038/s41531-025-01002-2

Li, Y., Yu, Z., Wu, P., & Chen, J. (2022). Ability of an altered functional coupling between resting-state networks to predict behavioral outcomes in subcortical ischemic stroke: A longitudinal study. Frontiers in Aging Neuroscience, 14, 933567. https://doi.org/10.3389/FNAGI.2022.933567/BIBTEX

Liebenthal, E., Binder, J. R., Spitzer, S. M., Possing, E. T., & Medler, D. A. (2005). Neural Substrates of Phonemic Perception. Cerebral Cortex, 15(10), 1621–1631. https://doi.org/10.1093/CERCOR/BHI040

Liu, B., Chen, C., Cai, P., Zhang, J., Yang, L., Chen, X., Ma, X., Jiang, X., Zhang, A., Song, L., & Jiang, L. (2026). The alterations in brain network functional gradients and dynamic functional connectivity in Alzheimer's disease: a resting-state fMRI study. *Frontiers in Aging Neuroscience*, *17*, 1716076. https://doi.org/10.3389/FNAGI.2025.1716076/TEXT

Lucas, A., Mouchtaris, S., Cornblath, E. J., Sinha, N., Caciagli, L., Hadar, P., Gugger, J. J., Das, S., Stein, J. M., & Davis, K. A. (2023). Subcortical functional connectivity gradients in temporal lobe epilepsy. *NeuroImage : Clinical*, *38*, 103418. https://doi.org/10.1016/J.NICL.2023.103418

Lv, H., Wang, Z., Tong, E., Williams, L. M., Zaharchuk, G., Zeineh, M., Goldstein-Piekarski, A. N., Ball, T. M., Liao, C., & Wintermark, M. (2018). Resting-State Functional MRI: Everything That Nonexperts Have Always Wanted to Know. *American Journal of Neuroradiology*, *39*(8), 1390–1399. https://doi.org/10.3174/AJNR.A5527

Madden, D. J., Bennett, I. J., Burzynska, A., Potter, G. G., Chen, N. kuei, & Song, A. W. (2011). Diffusion Tensor Imaging of Cerebral White Matter Integrity in Cognitive Aging. *Biochimica et Biophysica Acta*, *1822*(3), 386. https://doi.org/10.1016/J.BBADIS.2011.08.003

Mah, Y. H., Husain, M., Rees, G., & Nachev, P. (2014). Human brain lesion-deficit inference remapped. *Brain : A Journal of Neurology*, *137*(Pt 9), 2522–2531. https://doi.org/10.1093/brain/awu164

Marcus, D. S., Fotenos, A. F., Csernansky, J. G., Morris, J. C., & Buckner, R. L. (2010). Open Access Series of Imaging Studies (OASIS): Longitudinal MRI Data in Nondemented and Demented Older Adults. Journal of Cognitive Neuroscience, 22(12), 2677. https://doi.org/10.1162/JOCN.2009.21407

Marek, S., & Dosenbach, N. U. F. (2018). The frontoparietal network: function, electrophysiology, and importance of individual precision mapping. *Dialogues in Clinical Neuroscience*, *20*(2), 133. https://doi.org/10.31887/dcns.2018.20.2/smarek

Margulies, D. S., Ghosh, S. S., Goulas, A., Falkiewicz, M., Huntenburg, J. M., Langs, G., Bezgin, G., Eickhoff, S. B., Castellanos, F. X., Petrides, M., Jefferies, E., & Smallwood, J. (2016). Situating the default-mode network along a principal gradient of macroscale cortical organization. *Proceedings of the National Academy of Sciences of the United States of America*, *113*(44), 12574–12579. https://doi.org/10.1073/pnas.1608282113

Markello, R. D., Hansen, J. Y., Liu, Z. Q., Bazinet, V., Shafiei, G., Suárez, L. E., Blostein, N., Seidlitz, J., Baillet, S., Satterthwaite, T. D., Chakravarty, M. M., Raznahan, A., & Misic, B. (2022). neuromaps: structural and functional interpretation of brain maps. Nature Methods 2022 19:11, 19(11), 1472–1479. https://doi.org/10.1038/s41592-022-01625-w

Marti, E., Coll, S. Y., Doganci, N., & Ptak, R. (2025). Reorganized Functional Networks Underlie Working Memory Deficits After Right-Hemispheric Stroke. *The European Journal of Neuroscience*, *62*(10), e70336. https://doi.org/10.1111/ejn.70336

Mckeown, B., Strawson, W. H., Wang, H. T., Karapanagiotidis, T., Vos de Wael, R., Benkarim, O., Turnbull, A., Margulies, D., Jefferies, E., McCall, C., Bernhardt, B., & Smallwood, J. (2020). The relationship between individual variation in macroscale functional gradients and distinct aspects of ongoing thought. NeuroImage, 220, 117072. https://doi.org/10.1016/J.NEUROIMAGE.2020.117072

Meier, E. L., Johnson, J. P., & Kiran, S. (2018). Left frontotemporal effective connectivity during semantic feature judgments in patients with chronic aphasia and age-matched healthy controls. Cortex, 108, 173–192. https://doi.org/10.1016/J.CORTEX.2018.08.006

Meier, E. L. (2022). The role of disrupted functional connectivity in aphasia. Handbook of Clinical Neurology, 185, 99–119. https://doi.org/10.1016/B978-0-12-823384-9.00005-0

Meier, E. L., Kelly, C. R., & Hillis, A. E. (2022). Dissociable language and executive control deficits and recovery in post-stroke aphasia: An exploratory observational and case series study. *Neuropsychologia*, *172*, 108270. https://doi.org/10.1016/J.NEUROPSYCHOLOGIA.2022.108270

Meinzer, M., Flaisch, T., Breitenstein, C., Wienbruch, C., Elbert, T., & Rockstroh, B. (2008). Functional re-recruitment of dysfunctional brain areas predicts language recovery in chronic aphasia. *NeuroImage*, *39*(4), 2038–2046. https://doi.org/10.1016/J.NEUROIMAGE.2007.10.008

Melkas, S., Jokinen, H., Hietanen, M., & Erkinjuntti, T. (2014). Poststroke cognitive impairment and dementia: prevalence, diagnosis, and treatment. Degenerative Neurological and Neuromuscular Disease, 21. https://doi.org/10.2147/DNND.S37353

Memarian, N., Ferrari, P., Macdonald, M. J., Cheyne, D., De Nil, L. F., & Pang, E. W. (2012). Cortical activity during speech and non-speech oromotor tasks: A magnetoencephalography (MEG) study. *Neuroscience Letters*, *527*(1), 34. https://doi.org/10.1016/J.NEULET.2012.08.030

Menon, V. (2011). Large-scale brain networks and psychopathology: a unifying triple network model. *Trends in Cognitive Sciences*, *15*(10), 483–506. https://doi.org/10.1016/j.tics.2011.08.003

Menon, V., & D'Esposito, M. (2021). The role of PFC networks in cognitive control and executive function. *Neuropsychopharmacology*, *47*(1), 90. https://doi.org/10.1038/S41386-021-01152-W

Mesulam, M. -M. (1990). Large-scale neurocognitive networks and distributed processing for attention, language, and memory. *Annals of Neurology*, *28*(5), 597–613. https://doi.org/10.1002/ANA.410280502

Mesulam, M. (2002). Functional Anatomy of Attention and Neglect: from neurons to networks. *The Cognitive and Neural Bases of Spatial Neglect*, 32–45. https://doi.org/10.1093/acprof:oso/9780198508335.003.0002

Mesulam, M. (2005). Imaging connectivity in the human cerebral cortex: The next frontier? Annals of Neurology, 57(1), 5–7. https://doi.org/10.1002/ana.20368

Miraglia, F., Vecchio, F., Pappalettera, C., Nucci, L., Cotelli, M., Judica, E., Ferreri, F., & Rossini, P. M. (2022). Brain Connectivity and Graph Theory Analysis in Alzheimer's and Parkinson's Disease: The Contribution of Electrophysiological Techniques. *Brain Sciences*, *12*(3), 402. https://doi.org/10.3390/brainsci12030402

Mohr, H., Wolfensteller, U., Betzel, R. F., Mišić, B., Sporns, O., Richiardi, J., & Ruge, H. (2016). Integration and segregation of large-scale brain networks during short-term task automatization. *Nature Communications 2016 7:1*, *7*(1), 13217-. https://doi.org/10.1038/ncomms13217

Montefinese, M., Hallam, G., Stampacchia, S., Thompson, H. E., & Jefferies, E. (2021). Deficits of semantic control disproportionately affect low-relevance conceptual features: evidence from semantic aphasia. Aphasiology, 35(11), 1448–1462. https://doi.org/10.1080/02687038.2020.1814950

Moore, M. J., Demeyere, N., Rorden, C., & Mattingley, J. B. (2024). Lesion mapping in neuropsychological research: A practical and conceptual guide. *Cortex*, *170*(3), 38–52. https://doi.org/10.1016/j.cortex.2023.10.001

Moore, M. J., Gillebert, C. R., & Demeyere, N. (2021). Right and left neglect are not anatomically homologous: A voxel-lesion symptom mapping study. *Neuropsychologia*, *162*(5), 108024. https://doi.org/10.1016/j.neuropsychologia.2021.108024

Murphy, C., Jefferies, E., Rueschemeyer, S. A., Sormaz, M., Wang, H. ting, Margulies, D. S., & Smallwood, J. (2018). Distant from input: Evidence of regions within the default mode network supporting perceptually-decoupled and conceptually-guided cognition. *Neuroimage*, *171*, 393. https://doi.org/10.1016/J.NEUROIMAGE.2018.01.017

Murphy, C., Wang, H. T., Konu, D., Lowndes, R., Margulies, D. S., Jefferies, E., & Smallwood, J. (2019). Modes of operation: A topographic neural gradient supporting stimulus dependent and independent cognition. *NeuroImage*, *186*, 487–496. https://doi.org/10.1016/J.NEUROIMAGE.2018.11.009

Murphy, E., Forseth, K. J., Donos, C., Snyder, K. M., Rollo, P. S., & Tandon, N. (2023). The spatiotemporal dynamics of semantic integration in the human brain. *Nature Communications 2023 14:1*, *14*(1), 6336-. https://doi.org/10.1038/s41467-023-42087-8

Murphy, T. H., & Corbett, D. (2009). Plasticity during stroke recovery: from synapse to behaviour. *Nature Reviews Neuroscience 2009 10:12*, *10*(12), 861–872. https://doi.org/10.1038/nrn2735

Murray, L. L. (2012). Attention and Other Cognitive Deficits in Aphasia: Presence and Relation to Language and Communication Measures. *American Journal of Speech-Language Pathology*, *21*(2). https://doi.org/10.1044/1058-0360(2012/11-0067)

Myers, M. J., Labonte, A. K., Gordon, E. M., Laumann, T. O., Tu, J. C., Wheelock, M. D., Nielsen, A. N., Schwarzlose, R. F., Camacho, M. C., Alexopoulos, D., Warner, B. B., Raghuraman, N., Luby, J. L., Barch, D. M., Fair, D. A., Petersen, S. E., Rogers, C. E., Smyser, C. D., &

Sylvester, C. M. (2024). Functional parcellation of the neonatal cortical surface. *Cerebral Cortex*, *34*(2). https://doi.org/10.1093/CERCOR/BHAE047

Na, Y., Jung, J. Y., Tench, C. R., Auer, D. P., & Pyun, S. B. (2022). Language systems from lesion-symptom mapping in aphasia: A meta-analysis of voxel-based lesion mapping studies. NeuroImage : Clinical, 35, 103038. https://doi.org/10.1016/J.NICL.2022.103038

Nakamura, T., Hillary, F. G., & Biswal, B. B. (2009). Resting network plasticity following brain injury. *PloS One*, *4*(12). https://doi.org/10.1371/JOURNAL.PONE.0008220

Nashed, J. Y., Gale, D. J., Gallivan, J. P., & Cook, D. J. (2024). Changes in cortical manifold structure following stroke and its relation to behavioral recovery in the male macaque. Nature Communications 2024 15:1, 15(1), 1–17. https://doi.org/10.1038/s41467-024-53365-4

Neubert, F. X., Mars, R. B., Buch, E. R., Olivier, E., & Rushworth, M. F. S. (2010). Cortical and subcortical interactions during action reprogramming and their related white matter pathways. *Proceedings of the National Academy of Sciences of the United States of America*, *107*(30), 13240–13245. https://doi.org/10.1073/pnas.1000674107

Niessen, E., Fink, G. R., & Weiss, P. H. (2014). Apraxia, pantomime and the parietal cortex. NeuroImage : Clinical, 5, 42. https://doi.org/10.1016/J.NICL.2014.05.017

Noonan, K. A., Jefferies, E., Corbett, F., & Lambon Ralph, M. A. (2010). Elucidating the nature of deregulated semantic cognition in semantic aphasia: Evidence for the roles of prefrontal and temporo-parietal cortices. Journal of Cognitive Neuroscience, 22(7), 1597–1613. https://doi.org/10.1162/JOCN.2009.21289

Noonan, K. A., Jefferies, E., Visser, M., & Lambon Ralph, M. A. (2013). Going beyond inferior prefrontal involvement in semantic control: evidence for the additional contribution of dorsal angular gyrus and posterior middle temporal cortex. *Journal of Cognitive Neuroscience*, *25*(11), 1824–1850. https://doi.org/10.1162/jocn_a_00442

Nucci, M. P., Cotosck, K., Lukasova, K., Nitrini, R., Grady, C. L., Amaro, E., & Meltzer, J. A. (2026). Literacy modulates engagement of the right inferior frontal gyrus in phonological processing of spoken language. *Cortex*, *196*, 19–40. https://doi.org/10.1016/j.cortex.2025.12.007

Nudo, R. J., Milliken, G. W., Jenkins, W. M., & Merzenich, M. M. (1996). Use-dependent alterations of movement representations in primary motor cortex of adult squirrel monkeys. *Journal of Neuroscience*, *16*(2), 785–807. https://doi.org/10.1523/jneurosci.16-02-00785.1996

O'Donnell, L. J., & Westin, C. F. (2011). An introduction to diffusion tensor image analysis. *Neurosurgery Clinics of North America*, *22*(2), 185. https://doi.org/10.1016/J.NEC.2010.12.004

Obayashi, S. (2021). Cognitive and linguistic dysfunction after thalamic stroke and recovery process: possible mechanism. *AIMS Neuroscience*, *9*(1), 1. https://doi.org/10.3934/NEUROSCIENCE.2022001

Oberhuber, M., Hope, T. M. H., Seghier, M. L., Parker Jones, O., Prejawa, S., Green, D. W., & Price, C. J. (2016). Four Functionally Distinct Regions in the Left Supramarginal Gyrus Support Word Processing. Cerebral Cortex (New York, NY), 26(11), 4212. https://doi.org/10.1093/CERCOR/BHW251

Obermeyer, J., Schlesinger, J., & Martin, N. (2019). Evaluating the Contribution of Executive Functions to Language Tasks in Cognitively Demanding Contexts. *American Journal of Speech-Language Pathology*, *29*(1 Suppl), 463. https://doi.org/10.1044/2019_AJSLP-CAC48-18-0216

Olafson, E. R., Jamison, K. W., Sweeney, E. M., Liu, H., Wang, D., Bruss, J. E., Boes, A. D., & Kuceyeski, A. (2021). Functional connectome reorganization relates to post-stroke motor recovery and structural and functional disconnection. *NeuroImage*, *245*, 118642. https://doi.org/10.1016/J.NEUROIMAGE.2021.118642

Olson, I. R., Plotzker, A., & Ezzyat, Y. (2007). The Enigmatic temporal pole: a review of findings on social and emotional processing. Brain, 130(7), 1718–1731. https://doi.org/10.1093/BRAIN/AWM052

Olsson, C., Arvidsson, P., & Blom Johansson, M. (2019). Relations between executive function, language, and functional communication in severe aphasia. *Aphasiology*, *33*(7), 821–845. https://doi.org/10.1080/02687038.2019.1602813;WGROUP:STRING:PUBLICATION

Osiurak, F., Reynaud, E., Baumard, J., Rossetti, Y., Bartolo, A., & Lesourd, M. (2021). Pantomime of tool use: looking beyond apraxia. Brain Communications, 3(4), fcab263. https://doi.org/10.1093/BRAINCOMMS/FCAB263

Ovadia-Caro, S., Villringer, K., Fiebach, J., Jungehulsing, G. J., Van Der Meer, E., Margulies, D. S., & Villringer, A. (2013). Longitudinal effects of lesions on functional networks after stroke. Journal of Cerebral Blood Flow & Metabolism, 33(8), 1279. https://doi.org/10.1038/JCBFM.2013.80

Pandya, S., Zeighami, Y., Freeze, B., Dadar, M., Collins, D. L., Dagher, A., & Raj, A. (2019). Predictive model of spread of Parkinson's pathology using network diffusion. *NeuroImage*, *192*, 178. https://doi.org/10.1016/J.NEUROIMAGE.2019.03.001

Papageorgiou, G., Kasselimis, D., Angelopoulou, G., Laskaris, N., Tsolakopoulos, D., Velonakis, G., Tountopoulou, A., Vassilopoulou, S., & Potagas, C. (2024). Investigating Aphasia Recovery:

Demographic and Clinical Factors. Brain Sciences, 14(1). https://doi.org/10.3390/BRAINSCI14010007

Park, J. Y., Kim, Y. H., Chang, W. H. yuk, Park, C. hyun, Shin, Y. Il, Kim, S. T. ae, & Pascual-Leone, A. (2014). Significance of longitudinal changes in the default-mode network for cognitive recovery after stroke. *The European Journal of Neuroscience*, *40*(4), 2715–2722. https://doi.org/10.1111/ejn.12640

Pascual-Leone, A., Amedi, A., Fregni, F., & Merabet, L. B. (2005). The plastic human brain cortex. *Annual Review of Neuroscience*, *28*, 377–401. https://doi.org/10.1146/annurev.neuro.27.070203.144216

Patterson, K., Nestor, P. J., & Rogers, T. T. (2007). Where do you know what you know? The representation of semantic knowledge in the human brain. Nature Reviews Neuroscience 2007 8:12, 8(12), 976–987. https://doi.org/10.1038/nrn2277

Pedersen, R., Geerligs, L., Andersson, M., Gorbach, T., Avelar-Pereira, B., Wåhlin, A., Rieckmann, A., Nyberg, L., & Salami, A. (2021). When functional blurring becomes deleterious: Reduced system segregation is associated with less white matter integrity and cognitive decline in aging. *NeuroImage*, *242*. https://doi.org/10.1016/j.neuroimage.2021.118449

Pedreira, C., Mormann, F., Kraskov, A., Cerf, M., Fried, I., Koch, C., & Quiroga, R. Q. (2010). Responses of Human Medial Temporal Lobe Neurons Are Modulated by Stimulus Repetition. Journal of Neurophysiology, 103(1), 97. https://doi.org/10.1152/JN.91323.2008

Peraza, J. A., Salo, T., Riedel, M. C., Bottenhorn, K. L., Poline, J.-B., Dockès, J., Kent, J. D., Bartley, J. E., Flannery, J. S., Hill-Bowen, L. D., Lobo, R. P., Poudel, R., Ray, K. L., Robinson, J. L., Laird, R. W., Sutherland, M. T., Vega, A. de la, & Laird, A. R. (2023). Methods for decoding cortical gradients of functional connectivity. BioRxiv. https://doi.org/10.1101/2023.08.01.551505

Petrides, M., & Pandya, D. N. (2004). The Frontal Cortex. *The Human Nervous System: Second Edition*, 950–972. https://doi.org/10.1016/B978-012547626-3/50026-0

Philippi, C. L., Bruss, J., Boes, A. D., Albazron, F. M., Deifelt Streese, C., Ciaramelli, E., Rudrauf, D., & Tranel, D. (2020). Lesion network mapping demonstrates that mind-wandering is associated with the default mode network. Journal of Neuroscience Research, 99(1), 361. https://doi.org/10.1002/JNR.24648

Pincus, S. M. (1994). Greater signal regularity may indicate increased system isolation. *Mathematical Biosciences*, *122*(2), 161–181. https://doi.org/10.1016/0025-5564(94)90056-6

Pini, L., Salvalaggio, A., De Filippo De Grazia, M., Zorzi, M., de Schotten, M. T., & Corbetta, M. (2021). A novel stroke lesion network mapping approach: improved accuracy yet still low deficit prediction. Brain Communications, 3(4). https://doi.org/10.1093/BRAINCOMMS/FCAB259

Planton, S., Jucla, M., Roux, F. E., & Démonet, J. F. (2013). The "handwriting brain": A meta-analysis of neuroimaging studies of motor versus orthographic processes. *Cortex*, *49*(10), 2772–2787. https://doi.org/10.1016/j.cortex.2013.05.011

Ploner, C. J., Gaymard, B. M., Rivaud-Péchoux, S., & Pierrot-Deseilligny, C. (2005). The Prefrontal Substrate of Reflexive Saccade Inhibition in Humans. *Biological Psychiatry*, *57*(10), 1159–1165. https://doi.org/10.1016/J.BIOPSYCH.2005.02.017

Plowman, E., Hentz, B., & Ellis, C. (2012). Post-stroke aphasia prognosis: a review of patient-related and stroke-related factors. Journal of Evaluation in Clinical Practice, 18(3), 689–694. https://doi.org/10.1111/J.1365-2753.2011.01650.X

Pobric, G., Jefferies, E., & Ralph, M. A. L. (2007). Anterior temporal lobes mediate semantic representation: Mimicking semantic dementia by using rTMS in normal participants. Proceedings of the National Academy of Sciences of the United States of America, 104(50), 20137–20141. https://doi.org/10.1073/PNAS.0707383104/ASSET/D7886652-4A10-4E9B-A522-01C0DE1032A4/ASSETS/GRAPHIC/ZPQ0480784680001.JPEG

Price, C. J., & Crinion, J. (2005). The latest on functional imaging studies of aphasic stroke. Current Opinion in Neurology, 18(4), 429–434. https://doi.org/10.1097/01.WCO.0000168081.76859.C1

Price, C. J., Devlin, J. T., Moore, C. J., Morton, C., & Laird, A. R. (2005). Meta-analyses of object naming: effect of baseline. *Human Brain Mapping*, *25*(1), 70–82. https://doi.org/10.1002/HBM.20132

Price, C. J., Seghier, M. L., & Leff, A. P. (2010). Predicting Language Outcome and Recovery After Stroke (PLORAS). Nature Reviews. Neurology, 6(4), 202. https://doi.org/10.1038/NRNEUROL.2010.15

Price, C. J. (2012). A review and synthesis of the first 20 years of PET and fMRI studies of heard speech, spoken language and reading. NeuroImage, 62(2), 816–847. https://doi.org/10.1016/J.NEUROIMAGE.2012.04.062

Promjunyakul, N. on, Schmit, B. D., & Schindler-Ivens, S. (2013). Changes in hemodynamic responses in chronic stroke survivors do not affect fMRI signal detection in a block experimental design. *Magnetic Resonance Imaging*, *31*(7), 10.1016/j.mri.2013.02.009. https://doi.org/10.1016/J.MRI.2013.02.009

Purcell, J., Sebastian, R., Leigh, R., Jarso, S., Davis, C., Posner, J., Wright, A., & Hillis, A. E. (2017). Recovery of orthographic processing after stroke: A longitudinal fMRI study. Cortex, 92, 103–118. https://doi.org/10.1016/J.CORTEX.2017.03.022

Pustina, D., Avants, B., Faseyitan, O. K., Medaglia, J. D., & Coslett, H. B. (2018). Improved accuracy of lesion to symptom mapping with multivariate sparse canonical correlations. *Neuropsychologia*, *115*, 154–166. https://doi.org/10.1016/j.neuropsychologia.2017.08.027

Pützer, M., Moringlane, J. R., Sikos, L., Reith, W., & Krick, C. M. (2019). fMRI and acoustic analyses reveal neural correlates of gestural complexity and articulatory effort within bilateral inferior frontal gyrus during speech production. *Neuropsychologia*, *132*. https://doi.org/10.1016/J.NEUROPSYCHOLOGIA.2019.107129

Raj, A., Kuceyeski, A., & Weiner, M. (2012). A Network Diffusion Model of Disease Progression in Dementia. *Neuron*, *73*(6), 1204. https://doi.org/10.1016/j.neuron.2011.12.040

Rajda, C. M., Desabrais, K., & Levin, M. F. (2025). Relationships Between Cognitive Impairments and Motor Learning After Stroke: A Scoping Review. *Neurorehabilitation and Neural Repair*, *39*(2), 142–156. https://doi.org/10.1177/15459683241300458

Ramage, A. E., Aytur, S., & Ballard, K. J. (2020). Resting-State Functional Magnetic Resonance Imaging Connectivity Between Semantic and Phonological Regions of Interest May Inform Language Targets in Aphasia. Journal of Speech, Language, and Hearing Research : JSLHR, 63(9), 3051. https://doi.org/10.1044/2020_JSLHR-19-00117

Ramsey, L. E., Siegel, J. S., Baldassarre, A., Metcalf, N. V., Zinn, K., Shulman, G. L., & Corbetta, M. (2016). Normalization of network connectivity in hemi-spatial neglect recovery. Annals of Neurology, 80(1), 127. https://doi.org/10.1002/ANA.24690

Rao, R. P. N. (2024). A sensory–motor theory of the neocortex. *Nature Neuroscience 2024 27:7*, *27*(7), 1221–1235. https://doi.org/10.1038/s41593-024-01673-9

Rauschecker, J. P. (2010). An Expanded Role for the Dorsal Auditory Pathway in Sensorimotor Control and Integration. *Hearing Research*, *271*(1–2), 16. https://doi.org/10.1016/J.HEARES.2010.09.001

Rene del Jesus Gonzalez Alam, T., A Mckeown, B. L., Gao, Z., Bernhardt, B., Vos de Wael, R., Margulies, D. S., Smallwood, J., & Jefferies, E. (2022). A tale of two gradients: differences between the left and right hemispheres predict semantic cognition. *Brain Structure and Function*, *227*, 631–654. https://doi.org/10.1007/s00429-021-02374-w

Rezaei, A., Areshenkoff, C. N., Gale, D. J., De Brouwer, A. J., Nashed, J. Y., Flanagan, J. R., & Gallivan, J. P. (2025). Transfer of motor learning is associated with patterns of activity in the

default mode network. *PLOS Biology*, *23*(8), e3003268. https://doi.org/10.1371/journal.pbio.3003268

Riccardi, N., Nelakuditi, S., Den Ouden, D. B., Rorden, C., Fridriksson, J., & Desai, R. H. (2024). Discourse-and lesion-based aphasia quotient estimation using machine learning. https://doi.org/10.1016/j.nicl.2024.103602

Ripamonti, E., Frustaci, M., Zonca, G., Aggujaro, S., Molteni, F., & Luzzatti, C. (2018). Disentangling phonological and articulatory processing: A neuroanatomical study in aphasia. Neuropsychologia, 121, 175–185. https://doi.org/10.1016/J.NEUROPSYCHOLOGIA.2018.10.015

Roberts, S. M., Bruce, R., Hope, T. M. H., Geva, S., Anderson, S., Woodgate, H., Ledingham, K., Gajardo-Vidal, A., Lorca-Puls, D. L., Crinion, J. T., Leff, A. P., Green, D. W., & Price, C. J. (2024). The impact of pre-stroke formal education on language test performance in aphasic and non-aphasic stroke survivors. *Aphasiology*, *39*(11), 1480. https://doi.org/10.1080/02687038.2024.2434864

Robson, H., Sage, K., & Lambon Ralph, M. A. (2012). Wernicke's aphasia reflects a combination of acoustic-phonological and semantic control deficits: A case-series comparison of Wernicke's aphasia, semantic dementia and semantic aphasia. Neuropsychologia, 50(2), 266–275. https://doi.org/10.1016/J.NEUROPSYCHOLOGIA.2011.11.021

Roelofs, A. (2021). Phonological cueing of word finding in aphasia: insights from simulations of immediate and treatment effects. *Aphasiology*, *35*(2), 169–185. https://doi.org/10.1080/02687038.2019.1686748

Roeltgen, D. P., Heilman, K. M., & Roeltgen, D. (1985). Review of agraphia and a proposal for an anatomically-based neuropsychological model of writing. *Applied Psycholinguistics*, *6*(3), 205–229. https://doi.org/10.1017/S0142716400006184

Royer, J., Paquola, C., Valk, S. L., Kirschner, M., Hong, S. J., Park, B. Y., Bethlehem, R. A. I., Leech, R., Yeo, B. T. T., Jefferies, E., Smallwood, J., Margulies, D., & Bernhardt, B. C. (2024). Gradients of Brain Organization: Smooth Sailing from Methods Development to User Community. *Neuroinformatics 2024 22:4*, *22*(4), 623–634. https://doi.org/10.1007/s12021-024-09660-y

Rudrauf, D., Mehta, S., & Grabowski, T. J. (2008). Disconnection's renaissance takes shape: Formal incorporation in group-level lesion studies. *Cortex*, *44*(8), 1084–1096. https://doi.org/10.1016/j.cortex.2008.05.005

Saber-Moghadam, R., Zeinalzadeh, A., Jamali, J., Farzadfard, M. T., & Sobhani-Rad, D. (2024). Synergistic effects of combined motor and language interventions on stroke rehabilitation: a

holistic approach. *Frontiers in Human Neuroscience*, *18*, 1454491. https://doi.org/10.3389/fnhum.2024.1454491

Sagues, E., Alfaro, F., Ramos-Rodríguez, R., & García-Casares, N. (2025). Resting-state functional connectivity alterations in post-stroke cognitive impairment: a systematic review. *Brain Imaging and Behavior*, *19*(5), 1117. https://doi.org/10.1007/S11682-025-01013-W

Salvalaggio, A., de Filippo De Grazia, M., Zorzi, M., de Schotten, M. T., & Corbetta, M. (2020). Post-stroke deficit prediction from lesion and indirect structural and functional disconnection. *Brain*, *143*(7), 2173. https://doi.org/10.1093/brain/awaa156

Salvalaggio, A., de Filippo De Grazia, M., Zorzi, M., de Schotten, M. T., & Corbetta, M. (2020). Post-stroke deficit prediction from lesion and indirect structural and functional disconnection. Brain, 143(7), 2173. https://doi.org/10.1093/BRAIN/AWAA156

Sasse, L., Paquola, C., Dukart, J., Hoffstaedter, F., Eickhoff, S. B., & Patil, K. R. (2026). Individual identifiability following Procrustes alignment of functional gradients: effect of subspace dimensionality. *Communications Biology 2026 9:1*, *9*(1), 231-. https://doi.org/10.1038/s42003-025-09509-3

Saur, D., Lange, R., Baumgaertner, A., Schraknepper, V., Willmes, K., Rijntjes, M., & Weiller, C. (2006). Dynamics of language reorganization after stroke. *Brain*, *129*(6), 1371–1384. https://doi.org/10.1093/brain/awl090

Saygin, A. P., Dick, F., Wilson, S. W., Dronkers, N. F., & Bates, E. (2003). Neural resources for processing language and environmental sounds: Evidence from aphasia. *Brain*, *126*(4), 928–945. https://doi.org/10.1093/BRAIN/AWG082

Schaefer, A., Kong, R., Gordon, E. M., Laumann, T. O., Zuo, X.-N., Holmes, A. J., Eickhoff, S. B., & Yeo, B. T. T. (2018). Local-Global Parcellation of the Human Cerebral Cortex from Intrinsic Functional Connectivity MRI. Cerebral Cortex, 28(9), 3095–3114. https://doi.org/10.1093/CERCOR/BHX179

Scheffer, M., Kroeff, C., Steigleder, B. G., Klein, L. A., Grassi-Oliveira, R., & de Almeida, R. M. M. (2016). Right frontal stroke: extra-frontal lesions, executive functioning and impulsive behaviour. *Psicologia: Reflexão e Crítica 2016 29:1*, *29*(1), 28-. https://doi.org/10.1186/S41155-016-0018-8

Schevenels, K., Gerrits, R., Lemmens, R., De Smedt, B., Zink, I., & Vandermosten, M. (2022). Early white matter connectivity and plasticity in post stroke aphasia recovery. *NeuroImage : Clinical*, *36*, 103271. https://doi.org/10.1016/j.nicl.2022.103271

Schlemm, E., Cheng, B., Thomalla, G., & Kessner, S. S. (2023). Functional Lesion Network Mapping of Sensory Deficits After Ischemic Stroke. Stroke, 54(11), 2918–2922. https://doi.org/10.1161/STROKEAHA.123.044470/SUPPL_FILE/STR_STROKE-2023-044470D-A_SUPP2.PDF

Schlemm, E., Ingwersen, T., Königsberg, A., Boutitie, F., Ebinger, M., Endres, M., Fiebach, J. B., Fiehler, J., Galinovic, I., Lemmens, R., Muir, K. W., Nighoghossian, N., Pedraza, S., Puig, J., Simonsen, C. Z., Thijs, V., Wouters, A., Gerloff, C., Thomalla, G., & Cheng, B. (2021). Preserved structural connectivity mediates the clinical effect of thrombolysis in patients with anterior-circulation stroke. *Nature Communications 2021 12:1*, *12*(1), 1–12. https://doi.org/10.1038/s41467-021-22786-w

Schmidt, R., LaFleur, K. J. R., de Reus, M. A., van den Berg, L. H., & van den Heuvel, M. P. (2015). Kuramoto model simulation of neural hubs and dynamic synchrony in the human cerebral connectome. *BMC Neuroscience 2015 16:1*, *16*(1), 54-. https://doi.org/10.1186/s12868-015-0193-z

Schoonheim, M. M., Broeders, T. A. A., & Geurts, J. J. G. (2022). The network collapse in multiple sclerosis: An overview of novel concepts to address disease dynamics. *NeuroImage: Clinical*, *35*. https://doi.org/10.1016/j.nicl.2022.103108

Schumacher, R., Halai, A. D., & Lambon Ralph, M. A. (2019). Assessing and mapping language, attention and executive multidimensional deficits in stroke aphasia. *Brain : A Journal of Neurology*, *142*(10), 3202–3216. https://doi.org/10.1093/BRAIN/AWZ258

Schwarz, A., Holl, C. K., Brinkman, L., Stehman, A. J., Cardoso Ferreira, I., Soleimani, N., Farahmand, E., Settle, M., Sakthi, S., Vo, I., Olivares, N., Song, M. K., & Cramer, S. C. (2026). Disconnection syndromes and injury to neural systems after ischemic stroke. *Frontiers in Stroke*, *4*, 1643570. https://doi.org/10.3389/fstro.2025.1643570

Seeley, W. W., Menon, V., Schatzberg, A. F., Keller, J., Glover, G. H., Kenna, H., Reiss, A. L., & Greicius, M. D. (2007). Dissociable intrinsic connectivity networks for salience processing and executive control. *The Journal of Neuroscience : The Official Journal of the Society for Neuroscience*, *27*(9), 2349–2356. https://doi.org/10.1523/JNEUROSCI.5587-06.2007

Seewoo, B. J., Joos, A. C., & Feindel, K. W. (2021). An analytical workflow for seed-based correlation and independent component analysis in interventional resting-state fMRI studies. Neuroscience Research, 165, 26–37. https://doi.org/10.1016/J.NEURES.2020.05.006

Seghier, M. L., Patel, E., Prejawa, S., Ramsden, S., Selmer, A., Lim, L., Browne, R., Rae, J., Haigh, Z., Ezekiel, D., Hope, T. M. H., Leff, A. P., & Price, C. J. (2016). The PLORAS Database: A

data repository for Predicting Language Outcome and Recovery After Stroke. *Neuroimage*, *124*(Pt B), 1208. https://doi.org/10.1016/J.NEUROIMAGE.2015.03.083

Semrau, J. A., Herter, T. M., Scott, S. H., & Dukelow, S. P. (2015). Examining differences in patterns of sensory and motor recovery after stroke with robotics. *Stroke*, *46*(12), 3459–3469. https://doi.org/10.1161/STROKEAHA.115.010750

Serhan, Y., Darawshy, S., Wei, W., Margulies, D. S., Nenning, K. H., & Ovadia-Caro, S. (2025). Individual uniqueness of connectivity gradients is driven by the complexity of the embedded networks and their dispersion. *Brain Structure & Function*, *230*(6), 110. https://doi.org/10.1007/S00429-025-02976-8

Shao, X., Mckeown, B., Karapanagiotidis, T., Vos de Wael, R., Margulies, D. S., Bernhardt, B., Smallwood, J., Krieger-Redwood, K., & Jefferies, E. (2022). Individual differences in gradients of intrinsic connectivity within the semantic network relate to distinct aspects of semantic cognition. Cortex, 150, 48–60. https://doi.org/10.1016/J.CORTEX.2022.01.019

Sharif, M. S., Goldberg, E. B., Walker, A., Hillis, A. E., & Meier, E. L. (2022). The contribution of white matter pathology, hypoperfusion, lesion load, and stroke recurrence to language deficits following acute subcortical left hemisphere stroke. PLOS ONE, 17(10), e0275664. https://doi.org/10.1371/JOURNAL.PONE.0275664

Sheets, J. R., Briggs, R. G., Young, I. M., Bai, M. Y., Lin, Y. H., Poologaindran, A., Conner, A. K., O'Neal, C. M., Baker, C. M., Glenn, C. A., & Sughrue, M. E. (2021). Parcellation-based modeling of the supplementary motor area. *Journal of the Neurological Sciences*, *421*, 117322. https://doi.org/10.1016/J.JNS.2021.117322

Shi, K., Tian, D. C., Li, Z. G., Ducruet, A. F., Lawton, M. T., & Shi, F. D. (2019). Global brain inflammation in stroke. The Lancet Neurology, 18(11), 1058–1066. https://doi.org/10.1016/S1474-4422(19)30078-X

Shine, J. M., Müller, E. J., Munn, B., Cabral, J., Moran, R. J., & Breakspear, M. (2021). Computational models link cellular mechanisms of neuromodulation to large-scale neural dynamics. *Nature Neuroscience*, *24*(6), 765–776. https://doi.org/10.1038/S41593-021-00824-6

Siddiqi, S. H., Kording, K. P., Parvizi, J., & Fox, M. D. (2022). Causal mapping of human brain function. *Nature Reviews Neuroscience 2022 23:6*, *23*(6), 361–375. https://doi.org/10.1038/s41583-022-00583-8

Siegel, J. S., Ramsey, L. E., Snyder, A. Z., Metcalf, N. V., Chacko, R. V., Weinberger, K., Baldassarre, A., Hacker, C. D., Shulman, G. L., & Corbetta, M. (2016). Disruptions of network connectivity predict impairment in multiple behavioral domains after stroke. Proceedings of

the National Academy of Sciences of the United States of America, 113(30), E4367–E4376. https://doi.org/10.1073/PNAS.1521083113;WGROUP:STRING:PUBLICATION

Siegel, J. S., Seitzman, B. A., Ramsey, L. E., Ortega, M., Gordon, E. M., Dosenbach, N. U. F., Petersen, S. E., Shulman, G. L., & Corbetta, M. (2018). Re-emergence of modular brain networks in stroke recovery. *Cortex; a Journal Devoted to the Study of the Nervous System and Behavior*, *101*, 44. https://doi.org/10.1016/j.cortex.2017.12.019

Siegel, J. S., Shulman, G. L., & Corbetta, M. (2017). Measuring functional connectivity in stroke: Approaches and considerations. *Journal of Cerebral Blood Flow and Metabolism*, *37*(8), 2665–2678. https://doi.org/10.1177/0271678X17709198

Sihvonen, A. J., Vadinova, V., Garden, K. L., Meinzer, M., Roxbury, T., O'Brien, K., Copland, D., McMahon, K. L., & Brownsett, S. L. E. (2023). Right hemispheric structural connectivity and poststroke language recovery. Human Brain Mapping, 44(7), 2897–2904. https://doi.org/10.1002/HBM.26252

Silva, A. B., Liu, J. R., Zhao, L., Levy, D. F., Scott, T. L., & Chang, E. F. (2022). A Neurosurgical Functional Dissection of the Middle Precentral Gyrus during Speech Production. *The Journal of Neuroscience*, *42*(45), 8416. https://doi.org/10.1523/JNEUROSCI.1614-22.2022

Simic, T., Desjardins, M. È., Courson, M., Bedetti, C., Houzé, B., & Brambati, S. M. (2023). Treatment-induced neuroplasticity after anomia therapy in post-stroke aphasia: A systematic review of neuroimaging studies. *Brain and Language*, *244*, 105300. https://doi.org/10.1016/J.BANDL.2023.105300

Sinha, N., Nikki Arrington, C., Malins, J. G., Pugh, K. R., Frijters, J. C., & Morris, R. (2024). The reading-attention relationship: Variations in working memory network activity during single word decoding in children with and without dyslexia. *Neuropsychologia*, *195*, 108821. https://doi.org/10.1016/j.neuropsychologia.2024.108821

Smallwood, J., Bernhardt, B. C., Leech, R., Bzdok, D., Jefferies, E., & Margulies, D. S. (2021). The default mode network in cognition: a topographical perspective. *Nature Reviews. Neuroscience*, *22*(8), 503–513. https://doi.org/10.1038/S41583-021-00474-4

Smith, S. M., & Nichols, T. E. (2009). Threshold-free cluster enhancement: Addressing problems of smoothing, threshold dependence and localisation in cluster inference. NeuroImage, 44(1), 83–98. https://doi.org/10.1016/J.NEUROIMAGE.2008.03.061

Smith, S. M., Fox, P. T., Miller, K. L., Glahn, D. C., Fox, P. M., Mackay, C. E., Filippini, N., Watkins, K. E., Toro, R., Laird, A. R., & Beckmann, C. F. (2009). Correspondence of the brain's functional architecture during activation and rest. *Proceedings of the National Academy of*

Sciences of the United States of America, *106*(31), 13040–13045. https://doi.org/10.1073/PNAS.0905267106;PAGE:STRING:ARTICLE/CHAPTER

Solo, V., Poline, J. B., Lindquist, M. A., Simpson, S. L., Bowman, F. D., Chung, M. K., & Cassidy, B. (2018). Connectivity in fMRI: Blind Spots and Breakthroughs. *IEEE Transactions on Medical Imaging*, *37*(7), 1537. https://doi.org/10.1109/TMI.2018.2831261

Souter, N. E., Wang, X., Thompson, H., Krieger-Redwood, K., Halai, A. D., Lambon Ralph, M. A., Thiebaut de Schotten, M., & Jefferies, E. (2022). Mapping lesion, structural disconnection, and functional disconnection to symptoms in semantic aphasia. Brain Structure & Function, 227(9), 3043. https://doi.org/10.1007/S00429-022-02526-6

Spaccavento, S., Craca, A., Del Prete, M., Falcone, R., Colucci, A., Di Palma, A., & Loverre, A. (2013). Quality of life measurement and outcome in aphasia. Neuropsychiatric Disease and Treatment, 10, 27–37. https://doi.org/10.2147/NDT.S52357

Sperber, C., Griffis, J., & Kasties, V. (2022). Indirect structural disconnection-symptom mapping. *Brain Structure and Function 2022 227:9*, *227*(9), 3129–3144. https://doi.org/10.1007/S00429-022-02559-X

Sperber, C., Gallucci, L., Mirman, D., Arnold, M., & Umarova, R. M. (2023). Stroke lesion size – Still a useful biomarker for stroke severity and outcome in times of high-dimensional models. *NeuroImage : Clinical*, *40*. https://doi.org/10.1016/J.NICL.2023.103511

Sperber, C., Rosenzopf, H., Wawrzyniak, M., Klingbeil, J., Saur, D., & Karnath, H. O. (2025). Spatial neglect after subcortical stroke may reflect cortico-cortical disconnection. *Scientific Reports 2025 15:1*, *15*(1), 18544-. https://doi.org/10.1038/s41598-025-01703-x

Sporns, O., Faskowitz, J., Teixeira, A. S., Cutts, S. A., & Betzel, R. F. (2021). Dynamic expression of brain functional systems disclosed by fine-scale analysis of edge time series. *Network Neuroscience*, *5*(2), 405. https://doi.org/10.1162/NETN_A_00182

Sporns, O., Tononi, G., & Kötter, R. (2005). The human connectome: A structural description of the human brain. *PLoS Computational Biology*, *1*(4), 0245–0251. https://doi.org/10.1371/JOURNAL.PCBI.0010042

Stam, C. J., Jones, B. F., Nolte, G., Breakspear, M., & Scheltens, P. (2007). Small-world networks and functional connectivity in Alzheimer's disease. *Cerebral Cortex (New York, N.Y. : 1991)*, *17*(1), 92–99. https://doi.org/10.1093/CERCOR/BHJ127

Stanley, M. L., Moussa, M. N., Paolini, B. M., Lyday, R. G., Burdette, J. H., & Laurienti, P. J. (2013). Defining nodes in complex brain networks. *Frontiers in Computational Neuroscience*, *7*(NOV), 169. https://doi.org/10.3389/FNCOM.2013.00169/ABSTRACT

Stefaniak, J. D., Geranmayeh, F., & Lambon Ralph, M. A. (2022). The multidimensional nature of aphasia recovery post-stroke. *Brain*, *145*(4), 1354–1367. https://doi.org/10.1093/BRAIN/AWAB377

Stockert, A., Wawrzyniak, M., Klingbeil, J., Wrede, K., Kümmerer, D., Hartwigsen, G., Kaller, C. P., Weiller, C., & Saur, D. (2020). Dynamics of language reorganization after left temporo-parietal and frontal stroke. *Brain : A Journal of Neurology*, *143*(3), 844–861. https://doi.org/10.1093/brain/awaa023

Sun, L., Zhao, T., Liang, X., Xia, M., Li, Q., Liao, X., Gong, G., Wang, Q., Pang, C., Yu, Q., Bi, Y., Chen, P., Chen, R., Chen, Y., Chen, T., Cheng, J., Cheng, Y., Cui, Z., Dai, Z., … He, Y. (2025). Human lifespan changes in the brain's functional connectome. *Nature Neuroscience 2025 28:4*, *28*(4), 891–901. https://doi.org/10.1038/s41593-025-01907-4

Swinburn, K., Porter, G., & Howard, D. (2004). *CAT: Comprehensive Aphasia Test*. 175. http://books.google.com/books?id=MMVdPwAACAAJ&pgis=1

Swinburn, K., Porter, G., & Howard, D. (2012). Comprehensive Aphasia Test. *PsycTESTS Dataset*. https://doi.org/10.1037/t13733-000

Tao, Y., & Rapp, B. (2020). How functional network connectivity changes as a result of lesion and recovery: An investigation of the network phenotype of stroke. *Cortex; a Journal Devoted to the Study of the Nervous System and Behavior*, *131*, 17. https://doi.org/10.1016/J.CORTEX.2020.06.011

Tao, Y., & Rapp, B. (2021). Investigating the network consequences of focal brain lesions through comparisons of real and simulated lesions. *Scientific Reports 2021 11:1*, *11*(1), 2213-. https://doi.org/10.1038/s41598-021-81107-9

Tarantino, V., Burgio, F., Toffano, R., Rigon, E., Meneghello, F., Weis, L., & Vallesi, A. (2021). Efficacy of a training on executive functions in potentiating rehabilitation effects in stroke patients. *Brain Sciences*, *11*(8), 1002. https://doi.org/10.3390/BRAINSCI11081002/S1

Thiebaut De Schotten, M., Tomaiuolo, F., Aiello, M., Merola, S., Silvetti, M., Lecce, F., Bartolomeo, P., & Doricchi, F. (2014). Damage to white matter pathways in subacute and chronic spatial neglect: a group study and 2 single-case studies with complete virtual "in vivo" tractography dissection. *Cerebral Cortex (New York, N.Y. : 1991)*, *24*(3), 691–706. https://doi.org/10.1093/cercor/bhs351

Thiebaut de Schotten, M., Foulon, C., & Nachev, P. (2020). Brain disconnections link structural connectivity with function and behaviour. Nature Communications, 11(1), 1–8. https://doi.org/10.1038/S41467-020-18920-9

Thielen, H., Tuts, N., Welkenhuyzen, L., Lemmens, R., Wibail, A., Huenges Wajer, I. M. C., Lafosse, C., Mantini, D., & Gillebert, C. R. (2025). Post-stroke sensory hypersensitivity: insights from lesion-symptom and disconnection mapping. *Brain Communications*, *7*(3). https://doi.org/10.1093/braincomms/fcaf176

Thomas Yeo, B. T., Krienen, F. M., Sepulcre, J., Sabuncu, M. R., Lashkari, D., Hollinshead, M., Roffman, J. L., Smoller, J. W., Zöllei, L., Polimeni, J. R., Fisch, B., Liu, H., & Buckner, R. L. (2011). The organization of the human cerebral cortex estimated by intrinsic functional connectivity. *Https://Doi.Org/10.1152/Jn.00338.2011*, *106*(3), 1125–1165.

Thomason, M. E., Chang, C. E., Glover, G. H., Gabrieli, J. D. E., Greicius, M. D., & Gotlib, I. H. (2008). Default-mode function and task-induced deactivation have overlapping brain substrates in children. *NeuroImage*, *41*(4), 1493–1503. https://doi.org/10.1016/J.NEUROIMAGE.2008.03.029

Thompson, H. E., & Jefferies, E. (2013). Semantic control and modality: An input processing deficit in aphasia leading to deregulated semantic cognition in a single modality. *Neuropsychologia*, *51*(10), 1998–2015. https://doi.org/10.1016/j.neuropsychologia.2013.06.030

Thompson, H. E., Robson, H., Lambon Ralph, M. A., & Jefferies, E. (2015). Varieties of semantic 'access' deficit in Wernicke's aphasia and semantic aphasia. *Brain*, *138*(12), 3776. https://doi.org/10.1093/BRAIN/AWV281

Thompson, H., Davey, J., Hoffman, P., Hallam, G., Kosinski, R., Howkins, S., Wooffindin, E., Gabbitas, R., & Jefferies, E. (2017). Semantic control deficits impair understanding of thematic relationships more than object identity. Neuropsychologia, 104, 113. https://doi.org/10.1016/J.NEUROPSYCHOLOGIA.2017.08.013

Thompson, H. E., Almaghyuli, A., Noonan, K. A., barak, O., Lambon Ralph, M. A., & Jefferies, E. (2018). The contribution of executive control to semantic cognition: Convergent evidence from semantic aphasia and executive dysfunction. Journal of Neuropsychology, 12(2), 312–340. https://doi.org/10.1111/JNP.12142

Thompson, H. E., Noonan, K. A., Halai, A. D., Hoffman, P., Stampacchia, S., Hallam, G., Rice, G. E., De Dios Perez, B., Lambon Ralph, M. A., & Jefferies, E. (2022). Damage to temporoparietal cortex is sufficient for impaired semantic control. *Cortex*, *156*, 71–85. https://doi.org/10.1016/j.cortex.2022.05.022

Thompson-Schill, S. L., D'Esposito, M., Aguirre, G. K., & Farah, M. J. (1997). Role of left inferior prefrontal cortex in retrieval of semantic knowledge: A reevaluation. Proceedings of the National Academy of Sciences, 94(26), 14792–14797. https://doi.org/10.1073/PNAS.94.26.14792

Thompson-Schill, S. L., Jonides, J., Marshuetz, C., Smith, E. E., D'Esposito, M., Kan, I. P., Knight, R. T., & Swick, D. (2002). Effects of frontal lobe damage on interference effects in working memory. *Cognitive, Affective, & Behavioral Neuroscience 2002 2:2*, *2*(2), 109–120. https://doi.org/10.3758/CABN.2.2.109

Tompson, S. H., Falk, E. B., Vettel, J. M., & Bassett, D. S. (2018). Network Approaches to Understand Individual Differences in Brain Connectivity: Opportunities for Personality Neuroscience. *Personality Neuroscience*, *1*, e5. https://doi.org/10.1017/PEN.2018.4

Tscherpel, C., Mustin, M., Rosjat, N., Mais, L. T., Ziemann, U., Fink, G. R., Daun, S., & Grefkes, C. (2025). Evoked slow oscillations and dynamic network reorganization after stroke. *Brain Communications*, *7*(6). https://doi.org/10.1093/BRAINCOMMS/FCAF391

Tsiakiri, A., Giantsios, C., Vlotinou, P., Nikolaidou, A., Atanbori, J., Sohani, B., Aliyu, A., Mournou, A., Peristeri, E., & Frantzidis, C. (2024). Mapping brain networks and cognitive functioning after stroke: A systematic review. *Brain Organoid and Systems Neuroscience Journal*, *2*(4), 43–52. https://doi.org/10.1016/j.bosn.2024.08.001

Tuladhar, A. M., Snaphaan, L., Shumskaya, E., Rijpkema, M., Fernandez, G., Norris, D. G., & de Leeuw, F. E. (2013). Default Mode Network Connectivity in Stroke Patients. PLoS ONE, 8(6), 66556. https://doi.org/10.1371/JOURNAL.PONE.0066556

Uddin, L. Q., Nomi, J. S., Hébert-Seropian, B., Ghaziri, J., & Boucher, O. (2017). Structure and function of the human insula. *Journal of Clinical Neurophysiology : Official Publication of the American Electroencephalographic Society*, *34*(4), 300. https://doi.org/10.1097/WNP.0000000000000377

Underwood, R., Tolmeijer, E., Wibroe, J., Peters, E., & Mason, L. (2021). Networks underpinning emotion: A systematic review and synthesis of functional and effective connectivity. *NeuroImage*, *243*, 118486. https://doi.org/10.1016/J.NEUROIMAGE.2021.118486

Vallila-Rohter, S., & Kiran, S. (2012). Non-linguistic learning and aphasia: Evidence from a paired associate and feedback-based task. *Neuropsychologia*, *51*(1), 79. https://doi.org/10.1016/J.NEUROPSYCHOLOGIA.2012.10.024

Van Assche, M., Klug, J., Dirren, E., Richiardi, J., & Carrera, E. (2022). Preparing for a Second Attack: A Lesion Simulation Study on Network Resilience After Stroke. *Stroke*, *53*(6), 2038–2047. https://doi.org/10.1161/STROKEAHA.121.037372

van den Heuvel, M. P., & Hulshoff Pol, H. E. (2010). Exploring the brain network: A review on resting-state fMRI functional connectivity. *European Neuropsychopharmacology*, *20*(8), 519–534. https://doi.org/10.1016/J.EURONEURO.2010.03.008

van den Heuvel, M. P., & Sporns, O. (2011). Rich-Club Organization of the Human Connectome. *Journal of Neuroscience*, *31*(44), 15775–15786. https://doi.org/10.1523/JNEUROSCI.3539-11.2011

van den Heuvel, M. P., & Sporns, O. (2019). A cross-disorder connectome landscape of brain dysconnectivity. *Nature Reviews Neuroscience 2019 20:7*, *20*(7), 435–446. https://doi.org/10.1038/s41583-019-0177-6

van den Heuvel, M. P., Libedinsky, I., Quiroz Monnens, S., Repple, J., Sommer, I., & Cocchi, L. (2026). Investigating the methodological foundation of lesion network mapping. *Nature Neuroscience 2026*, 1–11. https://doi.org/10.1038/s41593-025-02196-7

Van Der Werf, Y. D., Scheltens, P., Lindeboom, J., Witter, M. P., Uylings, H. B. M., & Jolles, J. (2003).Deficits of memory, executive functioning and attention following infarction in the thalamus; a study of 22 cases with localised lesions. *Neuropsychologia*, *41*(10), 1330–1344. https://doi.org/10.1016/S0028-3932(03)00059-9

Van Hees, S., McMahon, K., Angwin, A., de Zubicaray, G., & Copland, D. A. (2014). Neural activity associated with semantic versus phonological anomia treatments in aphasia. *Brain and Language*, *129*(1), 47–57. https://doi.org/10.1016/j.bandl.2013.12.004

van Oers, C. A. M. M., Vink, M., van Zandvoort, M. J. E., van der Worp, H. B., de Haan, E. H. F., Kappelle, L. J., Ramsey, N. F., & Dijkhuizen, R. M. (2010). Contribution of the left and right inferior frontal gyrus in recovery from aphasia. A functional MRI study in stroke patients with preserved hemodynamic responsiveness. *NeuroImage*, *49*(1), 885–893. https://doi.org/10.1016/j.neuroimage.2009.08.057

Vanhaudenhuyse, A., Demertzi, A., Schabus, M., Noirhomme, Q., Bredart, S., Boly, M., Phillips, C., Soddu, A., Luxen, A., Moonen, G., & Laureys, S. (2011). Two distinct neuronal networks mediate the awareness of environment and of self. *Journal of Cognitive Neuroscience*, *23*(3), 570–578. https://doi.org/10.1162/jocn.2010.21488

Veldsman, M., & Brodtmann, A. (2019). Disconnectomics: Stroke-related disconnection and dysfunction in distributed brain networks. *International Journal of Stroke*, *14*(1), 6–8. https://doi.org/10.1177/1747493018806166

Veldsman, M., Werden, E., Egorova, N., Khlif, M. S., & Brodtmann, A. (2020). Microstructural degeneration and cerebrovascular risk burden underlying executive dysfunction after stroke. *Scientific Reports 2020 10:1*, *10*(1), 17911-. https://doi.org/10.1038/s41598-020-75074-w

Verma, K., Kumar, S., & Paydarfar, D. (2022). Automatic Segmentation and Quantitative Assessment of Stroke Lesions on MR Images. Diagnostics, 12(9), 2055. https://doi.org/10.3390/DIAGNOSTICS12092055

von Economo, C., & Koskinas, G. N. (2007). Atlas of Cytoarchitectonics of the Adult Human Cerebral Cortex: Translated, revised and edited with an Introduction and additional appendix material by L.C. Triarhou (Thessaloniki). With full-scale reproductions of the original 112 microphotographic plat…. *Atlas of Cytoarchitectonics of the Adult Human Cerebral Cortex*. https://doi.org/10.1159/isbn.978-3-8055-8289-6

von Monakow C. , Die Localization im Grosshirn und der Abbau der Funktion durch korticale Herde, 1914 Wiesbaden, GermanyJF Bergmann

Vos de Wael, R., Benkarim, O., Paquola, C., Lariviere, S., Royer, J., Tavakol, S., Xu, T., Hong, S. J., Langs, G., Valk, S., Misic, B., Milham, M., Margulies, D., Smallwood, J., & Bernhardt, B. C. (2020). BrainSpace: a toolbox for the analysis of macroscale gradients in neuroimaging and connectomics datasets. *Communications Biology*, *3*(1), 103. https://doi.org/10.1038/S42003-020-0794-7

Vos De Wael, R., Larivière, S., Caldairou, B., Hong, S. J., Margulies, D. S., Jefferies, E., Bernasconi, A., Smallwood, J., Bernasconi, N., & Bernhardt, B. C. (2018). Anatomical and microstructural determinants of hippocampal subfield functional connectome embedding. Proceedings of the National Academy of Sciences of the United States of America, 115(40), 10154–10159. https://doi.org/10.1073/PNAS.1803667115/-/DCSUPPLEMENTAL

Voytek, B., Davis, M., Yago, E., Barceló, F., Vogel, E. K., & Knight, R. T. (2010). Dynamic Neuroplasticity after Human Prefrontal Cortex Damage. *Neuron*, *68*(3), 401–408. https://doi.org/10.1016/j.neuron.2010.09.018

Wagner, S., Sebastian, A., Lieb, K., Tüscher, O., & Tadić, A. (2014). A coordinate-based ALE functional MRI meta-analysis of brain activation during verbal fluency tasks in healthy control subjects. BMC Neuroscience 2014 15:1, 15(1), 19-. https://doi.org/10.1186/1471-2202-15-19

Wang, L., Yu, C., Chen, H., Qin, W., He, Y., Fan, F., Zhang, Y., Wang, M., Li, K., Zang, Y., Woodward, T. S., & Zhu, C. (2010). Dynamic functional reorganization of the motor execution network after stroke. *Brain : A Journal of Neurology*, *133*(Pt 4), 1224–1238. https://doi.org/10.1093/BRAIN/AWQ043

Wang, X., Huang, C. C., Tsai, S. J., Lin, C. P., & Cai, Q. (2024). The aging trajectories of brain functional hierarchy and its impact on cognition across the adult lifespan. *Frontiers in Aging Neuroscience*, *16*, 1331574. https://doi.org/10.3389/FNAGI.2024.1331574/FULL

Wang, X., Margulies, D. S., Smallwood, J., & Jefferies, E. (2020). A gradient from long-term memory to novel cognition: Transitions through default mode and executive cortex. NeuroImage, 220, 117074. https://doi.org/10.1016/J.NEUROIMAGE.2020.117074

Wang, X., Gao, Z., Smallwood, J., & Jefferies, E. (2021). Both Default and Multiple-Demand Regions Represent Semantic Goal Information. Journal of Neuroscience, 41(16), 3679–3691. https://doi.org/10.1523/JNEUROSCI.1782-20.2021

Wang, X., Krieger-Redwood, K., Cui, Y., Smallwood, J., Du, Y., & Jefferies, E. (2024). Macroscale brain states support the control of semantic cognition. *Communications Biology 2024 7:1*, *7*(1), 926-. https://doi.org/10.1038/s42003-024-06630-7

Wang, X., Krieger-Redwood, K., Lyu, B., Lowndes, R., Wu, G., Souter, N. E., Wang, X., Kong, R., Shafiei, G., Bernhardt, B. C., Cui, Z., Smallwood, J., Du, Y., & Jefferies, E. (2024). The Brain's Topographical Organization Shapes Dynamic Interaction Patterns That Support Flexible Behavior Based on Rules and Long-Term Knowledge. Journal of Neuroscience, 44(22). https://doi.org/10.1523/JNEUROSCI.2223-23.2024

Wang, Y., Eichert, N., Paquola, C., Rodriguez-Cruces, R., DeKraker, J., Royer, J., Cabalo, D. G., Auer, H., Ngo, A., Leppert, I. R., Tardif, C. L., Rudko, D. A., Leech, R., Amunts, K., Valk, S. L., Smallwood, J., Evans, A. C., & Bernhardt, B. C. (2025). Multimodal gradients unify local and global cortical organization. Nature Communications 2025 16:1, 16(1), 1–16. https://doi.org/10.1038/s41467-025-59177-4

Wang, Z., Dai, Z., Gong, G., Zhou, C., & He, Y. (2015). Understanding structural-functional relationships in the human brain: A large-scale network perspective. *Neuroscientist*, *21*(3), 290–305. https://doi.org/10.1177/1073858414537560/ASSET/IMAGES/LARGE/10.1177_1073858414537560-FIG6.JPEG

Weber, S., Bühler, J., Bolton, T. A. W., & Aybek, S. (2025). Altered brain network dynamics in motor functional neurological disorders: the role of the right temporo-parietal junction. *Translational Psychiatry 2025 15:1*, *15*(1), 167-. https://doi.org/10.1038/s41398-025-03385-5

Westlin, C., Guthrie, A. J., Bleier, C., Finkelstein, S. A., Maggio, J., Ranford, J., MacLean, J., Godena, E., Millstein, D., Paredes-Echeverri, S., Freeburn, J., Adams, C., Stephen, C. D., Diez, I., & Perez, D. L. (2025). Delineating network integration and segregation in the pathophysiology of functional neurological disorder. *Brain Communications*, *7*(3). https://doi.org/10.1093/braincomms/fcaf195

White, B. R., Chan, C., Vandekar, S., & Shinohara, R. T. (2022). Statistical approaches to temporal and spatial autocorrelation in resting-state functional connectivity in mice measured with optical intrinsic signal imaging. Neurophotonics, 9(4). https://doi.org/10.1117/1.NPH.9.4.041405

Whitfield-Gabrieli, S., & Nieto-Castanon, A. (2012). Conn: a functional connectivity toolbox for correlated and anticorrelated brain networks. *Brain Connectivity*, *2*(3), 125–141. https://doi.org/10.1089/BRAIN.2012.0073

Whitney, C., Kirk, M., O'Sullivan, J., Lambon Ralph, M. A., & Jefferies, E. (2011). The Neural Organization of Semantic Control: TMS Evidence for a Distributed Network in Left Inferior Frontal and Posterior Middle Temporal Gyrus. *Cerebral Cortex*, *21*(5), 1066–1075. https://doi.org/10.1093/CERCOR/BHQ180

Wig, G. S., Laumann, T. O., & Petersen, S. E. (2014). An approach for parcellating human cortical areas using resting-state correlations. *NeuroImage*, *93*, 276–291. https://doi.org/10.1016/j.neuroimage.2013.07.035

Wild, C. J., Yusuf, A., Wilson, D. E., Peelle, J. E., Davis, M. H., & Johnsrude, I. S. (2012). Effortful Listening: The Processing of Degraded Speech Depends Critically on Attention. *The Journal of Neuroscience*, *32*(40), 14010. https://doi.org/10.1523/JNEUROSCI.1528-12.2012

Wilson, S. M., & Hula, W. D. (2019). Multivariate approaches to understanding aphasia and its neural substrates. *Current Neurology and Neuroscience Reports*, *19*(8), 53. https://doi.org/10.1007/S11910-019-0971-6

Wilson, S. M., & Schneck, S. M. (2021). Neuroplasticity in Post-Stroke Aphasia: A Systematic Review and Meta-Analysis of Functional Imaging Studies of Reorganization of Language Processing. Neurobiology of Language, 2(1), 22–82. https://doi.org/10.1162/NOL_A_00025

Winkler, A. M., Ridgway, G. R., Webster, M. A., Smith, S. M., & Nichols, T. E. (2014). Permutation inference for the general linear model. https://doi.org/10.1016/j.neuroimage.2014.01.060

Wolff, M., & Halassa, M. M. (2024). The mediodorsal thalamus in executive control. *Neuron*, *112*(6), 893–908. https://doi.org/10.1016/j.neuron.2024.01.002

Wu, K., Jiang, Y., Luo, J., Chen, Y., Peng, S., Kong, X., & Gong, G. (2025). Latent dimension linking functional connectivity with post-stroke deficits across multiple domains. *Brain Communications*, *7*(4). https://doi.org/10.1093/BRAINCOMMS/FCAF276

Wu, X., Liang, C., Bustillo, J., Kochunov, P., Wen, X., Sui, J., Jiang, R., Yang, X., Fu, Z., Zhang, D., Calhoun, V. D., & Qi, S. (2025). The Impact of Atlas Parcellation on Functional Connectivity Analysis Across Six Psychiatric Disorders. *Human Brain Mapping*, *46*(5), e70206. https://doi.org/10.1002/HBM.70206;JOURNAL:JOURNAL:10970193;WGROUP:STRING:PUBLICATION

Wulf, G., McNevin, N., & Shea, C. H. (2001). The automaticity of complex motor skill learning as a function of attentional focus. *The Quarterly Journal of Experimental Psychology. A, Human Experimental Psychology*, *54*(4), 1143–1154. https://doi.org/10.1080/713756012

Xiao, Y., Wang, D., Tan, Z., Luo, H., Wang, Y., Pan, C., Lan, Z., Kuai, C., & Xue, S. W. (2022). Charting the dorsal-medial functional gradient of the default mode network in major depressive disorder. Journal of Psychiatric Research, 153, 1–10. https://doi.org/10.1016/J.JPSYCHIRES.2022.06.059

Xing, S., Lacey, E. H., Skipper-Kallal, L. M., Jiang, X., Harris-Love, M. L., Zeng, J., & Turkeltaub, P. E. (2015). Right hemisphere grey matter structure and language outcomes in chronic left hemisphere stroke. *Brain*, *139*(1), 227. https://doi.org/10.1093/BRAIN/AWV323

Yan, X., Kong, R., Xue, A., Yang, Q., Orban, C., An, L., Holmes, A. J., Qian, X., Chen, J., Zuo, X. N., Zhou, J. H., Fortier, M. V., Tan, A. P., Gluckman, P., Chong, Y. S., Meaney, M. J., Bzdok, D., Eickhoff, S. B., & Yeo, B. T. T. (2023). Homotopic local-global parcellation of the human cerebral cortex from resting-state functional connectivity. *NeuroImage*, *273*, 120010. https://doi.org/10.1016/J.NEUROIMAGE.2023.120010

Yang, S., Meng, Y., Li, J., Li, B., Fan, Y. S., Chen, H., & Liao, W. (2020). The thalamic functional gradient and its relationship to structural basis and cognitive relevance. *NeuroImage*, *218*. https://doi.org/10.1016/j.neuroimage.2020.116960

Ye, B., Wei, D., & Pan, L. (2022). Montreal Cognitive Assessment of cognitive dysfunction after basal ganglia stroke. *Acta Neurologica Belgica*, *122*(4), 881. https://doi.org/10.1007/s13760-022-01967-4

Yeo BTT, Krienen FM, Sepulcre J, Sabuncu MR, Lashkari D, Hollinshead M, Roffman JL, Smoller JW, Zollei L, Polimeni JR, Fischl B, Liu H, Buckner RL (2011) The organization of the human cerebral cortex estimated by intrinsic functional connectivity. J Neurophysiol 106:1125–1165. https://doi.org/10.1152/jn.00338.2011

Yerys, B. E., Gordon, E. M., Abrams, D. N., Satterthwaite, T. D., Weinblatt, R., Jankowski, K. F., Strang, J., Kenworthy, L., Gaillard, W. D., & Vaidya, C. J. (2015). Default mode network segregation and social deficits in autism spectrum disorder: Evidence from non-medicated children. *NeuroImage: Clinical*, *9*, 223–232. https://doi.org/10.1016/J.NICL.2015.07.018

Yourganov, G., Fridriksson, J., Stark, B., & Rorden, C. (2017). Removal of artifacts from resting-state fMRI data in stroke. *NeuroImage : Clinical*, *17*, 297. https://doi.org/10.1016/J.NICL.2017.10.027

Zebhauser, P. T., Vernet, M., Unterburger, E., & Brem, A. K. (2019). Visuospatial Neglect - a Theory-Informed Overview of Current and Emerging Strategies and a Systematic Review on the

Therapeutic Use of Non-invasive Brain Stimulation. *Neuropsychology Review*, *29*(4), 397. https://doi.org/10.1007/s11065-019-09417-4

Zevgolatakou, E., Thye, M., & Mirman, D. (2022). Behavioural and neural structure of fluent speech production deficits in aphasia. *Brain Communications*, *5*(1), fcac327. https://doi.org/10.1093/BRAINCOMMS/FCAC327

Zhang, B., Schnakers, C., Wang, K. X. L., Wang, J., Lee, S., Millan, H., Howard, M., Rosario, E., & Zheng, Z. S. (2025). Infratentorial white matter integrity as a potential biomarker for post-stroke aphasia. *Brain Communications*, *7*(3). https://doi.org/10.1093/braincomms/fcaf174

Zhang, C., Xia, Y., Feng, T., Yu, K., Zhang, H., Sami, M. U., Xiang, J., & Xu, K. (2021). Disrupted Functional Connectivity Within and Between Resting-State Networks in the Subacute Stage of Post-stroke Aphasia. Frontiers in Neuroscience, 15, 746264. https://doi.org/10.3389/FNINS.2021.746264/BIBTEX

Zhang, X. H., Anderson, K. M., Dong, H. M., Chopra, S., Dhamala, E., Emani, P. S., Gerstein, M. B., Margulies, D. S., & Holmes, A. J. (2024). The cell-type underpinnings of the human functional cortical connectome. *Nature Neuroscience 2024 28:1*, *28*(1), 150–160. https://doi.org/10.1038/s41593-024-01812-2

Zhao, M. T., Gong, Q., Chen, R., & Jiao, Y. (2025). Cortical Hierarchy Collapse in Alzheimer's Disease: Connectome Gradient Compression as a Potential Biomarker. *Journal of Neuroscience Research*, *103*(12), e70099. https://doi.org/10.1002/JNR.70099

Zhao, Y., Halai, A. D., & Lambon Ralph, M. A. (2020). Evaluating the granularity and statistical structure of lesions and behaviour in post-stroke aphasia. Brain Communications, 2(2). https://doi.org/10.1093/BRAINCOMMS/FCAA062

Zhao, Y., Cox, C. R., Lambon Ralph, M. A., & Halai, A. D. (2023). Using in vivo functional and structural connectivity to predict chronic stroke aphasia deficits. Brain : A Journal of Neurology, 146(5), 1950–1962. https://doi.org/10.1093/BRAIN/AWAC388

Zhao, Y., Song, L., Ding, J., Lin, N., Wang, Q., Du, X., Sun, R., & Han, Z. (2017). Left Anterior Temporal Lobe and Bilateral Anterior Cingulate Cortex Are Semantic Hub Regions: Evidence from Behavior-Nodal Degree Mapping in Brain-Damaged Patients. The Journal of Neuroscience, 37(1), 141. https://doi.org/10.1523/JNEUROSCI.1946-16.2016

Zhu, T., Li, L., Song, Y., Han, Y., Zhou, C., Zhou, D., Zhang, F., Xue, Q., Liu, J., Zhao, L., Zhang, C., Lv, Y., & Han, X. (2019). Altered Functional Connectivity within Default Mode Network in Patients with Transient Ischemic Attack: A Resting-State Functional Magnetic Resonance Imaging Study. Cerebrovascular Diseases, 48(1–2), 61–69. https://doi.org/10.1159/000502884

Zuo, L., Dong, Y., Hu, Y., Xiang, X., Liu, T., Zhou, J., Shi, J., & Wang, Y. (2023). Clinical Features, Brain-Structure Changes, and Cognitive Impairment in Basal Ganglia Infarcts: A Pilot Study. *Neuropsychiatric Disease and Treatment*, *19*, 1171. https://doi.org/10.2147/NDT.S384726